THE UNIVERSITY OF NOTTINGHAM
Institute of Engineering Surveying and Space Geodesy

GPS ASSISTED HELICOPTER PHOTOGRAMMETRY FOR HIGHWAY PROFILING

Christopher Iain Harold Joy
BEng (Nottingham),1993

Thesis submitted to the University of Nottingham
for the degree of Doctor of Philosophy

April 1998

ABSTRACT

Roads are an integral part of today's lifestyle. Indeed, a modern and efficient economy requires a satisfactory road network. The road network in the United Kingdom faces ever-increasing demands with 94% of passenger travel and 92% of freight transport undertaken by road. Maintenance of the network is essential. Prior to the commencement of any maintenance scheme, an accurate highway profile is measured by undertaking a detailed topographic survey of the road surface and the adjacent verges. Traditionally, this is carried out by land surveyors using, for example, a theodolite, EDM and level.

Highway surveying by traditional methods is a slow, costly and dangerous process. A photogrammetric technique was devised by Photarc Surveys Ltd of Harrogate, UK to reduce the problems of speed, cost and safety. This helicopter based photographic system can yield topographic data at upto ±5mm rmse through photogrammetric analysis. It is necessary to install ground control points on the hard shoulder for use in the photogrammetric analysis.

This research investigates the potential of both conventional aerial triangulation and in-flight GPS assisted aerial triangulation for reducing this ground control requirement. The original photographic system is extended to integrate a GPS positioning system and the performance of this system is assessed through a series of field trials.

The results of the research show that the camera can be positioned by the GPS system to within 5 centimetres. The GPS positions can be included in the aerial triangulation to further reduce the requirement for ground control. It is shown that for mapping at the ± 5mm rmse level, there is no potential for height control reduction, even when GPS positions are used. However for mapping at upto ± 20mm, the GPS positions can enable a significant reduction in ground control.

ACKNOWLEDGEMENTS

The research undertaken for this thesis has been carried out in the Institute of Engineering Surveying and Space Geodesy (IESSG) at the University of Nottingham. The author acknowledges the advice from his academic supervisor, Dr Martin Smith, throughout the period of formal study and beyond.

The author would like to express his thanks to a number of people who have helped realise the research aims. Mr J C Boardman and Mr R M Stanbridge of Photarc Surveys Ltd for the support of the company and the continued advice. Dr D Lowe for his advice on integrated positioning systems. Also, thanks to the Engineering Faculty Workshop and notably Mr G Handley for his advice and assistance.

The author would like to make a special mention of thanks to the IESSG technicians, the late Mr P Clarke and the late Mr S Elliott.

I would express my gratitude to the friends and colleagues from the IESSG and the Department of Civil Engineering for providing a light hearted deviation from the serious business of research. This made my second three year sentence at the University all the more pleasant! Thanks to Dr Nigel Penna and Dr Douglas Smith for proof reading parts of this thesis.

Finally, to Lynn for her continued tolerance of all the evenings spent in front of the computer and her encouragement to get me to finish this thesis. Also, to my family for their emotional and financial support throughout my university years.

It was a long road..... but I got there in the end!

TABLE OF CONTENTS

8. AERIAL TRIANGULATION: TESTS AND RESULTS.....148

LIST OF FIGURES

LIST OF TABLES

Chapter 1

Introduction

1.1 The Role of Highway Profiling

Roads are an integral part of today's lifestyle. Indeed, a modern and efficient economy requires a satisfactory road network (for example for product distribution and tourism). The backbone of the road network in the United Kingdom is the 10,400 kilometre [*Highways Agency, 1996a*] motorway and trunk road network. This faces ever-increasing demands with 94% of passenger travel and 92% of freight transport undertaken by road [*BRF, 1997*]. The pressure on the road network is set to continue with predictions for growth suggesting that traffic volumes will continue to grow and vehicle ownership will increase by 16% by the year 2005 [*BRF, 1997*].

Management, development and maintenance of the motorway and trunk road network in the UK is the responsibility of the Highways Agency. They are committed to providing an efficient, reliable, safe and environmentally acceptable network through a rolling programme of road maintenance and

expansion [*Highways Agency, 1996b*]. The Highways Agency continually monitors the condition of the road network to prioritise road improvement schemes within available funding [*Highways Agency, 1996a*]. In 1995, the portfolio of road improvement schemes awaiting funding from either public or private sectors totalled 6.44 billion pounds [*Highways Agency, 1996b*].

Prior to the commencement of any maintenance scheme or road realignment work, it is essential to provide accurate highway profiles by undertaking a detailed topographic survey of the road surface and the adjacent verges [*Boardman, 1994*]. This data is then utilised by the highway engineers for procedure planning and material costing, because without a survey of the area, it is impossible to calculate new road alignments and levels. Traditionally, a highway profiling survey is carried out by first re-directing traffic from the area with traffic cones in a similar manner as would be required during the actual maintenance scheme [*DoT, 1996*]. A team of land surveyors can then carry out a topographic survey of the area using, for example, a theodolite, EDM and level.

1.2 Non-Contact Highway Profiling

Detailed land survey using instruments such as a theodolite and EDM is a slow and expensive process. The cost is increased by the need to close off road lanes to traffic, realised through lane rental from the Highways Agency, which costs upwards of £50,000 per kilometre per day [*Longdin and Browning, 1990*]. From a safety standpoint, it is undesirable to re-direct traffic with cones for anything but the most essential maintenance because of the link between roadworks and increased traffic accident rates. This danger of roadworks has been quantified by a Transport Research Laboratory study [*Hayes and Taylor, 1993*] which calculated that the risks associated with major roadworks are a 14% increase in personal injury rates on dual carriageways and an increase of 57% on motorways.

The solution to reducing the lane coning that is necessary for road maintenance is to employ a so called 'non-contact' method of surveying to acquire the highway profiles. This implies that the surveyor does not encroach onto the live carriageway, negating the need for lane coning. Two approaches have been developed by UK survey companies and can be summarised as:

- Profiling by reflectorless EDM
- Profiling by photogrammetry

The reflectorless EDM is a recent innovation and has found great use in places where the object is inaccessible. Glen Surveys Ltd of Orpington, UK have demonstrated the use of reflectorless EDM technology for highway profiling of short sections of UK trunk roads [*Jackson, 1996*]. The survey is conducted from the hard shoulder of the road and is capable of providing highway spot levels to ±5mm rmse. However, this approach requires the surveyor to manually move the EDM along to the next station which is very time consuming when many kilometres of highway are to be profiled.

A more dynamic approach has been operated for several years by Longdin and Browning Surveys of Swansea, UK. They have mounted the reflectorless EDM in a modified van to enable the observation station to be quickly moved along the hard shoulder [*Bennett, 1989*]. This speeds up the survey whilst maintaining the same ±5mm rmse accuracy.

The photogrammetric approach to highway profiling was originally developed by Photarc Surveys Ltd, a photogrammetric mapping company based in Harrogate, UK. This technique is the basis for the research and is now introduced.

1.3 Helicopter Photogrammetry

Photarc Surveys Ltd were approached in 1983 by West Yorkshire County Council and asked to undertake a topographic survey of two stretches of the M62 by some remote method such that lane coning was not necessary. With experience of developing novel photogrammetric techniques, the company devised a helicopter based photographic system which could yield high precision topographic data through photogrammetric analysis [*Boardman, 1994*].

Technically, the system comprises three distinct operations [*Stanbridge, 1993*]:

- Ground control survey
- Photograph acquisition
- Photogrammetric analysis

Using a helicopter flown as low as 75m altitude [*Boardman, 1994*] to obtain vertical stereo-photographic coverage of the motorway, pairs of photographs can be orientated in an photogrammetric plotter to produce a *stereomodel*. The altitude of the helicopter is maintained with a laser altimeter. Ground control points are required to orientate the model, such that image point measurements can be transformed into the corresponding ground coordinates in the object space. These ground control points are 10cm square white markers (shown in figure 5.1) which are established at the back of the hard shoulder at upto a 50m interval depending on the required precision of the highway survey. Permanent ground markers are also established at a 250m interval which is a requirement for the survey and setting out work done during the eventual road maintenance work.

The final data is typically provided to the client as a series of spot height strings along the various lanes of the highway or as a full topographical survey

[*Boardman, 1994*], formatted into an appropriate data format for input into a computer based highway design package such as MOSS [*Stanbridge, 1987*]. These spot heights can be reliably provided to ±5mm rmse precision as shown in table 1.1.

Contract Specified Precision (mm)	Photographic Scale	Control Interval (m)	Field Level Precision (mm)	Photogrammetric Precision (μm)
5	1:750	50	2	4
10	1:900	60	3	4
12	1:1050	70	3	4
15	1:1200	80	4	4
20	1:1500	100	5	4

Table 1.1 - Highway Contract Precisions And Related Scale/Control Requirements [*Boardman, 1994*]

Highway profiling by photogrammetry is nearly a true non-contact method unlike the aforementioned EDM approach which requires a surveyor to occupy the hard shoulder for the duration of the survey. This is particular important because of the danger of working on the hard shoulder adjacent to live traffic lanes. *Stanbridge* [1996] reports that the death of highway engineers during such a survey caused the Queensland Department of Transport in Australia to employ Photarc Surveys Ltd and their photogrammetric technique because of the clear safety benefits. Only the process of establishing the ground control markers at the back edge of the hard shoulder requires any intrusion onto the highway.

In addition to highway profiles for maintenance schemes, the use of a photographic technique also ensures that a full visual record is available to engineers [*Stanbridge, 1987*] for condition assessment of roadside furniture (lamp posts, signs, crash barriers).

1.4 Research Objectives

Although the actual survey procedure is remote through the use of a helicopter, it is necessary to install a number of ground control points on the hard shoulder for use in the photogrammetric analysis. This is an unfortunate caveat to an otherwise non-contact method because of the requirement for a survey team to work adjacent to live traffic lanes whilst coordinating these ground control points. Photarc Surveys Ltd had recognised this problem but were unable, because of commercial pressures, to investigate available photogrammetric techniques such as aerial triangulation which might reduce the requirement for ground control. Coupled with this possibility to reduce ground control were developments in an extension to aerial triangulation [*Ackermann, 1992a*] which enables the use of satellite positioning techniques for further reducing the same requirement for such ground control points in small scale mapping work.

This research was conceived after discussions between Photarc Surveys Ltd and the Institute of Engineering Surveying and Space Geodesy at the University of Nottingham. The primary aim is to investigate the potential of both conventional aerial triangulation and in-flight GPS assisted aerial triangulation for reducing the ground control requirement in large scale photogrammetric mapping of highways. The original photographic system that was developed for use in the helicopter is not capable of collecting GPS data during a photographic flight. Therefore, the research also involves extending the photographic system to integrate a GPS positioning system and assessing the performance of this system through a series of field trials.

1.5 Research Methodology

To achieve the objectives of this research, it is necessary to undertake the following work:

- Modify the photographic acquisition system to also obtain GPS positioning data
- Develop software to enable both conventional aerial triangulation and GPS assisted aerial triangulation
- Derive data to allow a comparison of the quality of aerial triangulation and the potential for ground control reduction

The integration of a GPS positioning system and a photogrammetric camera system has been evaluated for small scale mapping work [*Ackermann and Schade, 1993*]. This type of work uses a fixed wing aircraft which is different to the helicopter used in this research. The modification of the photogrammetric camera system posed a new challenge because of the unique operating environment and the need for the camera system to remain portable and available for commercial work [*Hansen and Joy, 1995*]. In order to achieve the integration, the emphasis is placed on:

- The design and development of an electronic control system for integrating the timing of the GPS receiver and the camera shutter mechanism
- The development of computer control software to support the electronic control system

The performance of the GPS-camera system is assessed through testing in three field trials. Specifically, the antenna phase centre coordinates derived from the GPS positioning system are compared to truth coordinates calculated by photogrammetric space resection. An assessment of the practical considerations for using a combined system is also given.

Aerial triangulation is a data processing technique for photogrammetric observations. No suitable aerial triangulation package was available at the IESSG for processing of GPS assisted aerial triangulation. The author has,

therefore, developed an aerial triangulation package which can use the GPS position data and is written as a framework for future research developments in this field.

The quality of the aerial triangulation of the test datasets is assessed through the comparison of different ground control configurations and different photographic configurations (the use of side strips of photography). The assessment of these configurations is based on an accuracy comparison of the derived coordinates of the measured ground points with a truth ground survey undertaken at the time of the photographic flight.

1.6 Thesis Outline

Since the system development was investigated in two distinct areas, aerial triangulation processing and the use of GPS, Chapter 2 provides a background to the aerial triangulation work and Chapter 3 contains an overview of the relevant GPS concepts. The integration of GPS and photogrammetry has been an active international research field over the last few years and provided the impetus for this work. In Chapter 4, the factors in combining the two techniques are detailed and the approaches which have been taken in other applications, such as forestry and small scale topographic mapping, are discussed. The field trials and datasets are introduced in Chapter 5 and further discussion is given to the methodology behind the aerial triangulation testing. The necessary hardware developments for the GPS-camera system are described and assessed in Chapter 6.

To assess the performance of aerial triangulation processing and the inclusion of GPS positioning data, it was necessary for the author to develop a core software package and several smaller applications. These are described in Chapter 7. Having detailed the hardware and software developments necessary to exploit aerial triangulation techniques and GPS positioning, the analytical investigations and comparisons are given in Chapter 8. Finally, in

Chapter 9 the conclusions drawn from the research and recommendations for future work are detailed.

Chapter 2

Aerial Triangulation

2.1 Introduction

A stereoscopic model is required for most aerial applications of modern photogrammetry, this being achieved with an analytical or digital stereoplotter. To locate the model in a ground based coordinate system, a framework of control points is required on the ground surface. Provision of such *ground control* can be a costly part of a photogrammetric survey.

Aerial Triangulation may be defined as "the process for the extension and provision of control information....as may be necessary for topographic or similar mapping" [*Ghosh, 1975*]. Traditionally, it has been used to provide ground coordinate points, but by using an appropriate technique it can also be used to calculate the orientation parameters of the photographs for subsequent orientation in the photogrammetric plotter. These orientation parameters are

the exposure station coordinates (X_0, Y_0 and Z_0) and three rotations (ω, ϕ and κ). The main advantage of aerial triangulation is that, even within large photographic blocks, it only uses a relatively small framework of surveyed ground points.

This chapter introduces the three main types of aerial triangulation in section 2.2 with a short discussion on early methods in section 2.3. The main sections concentrate on the technique of aerial triangulation using bundles (bundle estimation) which is implemented in the software. Section 2.4 introduces bundle estimation and section 2.5 discusses methods for refining measured photo coordinates. Section 2.6 details methods for applying a statistical evaluation to the results of an aerial triangulation and error analysis is detailed in section 2.7. A summary of this chapter is given in section 2.8.

2.2 Background

The orientation of a series of photographs by aerial triangulation is classified according to many different criteria, varying across the available literature. A useful classification, in the author's opinion, is based on the photographic unit which is analysed.

- Model - consisting of a pair of photographs
- Photograph - consisting of a single photograph

The order of this classification indicates the technological developments in photogrammetry since the early part of the twentieth century. The development of the first computers enabled the photogrammetrist to apply computational methods to aerial triangulation and the order represents an increase in computational effort. The aerial triangulation technique classification can be further refined to reflect the adjustment techniques:

- Polynomial Adjustment
- Section Adjustment
- Bundle Estimation

The *estimation* phrase modernises the concept of adjusting coordinates during each technique. Polynomial adjustment and section adjustment are now briefly discussed before the description of bundle estimation which is implemented in most modern aerial triangulation packages such as BINGO [*Krück, 1996*].

2.3 Early Methods in Aerial Triangulation

The polynomial adjustment and section adjustment methods use the model as the basic data unit. This means that the image points are measured in the model coordinate system. Once all of the points have been measured in all of the models, the models are joined into a block or strip and located into the ground coordinate system. Polynomial and section are two techniques which can be used to achieve this joining of the individual models.

2.3.1 Polynomial Adjustment

The procedure of polynomial adjustment works with strips of photography and is described by *Schut* [1967]. Two stages are apparent in the procedure:

- Formation of the strip from stereomodels
- Polynomial transformation of the strip onto the available ground control

The difficulty of polynomial estimation is the choice of a suitable polynomial transformation which describes the deformations which affect the strip. These deformations may be caused by:

- Curvature of the earth in the object space
- Observational errors
- Instrumental errors
- Atmospheric errors

Without careful consideration, the strip will be poorly transformed onto the available ground control. Further discussion of the observational errors that can cause deformation in a photogrammetric strip or block can be found in the discussion on the Bundle estimation (§2.5).

2.3.2 Section Adjustment

The procedure of section adjustment works directly with the models. A group of models are transformed into the ground coordinate system using a suitable transformation and common tie points in adjacent models.

Analytical processes like section adjustment were only feasible with the advent of the computer [*Wolf, 1983*]. One significant benefit of section adjustment is that the transformation can be achieved by a least squares process which can improve the overall precision.

Neither polynomial adjustment or section adjustment were investigated during this research because it was felt that the bundle estimation process was the most robust and most suitable for the introduction of GPS observations into the computation. There discussion is only included for completeness alongside the main discussion which now follows.

2.4 Bundle Estimation

The basic data unit in the bundle estimation is the photograph, and the method takes its name from the bundles of light rays which project the object space onto the negative at the instant of exposure (Figure 2.1). It is considered to be the most accurate method for performing aerial triangulation for the following reasons [*Ibrahim, 1995*]:

- the collinearity condition, which constitutes the functional model in a bundle estimation, is a good representation of the actual geometric situation without any serious approximations.
- the analytical or digital instruments used to obtain the image point observations have low instrumental errors (typically less than 3μm in an analytical instrument such as the Leica SD2000 or Zeiss P3 Planicomp).
- errors which might result from a relative or absolute orientation procedure are not propagated into the estimation process because they are not required in the measurement phase.

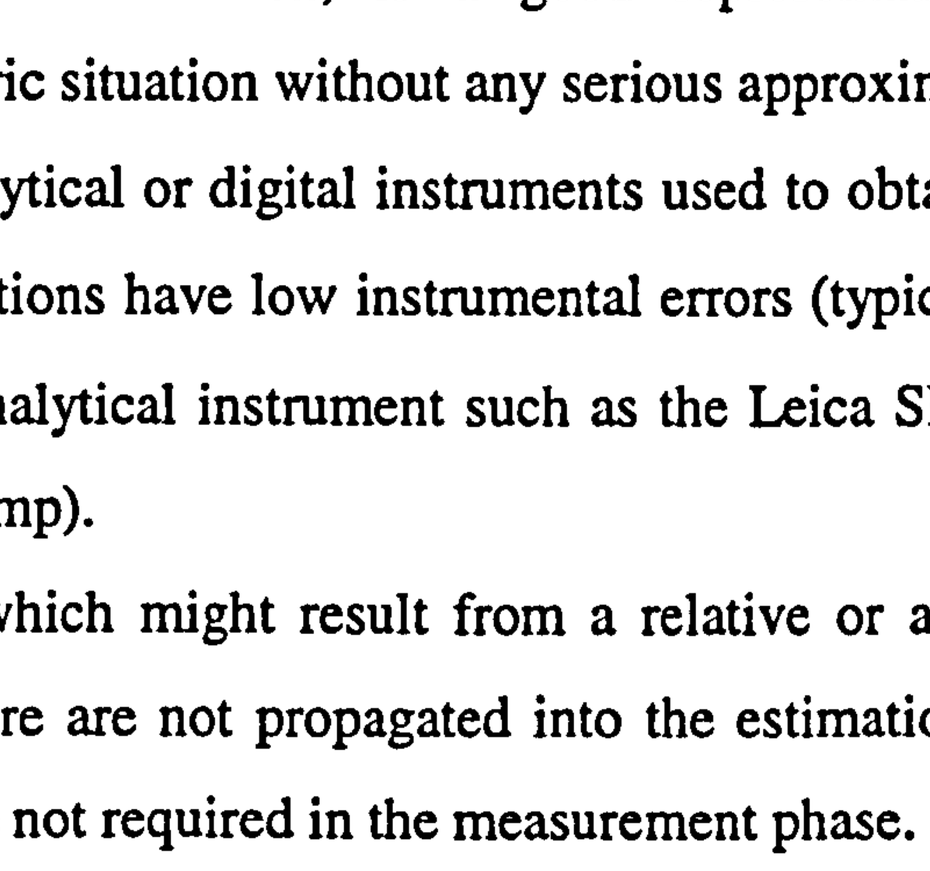

Figure 2.1 - The projective relationship between object and image space in a Bundle Estimation

The orientation parameters (§2.1) for each photograph are solved simultaneously using the process of the Best Linear Unbiased Estimate (BLUE), more commonly referred to as the Least Squares estimate. This technique is necessary because there are more observations in the computation than there are unknown parameters to be derived (redundancy).

2.4.1 Least Squares Principles

The method of least squares was developed over 150 years ago [*Slama, 1980*] and is used extensively in geodesy and photogrammetry. It is based on the principle of *maximum likelihood estimators* with two fundamental assumptions on the observations:

- the observations contain only random errors whose probability density function (pdf) is symmetrical and continuous (§2.7.3)
- all observations are mutually independant [*Slama, 1980*]

A least squares solution for the unknown parameters is achieved when the following condition is satisfied:

$$v^T W v \Rightarrow \text{minimum}$$

ie, the sum of the squares of the weighted (W) residuals (v) are a minimum. The weight matrix is the inverse of C_{ap}, the *a priori* covariance matrix of the observations [*Cross, 1972*] and is discussed in §2.4.6. A residual is the difference between the observed value and the computed value, giving a measure of the fit of the observations to the functional model (§2.4.2).

There are three main constituents to the least squares process, the *functional model*, the *computational algorithm* and the *statistical evaluation* of the results. The simplified relationship is illustrated in Figure 2.2.

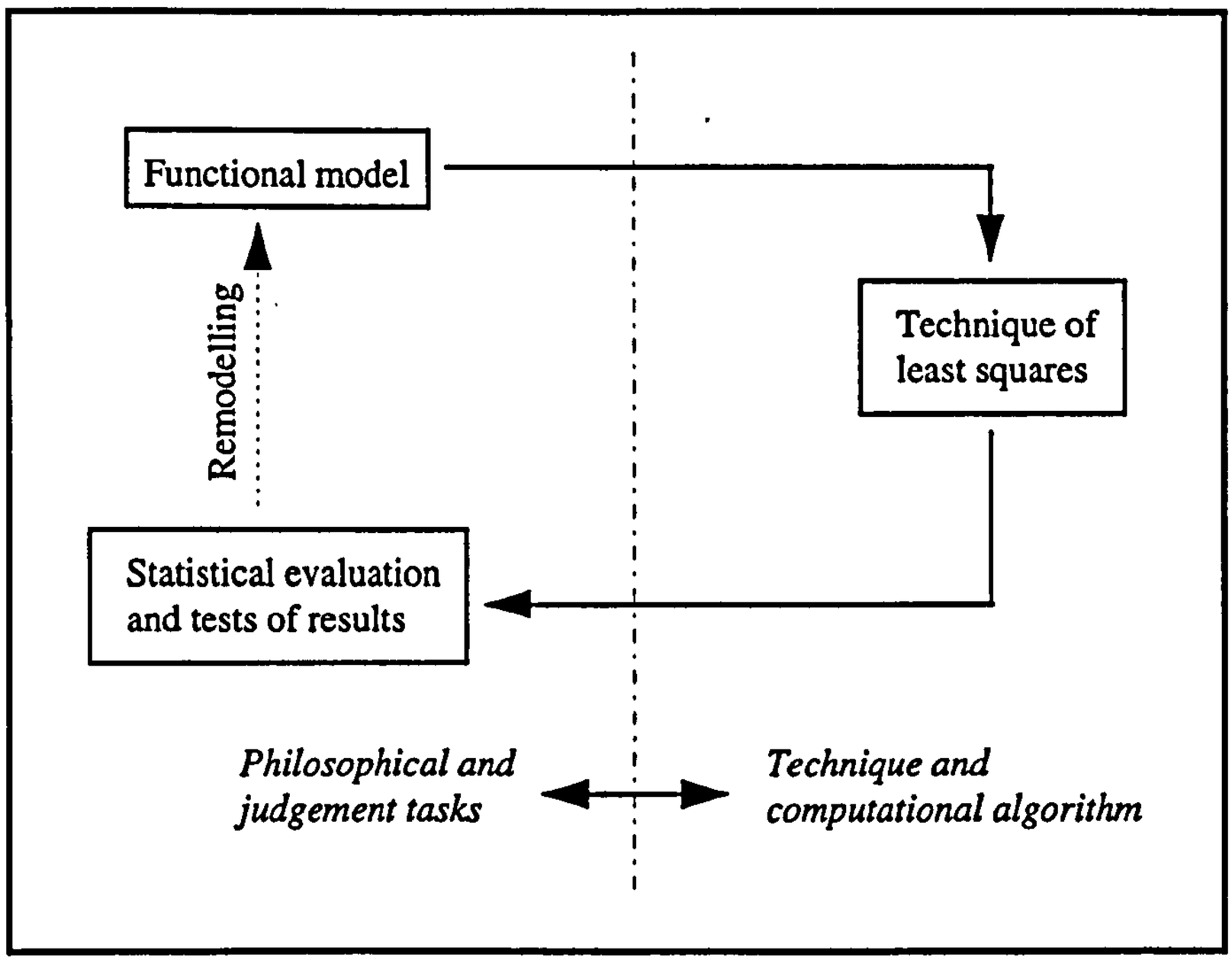

Figure 2.2 - The Components Of A Least Squares Process [*Mikhail, 1976*]

The following subsections discuss the factors involved in evaluating a solution of the unknown parameters. It will be seen that these typically contain unknown photograph orientation parameters (§2.1) and the coordinates of the ground points.

2.4.2 The Functional Model And The Collinearity Condition

The functional model relates the observed quantities to those which are to be determined by a series of observation equations. In the specific case of a photogrammetric bundle estimation, the primary observation equation describes the relationship between the image point measurements that are

obtained with the analytical or digital stereoplotter and the corresponding ground point coordinates. The collinearity condition can be used to develop such an equation.

The collinearity condition represents the actual situation at the time of exposing the photographic film over an object field (figure 2.1). A ray of light is assumed to be a straight line passing from the ground point, through the perspective centre of the camera, to the photographic image of that point. This assumption is valid because the effects of certain distortions are removed before or during the computation (§2.5). *"Analytical photogrammetry consists of mathematical modelling of the relationship between different [coordinate] systems"* [*Ghosh, 1988*].

The relationship between the image coordinates of the photo point and the ground coordinates of the ground point may be written as [*Ibrahim, 1995*]:

$$\begin{bmatrix} X_i \\ Y_i \\ Z_i \end{bmatrix} = \lambda_{ij} m^j \begin{bmatrix} x_i^j \\ y_i^j \\ -f \end{bmatrix} + \begin{bmatrix} X^j \\ Y^j \\ Z^j \end{bmatrix} \qquad \textbf{[2.1]}$$

where:

$[X_i \quad Y_i \quad Z_i]^T$	are the ground coordinates of ground point i
$[X^j \quad Y^j \quad Z^j]^T$	are the ground coordinates of the image station j (perspective centre)
$[x_i^j \quad y_i^j]^T$	are the image coordinates of ground point i in photograph j
λ_{ij}	is the scale factor associated with ground point i in photograph j
m^j	is the rotation matrix of photograph j which consists of elements for the three axes rotation parameters ω, ϕ and κ
f	is the camera principal distance

Equation 2.1 can be manipulated to form the non-linear observation equations shown in equations 2.2a and 2.2b. These equations are referred to as the collinearity equations, the most fundamental equations in analytical photogrammetry [*Slama, 1980*].

$$x_i^j = -f\frac{m_{11}^j\left(X_i - X^j\right)+m_{12}^j\left(Y_i - Y^j\right)+m_{13}^j\left(Z_i - Z^j\right)}{m_{31}^j\left(X_i - X^j\right)+m_{32}^j\left(Y_i - Y^j\right)+m_{33}^j\left(Z_i - Z^j\right)} \qquad \textbf{[2.2a]}$$

$$y_i^j = -f\frac{m_{21}^j\left(X_i - X^j\right)+m_{22}^j\left(Y_i - Y^j\right)+m_{23}^j\left(Z_i - Z^j\right)}{m_{31}^j\left(X_i - X^j\right)+m_{32}^j\left(Y_i - Y^j\right)+m_{33}^j\left(Z_i - Z^j\right)} \qquad \textbf{[2.2b]}$$

where:

m_{ab}^j is the rotation matrix element for image j and ab signifies a position in the rotation matrix

all other values take their previous definition

These equations form least squares observation equations and must be in a linear form before they are solved to give the unknown parameters. The collinearity equations can be linearised using Taylor's theorem [*Slama,1980*] and written as:

$$v_x = -\left[\begin{array}{l} f_x\left(x_a,\omega,\rho,\kappa,X_0,Y_0,Z_0,X_A,Y_A,Z_A\right)+\frac{\partial f_x}{\partial\omega}d\omega+\frac{\partial f_x}{\partial\rho}d\rho+\frac{\partial f_x}{\partial\kappa}d\kappa+ \\ \frac{\partial f_x}{\partial X_0}dX_0+\frac{\partial f_x}{\partial Y_0}dY_0+\frac{\partial f_x}{\partial Z_0}dZ_0+\frac{\partial f_x}{\partial X_A}dX_A+\frac{\partial f_x}{\partial Y_A}dY_A+\frac{\partial f_x}{\partial Z_A}dZ_A \end{array}\right] \Big/ \frac{\partial f_x}{\partial x_a} \qquad \textbf{[2.3a]}$$

$$v_y = -\left[\begin{array}{l} f_y\left(y_a,\omega,\rho,\kappa,X_0,Y_0,Z_0,X_A,Y_A,Z_A\right)+\frac{\partial f_y}{\partial\omega}d\omega+\frac{\partial f_y}{\partial\rho}d\rho+\frac{\partial f_y}{\partial\kappa}d\kappa+ \\ \frac{\partial f_y}{\partial X_0}dX_0+\frac{\partial f_y}{\partial Y_0}dY_0+\frac{\partial f_y}{\partial Z_0}dZ_0+\frac{\partial f_y}{\partial X_A}dX_A+\frac{\partial f_y}{\partial Y_A}dY_A+\frac{\partial f_y}{\partial Z_A}dZ_A \end{array}\right] \Big/ \frac{\partial f_y}{\partial y_a} \qquad \textbf{[2.3b]}$$

where:

v_x and v_y	are residual errors in the x and y measured image coordinates
$\frac{\partial f_x}{\partial \omega}$ and similar	are the partial derivative of the function with respect to an unknown parameter
$d\omega$ and similar	are a correction to the approximate value of the unknown parameter

The details of this linearising process have been documented in photogrammetric texts such as *Slama* [1980] and so are not be repeated here.

2.4.3 The Datum Problem

In a photogrammetric bundle adjustment using only image coordinates as measurements, the ground coordinates of the ground points are not estimable [*Cross and Cooper, 1988*]. To overcome this problem, which can be referred to as the datum problem, ground points coordinate observations are required.

The ground control used in photogrammetry has historically been coordinated by the traditional method of angles, distances and levels. The measurements themselves often form a least squares adjustment process where the final coordinates are the most likely coordinates based on the observations made. In medium and small scale mapping, these control coordinates can be held fixed in the bundle estimation because their accuracy is considered to be of a significantly higher order than that required of the work [*Cross and Cooper, 1988*]. However, in large scale photogrammetric work it may be more robust to introduce the ground control coordinates as weighted observation equations.

2.4.4 Ground Control Observation Equations

Ground control points are introduced into the bundle estimation as observations. Considering a ground point *a*, an observation equation can be written:

$$\begin{bmatrix} X_a \\ Y_a \\ Z_a \end{bmatrix} = \begin{bmatrix} \bar{X}_a \\ \bar{Y}_a \\ \bar{Z}_a \end{bmatrix} + \begin{bmatrix} v_x \\ v_y \\ v_z \end{bmatrix} \qquad [2.4]$$

where:

$\begin{bmatrix} X_a & Y_a & Z_a \end{bmatrix}^T$ are the ground coordinates of control point a

$\begin{bmatrix} \bar{X}_a & \bar{Y}_a & \bar{Z}_a \end{bmatrix}^T$ are the observed coordinates of control point a

$\begin{bmatrix} v_x & v_y & v_z \end{bmatrix}^T$ are the residuals of the control point a

The ground control observations equations are linearised by Taylor's theorem in a similar manner to §2.4.2.

2.4.5 The Computational Algorithm

The linearised observation equations form the linear model for *observation equations* whose general form is:

$$Ax = b + v \qquad [2.5]$$

where A is the design matrix of coefficients,

x is the vector of unknown parameters,

b is the right hand side vector, and

v is the vector of residuals.

In the simple case of a bundle estimation with image point observations and a network of ground control points, equation 2.5 can be written as:

$$\begin{bmatrix} A & B \\ 0 & I \end{bmatrix} \begin{bmatrix} \partial P \\ \partial G \end{bmatrix} = \begin{bmatrix} b_1 \\ b_2 \end{bmatrix} + \begin{bmatrix} v_1 \\ v_2 \end{bmatrix} \qquad [2.6]$$

where:

A and B	are design matrices containing the partial derivatives of the observed image coordinates with respect to the unknown position and orientation elements of the photographs, and the ground coordinates of the observed image points.
∂P and ∂G	are the corrections (§2.4.8) to be added to the approximate values of the position and orientation elements of the photographs, and the ground coordinates of the observed image points.
b_1 and b_2	are the relationship between the observed quantities and the computed quantities as given in the linear observation equations in the appropriate form.
v_1 and v_2	are the residuals associated with the observed image points and the ground control point coordinates respectively.
I	is the identity matrix.

It can be shown [*Cross, 1983*] that equation 2.5 can be developed to give the *normal equations*.

$$x = (A^T W A)^{-1} A^T W b = N^{-1} A^T W b \qquad [2.7]$$

where:

W is the weight matrix associated with the covariance matrix of the observations (§2.4.6)

all other values take their previous definition

The procedure for solving equation 2.7 to find the corrections to the unknown parameters, as applied in the software used in this research, is discussed later (§7.3.3). The solution notably involves an inversion of the normal equation matrix (N) which can be computationally intensive [*Mikhail, 1976*]. It is, however, possible to examine the structure of the normal equation matrix and utilise its properties to reduce some of the computational effort.

The form of the design matrix (A) produces a normal equation matrix which is *banded and bordered* (Figure 2.3). The non-zero elements of the matrix are represented by the black shapes, with the rest of the matrix consisting of zero elements.

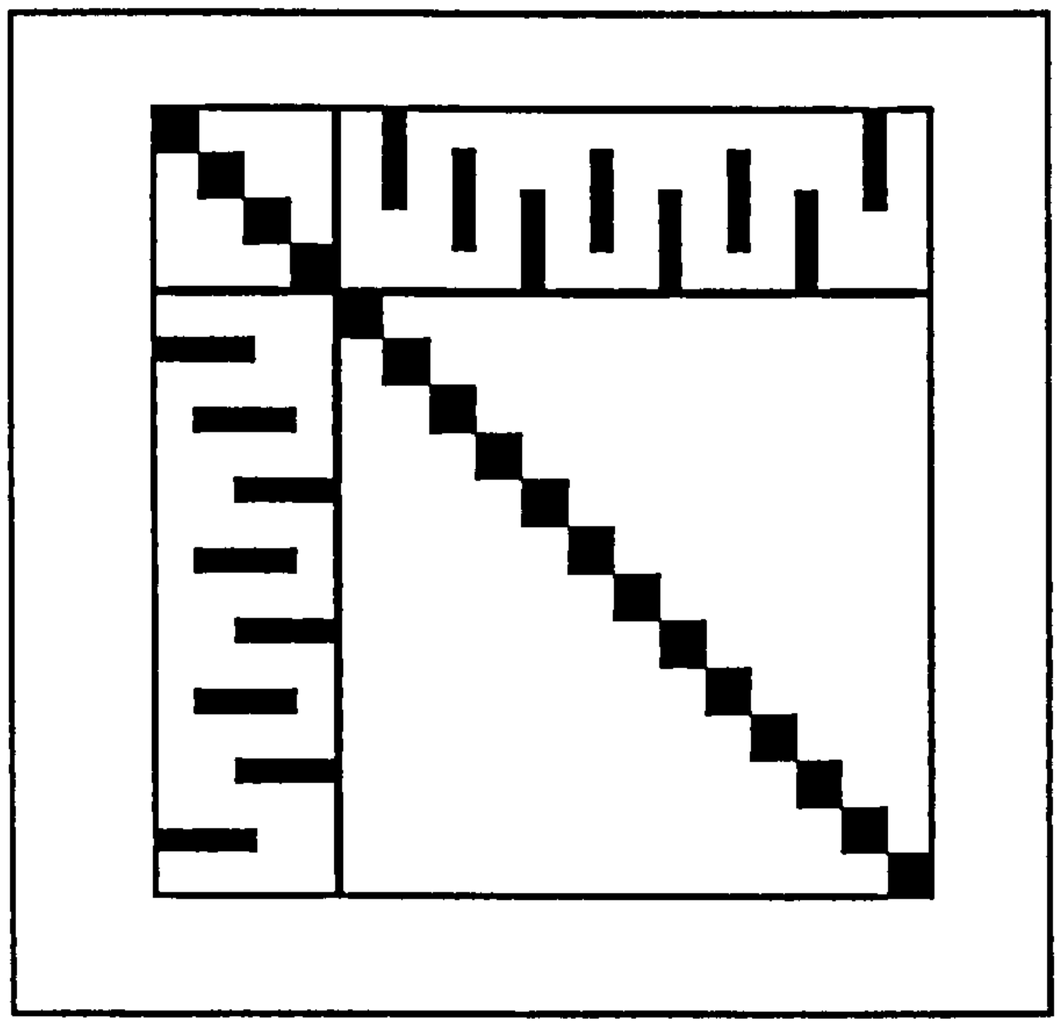

Figure 2.3 - The General Form of the Normal Equation Matrix

Matrices where only a small portion of the elements are non-zero are called *sparse matrices*. The exploitation of the properties of a sparse matrix can not only reduce the computational effort of calculating the inverse but also reduce

the computer memory which is required to store the matrix during a computation [*Mikhail, 1976*].

2.4.6 Weight Matrices

The weight matrix has been defined (§2.4.1) as the inverse of the *a priori* covariance matrix of the observations.

$$W = C_{ap}^{-1} \qquad [2.8]$$

The covariance matrix will be investigated further during the discussion on assessing the quality of a bundle estimation (§2.6). However, it is important to emphasise the use of this matrix at the beginning of the estimation process, such that the name *a priori* covariance matrix of the observations becomes clear.

The diagonal elements of the covariance matrix of the observations represent the variance of each of the observations. The variance of an observation is defined as *the square of the standard error* which is determined prior to the estimation (§2.4.7). The form of the matrix is shown below:

$$C_{ap} = \begin{bmatrix} \sigma_a^2 & 0 & 0 & 0 \\ 0 & \sigma_b^2 & 0 & 0 \\ 0 & 0 & \sigma_c^2 & 0 \\ 0 & 0 & 0 & \sigma_d^2 \end{bmatrix} \qquad [2.9]$$

A covariance matrix includes elements in the off-diagonal positions. Normally, observations are considered independent [*Cross, 1983*] and it is often too difficult to estimate their values. The matrix is simplified to have null values at these off-diagonal positions. The calculation of the *a priori* weight matrix for the bundle estimation from equation 2.9 is trivial:

$$W = C_{ap}^{-1}\begin{bmatrix} \sigma_a^{-2} & 0 & 0 & 0 \\ 0 & \sigma_b^{-2} & 0 & 0 \\ 0 & 0 & \sigma_c^{-2} & 0 \\ 0 & 0 & 0 & \sigma_d^{-2} \end{bmatrix} \qquad \textbf{[2.10]}$$

It can be seen from equations 2.8 and 2.10 that the weight of an observation is actually the reciprocal of the standard error squared.

2.4.7 Estimation of Observation Standard Error

To correctly estimate the *a priori* weight matrix in a bundle estimation, the observational standard error must be given. This procedure requires a personal assessment of the potential error in an observation or series of homogenous observations, often using some external indicators:

- Previous performance
- Comparison with a known value
- Repeated measurement

Correct estimation of standard errors is often viewed as a function of experience in analysing the equipment and environment used to obtain the observations. In the photogrammetric case of image point observations, photographic quality, instrument calibration results, object dimensions and observer ability can all affect the observational standard error between successive projects.

2.4.8 Termination of The Iterative Process

A set of approximate values of the unknown parameters is required for the least squares computation and the vector x of unknowns (§2.4.5) is actually corrections to these approximations. It is important to seek approximate

values which are close to the true values, since a non-linear problem may have several solutions.

The whole process of bundle estimation is actually iterative, with the approximate values of iteration n being updated by the corrections x to form the approximations for iteration $n+1$. The size of the corrections to the approximate values will converge to the point where the parameters and residuals change by insignificant amounts. It is the responsibility of the user to define the required tolerance which the corrections must satisfy before the iterative process is terminated. It has been found that appropriate termination criteria for the high accuracy requirements of this research are:

- Photograph rotation corrections $< 1 \times 10^{-5}$ radians
- Position corrections $< 1 \times 10^{-4}$ metres

A bundle estimation will usually converge to satisfy these termination criteria within 5 to 10 iterations.

2.5 Refining Measured Photo Coordinates

The simple collinearity equations (§2.4.2) assume that the image point coordinate measurements contain no systematic errors. This is not generally the case and the major error sources can summarised as:

- Analytical Plotter Errors
- Film and Platen Deformations
- Principal Point Displacement
- Lens Distortions
- Earth Curvature
- Atmospheric Refraction

2.5.1 Analytical Plotter Error

The photogrammetric measuring instrument is an analytical plotter from which the XY rectangular coordinate observations are measured or derived. The errors can occur from any of three defects:

- The measurement coordinate axes are not orthogonal
- The axes suffer from curvature and weave
- There exists a scale difference along the axes

Calibration of an analytical plotter is normally effected by the use of a precision glass plate with reseau crosses etched onto one surface. Measured coordinates can be compared with calibrated coordinates to establish parameters to model the error.

Modern plotters, specifically the Leica SD2000 Analytical Plotter stage plates, are manufactured to minimise any errors. In a typical calibration of the stage plates on the instrument installed at Nottingham, the measurement precision has been found to be approximately 2μm. The detailed calibration data is used internally by the Leica software to compensate the photograph coordinates during measurement.

2.5.2 Film And Platen Deformations

Correction of the errors which exist as a result of deformations in the film and platen is enabled by the transformation of the analytical plotter coordinate system into the fiducial coordinate system. This transformation compensates for the analytical plotter axes not being parallel to the fiducial axes and having different scales.

Modern photogrammetric cameras such as the Zeiss UMK 10/1318 universal camera have four fiducial marks which are exposed onto the film simultaneously with the image. These fiducial marks may be a cross or dot (figure 2.4) and are situated as side or corner fiducials. Their coordinates are obtained from the camera calibration certificate.

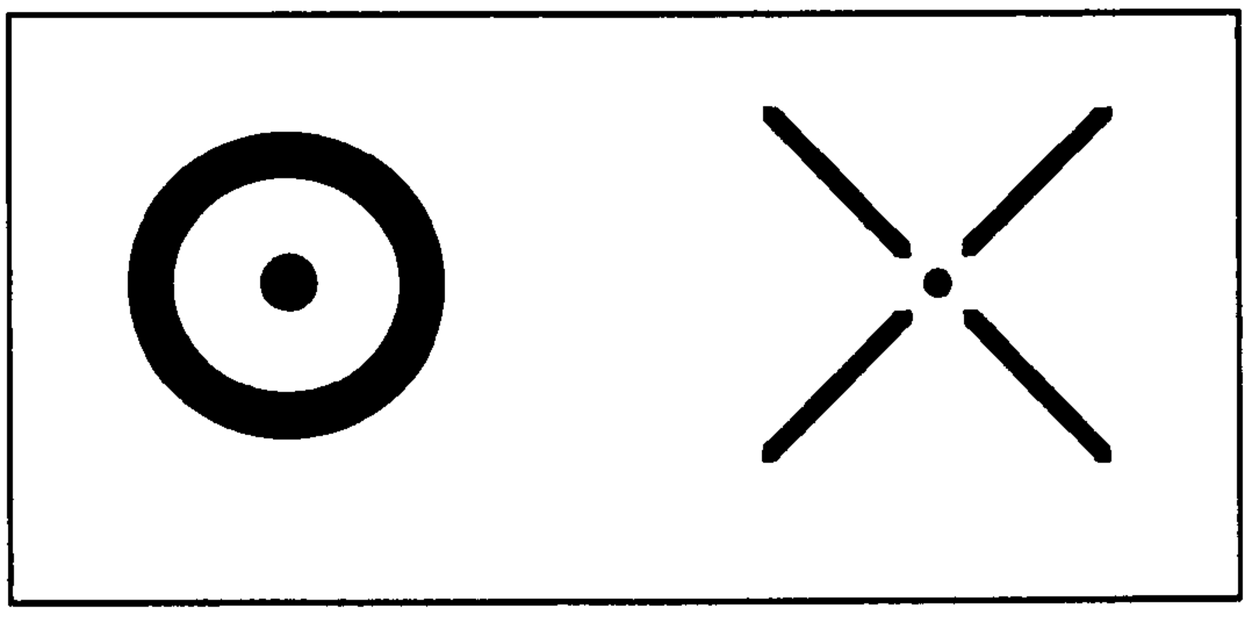

Figure 2.4 - The Fiducial Marks

An affine transformation [*Smith and Moore, 1998*] can be used with measurements made on the fiducials to transform the analytical plotter coordinates into true fiducial coordinates. The effects of film deformation and non-perpendicularity of the axes are accounted for during the process which also provides the scale, rotation and transformation required to gain measurements in the fiducial coordinate system.

2.5.3 Principal Point Displacement

The measured image points with coordinates in the fiducial coordinate system will have a coordinate system origin at the *indicated* principal point. This may not coincide with the *calibrated* principal point. A translation is required to correct for this error according to:

$$\begin{bmatrix} x_s \\ y_s \end{bmatrix} = \begin{bmatrix} x \\ y \end{bmatrix} - \begin{bmatrix} x_0 \\ y_0 \end{bmatrix} \qquad [2.11]$$

where:

x_s and y_s	are the coordinates of a point in the fiducial system with an origin at the *calibrated* principal point
x_0 and y_0	are the coordinates of the point in the fiducial system with an origin at the *indicated* principal point
x and y	are the offsets measured from the *indicated* principal point.

The coordinates x_0 and y_0 are determined from calibration and are included in the camera calibration certificate.

2.5.4 Lens Distortions

Distortions present in the lens can cause the rays of light to be deviated from their assumed paths, which displaces the imaged position and causes an error in the photograph measurements. Although several types of distortion exist, the radial distortion is the most effective [*Wolf, 1983*] and considered here.

It can be shown [*Moffitt, 1980*] that the radial lens distortion is represented by:

$$x_c = x\left(1-\frac{\delta_r}{r}\right) \qquad \textbf{[2.12a]}$$

$$y_c = y\left(1-\frac{\delta_r}{r}\right) \qquad \textbf{[2.12b]}$$

where δ_r is the radial distortion at a radial distance r from the principal point and can be represented by a polynomial of the form:

$$\delta_r = k_0 r + k_1 r^3 + k_2 r^5 + \cdots \qquad \textbf{[2.13]}$$

where k_x is a coefficient defining the shape of the polynomial curve.

2.5.5 Earth Curvature Correction

The ground coordinate system is conveniently taken to be a three dimensional XYZ cartesian coordinate system. However, this is contrary to surveying practice where heights are measured normal to the *equipotential surface* closest to the surface of the earth, and XY coordinates are measured on a plane coordinate system. It becomes necessary, particularly for high altitude photography, to correct for this coordinate system discrepancy.

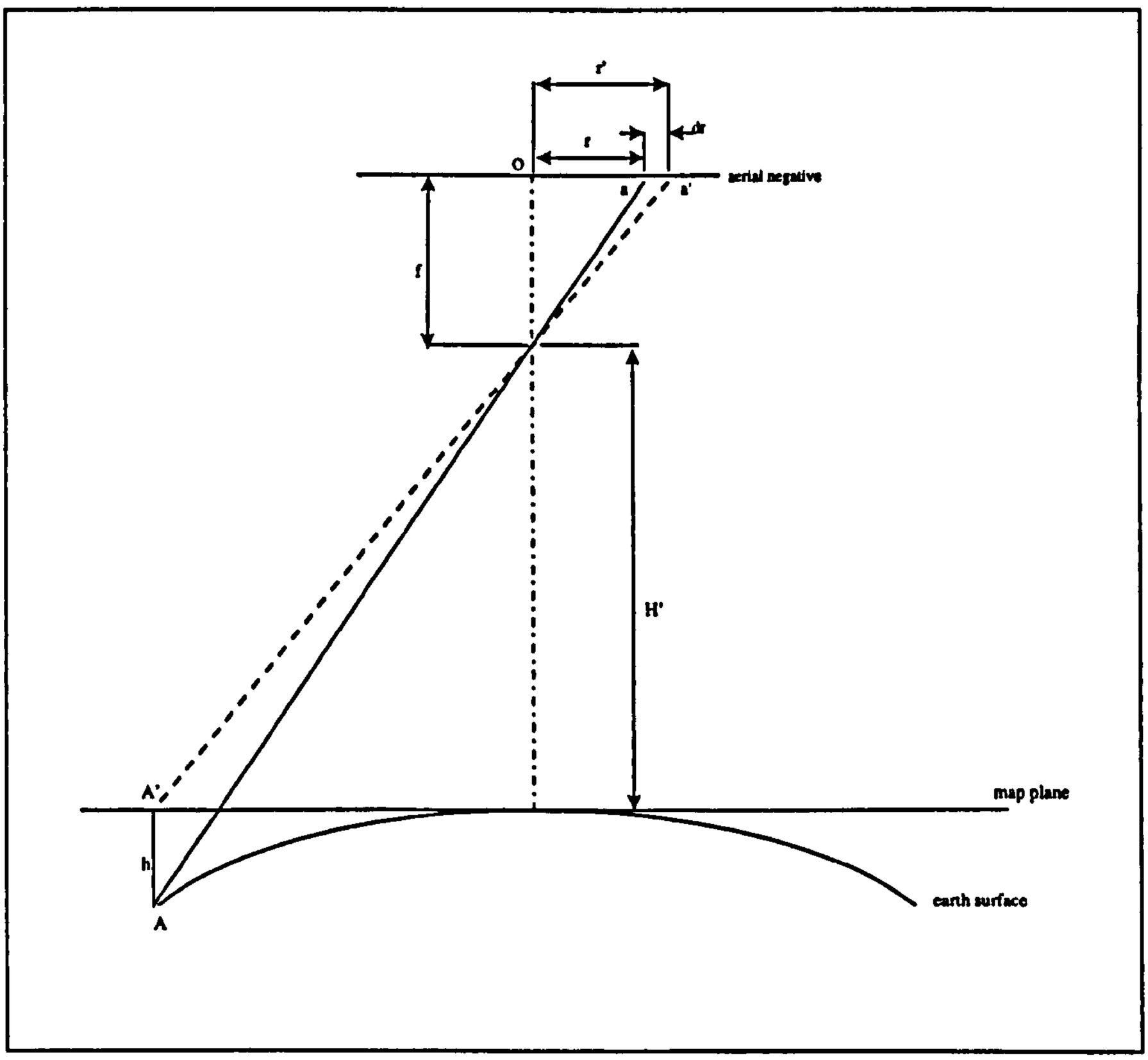

Figure 2.5 - Earth Curvature Correction

The coordinate system discrepancy, d_E, is given by [*Wolf, 1983*]:

$$d_E = \frac{r^3 H^{'}}{2f^2 R} \qquad \textbf{[2.14]}$$

where:

$H^{'}$ is the flying height above the average terrain elevation in metres

R is the radius of the earth in metres (6372200 metres)

r is the radial distance between the point and the principal point in millimetres

f is the camera principal distance in millimetres

The computed value for d_E is used to calculate the corrected image coordinates by replacing δ_r in equations 2.12a and 2.12b by $-d_E$.

The analytical plotter used in this research applies the earth curvature correction to the image coordinates at the time of measurement. The flying height for highway profiling can be as low as 75m which makes this error source negligible.

2.5.6 Atmospheric Refraction Correction

Light rays from the object field pass through the atmosphere, which has a decreasing density gradient with increased height. Such a ray of light which passes from a ground point to the camera lens will be refracted into a curved path away from the vertical. This deviation from a straight line is by a radial magnitude d_r, illustrated below:

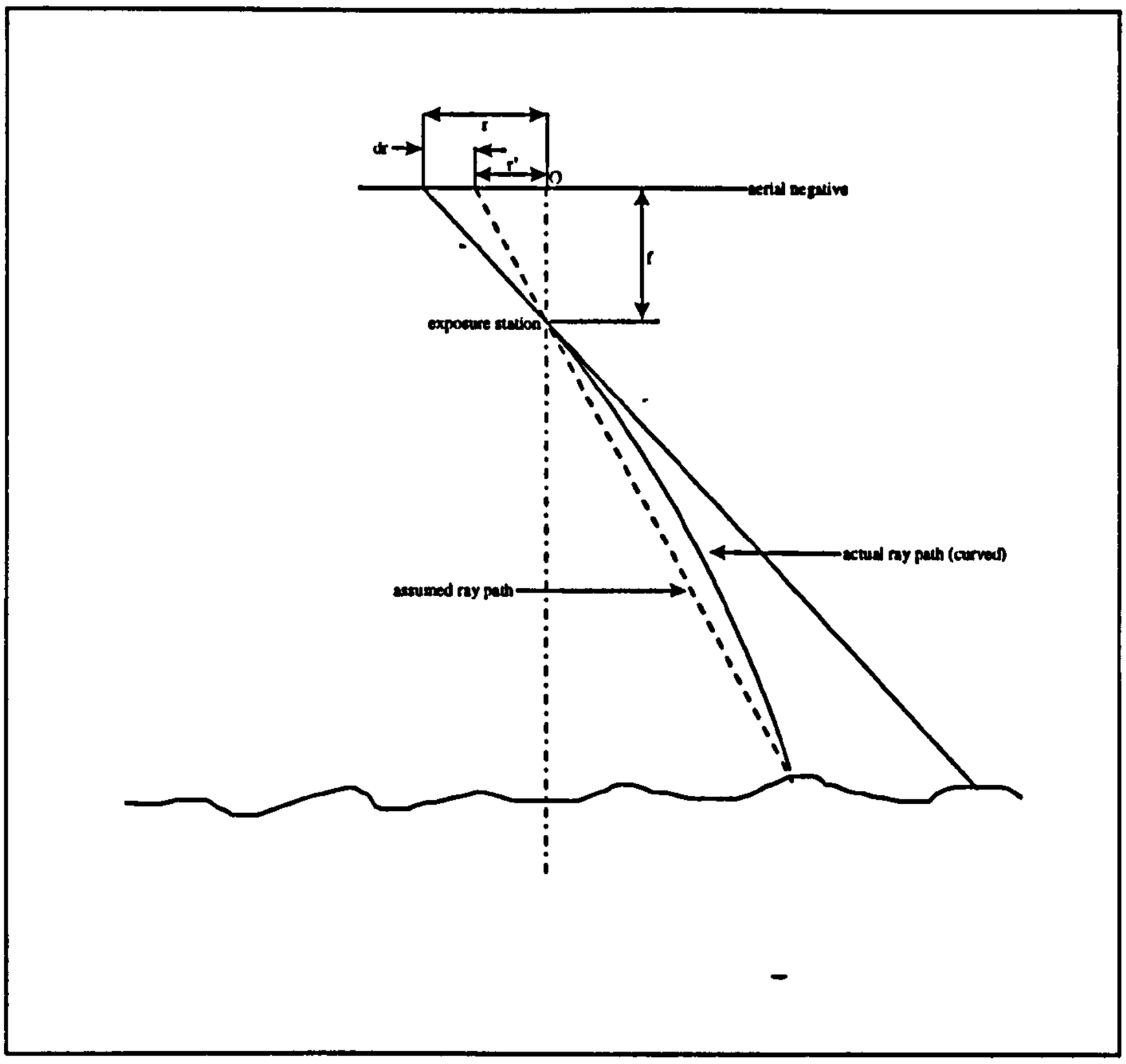

Figure 2.6 - Atmospheric Refraction Correction

To correct the measured photo coordinates for this effect, equation 2.15 enables the value of d_r to be calculated [*Moffitt, 1980*]:

$$d_r = K\left(r + \frac{r^3}{f^2}\right) \qquad \textbf{[2.15]}$$

where:

r is the radial distance of the point from the principal point

f is the camera principal distance

K is a variable which must be determined

The ARDC (Air Research and Development Command) of the US Air Force have derived a model to calculate the value of K [*Moffitt, 1980*]:

$$K = \left[\frac{2410H}{H^2 - 6H + 250} - \frac{2410h}{h_2 - 6h + 250}\left(\frac{h}{H}\right) \right] * 10^{-6} \qquad \textbf{[2.16]}$$

where:

H is the flying height above the datum in kilometres

h is the height of the object point above the datum in kilometres

The computed value for d_r is used to calculate the corrected image coordinates by replacing δ_r in equations 2.12a and 2.12b by d_r, in a similar manner to that described for earth curvature correction.

The analytical plotter used in this research applies the atmospheric refraction correction to the image coordinates at the time of measurement. The flying height for highway profiling can be as low as 75m which makes this error source negligible.

2.5.7 The Self-Calibrating Bundle Estimation

It is possible to take an alternative approach to refining the measured image coordinates by combining it into the estimation process. If the systematic errors present in the image point observations are to be recovered in this way, it becomes necessary to extend the finctional model. The concept of the self-calibrating estimation is to include additional parameters which model the systematic errors without the need for any purposely-made observations. It is discussed later in this chapter (§2.7.1).

2.6 Statistical Evaluation Of A Least Squares Solution

It has already been discussed that the reason for computing a bundle estimation is to find the position and orientation of the photographic exposures and the coordinates of all the observed ground points. Once the computation is completed, there are two questions to be asked:

- Are there any error sources which affected the estimation process?
- If not, how well were the unknown parameters evaluated?

The remaining sections of this chapter discuss the investigations which are necessary to address these two questions and achieve a reliable solution for the bundle estimation.

2.6.1 Accuracy And Precision

There are two useful indicators of the quality of an estimation process. These are *accuracy* and *precision*.

Accuracy may be defined as the deviation of a measured or estimated quantity from its true value. It is usually determined by comparing the estimate to the truth. The concept of truth in reference to position and orientation is however false, since it is never known. The definition of accuracy is refined to refer to the comparison of the estimate with a value determined by a measurement of a higher order of accuracy.

In this research, the truth for comparison against the ground point coordinate estimates is taken as the final coordinates from the ground survey. All the

ground points are targeted (including tie points) and these are coordinated by ground survey to allow an assessment of accuracy of the bundle estimation.

Precision is the agreement between repeated measurements or estimated quantities. It is usually determined by means of a standard deviation (σ). Specific measures of precision are discussed later in this chapter (§2.6.6).

2.6.2 Least Squares Residuals

Once the least squares computation process has been successfully terminated, it is possible to examine the residuals of the observations. These residuals are the amount by which an observation has been altered during the computation. Recalling equation 2.5, we can write the vector of residuals (v) as:

$$v = Ax - b \qquad \textbf{[2.17]}$$

2.6.3 The *A Posteriori* Unit Variance

The *a posteriori* unit variance, denoted σ_0^2 , is computed after the least squares computation. This is achieved from the following formula:

$$\sigma_0^2 = \frac{v^T W v}{n - m} \qquad \textbf{[2.18]}$$

where:

n is the number of observations,

m is the number of unknowns, and

v, W are defined in equations 2.5 and 2.7 respectively

It can be shown [*Cross, 1983*] that if this *a posteriori* unit variance σ_0^2 is significantly different from unity then the variances of the observations have been incorrectly estimated. This assumes that there are no gross errors present in the measurements and that the functional model is correct [*Cross, 1982*].

Cross [1983] illustrates that when the unit·variance is significantly different from unity, the observation variances have been underestimated by a factor of $1/\sigma^2$. This assumes that the observations in the least squares estimation are homogenous. In an estimation which uses heterogenous groups of observations, careful consideration should be given to the possible effect on the other observations when the variances of one group are poorly estimated.

2.6.4 Covariance Analysis

It is possible to investigate the precision of a bundle estimation. This is most conveniently enabled [*Cross, 1983*] by the derivation of the covariance matrices from the least squares process. There are, in fact, three covariance matrices which can be derived:

- Covariance matrix of the observations, C_l
- Covariance matrix of the parameters, C_x
- Covariance matrix of the residuals, C_v

The significance and derivation of the *a priori* covariance matrix of the observations has already been introduced (§2.4.6). However, a distinction should be noted between the values which are derived for the *a priori* matrix discussed and those which are derived from the actual least squares process. These matrices are the *a posteriori* matrices and hold important information about the quality of the bundle estimation.

It can be shown [*Cross, 1983*] that the definition of C_l, the covariance matrix of the estimated observed quantities is given as:

$$C_l = A\left(A^T W A\right)^{-1} A^T \qquad \textbf{[2.19]}$$

Similar expressions can be derived for C_x, the covariance matrix of the parameters and C_v, the covariance matrix of the residuals:

$$C_x = \left(A^T W A\right)^{-1} \qquad \textbf{[2.20]}$$

$$C_v = W^{-1} - A\left(A^T W A\right)^{-1} A^T \qquad \textbf{[2.21]}$$

where:

A is the matrix of the observations

W is the weight matrix

The most important covariance matrix in surveying and geodesy is C_x, as it holds information on the precision of the determined parameters. The matrix C_v is often used in statistical testing. C_l is seldom used because the greater interest is in the parameters.

2.6.5 Measures of Precision

The diagonal elements of the covariance matrix of the parameters, C_x, can yield a direct measure of precision for each determined parameter. In the case of a conventional bundle estimation where photograph positions and orientations and ground control point coordinates are to be determined, the square root of the relevant diagonal element yields the standard deviation of that parameter. It is therefore a simple matter to quote the parameter with this assessment of how well it has been determined.

It is sometimes valid to further simplify the measures of precision for a series of homogeneous observations. This can be the case when many sets of parameters must be compared for relative precision. A popular measure is the simple average and is the preferred single measure of precision because of the ease of calculation [*Cross, 1983*].

Although single measures of precision are effective in comparing many datasets, they hold limited information. A more detailed consideration of the parameter standard errors is most profitable in comparing datasets.

2.7 Error Analysis

Once the computation process has been successfully terminated, it is important to examine the results for signs of errors in either the observations or the observational model. Statistical testing enables statements to be made on the probability of a particular event occuring. Three types of error may be present in the estimation process:

- Gross errors
- Systematic errors
- Random errors

It is important to give careful consideration to the effective detection and correction of these errors in the observations. The following sub-sections discuss some of the techniques and tests that may be employed.

2.7.1 Systematic Errors And The Self-Calibrating Bundle Estimation

A systematic error can be seen to have a cumulative or constant effect [*Ibrahim, 1995*]. It is sometimes possible to formulate an analytical expression to describe the effect and correct it accordingly.

The most fundamental consideration of systematic errors is seen in the manufacture of photogrammetric cameras. There are known discrepancies between the collinearity condition which describes the path of a light ray from object point to image point, and the physical reality [*Granshaw, 1980*]. These camera lens distortions (§2.5.4) are *calibrated* at a regular interval and described in the *camera calibration certificate.* It is essential that all photogrammetric cameras possess a current certificate so that these distortions can be compensated in the stereoplotter.

It has been noted [*Granshaw, 1980*] that the *a priori* compensation of systematic errors in the photogrammetric camera is not fully effective. Residual errors still exist and are propagated into the bundle estimation process. The most robust method for treatment of systematic errors in a bundle estimation has been proved to be the technique of self calibration, where additional parameters are included in the fundamental model (§2.4.2) to model any residual errors.

Use of this enhancement to the basic bundle estimation model has been studied by many prominent researchers such as *Grün* [1982] and *Jacobsen* [1982]. Further detail on this technique is not included herein because it was not possible to explore the effects during the research. However, it should be noted that, although parameters can be introduced to model many different systematic effects, it can be detrimental to the estimation process if those parameters are poorly selected.

2.7.2 Random Errors And The Normal Distribution

A random error is caused by either the inability to make an exact measurement or by some other uncontrollable variation [*Slama, 1980*]. Random errors will always be present in a set of measurements, in this case a series of image point observations, and cannot be removed by modifying the functional model as with the systematic error.

Since random errors will always exist in a series of photogrammetric observations, some test should be applied to ensure that the errors do not adversely affect the estimation process. Statistical testing requires some knowledge of the *probability density function* (pdf) associated with the observations, which describes the probability that they will lie within a particular numerical range [*Cross, 1983*]. The most popular pdf associated with random errors is the normal distribution. The justification for the use of this particular distribution is found with the central limit theorem. This concludes that:

"....A random sample from any distribution....is approximately normal....." [*Cranshaw and Chambers, 1984*]

The use of the normal distribution as a basis for statistical testing in the bundle estimation propagates the common misconception [*Cross and Cooper, 1988*] that the least squares process can only be applied to observations which follow this distribution. It is in fact only true that the pdf of the observations must be symmetrical and continuous. However, since the normal distribution is a pre-requisite for the statistical testing, this point is only of minor interest.

2.7.3 Gross Error Detection

The gross error is sometimes referred to as a mistake, blunder or outlier, suggesting that it is caused by some incorrect measuring procedure. In the case of photogrammetric image point measurements in a stereoplotter, this is usually human error by the operator causing poor measurement of a point. The process of data manipulation or transfer throughout a photogrammetric project can also introduce incorrect data. *Hawkins* [1980] describes the outlier as "*an observation that deviates so much from other observations as to arouse suspicions that it was generated by another mechanism*". Gross errors seriously compromise the bundle estimation and demand attention so that they can be effectively removed from the observations.

From a statistical viewpoint, the gross error has been effectively described. *Ibrahim* [1995] states that "*when carrying out a statistical test for outliers, a so-called test statistic is computed. The pdf of the statistic is known and, if its value is so high that it can only be expected to be exceeded in (say) 1% of cases, it is assumed that the observation must have been generated by another process (ie. it is centred about a different mean) and is highlighted as a possible outlier (for probable rejection).*" This idea of calculating a test statistic for each observation and comparing this against some pre-determined tolerance is the basis for gross error detection. There are many methods available, broadly classified as:

- Pre-estimation detection techniques
- Post-estimation detection techniques

Full consideration will not be given herein to all the methods as they have not been applied in the software. Only an overview is provided to introduce some of the latest techniques, alongside those which have been implemented by the author. The reader is referred to *Ibrahim* [1995] and *El-Hakim* [1981] for detailed discussions on gross error detection.

(i) Repeated Measurement

The repeated measurement of an observed quantity is employed as a pre-estimation detection technique. It is common practice in ground survey and photogrammetric image point measurement, to check the mean and standard deviation of a quantity which has been observed many times. It becomes possible to identify any quantities which may contain an outlier by simple inspection of these statistics. Personal judgement plays an important role in this technique, as it must be clear as to what deviation around the mean value should be expected.

An extension to this simple technique is described in *Cross* [1983] where the mean and standard deviation of the series of observations, $x_{1...n}$, are used to calculate a test statistic, r_i, according to:

$$r_i = \frac{(x_i - \bar{x})}{s} \qquad [2.22]$$

where:

x_i is the ith observation in the series

$\bar{x}$ is the mean of the series of observations

s is the standard deviation of the series of observations

To test if any of the observations are an outlier, it is necessary to propose a hypothesis (H_0) for testing.

H_0: x_i comes from a normal distribution with mean, $\bar{x}$, and standard deviation, s.

H_A: x_i comes from a normal distribution with mean, $\bar{x}$ + error, and standard deviation, s.

The test statistic is compared with the tabulated value from the normal distribution tables and the observation rejected if the tabulated value is smaller. This is in accordance with the alternate hypothesis, H_A, saying that the observation does not come from the normal distribution described by the calculated mean and standard deviation.

Another method, more suited to a small series of observations is discussed in *Cross* [1983] where the subject of error detection from repeated measurements is dealt with in detail.

(ii) Baarda Data Snooping

Baarda Data Snooping is a sophisticated method of post-estimation error detection. It has been implemented in many software programs such as *El-Hakim* [1984]. The description given here uses equations taken from both *Cross* [1983] and *Ibrahim* [1995] who derive the necessary quantities.

The technique assumes that only one gross error exists in the observations although, in practice, it is possible that several gross errors might exist. The possibility of simultaneous detection of multiple gross errors has been investigated but is beyond the scope of this research.

The Baarda test is repeated for each observation, explaining the data snooping reference. The test uses a test statistic which it can be shown [*Cross, 1983*] is given by:

$$w_i = \frac{\hat{v}_i}{\sigma_{\hat{v}_i}} \qquad [2.23]$$

where:

$\hat{v}_i$ is the residual of observation i

$\sigma_{\hat{v}_i}$ is the standard deviation of $\hat{v}_i$

To derive a criterion for identification of a gross error, a hypothesis must be formulated:

H_0: w_i comes from a normal distribution with mean, 0, and standard deviation, unity.

H_A: w_i comes from a normal distribution with a different mean and standard deviation.

The process of testing the hypothesis and testing for the presence of a gross error in the observations can be described by the following steps:

- Calculate the least squares residual for each observation
- Calculate the standard deviation of the residual from the covariance matrix of the residuals (§2.6.4)
- Compute the test statistic according to equation 2.23
- Select a level of significance (eg. 95%, 99% and 99.5% are typical) and determine the critical value, w_c, from normal distribution tables
- If $w_i \geq w_c$, then the observation should be flagged as suspicious and a candidate for rejection.

Cross [1983] comments on the suitability of the Baarda technique. He says that "*it is strictly only correct when each value of* $\sigma_{\hat{v}_i}$ *truly reflects the population from which it is drawn. This will only be the case when we are sure that we are using the correct ..(weight matrix)...*". An alternative approach to testing for gross errors is the Tau test.

(iii) The Tau Test

The Tau test is another sophisticated method of gross error detection and is employed as a post-estimation technique. It takes its name from the alternative pdf, the τ-distribution, which it uses to assess the test statistic:

$$\tau_i = \frac{\hat{v}_i}{\sigma_{\hat{v}_i}} \qquad [2.24]$$

where:

$\hat{v}_i$ is the residual of observation i

$\sigma_{\hat{v}_i}$ is the standard deviation of $\hat{v}_i$

The important condition for testing against the τ-distribution is that the unit variance is unity. The implementation of the tau test is described by *Sleeman* [1992] and also by *Ibrahim* [1995]. The technique proceeds as follows:

- Calculate the least squares residual for each observation
- Calculate the standard deviation of the residual from the covariance matrix of the residuals (§2.6.4)
- Calculate the square root of the *a posteriori* unit variance (§2.6.3)
- Compute the test statistic according to equation 2.24
- Select a level of significance (eg. 95%, 99% and 99.5% are typical) and determine the critical value, τ_c, from tables
- If $\tau_i \geq \tau_c$, then the observation should be flagged as suspicious and a candidate for rejection.

2.8 Summary

Aerial triangulation allows a large number of ground points and exposure stations to be coordinated from a relatively small framework of surveyed ground points. There are many techniques but bundle estimation is the most recent and most appropriate for this research.

Bundle estimation is based on the principles of least squares. The functional model, which relates the observations to the unknown parameters, is solved by an iterative process to give the ground coordinates of measured image points and the orientation parameters of the photographs. The observations typically constitute image point measurements from an analytical plotter and the ground control coordinates from a prior ground survey.

There are several corrections which can be made to image point measurements to remove inherent errors. These systematic errors can also be removed by extending the functional model with additional unknown parameters.

Once the unknown parameters have been calculated, it is possible to statistically evaluate the results of the solution. Several techniques are available.

Chapter 3

Surveying and Navigation With GPS

3.1 Introduction

The NAVSTAR GPS (NAVigation Satellite Timing And Ranging Global Positioning System), more commonly referred to as *GPS*, is a space based radio navigation system. It was developed by the Joint Program Office (JPO) in the early 1970s, under the instruction of the United States Department of Defense (DoD), as a replacement for Transit, an earlier United States Navy positioning system [*Tsakiri, 1995*]. It was designed to provide a world wide, all-weather, passive and instantaneous three dimensional positioning service to the combined United States military community.

The Global Positioning System is introduced in section 3.2. Section 3.3 discusses the reference time frame, and the reference coordinate system is discussed in section 3.4. The satellite signals are detailed in section 3.5.

Section 3.6 discusses potential GPS error sources. GPS positioning in surveying is discussed in section 3.7 and GPS navigation techniques are discussed in section 3.8. A summary is given in section 3.9.

3.2 The Global Positioning System

The GPS system may be considered as composing of three segments, the Space Segment, the Control Segment and the User Segment.

3.2.1 The Space Segment

The Space Segment is the constellation of satellites orbiting the earth at a nominal altitude of 20200km. The initial plan was for a 24 satellite constellation, evenly distributed in 6 orbital planes at an equatorial inclination of 55° [*Leick,1995*]. The current constellation consists of 21 satellites and 3 active spares.

The first series of satellites were referred to as the Block I satellites and were prototypes to test the concept and performance of the system. In the late 1980s, the newer series of Block II satellites began their operational life, as a result of the experiences gained with the Block I satellites. The main difference between these two generations is the Block II satellites' ability to apply signal degradation (§3.6).

There have been two milestones in the history of GPS. Initial Operational Capability (IOC) was declared on 8 December 1993 when 24 GPS satellites were successfully operated simultaneously [*Leick, 1995*]. Several years of further development and satellite launches led to the declaration of Full Operational Capability (FOC) on 27 April 1995. Testing and development is continuing with the launch of the Block IIF (Follow-On) satellites.

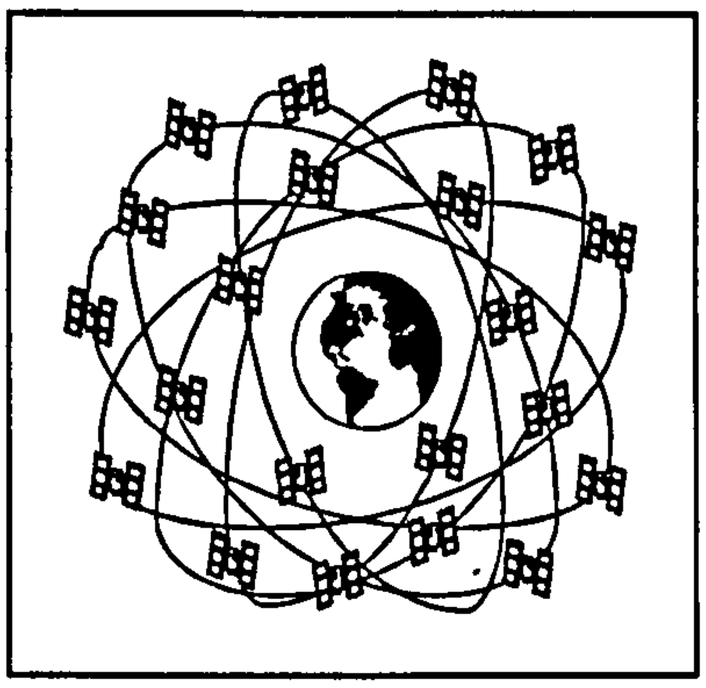

Figure 3.1 - Conceptual View of the GPS Satellite Constellation Above the Earth [*Beamson, 1995*]

Each satellite operates on its own time which is defined by an onboard atomic clock. All satellite transmissions (§3.5) are estimated from this timing mechanism.

3.2.2 The Control Segment

The Operational Control Segment (OCS) maintains and supports the GPS system and a tracking network. This tracking network is operated from 6 sites across the globe, including a Master Control Station (MCS) at Falcon Airforce Base in the USA [*Leick, 1995*]. The network enables effective tracking of every satellite for 90% of its orbit.

Tracking data is coordinated at the MCS and used to predict satellite orbits and clock errors (referred to as the *ephemeris*). This *broadcast ephemeris* is uploaded to the satellites every 24 hours.

3.2.3 The User Segment

The User Segment consists of the equipment which is required to receive the signals transmitted from the satellites. Since GPS is a passive positioning system, the equipment is commonly referred to as a *GPS Receiver.*

The characteristics of receivers vary throughout the field of surveying and navigation. The type of receiver used is particularly dependent on the required accuracy of the application. In high precision work, a dual frequency geodetic receiver is often used. This can access both the *carrier phases* as well as the *codes* of the signal (§3.5).

An incoming signal from a satellite will be received by the antenna of the GPS receiver system. The signal is then passed into the electronic components of the main receiver unit. The objective at this point is *signal acquisition* whereby an internally generated copy is compared with the incoming signal to find a maximum correlation. Once this is achieved the receiver engages in *signal tracking*. A brief discussion of code acquisition can be found in §3.5. For further details of receiver correlation techniques the reader is referred to *Tsakiri* [1995].

3.3 GPS Reference Time

The principles of GPS positioning are dependent on precise time measurements. Therefore, it is essential to have a precise time frame to which the different clocks can be referenced.

GPS time is a uniform atomic time synchronised by the Control Segment. Two caesium beam frequency standards and three hydrogen maser standards are maintained by the MCS and ultimately referenced to the Universal Coordinated Time (UTC) standard at the US Naval Observatory in

Washington DC. The expected offset between GPS time and UTC does not deviate by more than 1 millisecond. However, there is a requirement to adjust the time offset periodically by a leap second. This is because the leap seconds cannot be incorporated into GPS without interfering with the positioning requirements of the system. Since the official start of GPS operations (6 January 1980), there have been 10 leap seconds introduced to the GPS-UTC offset.

The stability in the GPS time frame which is introduced by the use of highly accurate and expensive clocks in the Space Segment is an important advantage of the GPS design. This allows the user to employ a crude quartz crystal clock in the receiver without any degredation in performance.

3.4 GPS Reference System (WGS84)

The orbits of the GPS satellites and the station coordinates are computed in the World Geodetic System of 1984 (WGS84). This global coordinate reference system is earth fixed and earth centred with an implied origin at the centre of mass of the earth [*Hubbard, 1995*]. The need for this system arose with the advent of satellite-based positioning and the difficulty of relating stations coordinated in different regional datums. WGS84 developed from the original US DoD World Geodetic Systems of 1966 (WGS66) and 1972 (WGS72) and is defined by over 1500 ground points [*Tsakiri, 1995*].

3.5 The Signal Structure

The NAVSTAR GPS is termed a one way ranging system, meaning that signals are transmitted from the satellites to the receivers. This passive positioning system enables there to be an unlimited number of users, and it also retains ultimate control with the United States military.

The need for precise time synchronisation has been mentioned (§3.3). The precise timing frequencies on board each satellite form the fundamental frequency from which all the base frequencies are derived. This fundamental frequency emitted by the satellite oscillators is 10.23 MHz [*Hubbard, 1995*].

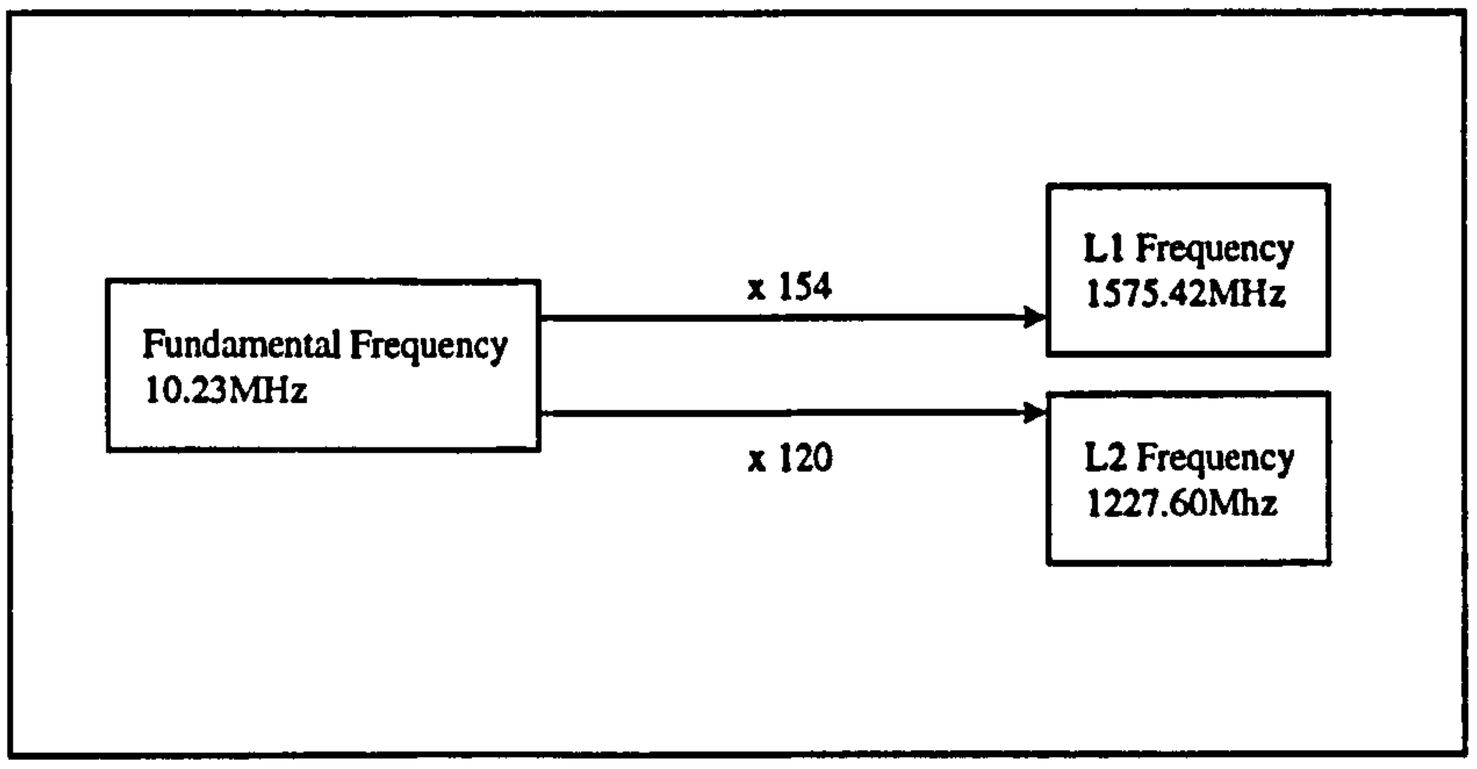

Figure 3.2 - The GPS Signal Carrier Frequencies

The GPS system was designed with two transmission or carrier frequencies upon which information is modulated. The L1 frequency transmits at 1575.42MHz and the L2 frequency transmits at 1227.60MHz. Figure 3.2 shows that these are both multiples of the fundamental frequency.

Since each satellite is synchronised to use the same fundamental and carrier frequencies, there must be a unique identification to allow the receiver to identify a unit within the constellation. Codes termed Pseudo Random Noise (PRN) are modulated on to the carrier frequencies and are unique to each satellite [*Leick, 1995*]. Three codes are currently in operational use, the Coarse Acquisition (C/A) code, the Precise Code (P) and the signal degradation code (W).

3.5.1 The Coarse Acquisition Code

The C/A code is only modulated on to one of the two carrier frequencies, the L1 frequency. It can be identified by a given PRN number, which is a common method of reference for the satellites. The code has a frequency of 1.023MHz which is utilised as a sequence of 1023 binary digits repeating every millisecond. This millisecond repeating nature of the code encourages a fast acquisition by the receiver.

Acquisition of the code by the receiver is by a correlation technique. The satellite code is received and compared with an internally generated code. Phase shifting (§3.7.1) of the generated code allows a signal harmony to be found and at this point the receiver is deemed to have *locked-on* to the signal.

3.5.2 The Precise Code

The P Code is modulated on to both the L1 and L2 frequencies and has a frequency of 10.23MHz, ten times faster than the C/A code. There is only one P code and this is 38 weeks long and reset at midnight every Saturday/Sunday. Each satellite transmits its own 7 day portion of the code as well as an identification contained in the Navigation Message (§3.5.3). This identification is the Hand Over Word (HOW) and informs the receiver of which P code portion is being transmitted.

Although acquisition of the P code is again effected by a signal correlation, this is often hindered by the US Military. National security policy dictates that the P code should be encrypted (by the W code) to form the Y code which cannot be decomposed by unauthorised users.

3.5.3 The Navigation Message

The Navigation Message is a data stream used to provide the user with position and status information for each satellite. It is transferred by superimposition on the L1 and L2 carrier frequencies. The information is provided with the data required to obtain an initial satellite position, repeating at a 30 second interval. The full *almanac* requires a 12.5 minute observation time to be transmitted to the user.

The message provides several important types of information. These include the system time, the Hand Over Word (HOW) for effective P code tracking, satellite clock and ionosphere correction parameters, satellite ephemerides and satellite health status.

3.5.4 Dilution of Precision

The precision of a GPS position solution is dependent on the geometry of the satellite constellation [*Bingley, 1993*]. If all the satellites are at a low elevation then the quality of the height position component may be poor. Conversely, if the satellites are at a high elevation, the quality of the plan position component may be poor. Optimum geometry constitutes satellites at both high and low elevations, evenly spaced around the horizon [*Hansen, 1996*].

The effect of this constellation can be quantified by one of several Dilution Of Precision (DOP) values:

- PDOP Positional DOP
- GDOP Geometric DOP
- VDOP Vertical DOP
- HDOP Horizontal DOP

It is generally seen that position solutions with a low DOP value are of a higher quality. The PDOP value, related to the three dimensional position (X, Y and Z axes), is used in this thesis to analyse the performance of the GPS-Photogrammetry system (§6.5.1). Further discussion of Dilution of Precision can be found in *Tsakiri* [1995].

3.6 GPS Error Sources

Gross, systematic and random error sources can affect the GPS derived position. Mostly, these errors are a function of the operating environment of the entire system, but some have been purposely introduced to maintain a higher instantaneous position accuracy for authorised users. A definitive consideration of error sources can be found in GPS texts such as *Leick* [1995]. A brief overview of the most prominent errors in GPS navigation is provided in this section.

3.6.1 Anti-Spoofing

During the design of GPS, the US DoD decided to implement two levels of user accuracy. The Precise Positioning Service (PPS) was designed with an instantaneous navigational accuracy of under 20 metres and was reserved for the military community. The Standard Positioning Service (SPS) was designed as a suitable degradation of the PPS accuracy with a 100 metre horizontal and 156 metre vertical accuracy [*Hansen, 1996*].

To deny use of the PPS to unauthorised users, an error source known as *Anti-Spoofing* was implemented in the satellite signal. The P-code is encrypted to form the Y-Code which cannot be measured without a special code, the W-Code. The W-Code is only supplied to authorised users who can then use it to generate a Y-Code and consequently position to PPS levels.

The original intention was that Anti-Spoofing of the signal alone would be sufficient to significantly degrade the positional accuracy attainable by unauthorised users. However, the C/A code was actually capable of 30 metre accuracy, so the US DoD introduced a further satellite based error source known as *Selective Availability.*

3.6.2 Selective Availability

Selective Availability is a combination of two error sources, *epsilon* and *dither.* Epsilon is the process of altering a satellite's broadcast ephemeris which produces a gradual decay in its accuracy. Dither is the process of manipulating the satellite clock such that the clock offset from GPS system time varies in an unpredictable way. The implementation of Selective Availability was successful in limiting instantaneous (single point) positioning accuracy to the intended SPS level. Its effects can be overcome by authorised users who have access to the SA algorithms.

3.6.3 Atmospheric Errors

The GPS signals are affected by the earth's atmosphere as they propagate to the user's antenna. For GPS positioning, the atmosphere can be considered to be composed of two strata; the ionosphere and the troposphere.

The ionosphere can be considered to extend from about 50km to 1000km above the earth's surface and consists of both charged particles and free electrons which are created by ultra-violet and X-ray radiation from the sun. Ionospheric errors are frequency dependent because of the changing properties of this layer, further details of which can be found in *Dodson et al* [1993].

The effects of the ionosphere can be eliminated by simultaneous observation on both L1 and L2 frequencies [*Shardlow, 1994*]. If, however, the user is operating a single frequency receiver, then this ionospheric delay remains a large error source and must be modelled. Differencing techniques only eliminate the ionospheric effects on short baselines [*Tsakiri, 1995*].

The troposphere can be considered to extend from the earth's surface to the ionosphere. It affects equally both the measurement of GPS pseudoranges (§3.7.1) and signal phase (§3.7.2) and cannot be removed by dual frequency observations. Elimination of tropospheric delay is dependant on implementing a suitable model, unless the baselines are short, when differencing techniques are sufficient.

Tropospheric delay can be conveniently represented as *wet* and *dry* delay. The dry delay is a function of pressure and accounts for 90 percent of the total effect. The wet delay is a function of the partial water vapour pressure along the line of sight to the satellite. Adequate modelling of the tropospheric delay remains a difficult problem and the reader is referred to *Shardlow* [1994] for a more indepth discussion.

3.6.4 Multipath

A GPS signal may not travel directly between the satellite antenna and the user's antenna. It is common for it to be reflected off one or more objects before it reaches the user [*Shardlow, 1990*]. Multipath errors occur when both a reflected and a direct (true) signal arrive at the user's antenna. The resulting interference at the antenna causes a positional error at the station [*Hansen, 1996*].

Multipath errors are systematic and are predominantly caused by the station environment. This environment will only be clean (multipath free) if there are no reflective surfaces around the antenna. Longer observation periods can also

be employed to average out the effects of multipath on the position determined [*Shardlow, 1990*]. Multipath averaging is only useful for static positioning

In kinematic positioning, it is not possible to utilise the aforementioned techniques because of the dynamic environment. Instead, it may be possible to use special antenna or receiver technology. . Multipath rejection is the reason for antennas being manufactured with a ground plane attached. Some antennae, such as those with the special choke-ring design are affected less by multipath.

GPS receiver technology is also a method for multipath error reduction [*Hansen, 1996*]. Mathematical analysis can be performed on an incoming signal to remove frequencies within the range of expected multipath frequency. Most prominent at the time of writing is the Multipath Elimination Technology [*NovAtel, 1995*] implemented by the NovAtel Corp.

Attempts have also been made to develop site specific multipath models. The principle of this approach is that errors can be filtered by applying a model which describes the error magnitude at any azimuth. Further details of this approach can be found in *Hardwick and Liu* [1995].

3.6.5 GPS Receiver Technology

The continued technological developments in receiver design have successfully reduced the error sources in the user segment of the GPS system. Both the GPS antenna and the GPS receiver can be considered in the reduction of possible error sources.

Antenna design has already been introduced in the discussion of multipath. The ground plane is a common method of reducing this reflection of the GPS signal. Special antenna designs and multipath absorbing materials have also been employed.

GPS receivers are affected by two error sources, namely measurement noise and internal clock errors [*Hansen, 1996*]. The measurement noise relates to the precision by which a receiver can measure a satellite signal. Improved *correlation* techniques have increased this measurement precision in modern receivers [*Roberts, 1997*]. Meanwhile, the GPS receiver clock is an inexpensive quartz crystal clock by comparison to the atomic clocks found in the space segment (§3.2.1). When relative positioning (§3.7.4), the receiver clock error is eliminated by the positioning differencing algorithms. In stand-alone positioning, the receiver clock must be estimated as an unknown, requiring extra satellite observations (§3.7.3).

The most recent notable development in GPS receiver technology is the proprietary algorithm which can be utilised to overcome the encryption of the P-code (§3.5.3). The first commercially available system is called *Z-tracking* and is available on receivers manufactured by Ashtech, Inc. [*Roberts, 1997*].

3.7 GPS Positioning for Surveying

Since the initial conception of GPS, it has grown to be a major measurement and positioning tool in many applications of surveying. The measurement strategy may employ either the *pseudo-range* observable or the *carrier phase* observable, depending on the required accuracy of the final position. In this section, the most pertinent techniques of GPS positioning *for this research* will be introduced. A fuller treatment may be found in *Leick* [1995].

3.7.1 The Pseudo-Range Observable

The GPS receiver is able to compare the incoming timing code from the satellite to a timing code which is generated internally. The two codes are out

of alignment (see figure 3.3) and this difference is representative of the time of travel between the satellite and the receiver. A range calculation can then be made by multiplying this time of travel by the speed of light.

The range measurement is termed a *pseudo*-range because there are errors which affect this observable, notably the offset between the time of the atomic clock in the satellite and the quartz clock in the receiver. The pseudo-range is the primary GPS observable and its measurement constitutes the two fundamental positioning services (§3.6.1).

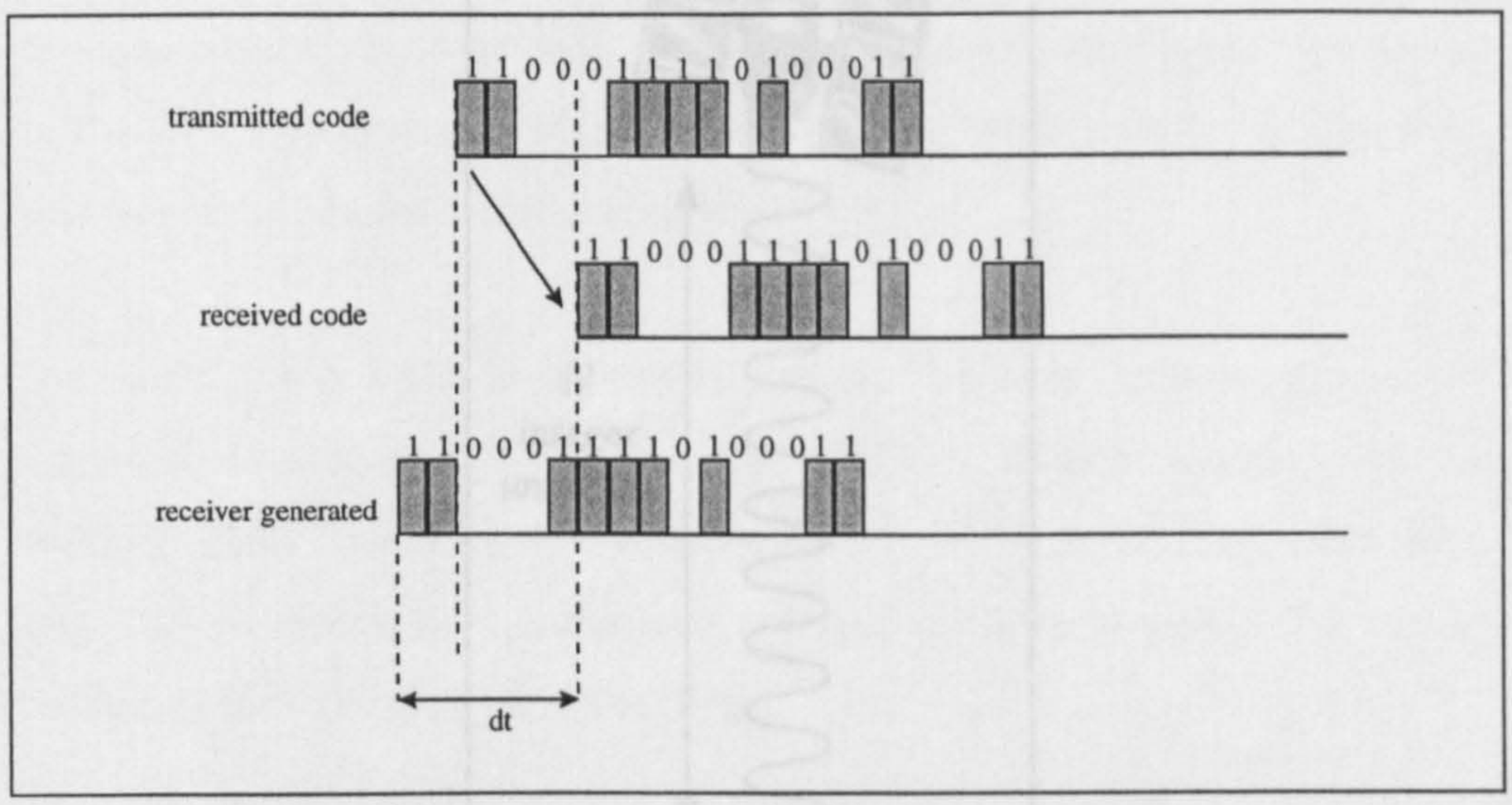

Figure 3.3 - Acquiring The C/A Code [*Leick, 1995*]

It will become clear that, for high accuracy survey and navigation, it is necessary to make additional observations on the incoming signal. This *carrier phase* observable is now discussed.

3.7.2 The Carrier Phase Observable

The two carrier signals have been introduced (§3.5.1) as enabling transfer of the C/A and P codes and the navigation message from satellite to receiver.

However, these signals can be modified to remove the aforementioned codes to produce two *clear* carrier frequencies.

A modern receiver is able to measure the phase of this carrier wave to a resolution of a few millimetres. Unfortunately, the signal is *ambiguous* because the receiver cannot measure the *integer* number of whole wavelengths from the satellite to the receiver (figure 3.4).

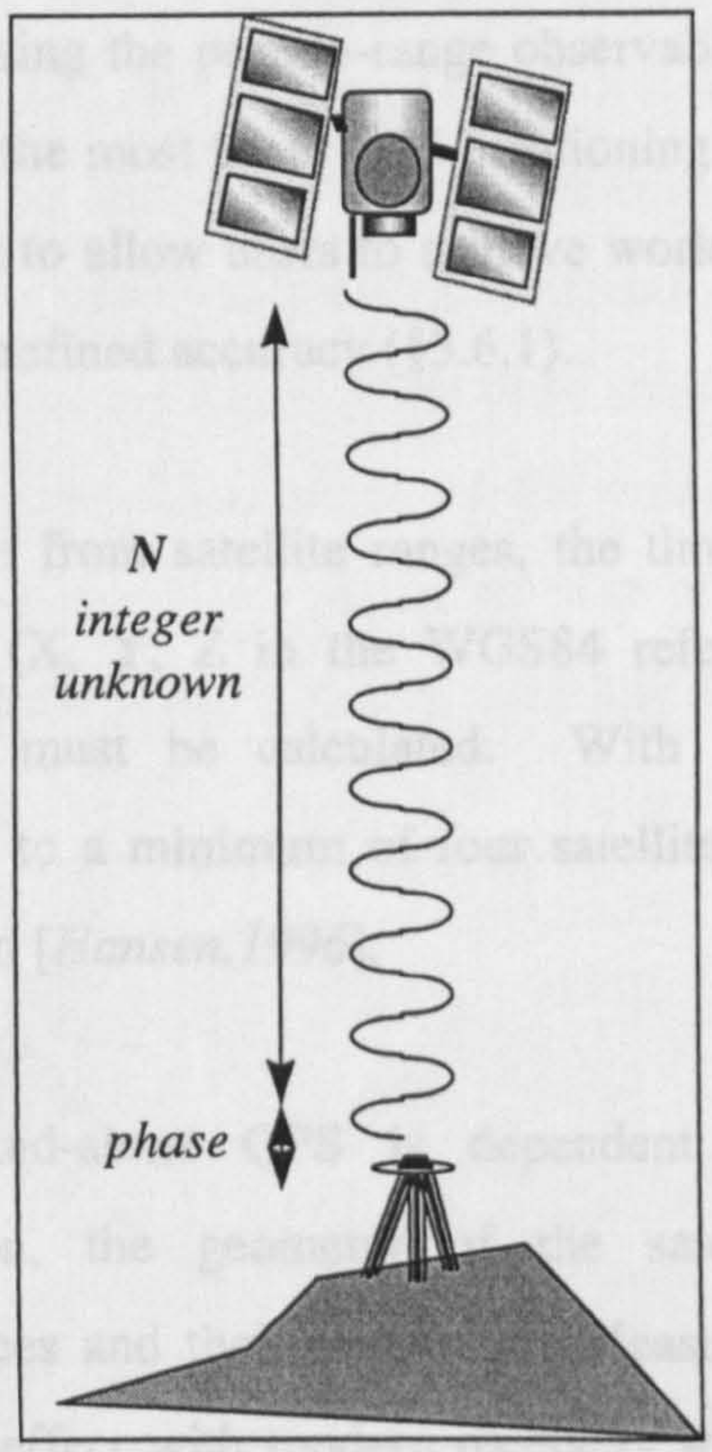

Figure 3.4 - The Carrier Phase Ambiguity [*IESSG, 1997*]

When the receiver begins tracking the signal, it selects an arbitrary integer value. As a result, all the carrier phase readings are relative to the *integer ambiguity* at the beginning of the current tracking period. This must be resolved in order to ultimately obtain an accurate position.

If the receiver is unable to continuously track the satellite because it *loses lock* on the signal, then another integer ambiguity is introduced when the satellite is

re-acquired and tracking begins again. This is the *cycle slip* problem [*Tsakiri, 1995*]. Although GPS positioning from the carrier phase observable enables a greater accuracy of survey or navigation, the existence of *cycle slips* in the data set presents a challenge to the positioning algorithms employed in GPS data processing software.

3.7.3 Stand-Alone GPS Positioning

Absolute positioning using the pseudo-range observable, hereafter referred to as stand-alone GPS, is the most basic GPS positioning technique. The design of the GPS system was to allow users to achieve world-wide navigation from this technique to a pre-defined accuracy (§3.6.1).

To calculate a position from satellite ranges, the three unknown geocentric Cartesian coordinates (X, Y, Z in the WGS84 reference system) and the receiver clock offset must be calculated. With these four unknowns, observations are made to a minimum of four satellites to enable the user to *trilaterate* their position [*Hansen,1996*].

The accuracy of stand-alone GPS is dependent on the pseudo-range measurement precision, the geometry of the satellites considered and systematic errors sources and their treatment. Measurement resolution does not have a significant effect with modern receivers which are capable of one metre resolution. The most significant error is the Selective Availability (SA) induced systematic errors (§3.6.2). A non-military user can expect a stand-alone accuracy at the 100 metre level [*Leick, 1995*].

3.7.4 Static GPS Surveying

Many survey applications require positional accuracies at the decimetre level and this cannot be acheived using the pseudo-range observable. Instead, the carrier phase GPS observable must be employed.

Static GPS surveying is almost always a relative positioning technique, where concurrent observations are made from the unknown point and a point of high accuracy with known WGS84 coordinates (which are fixed or highly constrained). A conceptual connection or *baseline* is initiated between the two points in the processing software. It is most common to use the *double difference carrier phase observable* which combines the observations at both stations to reduce and remove many of the error sources which contaminate a stand-alone GPS solution. Calculation of the coordinates of the unknown point requires a long observation period as it is necessary for the satellite constellation to change sufficiently to gain a reliable solution.

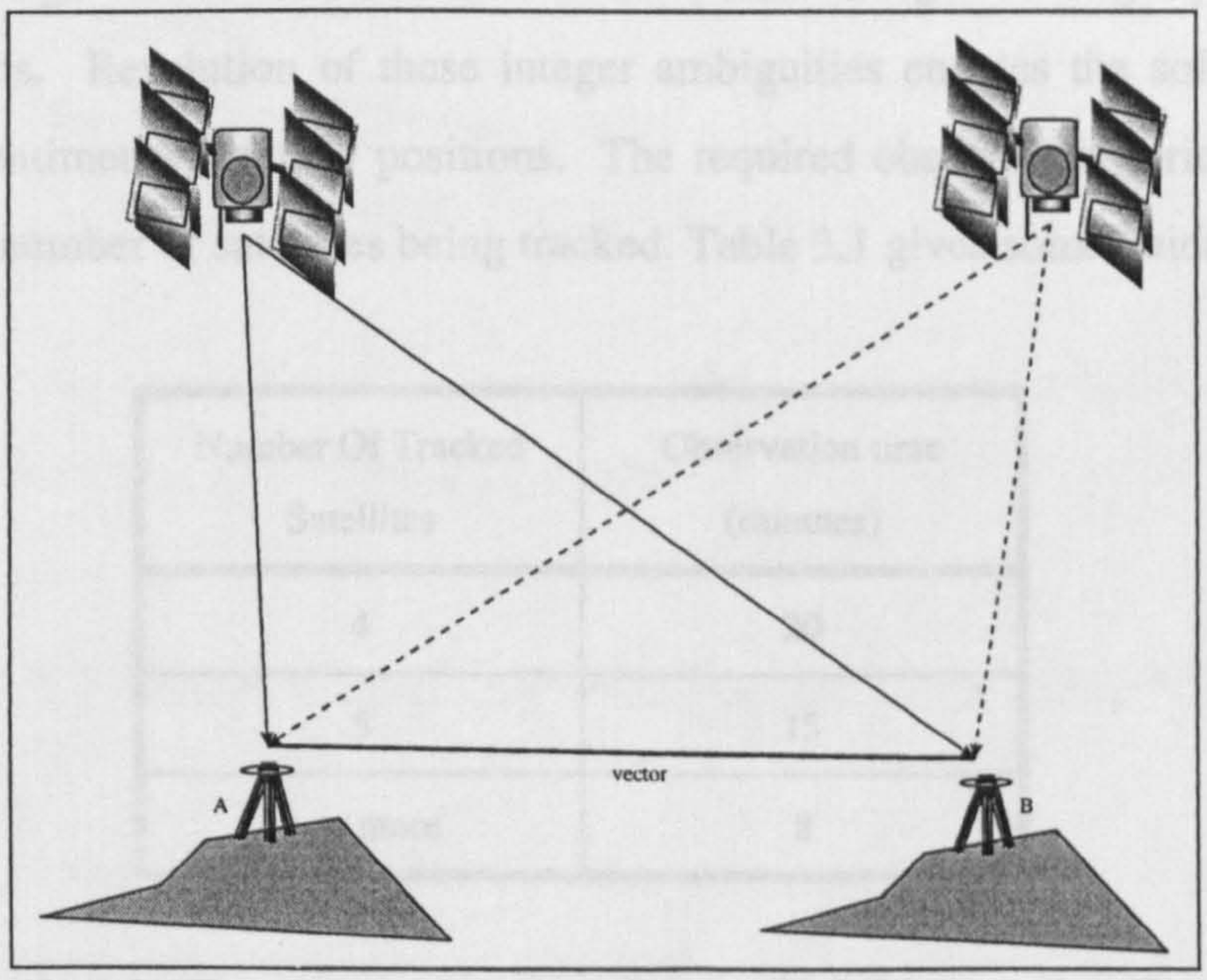

Figure 3.5 - Relative GPS Positioning

When centimetre level accuracy is required, a typical static survey session lasts between 30 minutes and 1 hour (depending on the baseline length), although this can be extended to many hours or even multiple sessions to derive very high accuracy point coordinates. A static baseline can achieve coordinate determination accuracy to 1cm ±1ppm [*Trimble Navigation, 1992*].

3.7.5 Fast-Static GPS Surveying

There is an obvious productivity overhead in static GPS surveying with the necessary long observation periods. Fast-Static GPS, also referred to as *Rapid-Static GPS*, reduces the observation time for short baselines (under approximately 20 kilometres).

The algorithms for Fast-Static GPS have been implemented in many commercial packages, including the Trimble WAVE and Ashtech PNAV softwares. They employ a combination of dual frequency observations, pseudo-range observations and carrier phase integer ambiguity search algorithms. Resolution of these integer ambiguities enables the software to derive centimetre accuracy positions. The required observation period varies with the number of satellites being tracked. Table 3.1 gives some guidance.

Number Of Tracked Satellites	Observation time (minutes)
4	20
5	15
6 or more	8

Table 3.1 - Recommended Fast-Static GPS Observation Times

[*Trimble Navigation, 1992*]

The accuracy of Fast-Static GPS is about 2cm ± 1ppm. Although static GPS enables considerably improved accuracies to be achieved (depending on baseline length, observation time and processing method), Fast-Static GPS is acceptable for tasks such as photogrammetric ground control measurement.

3.8 GPS Navigation Techniques

Stand-alone GPS positioning has been discussed as the most primitive form of GPS surveying and navigation. For greater accuracy, it becomes necessary to employ some form of relative positioning such as the two static techniques for coordinating a pre-defined number of survey points.

Kinematic GPS techniques are utilised in the case of GPS navigation or survey applications where the measuring body is in continuous motion. Considering a simplified overview of available techniques, they can be summarised as:

- Differential GPS
- Phase smoothed pseudo-ranges
- *On the Fly* ambiguity resolution

The following sections provide an introduction to each of these techniques and compare their relative positioning qualities.

3.8.1 Differential Pseudo-Range GPS (DGPS)

Differential Pseudo-Range GPS, hereafter referred to as DGPS, is a relative positioning technique whereby the user calculates a position relative to another point with known coordinates. It is similar in application to a *single difference pseudo-range solution* which combines the observations at both stations to reduce and remove the error sources which contaminate a stand-alone GPS

solution. Table 3.2 summarises those error sources in stand-alone GPS, and the possible improvement provided by DGPS.

The known point, or *reference station*, in DGPS has coordinates which have been determined to a very high degree of accuracy. When observations are subsequently made at this reference station (in conjunction with observations at an unknown point), the measured pseudo-range can be compared against a pseudo-range computed with knowledge of the station coordinates. A correction to the pseudo-range can be derived for each tracked satellite and then transmitted to the user via a radio link.

Error Source	Stand-Alone (metres)	Differential (metres)
Ephemeris	5 - 20	0 - 1
Satellite Clock	5 - 10	0
Ionosphere	15 - 20	2 - 3
Troposphere	3 - 4	1
Multipath	2	2
Receiver Noise	2	2
Selective Availability	50	0

Table 3.2 - Comparison of Error Magnitudes in Stand Alone and Differential GPS [*Moore, 1993*]

The correction to the user's measured pseudo-range combines the receiver clock, satellite orbit, atmospheric effect and selective availability errors. It is a robust positioning technique which provides 3 to 6 metre positional accuracy [*Moore, 1993*].

3.8.2 Phase Smoothed Pseudo-Ranges

Pseudo-range observations enable robust low accuracy positioning. In contrast, the use of carrier phase observations can enable high accuracy positioning when computed relative to a fixed point with accurately known coordinates. However, it is subject to periods where the receiver is unable to track the carrier signal, the so called *cycle slips*. A compromise solution is to combine both observables to achieve a robust positioning technique which is suitable for many kinematic applications.

Phase smoothing of pseudo-range measurements uses the change in range between successive carrier phase measurements to produce more accurate pseudo-range measurements. The technique is valid because the change in range for pseudo-ranges is approximately equal to the change of the carrier phase, which can be more precisely measured.

Further details of phase smoothing algorithms can be found in *Hansen* [1996].

3.8.3 *On the Fly* Ambiguity Resolution

On the Fly GPS is a technique where the ambiguities are resolved without an initial static observation period. The aims can be summarised [*Hansen, 1996*] as:

- Centimetric relative positioning
- No requirement to start at a point of known position
- No requirement to ever remain stationary to derive a point position
- Continued positioning after cycle slips
- Ability to implement the algorithms for real-time positioning
- High system integrity (protection against failure and incorrect positioning)

GPS systems based around *On the Fly* Ambiguity Resolution are the ultimate in precise positioning for navigation, placing no operational restrictions on the user and providing instantaneous positioning if used in a real-time mode of operation.

It has been discussed (§3.7.2) that it is necessary to resolve the integer ambiguity to its true integer value in order to utilise the carrier phase observable and derive high precision point positions. However, special search algorithms incorporating the principle of least squares can be used to estimate these integer ambiguities and so, because of inherent errors, these can only be considered as estimates of the true value. Without specialised enhancements to the basic least squares model, errors such as those caused by incorrect modelling of the atmosphere, which affects the satellite signals, would cause incorrect determination of the ambiguity unknowns.

The subject of ambiguity resolution algorithms is beyond the scope of this thesis. Further information can be found in the work of *Hansen* [1996] who developed the NOTF kinematic software after the founding work of *Walsh* [1994]. It is sufficient here to appreciate that the techniques employ complex relationships between the satellite signals to search for the most likely integer value of the satellite ambiguity, and use statistical testing to ensure that an incorrect integer does not propagate into the final position.

3.9 Summary

The Global Positioning System is a world wide, all-weather, passive and instantaneous three dimensional positioning service.

GPS can provide great flexibility for surveying or navigation. Point positions can be derived at the centimetre level when relative positioning is used.

The performance of GPS can be adversely affected by the operating environment. The reflection of GPS signals and the shielding of satellites to reduce the number of tracked satellites can hinder positional accuracies. Despite modern software algorithms, GPS users must be careful to miminise possible error sources during survey or navigation.

Chapter 4

The Integration Of GPS And Photogrammetry

4.1 Introduction

When GPS was emerging as a important tool in surveying and navigation, the photogrammetric community began to identify areas where this new technique could be utilised. These areas can be summarised [*Ackermann, 1986*]:

- Air survey flight navigation to ensure accurate positioning of exposures
- To provide camera orientation parameters for use in aerial triangulation
- To provide camera orientation parameters for direct orientation of photographs for analytical mapping procedures
- Calibration of new types of airborne sensors

Presently, the two most practically useful roles are the use of GPS for air survey flight navigation and for aerial triangulation.

Air survey flight navigation is an essential part of a photogrammetric flight because the flight lines over the object space must be pre-determined to gain suitable photographic coverage of the area. This planning was traditionally done manually from existing map sheets [*Burnside, 1985*], making it difficult to achieve the precise overlaps and effective aircraft guidance which contribute to the economic benefits of photogrammetric mapping [*Leica, 1996*]. The advent of GPS (and the use of small scale digital maps) enabled commercial companies to develop computer based navigation systems to complement their aerial camera systems and replace this manual planning process.

Carl Zeiss and Leica are the two most prominent aerial photogrammetric camera manufacturers. They have both developed GPS supported flight management systems to enhance the use of their cameras in photogrammetric mapping. They are called *T-Flight* and *Ascot* respectively and provide the aerial camera operator with tools ranging from flight mission planning to automated exposure control and export of GPS antenna positions for aerial triangulation. Near real-time display of aircraft position superimposed onto the flight plan is also provided on the operator console [*Becker and Barriere, 1993*].

The use of such extensive software and hardware solutions is not applicable in this research. This is because they are tightly coupled to large format aerial camera systems such as the Leica RC30 or the Zeiss LMK which can include advanced features such as gyro-stabilised camera mounts and forward motion compensation [*Leica, 1996*]. Fortunately, the photographic sorties for highway mapping are relatively short and the flight path is clearly defined by the centre-line of the highway. If any additional side strips are required then they can be guided by similar natural features [*Boardman, 1996*].

The main concern of this chapter, and this research, is the use of GPS as an aid to aerial triangulation. This means that GPS is used to determine the camera station coordinates for inclusion into the aerial triangulation process as additional observations [*Ackermann and Schade, 1993*]. Traditionally, these orientation elements have come from an indirect orientation method [*Ackermann, 1986*] because they are obtained by measurement of image points and ground control points.

If the camera station coordinates can be directly determined prior to the aerial triangulation process, then there could be a reduced requirement for the ground control points which enable an indirect determination of the same unknown orientation parameters (§2.4.2). Two distinct topics for discussion can be identified:

- The practical integration of GPS into the photogrammetric camera system to measure the perspective centre coordinates at each exposure station
- The mathematical techniques which enable these coordinate observations to be included into the aerial triangulation process

The physical integration of a GPS positioning system and a photogrammetric camera system is discussed in section 4.2. The extension of the conventional aerial triangulation mathematical model to include GPS observations is detailed in section 4.3 and a summary is given in section 4.4.

4.2 Physical Integration

The primary data source for modern photogrammetry is specialist photography taken with a calibrated camera. This camera is often mounted in a dedicated mount in the floor of a fixed wing aircraft [*Diete, 1990*]. The *photographic*

sortie is undertaken by trained personnel who follow careful procedures to ensure that the resultant photography is suitable for photogrammetric analysis [*Burnside, 1995*]. To integrate GPS data collection into this sortie is complex if the positional data is to be derived with the same reliability as the traditional photographic data. A number of fundamental points become apparent [*Hansen and Joy, 1995*]:

- Where is the GPS antenna to be mounted?
- How can the GPS antenna be related to the perspective centre of the camera?
- How can GPS positions be attributed to a photographic exposure time?
- What quality of GPS positioning data can be acquired, and how can this be processed?

To successfully integrate a GPS positioning system and a photogrammetric camera system, each of these points must be considered. The following sub-sections address these fundamental questions from a generalised standpoint. Specific discussions on the decisions made for this research can be found in chapter 6 which details the Nottingham GPS-Camera system.

4.2.1 GPS Antenna Location

The GPS antenna should be mounted on the aircraft in a position where it is free to receive the GPS signals with minimum obstruction [*Kinlyside, 1988*]. The effects of multipath and cycle slips have already be introduced (§3.6) and it is important to minimise their effects. Recommended locations [*Curry and Schuckman, 1993*] for the antenna are:

- On the fuselage directly over the camera
- On the tip of the vertical stabilising fin at the rear of the aircraft

Mounting the antenna on the fuselage has often been the favoured location since it is in close proximity to the camera [*Lucas and Mader, 1989*]. This can greatly simplify the calibration of the GPS antenna - camera offset vector (§4.2.2) and minimise the effects of the offset vector in small scale photography where a gyro-stabilised mount is utilised [*Ackermann, 1994*]. However, it may also be susceptible to multipath during the flight and prone to cycle slips as the aircraft turns and banks its wings between strips of photography. Fuselage mounting of GPS antennas involves modification to the fuselage according to the regulations of the Civil Aviation Authority (CAA) and the Federal Aviation Authority (FAA). This is an official approval process with can be as time consuming and costly as the initial installation of the photogrammetric camera mount since the aircraft must be approved for flight.

The vertical stabilising fin at the rear of a fixed wing aircraft is the more novel location and it is less susceptible to the multipath and cycle slip effects. The mounting of the antenna can be simple because some aircraft already have a strobe light mount which can be adapted [*Curry and Schuckman, 1993*]. However, the measurement of the offset vector is more complex because of the increased distance between the antenna and the camera. It has also been suggested [*Scott, 1994*] that the similar stabilising fin found on a helicopter is prone to excessive vibration and flexure during flight which may be detrimental to the electronics of the GPS antenna and may also introduce an error into the calibrated offset vector.

GPS antennas have been mounted on helicopters for specific applications. *Sylvander* [1991] reports on the use of GPS antenna positioning as an aid to forestry feature identification. The antenna was mounted on the rear boom of the helicopter, midway between the main fuselage and the rear fin. If the rear boom of a helicopter is tapered then it is possible that the vibration and flexure would be minimised by mounting at the wider end, making it a suitable location [*Scott, 1994*].

Another alternative is discussed in *Biggs et al* [1989], where the airborne sensor was deployed on a horizontal boom below the fuselage of the helicopter. The GPS antenna was also located on the same boom. This approach has the advantage of placing the antenna close to the sensor to simplify any necessary calculation of the sensor position from the GPS antenna phase centre position.

4.2.2 GPS Antenna - Camera Offset Vector

The principle behind integrating GPS into the photogrammetric system is to measure the coordinates of the camera perspective centre in the ground coordinate system. However, it is not possible to obtain this measurement directly because the perspective centre is internal to the camera's optical system.

The GPS antenna phase centre can be measured through a suitable kinematic processing technique (§3.8) and an observation equation derived to relate this to the camera perspective centre. The two points are related through an offset vector between them. This GPS antenna - camera offset vector must be accounted for by some measurement process [*Jacobsen, 1993*] before the GPS coordinates can contribute to the position exterior orientation of the camera stations.

There are two components to the offset vector:

- The inter-nodal vector within the camera lens system
- The exit nodal point to antenna phase centre vector

The collinearity equations (§2.4.2) are based on a simplification of the physical lens system of a camera, shown in Figure 4.1a, where the entrance nodal point and exit nodal point are assumed to be coincident and this point

becomes simply known as the perspective centre. However, the physical situation (Figure 4.1b) shows two points which are displaced along the Z-axis of the fiducial coordinate system. This inter-nodal vector must be measured as it contributes to the total vector between the camera perspective centre (the entrance nodal point) and the GPS antenna phase centre.

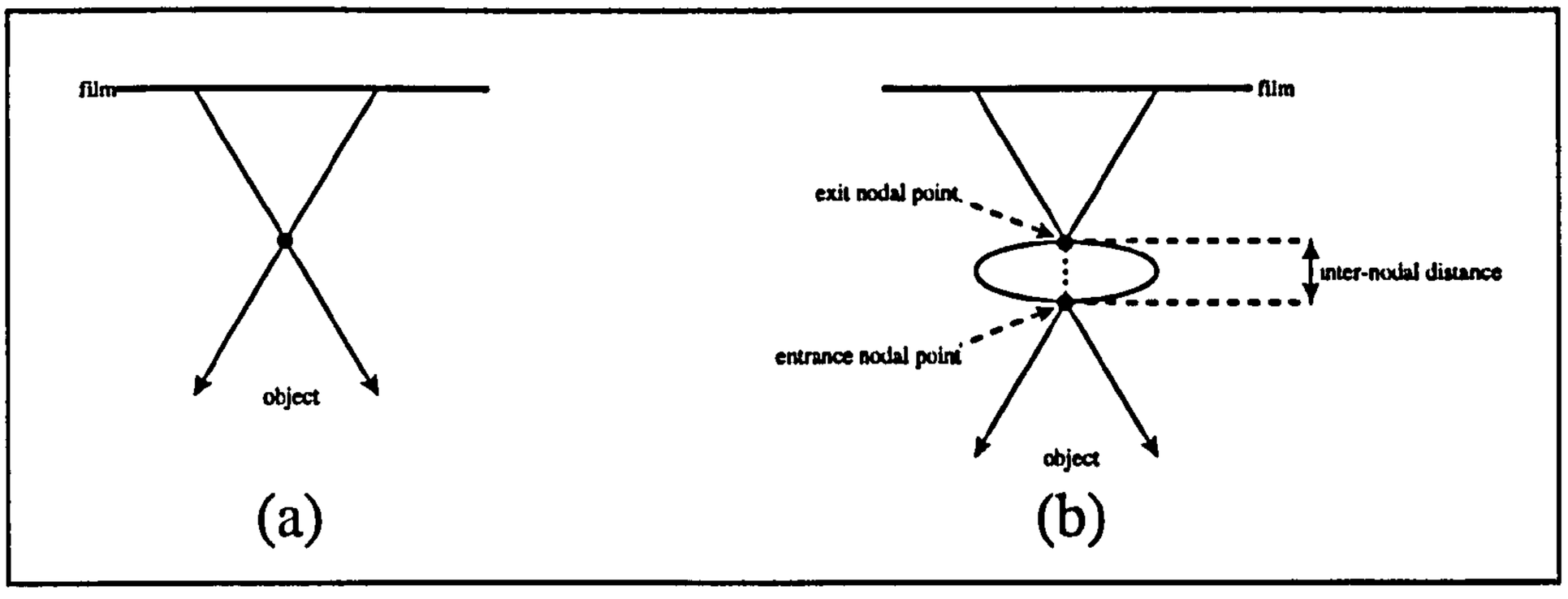

Figure 4.1 - The (a) Simplified and (b) Physical Path Of A Light Ray Through The Camera Lens System, after [*Jacobsen, 1993*]

Measurement of the inter-nodal vector is part of the design and manufacture of the photogrammetric camera and so must be supplied by the camera manufacturer. The vector for the UMK 10/1318 camera with a 100mm focal length, used throughout this research, is 40.45mm along the fiducial Z-axis [*Wickens, 1994*].

A typical aerial camera such as the Zeiss LMK is typically operated inside a *gyro-stabilised* mount which maintains the camera in a nominal horizontal plane above the ground surface despite any roll of the aircraft [*Klose, 1990*]. This has the effect that the offset vector between the exit nodal point and antenna phase centre does not remain constant, but is constantly changing [*Merchant, 1993*]. It would be necessary to make extra in-flight observations to derive this vector at each exposure station [*Ackermann and Schade, 1993*]. A simpler solution is to operate the camera in a *locked-down* mode [*Lucas, 1987*] so that the camera and aircraft roll in unison. This is generally

acceptable for commercial photographic sorties where the weather is good enough to ensure good flying conditions and the pilot is experienced at flying the pre-determined flight lines [*Boardman, 1996*]. If the offset vector is constant throughout the flight then it can be measured before the flight by either industrial surveying or close-range photogrammetry [*Grün et al, 1993*].

4.2.3 Exposure Control And Identification

Processed GPS data will provide point positions at a pre-determined interval known as the *epoch interval* (eg. 0.5 seconds) which can be user-defined in some receivers [*Ashtech, 1994*]. With these positions only derived at intervals along the flight line (figure 4.2), it is essential to relate the camera exposure station points, which can occur at any point along this same flight line, to the epochs.

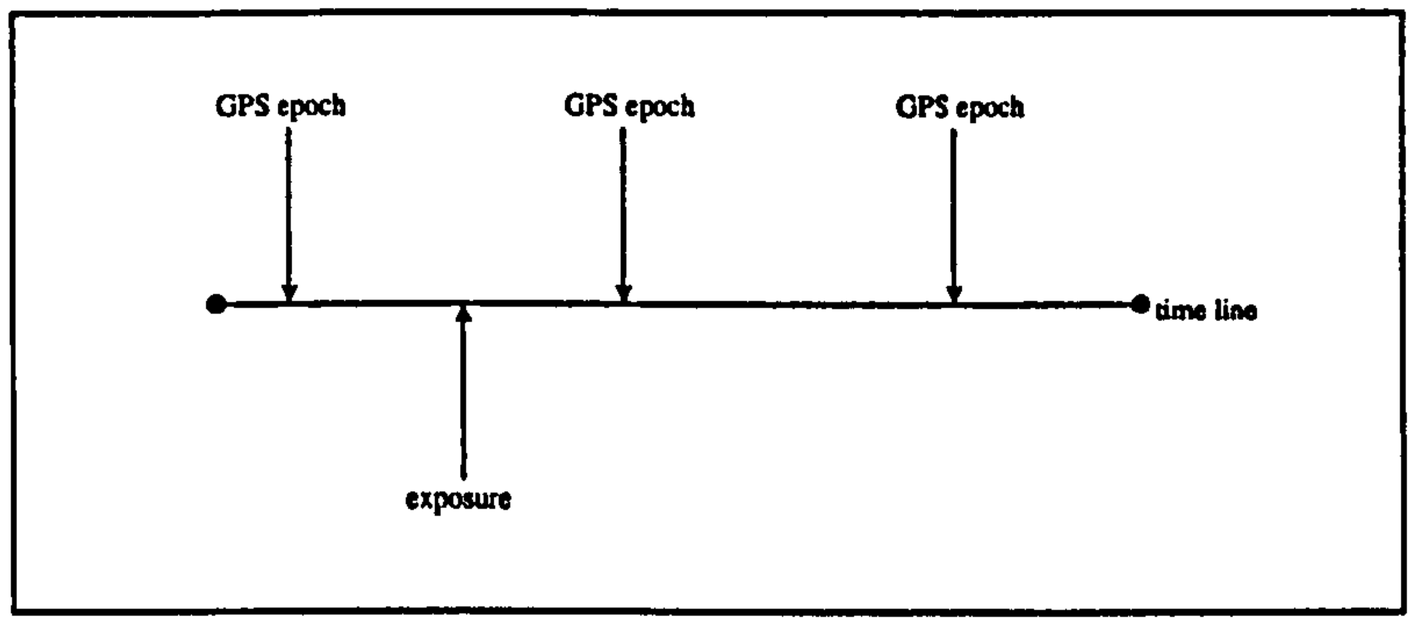

Figure 4.2 - The Relationship Between GPS Epoch And Photographic Exposure Times

The electronic integration of the photogrammetric camera and the GPS receiver can provide the required time synchronisation. There are two techniques to consider [*Hansen and Joy, 1995*]:

- The use of a discrete timing pulse from the camera into the GPS receiver

- The use of the One Pulse Per Second (1PPS) output from the receiver

(i) Camera Timing Pulse

A photogrammetric camera can be modified to output a discrete timing pulse, which can be fed to the GPS receiver and recorded in an event file.

Modern aerial cameras have this timing pulse available for output, and these are usually repeatable at the nanosecond level [*Curry and Schuckman, 1993*]. Older cameras can have a diode fitted into the image plane and this calibrated to the so called *instant of exposure* [*Jacobsen, 1991*] as shown in Figure 4.3. This calibration must be done carefully because of the positional error that could be introduced by a systematically incorrect timing pulse. The aircraft in a small scale photographic run might typically fly at 200 kilometres per hour which would cause 6 centimetres of positional error for every 1 millisecond of timing error [*Jacobsen, 1991*].

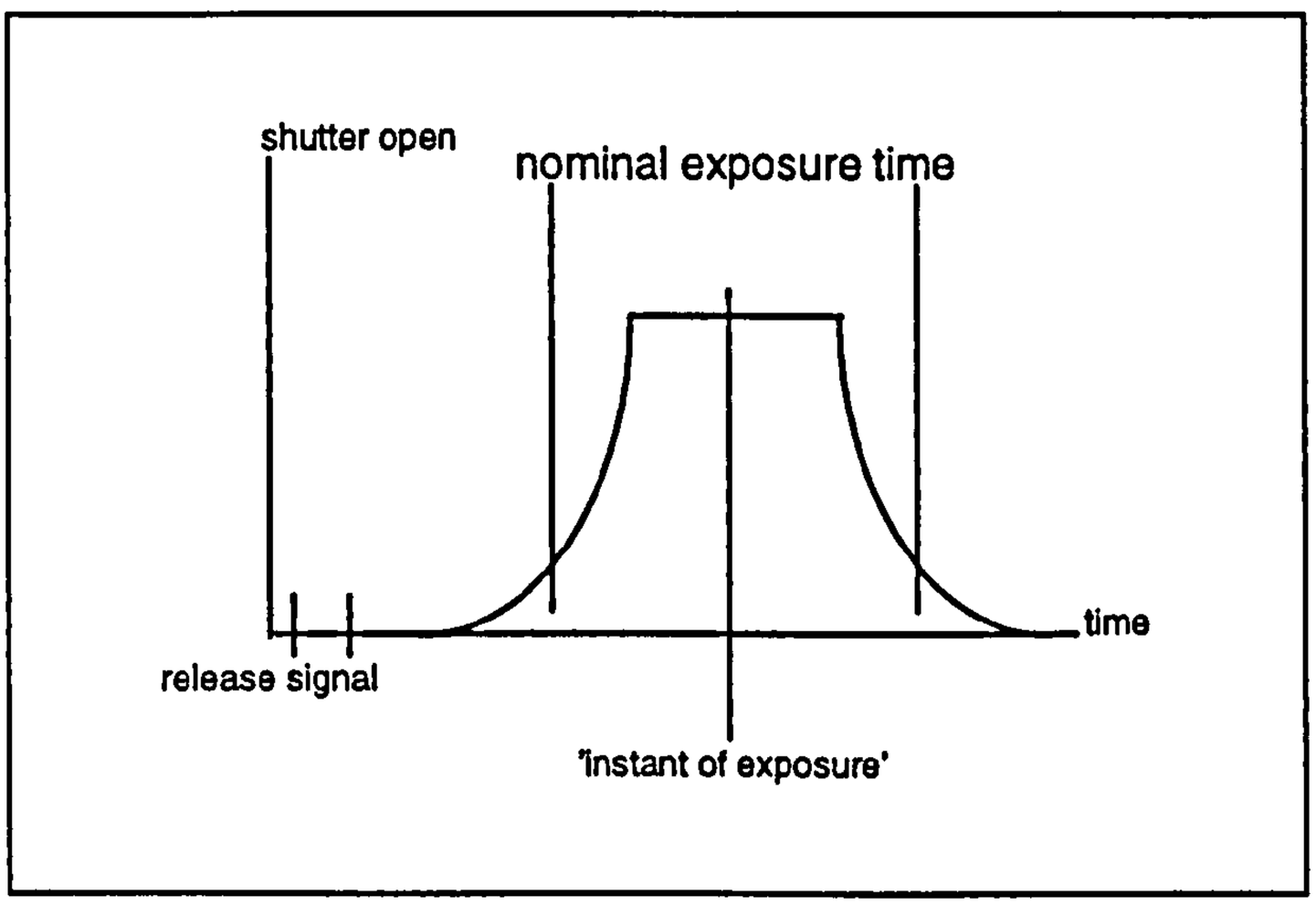

Figure 4.3 - The instant of exposure [*Jacobsen,1991*]

The timing pulse is usually fed directly to the GPS receiver. In the case of the Ashtech Z12 Geodetic receiver used for the final flight trials (§6.3.2), this timing pulse or *trigger signal* is fed in via a 'Camera In' port at the rear of the

receiver unit. A time stamp is recorded in the GPS receiver memory and is accurate to one microsecond. It is possible to configure the time stamping of the event at either the rising (start) or falling (end) edge of this signal [*Ashtech, 1994*].

The file of time stamps must be downloaded from the GPS receiver at the end of the photogrammetric flight, and is presented as a simple ASCII text file. If an exposure has occured at a time between two positional epochs, then the position must be interpolated. Two popular methods of interpolation are linear and least squares matching [*Jacobsen, 1993*]. Unfortunately, the interpolation of camera station coordinates between two GPS epoch positions is likely to introduce some degree of positional error [*Grüen et al, 1993*].

(ii) 1PPS Output From The GPS Receiver

Some GPS receivers can be programmed to output an electronic pulse which can be fed into the electronic firing mechanism of a photogrammetric camera to initiate shutter opening.

The use of the PPS output pulse to fire the camera shutter is a method for negating the need for interpolation of the exposure time between GPS epoch positions [*Ackermann, 1992b*]. In this case, the camera shutter would fire when the PPS signal is output precisely on a GPS epoch. With position and exposure occuring at the same time, no position interpolation would be necessary and no error would be introduced.

In practice, there is actually an inherent error in this type of system. The delay between the time that the PPS signal is output and the time that the camera reaches the instant of exposure (figure 4.3) can introduce an uncertainty of many milliseconds. This error can be referred to as the time synchronisation error (§6.6.1). In the same way as the instant of exposure pulse must be

calibrated to prevent a systematic positional error, it is important to allow for this error source.

It is possible, in the Ashtech Z12 receiver, to offset the PPS pulse against the GPS epoch interval to remove any effect of this delay [*Ashtech, 1994*]. The calibration of the PPS delay is discussed along with the design of the Nottingham GPS-Camera system (§6.6.1).

(iii) A Combined Approach (The Nottingham System)

The use of a camera timing pulse and the PPS output of the GPS receiver are not only discrete methods for exposure control and identification. It will be seen (§6.2.2) that a highly capable solution can be achieved by combining both into a complimentary approach:

- PPS signal to fire the camera
- The same PPS signal used as a camera timing pulse to record the exposure for time and performance verification

The most significant advantage to this approach, which is used in the Nottingham System, is that the PPS signal behaves like a feedback loop. This loop verifies whether the exposure has occured at the correct time.

4.2.4 GPS Data Processing

Modern GPS receivers are able to collect raw satellite data at upwards of 1Hz rate. When the GPS antenna is moving, as with so called kinematic applications such as a photogrammetric flight, this is particularly important for recovering the true flight path in the WGS84 coordinate system. Processing GPS data from a moving object can be hampered by [*Roberts, 1997*]:

- The initial integer ambiguity
- Cycle slips

The early GPS positioning techniques required the user to collect some data purely for resolving the initial integer ambiguity [*Ackermann, 1992d*]. This was achieved by collecting data whilst the aircraft was still on the runway before takeoff. Subsequent antenna positions could be obtained only to the point where the antenna lost lock on any satellite during the flight. With a long photogrammetric flight necessary for small-scale mapping, this is a significant caveat because the loss of lock could be easily caused by banking of the aircraft between photographic strips or even in travelling to the survey area [*Ackermann, 1994*].

Recent developments have produced new GPS positioning algorithms for kinematic GPS data. It is no longer necessary to collect data for resolving the initial integer ambiguity as this can be reliably resolved on-the-fly with only a few seconds of GPS data [*Hansen and Joy, 1995*].

Two GPS processing packages are used to derive antenna positions from the raw GPS data of the field trials in this research. The initial package is the NOTF suite, developed at the IESSG [*Hansen, 1996*]. All the early work is done with this package because it employs a purpose-built on-the fly algorithm to derive positions even after cycle slips in the raw data. Unfortunately, the NOTF package is only suitable for internal research work as it does not employ a intuitive interface and can be complex to use.

The final flight trial (§5.2.3) uses the Ashtech PRISM and PNAV software packages. PNAV is a commercial package which uses an on-the-fly kinematic algorithm. Its main advantage is the graphical user interface and simple reporting tools which makes it much easier to use than the NOTF package. The use of a commercial package made the GPS processing aspects of the flight trial progress quickly. The relative performance of PNAV and NOTF has been testing by *Hansen* [1996] and shown to not be significantly different.

4.3 GPS Assisted Aerial Triangulation

If GPS antenna phase centre coordinates are to contribute to the aerial triangulation process, the functional model (§2.4.2) must be extended to include this new type of observation. This section describes how the GPS antenna observations can be included into the bundle estimation.

4.3.1 Observation Equations

The functional model in a bundle estimation has already been introduced as a series of observations equations. These relate some observed quantity to unknown parameters which are to be determined. In the traditional bundle estimation process implemented in this research, the observed quantities are image point observations on the photographs, and ground coordinates derived from a prior ground survey.

To include the GPS antenna phase centre observed coordinates, the functional model of the triangulation must be extended with additional observation equations. The observation equation for GPS antenna coordinates can be written as:

$$\begin{bmatrix} X^i_{GPS} \\ Y^i_{GPS} \\ Z^i_{GPS} \end{bmatrix} = \begin{bmatrix} X^i_0 \\ Y^i_0 \\ Z^i_0 \end{bmatrix} + R. \begin{bmatrix} x^i_e \\ y^i_e \\ z^i_e \end{bmatrix} \qquad [4.1]$$

where:

$\begin{bmatrix} X^i_{GPS} & Y^i_{GPS} & Z^i_{GPS} \end{bmatrix}^T$ are the coordinates of the ith GPS antenna phase centre in the local coordinate system

$\begin{bmatrix} X_0^i & Y_0^i & Z_0^i \end{bmatrix}^T$	are the coordinates of the ith photograph perspective centre in the local coordinate system
R	is the rotation matrix describing the orientation of the photograph
$\begin{bmatrix} x_e^i & y_e^i & z_e^i \end{bmatrix}^T$	is the eccentricity vector from the ith photograph perspective centre to the GPS antenna phase centre in the fiducial coordinate system

The observation equation for GPS antenna coordinates as shown in non-linear. To include this in the bundle estimation functional model, it must be linearised by Taylor's theorem in the same way that the collinearity equations were linearised.

In this research, the eccentricity vector is pre-calibrated by theodolite intersection (§6.7.7) and so can be considered as a constant in the linearising process. The linear observation equation contains only unknown parameters for the position and orientation of the photograph. The computational algorithm of equation 2.5 is extended to the form shown below:

$$\begin{bmatrix} A & B \\ 0 & I \\ C & 0 \end{bmatrix} \cdot \begin{bmatrix} \delta P \\ \delta G \end{bmatrix} = \begin{bmatrix} b_1 \\ b_2 \\ b_3 \end{bmatrix} + \begin{bmatrix} v_1 \\ v_2 \\ v_3 \end{bmatrix} \qquad [4.2]$$

where:

A and B	are design matrices containing the partial derivatives of the observed image coordinates with respect to the unknown position and orientation elements of the

photographs, and the ground coordinates of the observed image points.

C — is the design matrix containing the partial derivatives of the GPS antenna phase centre coordinates with respect to the unknown position and orientation elements of the photographs

∂P and ∂G — are the corrections to be added to the approximate values of the position and orientation elements of the photographs, and the ground coordinates of the observed image points.

b_1 , b_2 and b_3 — are the relationship between the observed quantities and the computed quantities as given in the linearised observation equations in the appropriate form.

v_1 , v_2 and v_3 — are the residuals associated with the observed image points and the ground control point coordinates respectively.

This approach to the extension of a traditional bundle estimation model to include GPS antenna phase centre observation equations is the most straightforward method. It does not introduce any additional unknown parameters because the eccentricity vector is pre-calibrated.

4.3.2 The Datum Problem

Inclusion of the GPS observation equations into the bundle estimation process provides information on the absolute coordinate system. This enables the calculation of the orientation parameters of the exposure stations and the

ground coordinates of observed ground points. It is feasible to proceed through this bundle estimation without providing any traditional ground control to the equation system, since the definition of the ground coordinate system comes from the GPS observations. However, the GPS observations refer to the WGS84 coordinate system (§3.4) and photogrammetric results are usually wanted in some national or local coordinate system [*Ackermann, 1992c*].

It is common to include a minimum network of ground control points in the bundle estimation to define the transformation from WGS84 into the national coordinate system. These points must have their position calculated in both coordinate systems to enable this transformation process to take place within the bundle estimation software. In a photogrammetric block which is to be triangulated with GPS exposure stations, the ground control points are normally chosen in the four corners of the block [*Ackermann, 1992d*] or at the extremeties if the block is of an irregular shape. This gives a transformation which is effective across the whole block.

4.3.3 Shift and Drift Parameters

The kinematic GPS positional accuracy has been investigated in several prominent photogrammetric flights by comparing it to the positions derived from the photogrammetric block adjustment [*Ackermann, 1992a*]. It has been suggested that the GPS antenna positions show systematic errors or drift errors caused by incorrect ambiguity resolution and cycle slips in the raw data [*Freiss, 1991*]. To suppress or eliminate these errors and so improve the accuracy of the GPS positions, the GPS observation equations can be extended to include linear drift parameters [*Colomina, 1993*]. The use of linear parameters is valid if the errors are assessed separately for each strip [*Ackermann and Schade, 1993*]. The modified GPS observation equation can be written:

$$\begin{bmatrix} X^i_{GPS} \\ Y^i_{GPS} \\ Z^i_{GPS} \end{bmatrix} = \begin{bmatrix} X^i_0 \\ Y^i_0 \\ Z^i_0 \end{bmatrix} + R.\begin{bmatrix} x^i_e \\ y^i_e \\ z^i_e \end{bmatrix} + \left(\begin{bmatrix} a_x \\ a_y \\ a_z \end{bmatrix} + \begin{bmatrix} b_x \\ b_y \\ b_z \end{bmatrix} .(t - t_0) \right)_k \qquad [4.3]$$

where:

$\begin{bmatrix} X^i_{GPS} & Y^i_{GPS} & Z^i_{GPS} \end{bmatrix}$ are the coordinates of the ith GPS antenna phase centre in the local coordinate system

$\begin{bmatrix} X^i_0 & Y^i_0 & Z^i_0 \end{bmatrix}$ are the coordinates of the ith photograph perspective centre in the local coordinate system

R is the rotation matrix describing the orientation of the photograph

$\begin{bmatrix} x^i_e & y^i_e & z^i_e \end{bmatrix}$ is the eccentricity vector from the ith photograph perspective centre to the GPS antenna phase centre in the fiducial coordinate system

$\begin{bmatrix} a_x & a_y & a_z \end{bmatrix}^T$ are the shift parameters for the kth photograph strip

$\begin{bmatrix} b_x & b_y & b_z \end{bmatrix}^T$ are the time dependant drift parameters for the kth photograph strip

$(t - t_0)$ is the time from the instant of time to which the shift parameters of the kth photograph strip apply

The introduction of this extended GPS observation equation introduces further unknown parameters so it becomes necessary to extended the normal equation matrix to include these terms. Special consideration must be given to the configuration of the photographic block and the ground control if the shift and drift parameters are to be determined [*Ackermann, 1992b*].

Figure 4.4a shows the configuration of ground control that is necessary in a photographic block where no additional parameters are to be determined. The four control points enable the transformation from the WGS84 coordinate system of the GPS positions to the local coordinate system used for mapping. However, if the shift and drift parameters are included, this configuration is not adequate. Two possible solutions exist and are shown in Figure 4.4b and c. Two chains of vertical control points can be included along the sides of the block, or two cross strips of photography can be flown.

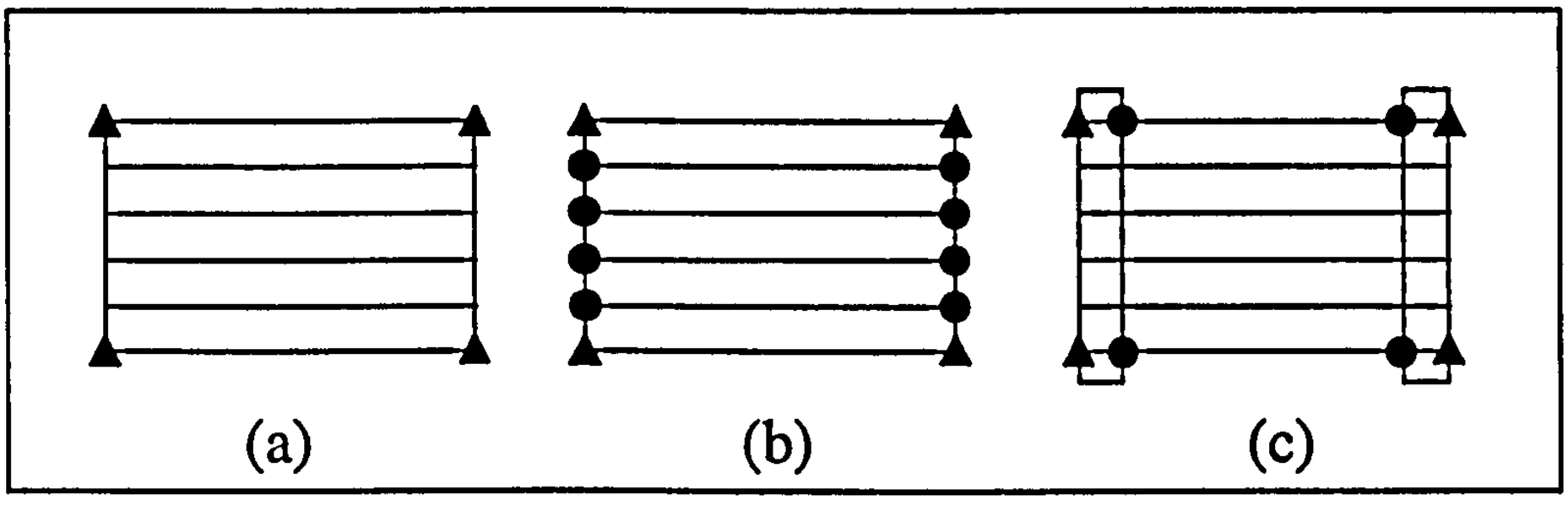

Figure 4.4 - Block Configuration for GPS-Triangulation

[*Ackermann, 1992c*]

The most popular solution [*Ackermann, 1992d*] is to use the additional cross strips approach to stabilise the aerial triangulation solution and successfully determine all the unknown parameters. This process of including additional photography or control points is known as block stabilisation [*Krück, 1996*].

The use of shift and drift parameters in the bundle estimation has certain operational advantages. The photogrammetrist can accept problems in the GPS data and use the bundle estimation process to remove the adverse effects

of poor kinematic position determination [*Ackermann, 1992b*]. However, the required parameters would be reduced or elimated if the kinematic positioning algorithm employed was reliable and accurate [*Ackermann and Schade, 1993*].

4.3.4 BINGO - A New Approach

The inclusion of shift and drift parameters into the functional model of the bundle estimation is not perfect because of the need to increase the number of control points or to introduce cross strips of photography to stabilise the block.

A new approach to the use of GPS data in the bundle estimation has been developed by GIP mbH, a software house based in Aalen, Germany. An extended functional model has been developed [*Krück, 1996*] which allows information about any unresolved integer ambiguities (§3.7.2) to be included in the estimation for subsequent resolution. The principle is not to model the errors caused by incorrect or failed ambiguity resolution in the GPS data processing stage, but to directly resolve the ambiguities by taking into account the photogrammetric image measurements and the photogrammetric ground control points. This is similar to performing a combined bundle estimation with raw ground survey observations rather than using the derived ground control point coordinates calculated from only the survey observations themselves (§5.4.4). A more rigorous result is achieved in such cases because all the information (the observations) are used simultaneously to find the unknown parameters.

The major advantage of this new approach is that no unnecessary parameters are introduced into the bundle estimation and the cross strips of photography are no longer required [*Krück, 1996*]. This reduction in either photography or control points is of great economical benefit. The pre-requisite for implementation is GPS data processing software which can provide certain additional data about the satellite constellation and which ambiguities are unresolved.

At the time of writing, the BINGO approach has been reported in *Krück* [1997] and tested with real block data and it is expected that other aerial triangulation software packages will be enhanced to include this new approach. However, a commercially viable solution is still in development [*Krück, 1997*] so it can only be seen as a promising development for future GPS-Triangulation work.

4.4 Summary

Aerial triangulation has already been introduced in chapter 2 as a method for reducing the requirement for ground control in photogrammetric mapping. A further reduction might be achieved by the integration of a in-flight GPS positioning system into the photogrammetric camera system. This would provide observations of the camera station coordinates which are otherwise indirectly determined in a traditional triangulation.

The integration of GPS and photogrammetry can only be achieved by overcoming several fundamental difficulties. The GPS antenna must be positioned on the aircraft to receive satellite data with the minimum of obstruction. The offset vector between the camera and the GPS antenna must be pre-calibrated or measured during the flight. The GPS positions are derived at a regular interval and this may not coincide with the instant of exposure of the camera, so a time offset must be calibrated.

If the camera-antenna offset vector is pre-calibrated then no additional unknown parameters are introduced into the bundle estimation. A simple observation equation can be derived to relate the measured GPS antenna phase centre to the camera perspective centre.

Chapter 5

Field Trials And Data Sets

5.1 Introduction

The primary aim of this research is to investigate the potential of both conventional aerial triangulation and GPS assisted aerial triangulation for reducing the control requirement in large scale photogrammetric mapping of highways. The original photographic system that was developed for use in the helicopter (§1.3) is not capable of collecting GPS data during a photographic flight. Therefore, the research also involves extending the photographic system to integrate a GPS positioning system.

To realise the aims of the research, it is necessary to undertake a series of practical field trials. These are used to investigate the feasibility and performance of the GPS-photogrammetry system at two discrete levels:

- Field performance of the hardware and associated software
- Numerical performance of the conventional and GPS assisted aerial triangulation concepts.

Section 5.2 introduces the hardware developments with a general description of the components of the GPS camera system. Section 5.3 describes the three primary field trials used in this research and discussed in the later chapters. Section 5.4 introduces the aerial triangulation dataset that is analysed in Chapter 8. Section 5.5 explains the observations that are used in the aerial triangulation and a summary is given in Section 5.6.

5.2 Hardware Overview

The Nottingham GPS-camera system is a development of the original camera system developed by Photarc Surveys Limited. The following sub-sections provide an overview of the primary hardware components.

5.2.1 The Camera Mount and Aerial Platform

The camera mount used for the photography was developed by Photarc Surveys Ltd after experimentation with a simpler version [*Boardman, 1994*] and is shown in Plate A.2. A major advantage of the design is that it did not require prior approval from the Civil Aviation Authority (CAA), who govern all alterations to the airframe of UK registered aircraft and helicopters [*Scott, 1994*]. Instead, a special frame called a *skymount* is fitted in the rear compartment of the Bell 206 helicopter, and the camera mount is bolted on [*Boardman, 1994*].

The camera mount has a rigid frame to allow secure attachment to the *skymount*. Below this is a ball and socket joint which connects the camera cradle to the upper frame. This allows the cradle to be moved throughout the flight, which is often important to maintain a low crab angle and prevent excessive κ rotation [*Boardman, 1994*].

5.2.2 The Zeiss UMK 10/1318 Universal Camera

The photogrammetric camera used in this research was the Zeiss UMK 10/1318 U universal survey camera. It is a film camera with a focal length of 99.27mm. The radial distortion parameters can be seen in Table 5.1. The film magazine has a vacuum back to aid film flattening and can typically accommodate around 80 exposures on a film roll.

Radial Distance (mm)	Distortion (μm)
15	+5
25	+8
40	+6
50	+2
70	-6

Table 5.1 - Radial Distortion Properties of Zeiss UMK 10/1318 Camera

Although not specifically designed for aerial photography, the UMK has found some applications in helicopters and small planes [*Stirling et al, 1992*]. The camera can be seen in Plate A.3.

5.2.3 The GPS Receiver

The two GPS-camera systems described in §6.3 and §6.6 use different GPS receivers because this corresponded to the availability of such hardware at the IESSG at the time of the field trials. The original Mk I system uses the Trimble 4000 SSE dual frequency geodetic receiver which is a high accuracy receiver predominantly used in surveying and mapping [*Trimble, 1992*]. The final Mk II system uses the Ashtech Z12 dual frequency geodetic receiver which is also used in surveying and mapping but has some additional features which make it suitable for navigation [*Ashtech, 1994*]. Both receivers consist of a receiver unit which is connected to an antenna (for receiving the GPS satellite signals) by cable.

Both GPS receivers are capable of generating a pulse-per-second (PPS) signal which is synchronised with the GPS measuring epochs. This signal is a low to high pulse (figure 5.1) and is nominally 1 millisecond in duration.

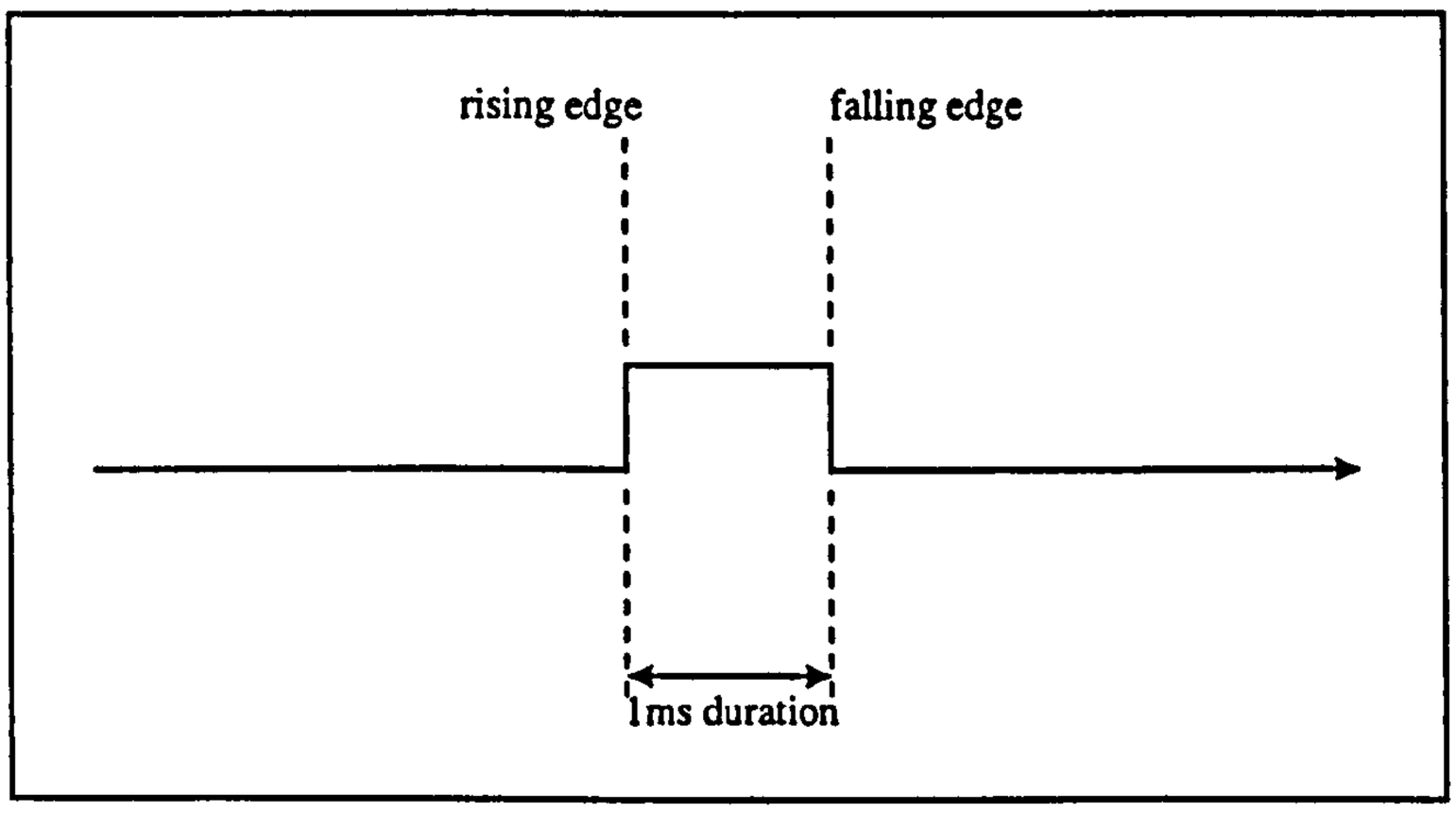

Figure 5.1 - The One-Pulse-Per-Second (PPS) Signal

The Trimble GPS receiver can output the PPS signal at a 1 second interval. In contrast, the Ashtech GPS receiver is user programmable and the period of the PPS signal can be changed from a 0.5 second interval to a maximum of 60

seconds. The PPS signal can also be offset from the GPS epoch time by upto 500 milliseconds, which is not possible in the Trimble receiver. The importance of these additional receiver facilities to this research is discussed in §6.7.2

The Zeiss UMK camera was tested in the laboratory to evaluate the feasibility of using the PPS signal to initiate the camera shutter mechanism. The use of the 1 millisecond signal was not successful and it was discovered that a longer signal was required. The signal duration that is required to initiate the camera shutter mechanism was found to be 50 milliseconds.

5.2.4 Lucas Accustar Tilt Sensors

The tilt sensors that were integrated into the GPS-camera system were borrowed from another research project at the IESSG. They consist of two electronic clinometers manufactured by Lucas which were mounted orthogonally within a perspex housing. Each tilt sensor has a theoretical resolution of 0.001°, although practically this is affected by the measurement system (§6.3.3).

The sensors are electronic and have no moving parts [*Lucas, 1992*]. When rotated about the sensitive axis, the sensor provides a linear electrical variation which is converted to raw angular data (§6.3.3).

Throughout this research, both sensors were connected in Analog mode to an Analog to Digital converter. This converter enables the angular variations to be derived from the electrical variation.

5.3 Field Trials

Three primary field trials were undertaken during the course of this research. These were used for critical assessment of system developments up to that date. In addition, it will be seen that the Pontefract field trails were used to collect datasets for the conventional and GPS assisted aerial triangulation work.

5.3.1 Pontefract 1994 (March 1994)

One of the primary goals in the first six months of the research was to develop and test a preliminary GPS-camera system in the true helicopter environment [*Smith and Joy, 1995*]. The aim of this trial was to test early ideas and to gain valuable practical experience to assist the subsequent developments.

The test site was chosen to be close to the helicopter's base to reduce unnecessary flying time to another test site. It was also important to have easy access to the test site for ground control survey work and preparation. The location was a private airfield near Pontefract, UK, which is operated by the helicopter charter company used for all the commercial photogrammetric work. This site had a grass runway, with an 800m length and 18m width (at the time of the 1994 trial), and the surrounding fields could be used to simulate a typical highway environment. The ground control was established at a 40m interval along a 160m section of the runway and coordinated using theodolite, EDM and digital level. A local coordinate system of Eastings, Northings and Height was defined using an arbitrary local origin. The plan coordinates of the control points were calculated to a precision of 0.010m and the height coordinates to a precision of 0.002m.

All previous commercial projects by Photarc Surveys Ltd used a 10 centimetre square blank white target for the ground control points [*Boardman, 1994*]

which is shown in Figure 5.2a. As part of this first field trial, consideration was given to the use of an alternate design which might improve ground control measurement during the observation phase of the aerial triangulation process. A combination of the original blank target and a newer black and white quadrant design, shown in Figure 5.2b were coordinated throughout the test field.

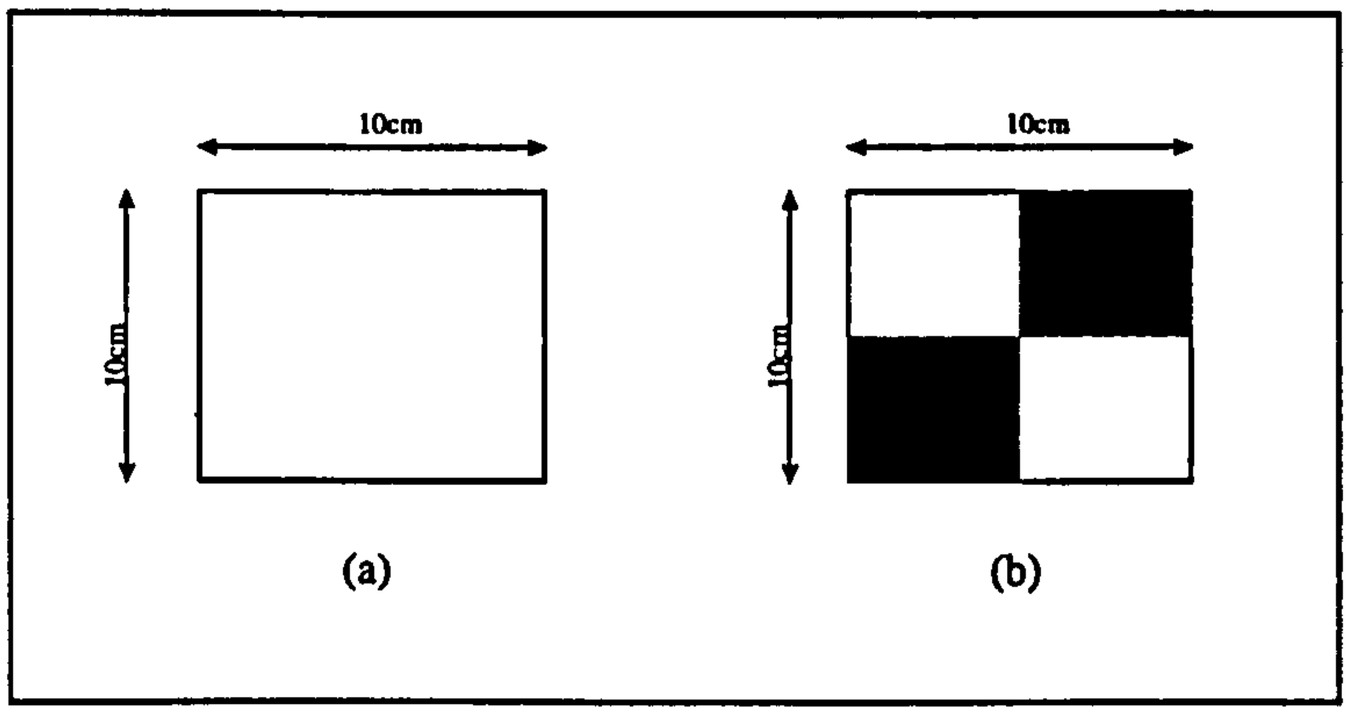

Figure 5.2 - Ground Control Target Design

A 30 minute flight was undertaken on 23rd March 1994 at 1.30pm. This timing combined the optimum GPS satellite constellation with the optimum light conditions for good photography. Unfortunately, the weather conditions were not ideal with high winds and some light rain. These conditions would not have been suitable for work on a production survey [*Smith and Joy, 1995*]. The photography and GPS antenna coordinates obtained from the Pontefract 1994 trial are discussed in §5.4.1.

5.3.2 Medical School Trial (August 1995)

The development of the Mk II GPS-Camera system (§6.5) required a simple field trial to quantify the improvement in operational performance over the original Mk I system. Unlike the Pontefract trials, the Medical School trial was only intended to assess the performance of the GPS-camera system

hardware. The photography was not to be used for any aerial triangulation investigations.

A building facade at the Queens Medical Centre in Nottingham, UK was used to obtain photography with ground control targets across its full area. With the GPS-camera system rotated on to its side (Plate A.1), the building facade was large enough to obtain this photography. The ground control was printed as the 10cm quadrant design previously shown in Figure 5.2b on adhesive labels. These were attached to the outside of the windows at an equal spacing across each floor of the building. The ground control was coordinated using theodolite and EDM from a pre-coordinated control network in the adjacent car-park.

The trial was undertaken on the morning of 19th August 1995 to minimise building shadow over the object space. Unfortunately, the UMK camera had developed an intermittent shutter fault which caused some double exposures and severe image movement. This fault meant that only 2 exposures, both at the end of the intended 5 photograph strip, were suitable for analysis. After analysis of these two exposures (§6.7), there was no requirement for a repeat field trial to overcome the camera problems.

5.3.3 Pontefract 1996 (August 1996)

After minor modifications to the Mk II GPS Camera system as a result of the experience gained during the Medical School trial, a final full-scale flight trial was undertaken. This Pontefract 1996 flight trial was the culmination of all the research. It was used to enable a final critical assessment of the performance of the GPS-camera system in the helicopter environment and to obtain suitable data for the aerial triangulation tests that are described in Chapter 8.

The chosen location for this field trial was the same grass runway used in the Pontefract 1994 trial. Since this was to be the final field trial, a larger section of the runway was used. With the requirement for permanent ground markers in a commercial survey (§1.3), a 750m section was selected. The ground control was established at a 50m interval along the runway and coordinated using theodolite, EDM and level. A local coordinate system of Eastings, Northings and Height was defined using an arbitrary local origin in the same manner as the Pontefract 1994 trial and the survey observations were adjusted using a least squares based software package called HORNET [*Sleeman, 1992*]. The level information was calculated directly from the levelling observations with overlapping observations to provide an independent check.

Unfortunately, the results of the ground survey identified that some of the latter control points were poorly coordinated because of site restrictions. The final section was reduced to 500m (twice the 250m permanent ground marker interval). The plan coordinates of the control points were calculated to a precision of 0.010m and the height coordinates to a precision of 0.002m.

The site was flown at 75m above the ground. This height is given by a radio-altimeter [*Boardman, 1994*] which bounces a signal off the ground continuously. A photographic sortie flown at this height gives 1:750 scale photography, which is usually used for commercial contracts requiring a ground point rmse of 5mm.

5.4 Aerial Triangulation Data Sets

The aerial triangulation tests in this research were performed using data from both of the Pontefract field trials. The preliminary conventional aerial triangulation tests were undertaken with the Pontefract 1994 dataset and the results were used to test the feasibility of using aerial triangulation in large

scale highway mapping. The results of these tests are given in *Smith and Joy* [1995] and not repeated here because they were only interim results.

The main conventional aerial triangulation and GPS assisted aerial triangulation tests were undertaken with the Pontefract 1996 dataset. This is because the trial had yielded both good quality photography and GPS antenna phase centre positions for all the photographic exposures.

5.4.1 Pontefract 1994 Photograph Block

The Pontefract 1994 photography consists of 3 photograph strips of 5 frames length with a conventional 60% forward overlap between exposures [*Smith and Joy, 1995*] and a 75% lateral overlap between the strips. The GPS observations collected during the flight did not yield sufficient antenna phase centre coordinates for GPS Aerial Triangulation analysis. However, two coordinates were derived to test the coordinate recovery of the system (§6.4.1).

5.4.2 Pontefract 1996 Photograph Block

The culmination of the hardware developments was the Pontefract 1996 field trial and the resulting data set. The photography consists of 3 photograph strips of 11 frames length with a conventional 60% forward overlap between exposures and a 75% lateral overlap between the strips.

GPS antenna phase centre coordinates were obtained for all the photographs after processing the raw data through the PNAV kinematic GPS software (§4.2.4). Tilt data was also collected.

5.5 Observations In The Aerial Triangulation

Aerial triangulation using the method of bundle estimation is theoretically capable of using many types of observations. The only requirement is that there is a suitable functional model which describes the relationship of the observations to the unknown values which are to be determined. For the specific case investigated in the aerial triangulation tests of this research, the following observations types are employed.

- Image Coordinates
- Ground Control Point Coordinates
- GPS Antenna Phase Centre Coordinates

These different categories of observation are now discussed.

5.5.1 Image Point Observations

The measurement process of aerial triangulation was undertaken on the Leica SD2000 analytical stereoplotter at the University of Nottingham. Through an appropriate software interface, in this case the AETRI package [*Leica, 1993*], image points can be measured and recorded as a file of (x,y) image coordinates.

The coordinate system used to define the points of interest is the fiducial coordinate system (figure 5.3). This system is defined by the so-called fiducial marks on the photograph, whose coordinates are given in the camera calibration certificate.

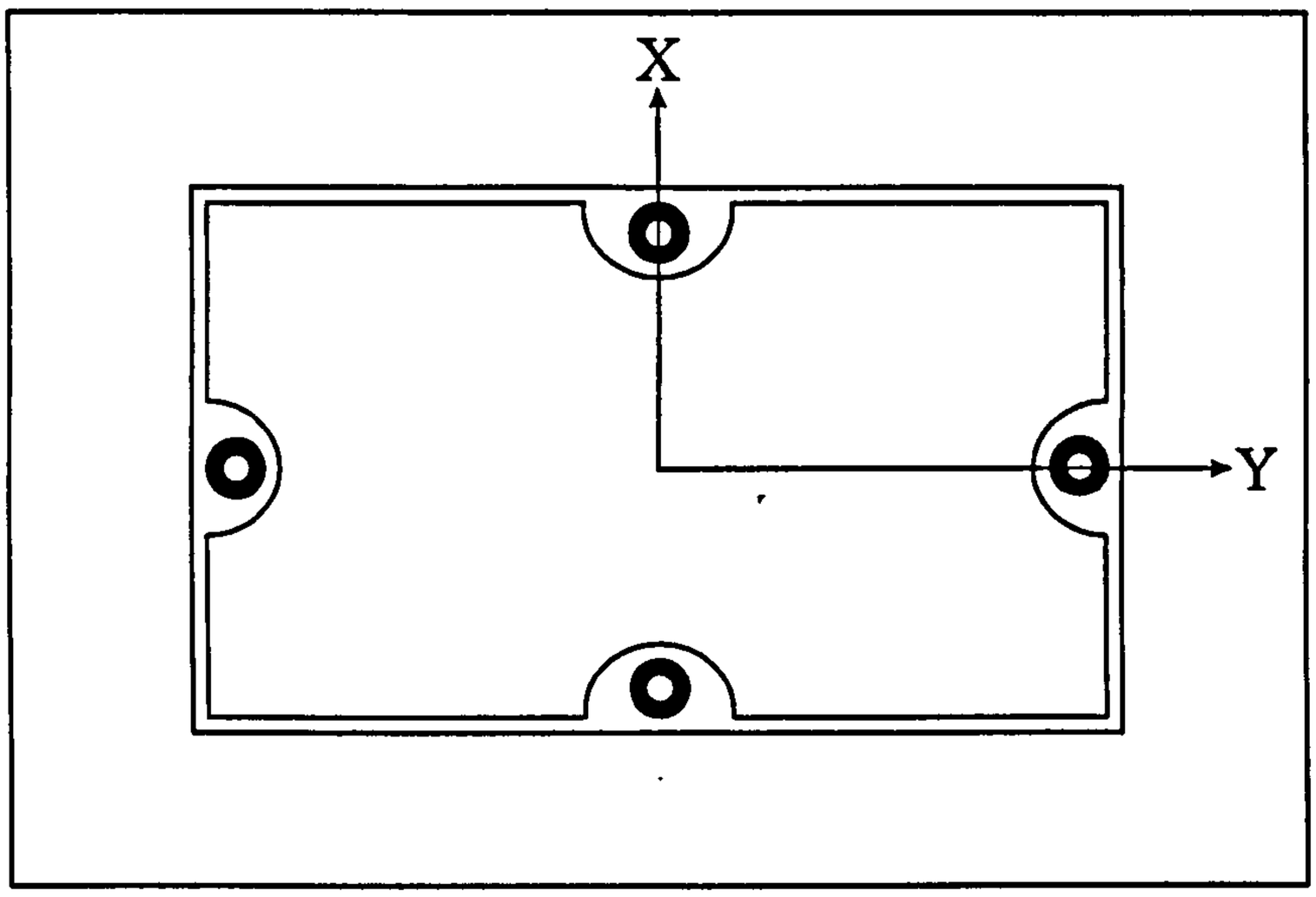

Figure 5.3 - The Fiducial Coordinate System

Image coordinates can be considered as raw observations in the Bundle Estimation, although certain additional distortion parameters (§3.5) can be corrected at the measurement stage to refine the observations.

Within the overlap of a pair of exposures, a standard observation pattern was adopted for the image point observations. 10 points were measured on the images as shown in Figure 5.4.

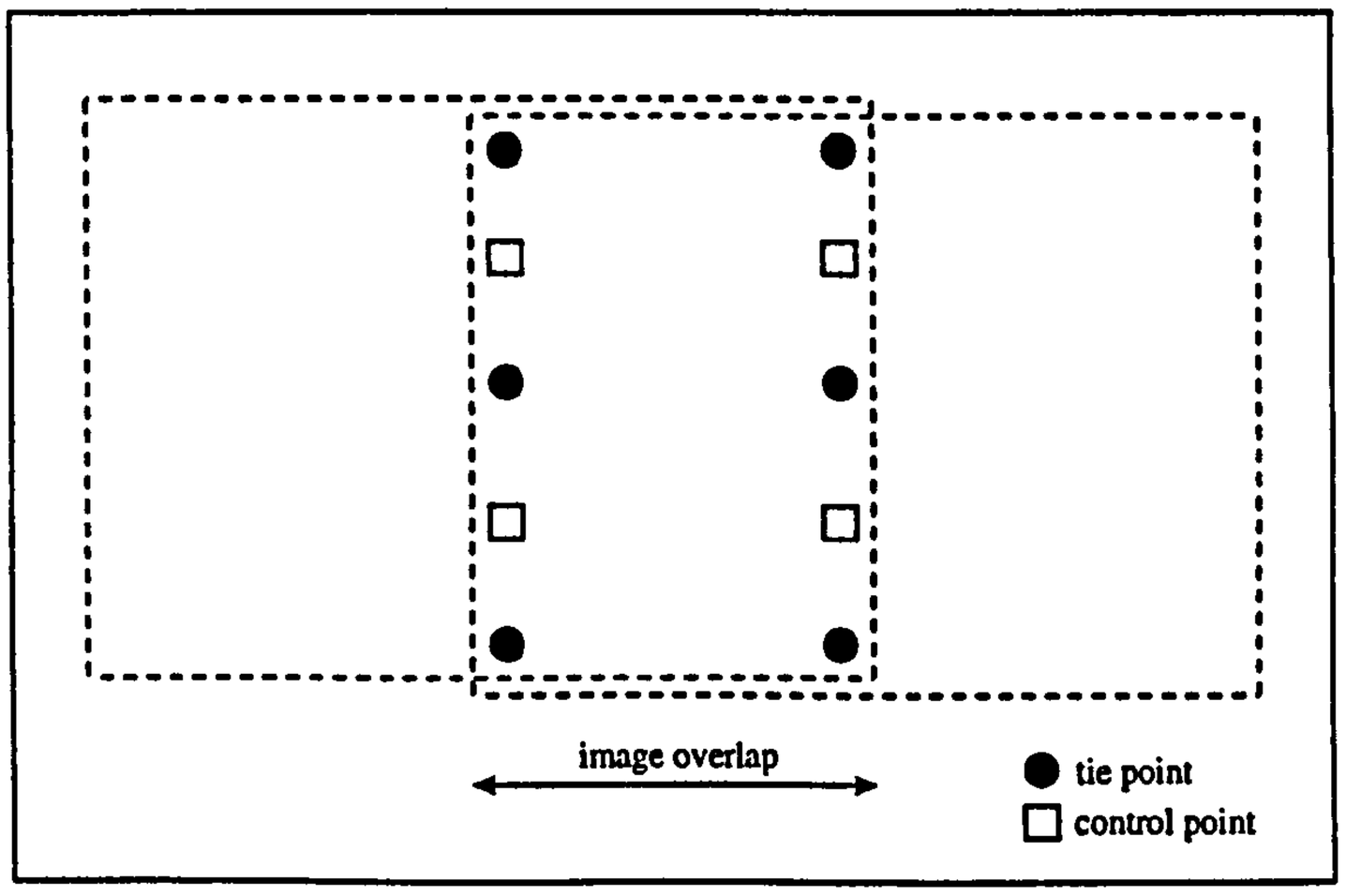

Figure 5.4 - The image point observation pattern

Towards the left and right edges of the model, a group of five points were measured perpendicular to the flight direction. It can be seen that two of these five points are the control points which are separated by the standard width of a three lane motorway.

The other three points are the tie points, marked on the ground by targets for convenience and because the test field was void of suitable texture for repeatable ground point measurement. Marking of the tie points with ground markers ensured that the same point was always measured on different exposures. The centre tie point represents a measurement made on the central reservation of the highway.

5.5.2 Ground Point Observations

Establishing a ground control network within the field of a photographic block usually involves the measurement of angles, distances and height differences between ground stations. The survey observations are used to derive ground control coordinates in a pre-defined coordinate system which may be defined at the local level, the national level (such as OSGB36) , or the global level (such as WGS84).

The use of ground control points in an aerial triangulation produces a two stage estimation process. The control coordinates are derived from a separate calculation which is based on the technique of least squares and uses the observations obtained by theodolite, EDM and level. These observations are not subsequently used in the aerial triangulation. Instead, the calculated coordinates of the ground control points are used as observations with an appropriate assessment of their precision. This is further discusses in §5.5.4.

5.5.3 GPS Antenna Phase Centre Observations

The implementation of GPS assisted aerial triangulation introduces another stage in the overall estimation process. The coordinates of the antenna phase centre are derived from satellite observations (§4.8) by least squares based GPS software (§4.2.4). The satellite observations are not included in the subsequent Bundle Estimation which uses only the functional relationship between the antenna phase centre and the perspective centre of the camera.

5.5.4 Rigorous Aerial Triangulation

Given the three observation groups used in a GPS assisted aerial triangulation, it might seem more rigorous to use all available observation in a single least squares computation. A functional model might be derived to relate the different groups and so remove the requirement for intermediate coordinate estimations.

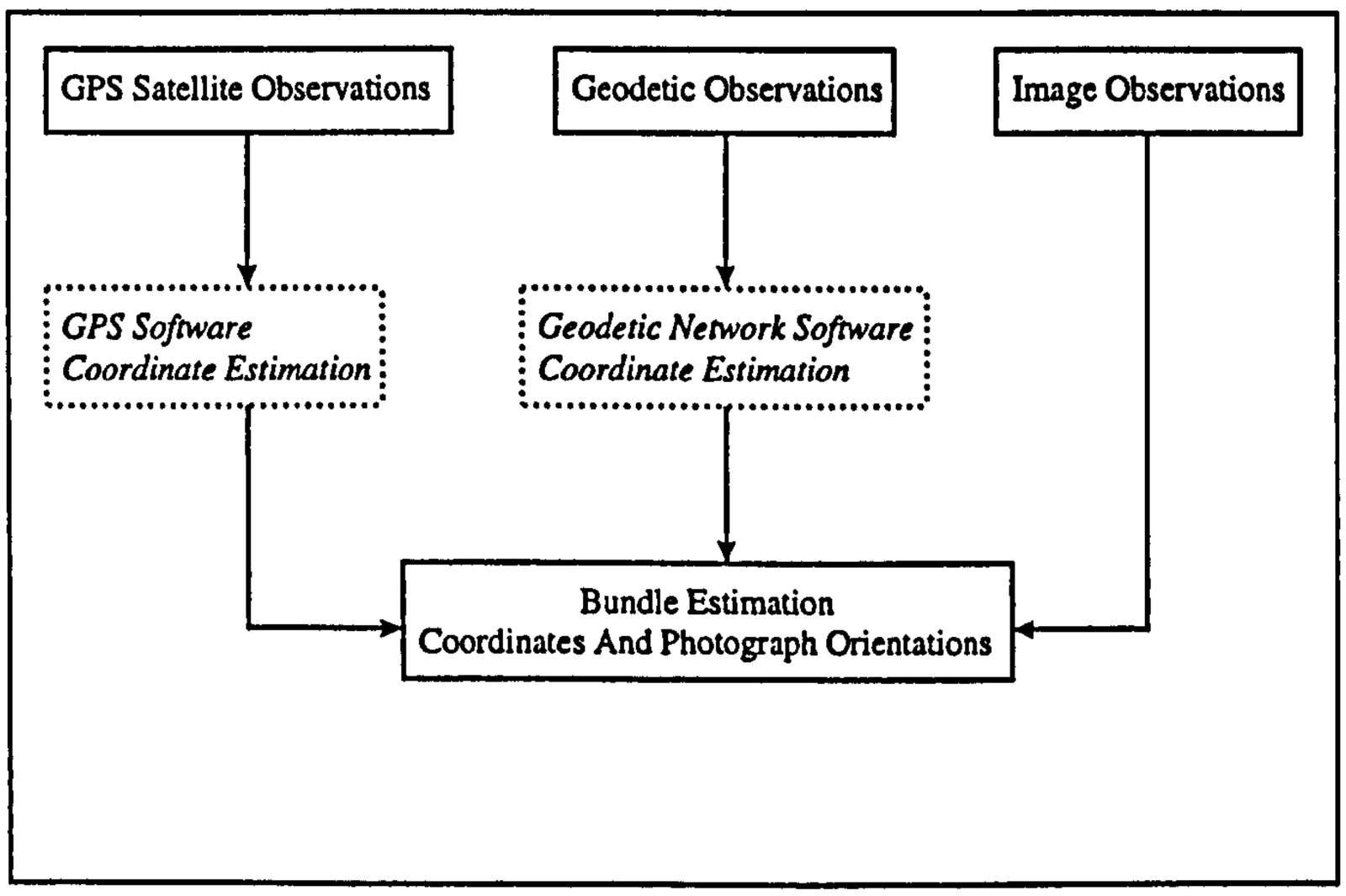

Figure 5.5 - Rigorous Bundle Estimation By Removing Intermediate Software

The inclusion of geodetic observations into the functional model of a bundle estimation has been implemented in commercial software such as the BINGO-F suite [*Krück,1997*]. This package is also able to use raw GPS data from specially adapted GPS software (§4.3.4).

The analysis in this research programme has used intermediate software (figure 5.5) to estimate both the ground coordinates and the GPS antenna phase centre coordinates. The functional model in TABBY (§7.3) does not implement least squares observation equations for raw geodetic observations or GPS observations.

5.6 Summary

Three field trials have been conducted to test the operational performance of the integrated system. Photogrammetric and geodetic data sets have been derived from these trials to validate the performance of the photogrammetric system in an aerial triangulation process.

The aerial triangulation processing utilises image point observations, coordinated ground control points and GPS antenna phase centre coordinates. The software does not implement the capability of including the raw geodetic observations into a single triangulation.

Chapter 6

Nottingham GPS-Camera System: Development and Performance.

6.1 Introduction

The original photographic system (§1.3) that was developed by Photarc Surveys Limited is not capable of collecting GPS data during a photographic flight. It is therefore necessary to extend the photographic system to integrate a GPS positioning system.

The principles and considerations for integrating a photogrammetric camera system and a GPS positioning system have been introduced in Chapter 4. A preliminary system (referred to as Mk I) was developed and assessed through the Pontefract 1994 field trial. As a result of the experiences of this trial, a revised system was developed (referred to as the Mk II system) and assessed through both the Medical School field trial and the Pontefract 1996 field trial.

This chapter introduces the concept of developing the original camera system in section 6.2. The Mk I system is introduced in section 6.3. The performance of the Mk I system in the Pontefract 1994 field trial is given in section 6.4. The experiences from the Pontefract 1994 trial showed several areas of the system that would benefit from further development. These are discussed in section 6.5 and the resulting Mk II system is introduced in section 6.6. The performance of the Mk II system in the Medical School field trial is given in section 6.7. Section 6.8 discusses the practical aspects of using the Nottingham GPS-camera system in the helicopter environment and the performance in the Pontefract 1996 field trial is given in section 6.9. A summary is given in section 6.10.

6.2 Development Overview

The Nottingham GPS-camera system uses the original camera system, developed by Photarc Surveys Limited, as the base component. Preliminary theoretical analysis [*Smith and Joy, 1996b*] had studied the requirement for positioning the perspective centre of the camera using GPS instead of ground control points. This showed that the plan position would be required at ±0.025m RMSE and the height position at ±0.007m RMSE for the highest contract specification of ±0.005m (§1.3). This would be relaxed for the lower contract specifications. Alternatively, centimetric level GPS positioning might satisfy the requirement for highway mapping at the lower contract specifications of 0.010m and 0.020m RMSE, or for other applications.

There was a requirement that the camera only system would be available for use on commercial contracts both during the research and when a GPS positioning system is not required. This requirement produces two key aims for the development:

- The new system had to be as portable and simple to operate as the original camera system
- The additional components must be removable

The following sub-section provide a background to the integration of the GPS positioning system.

6.2.1 Hardware Integration

A requirement of an integrated GPS-camera system is that the GPS derived positions can be related to the camera exposure time. The theory of exposure control and identification has been discussed (§4.2.3) and can be achieved by using one of two techniques [*Hansen and Joy, 1995*]:

- The use of a discrete timing pulse from the camera into the GPS receiver
- The use the One Pulse Per Second (1PPS) output from the receiver

The use of a camera timing pulse involves the interpolation of the exposure position from the two adjacent GPS positions (§4.2.3). However, a helicopter moves at a typical ground speed of 25 kilometres per hour and, because of air turbulence, its motion can be less linear than a fixed wing aircraft moving at a typical ground speed of 200 kilometres per hour [*Hansen and Joy, 1995*].

An alternate approach is to utilise the GPS one-pulse-per-second (1PPS) timing signal to fire the camera (§4.2.3). This approach truly synchronises the photographic exposure with the GPS time epochs, once a correction has been made for the instant of exposure offset (§6.5.1). It is used in the Nottingham GPS-camera system.

6.2.2 Portability Issues

The original camera system is portable because it is not permanently attached to the helicopter, unlike large format aerial cameras which are installed into a dedicated fixed wing aircraft [*Boardman, 1994*]. The camera mount is attached to a *skymount* instead of the helicopter airframe which decouples it from a dedicated helicopter. The original camera system can be deployed in any area where a Bell 206 helicopter, the most popular civilian helicopter in the world, is available. Since the *skymount* is a standard fitting for this type of helicopter, it may either be available with the helicopter or can be shipped to site with the camera [*Stanbridge, 1996*].

One of the key aims of the development of the GPS-camera system (§6.2) was to design and implement a system which was as portable as the original system. However, it is common practice (§4.2.1) to locate the GPS antenna where it is free to receive the GPS signals with the minimum of obstruction. The recommended locations may require modification to the aircraft fuselage which, in addition to being costly and time consuming, makes the system less portable because this must be repeated for every aircraft which is used for the photographic flights.

The location of the GPS antenna for the Mk I system is discussed in §6.3.4 and for the Mk II system in §6.5.3.

6.2.3 Removable Components

A requirement at the beginning of the research was that the original camera system would be available for use on commercial contracts. This meant that the additional components of the GPS-camera system should:

- require no modifications to the photogrammetric camera
- should be modular and easy to remove

All the components of the GPS-camera system can be decoupled from the camera mount when the GPS positioning capability is not required. The cornerstone of the integration is the electronic control system which is discussed in §6.3.2 for the MK I system and §6.6.3 for the Mk II system.

6.3 Mk I (Prototype) System

There are four hardware components that are used in the GPS-camera system. They can be summarised as:

- A Camera
- A Positioning System
- An Orientation System
- A Timing Control System

The orientation system used in this research is a pair of tilt sensors which were available from another research project. Although, the main focus of the hardware development was to integrate a GPS positioning system, the opportunity was available to investigate the measurement of camera orientation.

At the start of this research, there was an opportunity for early flight experience [*Smith and Joy, 1995*]. A preliminary GPS-camera system was developed in order to gain a practical understanding of the integration of a photogrammetric camera and a GPS positioning system. The following sub-sections detail the components of this Mk I system.

6.3.1 The Electronic Control System

The principle of synchronising the GPS receiver and the photogrammetric camera, as defined in §6.2.1, uses the PPS signal of the GPS receiver. Essentially, the pulse is used to fire the camera shutter mechanism and because this is synchronised to the GPS epoch (the time when the GPS position data is recorded), the timing of the two systems is synchronised and no interpolation is required.

Although the PPS signal is used to synchronise the GPS receiver and camera, the camera operator must still press a button to indicate when the helicopter has reached the correct position for the photographic exposure. An electronic control system is required to give the camera operator control over the photographic exposures, whilst firing the camera with the PPS output of the GPS receiver. An overview of the operation is shown in figure 6.2.

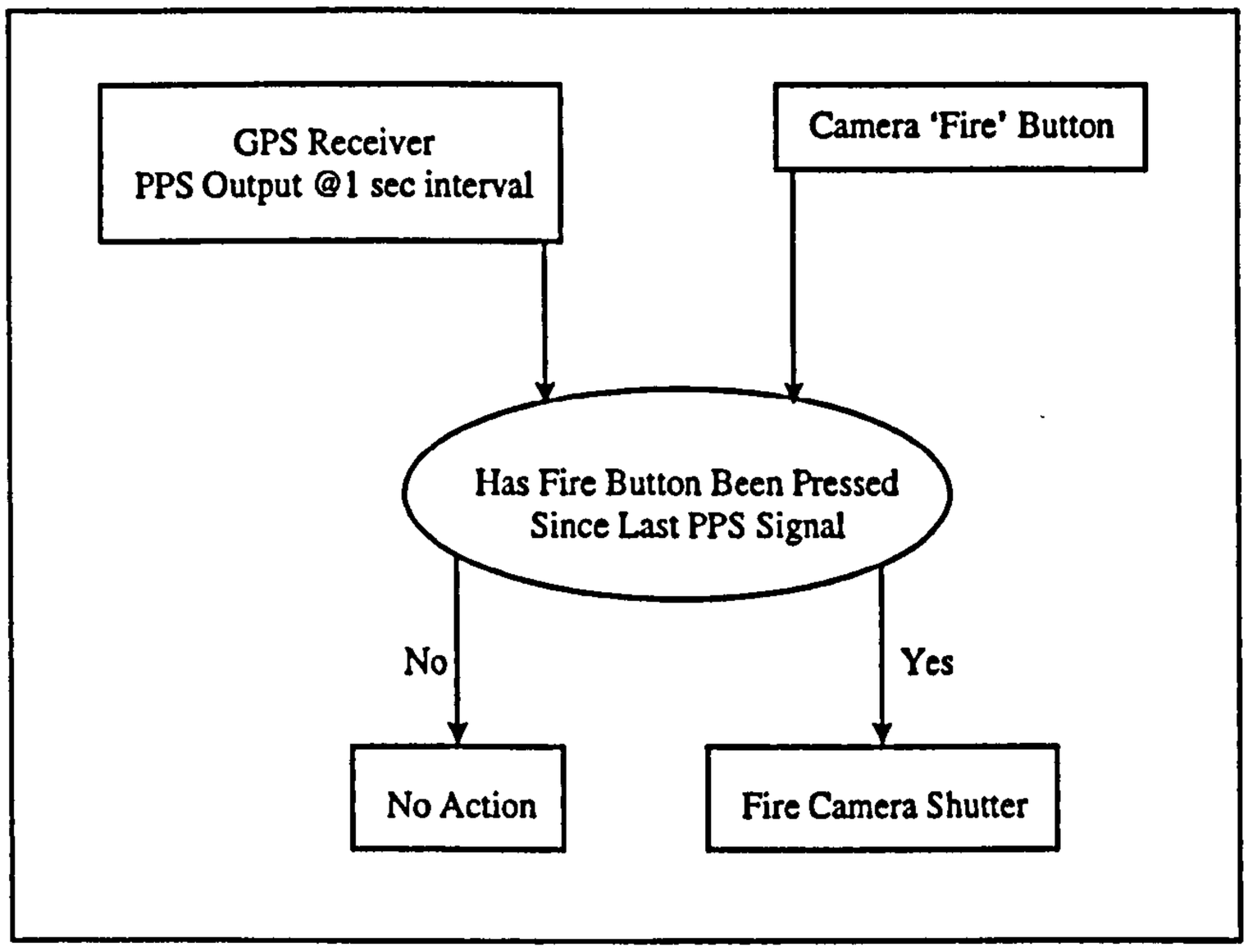

Figure 6.2 - The Electronic Control System

It receives input from both the GPS receiver and the camera 'fire' button. The 1PPS signal is sent at a 1 second interval and each time it is received by the electronic control system, the system chooses what action to take. If the

camera 'fire' button has been pressed since the last PPS signal was received, the action is to use the pulse to fire the camera shutter. If, however, the camera 'fire' button has not been pressed by the camera operator, no action is taken and the system resets to await the next 1PPS signal from the GPS receiver.

Additional circuitry was also required to extend the duration of the 1 microsecond PPS timing pulse to reliably fire the camera, in accordance with the testing described in §5.2.3.

6.3.2 Integration Overview

The interaction between each of the components of the Mk I system is shown in Figure 6.3.

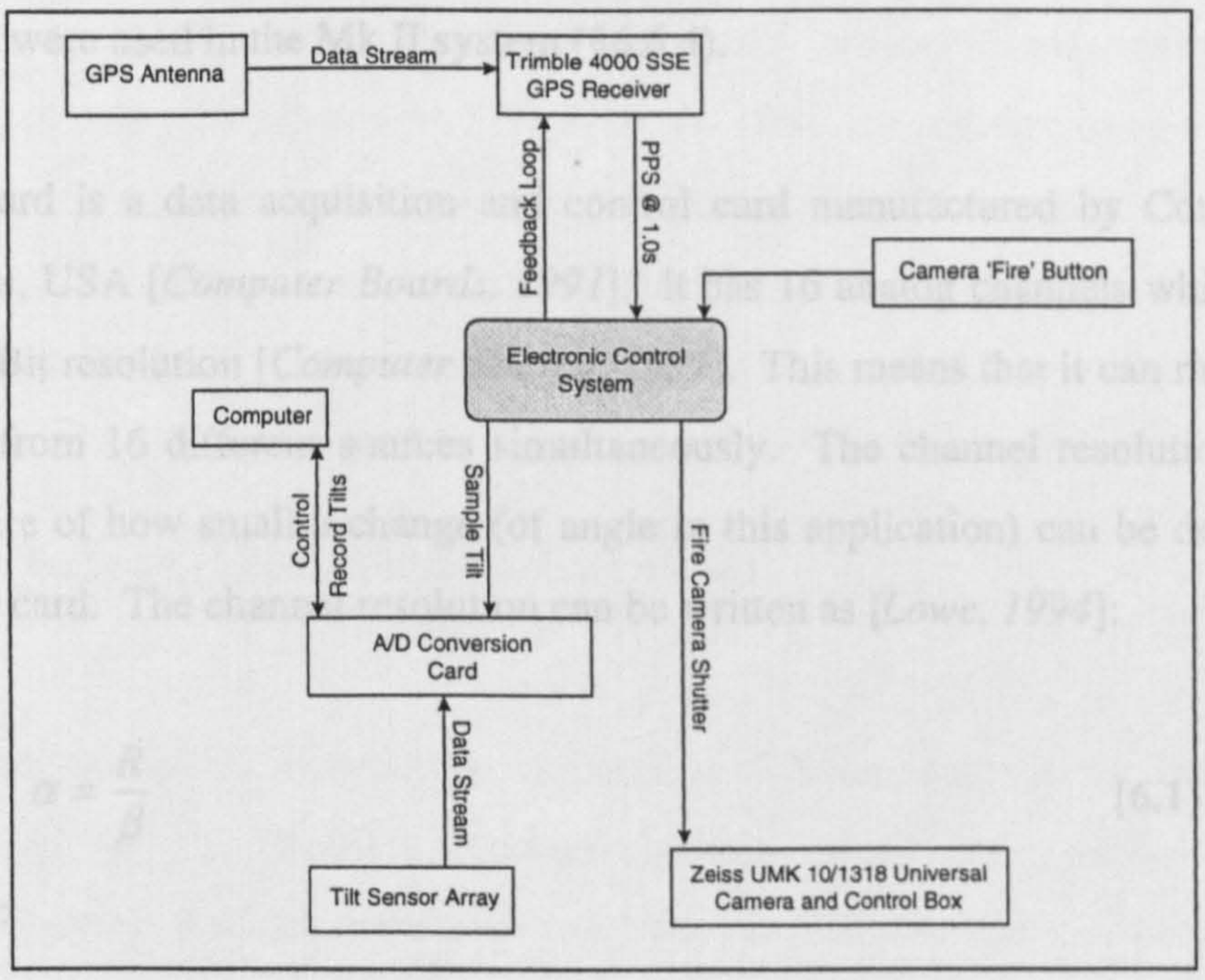

Figure 6.3 - Schematic Diagram Of The Mk I GPS-Camera System

At the centre of the schematic diagram is the electronic control system which is positioned to receive input from both the GPS receiver and the camera 'fire' button. This is the same principle that has been described in §6.3.2. When the PPS signal is used to 'fire' the camera, the signal is also used trigger the tilt sensor measurement system. This system uses computer software to control the A/D conversion card and the recording of tilt values. The data stream between the tilt sensor array and the A/D card is constant. However, the tilt values will only be recorded when the PPS signal trigger is received from the electronic control system.

6.3.3 The A/D Conversion Card

The Analog to Digital converter card is needed to convert the electrical output of the tilt sensors into angular measurements. It is used in both the Mk I system and the Mk II system. However the card has several other capabilities which were used in the Mk II system (§6.6.4).

The card is a data acquisition and control card manufactured by Computer Boards, USA [*Computer Boards, 1991*]. It has 16 analog channels which are of 12 Bit resolution [*Computer Boards, 1991*]. This means that it can measure input from 16 different sources simultaneously. The channel resolution is a measure of how small a change (of angle in this application) can be detected by the card. The channel resolution can be written as [*Lowe, 1994*]:

$$\alpha = \frac{R}{\beta} \qquad [6.1]$$

where:

$$\beta = 2^x \qquad [6.2]$$

and

α is the practical resolution of the sensor system (angular seconds of arc),

R is the working range of the tilt sensor (angular seconds of arc),

β is the total number of bit values in a single channel,

x is the resolution of the analog channel (bits).

From equation 6.1 and 6.2, it can be shown that the resolution of each analog channel (and hence the combined system of sensor and A/D card) is 79 arc seconds.

Importantly for the Mk II system, the A/D card also contains an on board pacer clock and triggering inputs / outputs (§6.6.5).

Operation of the data acquisition card is enabled by a series of software functions written in the ANSI C programming language. These functions allow the card to be fully software configurable, as well as allowing real-time operation. The software for both the Mk I and Mk II systems, was coded on an IBM-compatible personal computer within the *MS-DOS* environment and compiled using the *Microsoft C 5.1 compiler suite*. In addition to controlling the operation of the card, the control software written for this research allows real time conversion of the raw bit values and recording of the tilt values. It is discussed in §6.6.5.

6.3.4 GPS Antenna Location

The importance of maintaining a portable GPS-camera system has been discussed (§6.2.2). The GPS antenna was located on the side of the helicopter, directly attached to the camera mount by a vertical pole and can be seen in Plate A.3. It was accepted that there may be problems with reception of the GPS signals and multipath from the airframe [*Smith and Joy, 1995*]. However, this was the most straightforward approach to integrating the GPS antenna whilst maintaining the portability of the overall system.

6.4 Pontefract 1994 Performance Evaluation

The Pontefract 1994 field trial was undertaken at a private airfield in Pontefract, UK which is operated by the helicopter charter company used for all the UK commercial photogrammetric contract work of Photarc Surveys Limited (§5.3.1). The aim, apart from obtaining photography for ongoing aerial triangulation tests (§5.3), was to assess the performance of the GPS-camera system. Three performance criteria were identified:

- Control System Performance
- GPS Antenna Location and Position Quality
- Tilt Sensor Performance

The following sub-sections discuss the performance evaluation of the system and the resulting recommendations for improvement.

6.4.1 Antenna Phase Centre Coordinate Recovery

The field trial was undertaken within strict time constraints [*Smith and Joy, 1995*] and initial analysis of the GPS data showed that the GPS antenna had only been able to receive signals from between two and four satellites during the flight [*Hansen and Joy, 1995*]. Although the flight was 30 minutes long, only one short section of the GPS data could be processed through the NOTF Kinematic GPS software and used to evaluate the positioning performance of the GPS system.

The GPS antenna phase centre coordinates for two frames were calculated using photogrammetric space resection. A residual vector was computed from the photogrammetrically derived coordinates of the GPS antenna minus the measured coordinates from the NOTF software. Table 6.1 summarises the coordinate recovery.

Frame Number	Residual Vector (m)			Vector Magnitude Between Solutions (m)
	dX (m)	dY (m)	dZ (m)	
30 (OTF L2)	0.17	0.13	-0.14	0.25
30 (OTF L1)	0.14	-0.10	-0.05	0.18
31 (OTF L2)	-0.26	-0.06	-0.11	0.29
32 (OTF L1)	-0.13	-0.04	0.28	0.31

Table 6.1 - Residual between the GPS antenna phase centre coordinates from photogrammetric 'truth' calculation and those from NOTF [*Hansen and Joy, 1995*]

The table shows that there is a large discrepancy along all three axes, with the positioning being particularly poor along the x axis. Overall, the magnitude of the position vector is between 18 and 31 centimetres. There are several possible reasons for such a large discrepancy:

- Multipath
- Satellite geometry
- Electronic control system errors

The location of the GPS antenna, at the side of the helicopter, could have caused multipathing (§3.6.4) of the GPS signals. This is known to introduce positional errors [*Shardlow, 1990*]. The satellite geometry (§3.5.4) is likely to have been poor because the helicopter shielded the GPS antenna from half of the sky. The GPS data showed a positional dilution of precision of 12 which could have generated a position shift of several centimetres alone [*Hansen and Joy, 1995*].

Another possible error in the Mk I system is the timing of the electronic control system. This is discussed in §6.5.1.

6.4.2 Tilt Sensor Angle Recovery

The measured tilt sensor angles were tested in the same way as that described in §6.4.1. A residual tilt value was calculated from the photogrammetrically derived 'truth' tilt minus the measured tilt value. Five photographic exposures were chosen for the tilt recovery evaluation and the results are summarised in table 6.2.

Frame Number	Tilt Sensor (°)	Calculated 'Truth' (°)
19	+2.92	-0.23
20	+0.36	+0.12
21	+3.99	-2.28
22	+2.78	-2.47
30	+0.24	+0.19

Table 6.2 - Calculated and measured tilts for a subset of the photographic exposures [*Smith and Joy,1995*]

It can be seen that there is a poor agreement between the measured and calculated tilt values. Only frames 20 and 30 are broadly close to the calculated value. It has been noted (§5.2.1) that the weather was not optimum and it is possible that this could effect the sensor performance because the camera mount was subject to wind buffeting.

6.4.3 Operational Performance

Although the Mk I system operated adequately throughout the flight trial, the position and orientation aspects were far below the quality which can be expected of kinematic GPS processing in alternative environments such as those described in *Hansen* [1995]. In conditions of good satellite geometry

(§3.5.4) and low multipath (§3.6.4), 2-3 centimetre positioning would be expected.

6.4.4 Tilt Sensor Appraisal

After analysing the tilt data from the Pontefract 1994 trial, it was suspected [*Lowe, 1994*] that the inherent damping of the tilt sensors was proving excessive in this highly dynamic environment. This was investigated during a series of laboratory trials to obtain controlled experimental data and quantify the sensor performance.

In principle, the sensor was moved between two fixed angles of tilt in an accurately measured time. The sensor data was then plotted to derive two variables:

- Velocity of movement between the two tilt angles
- The delay between ceasing sensor motion and the sensor reading the correct tilt

Figure 6.4 shows the typical form of the test data.

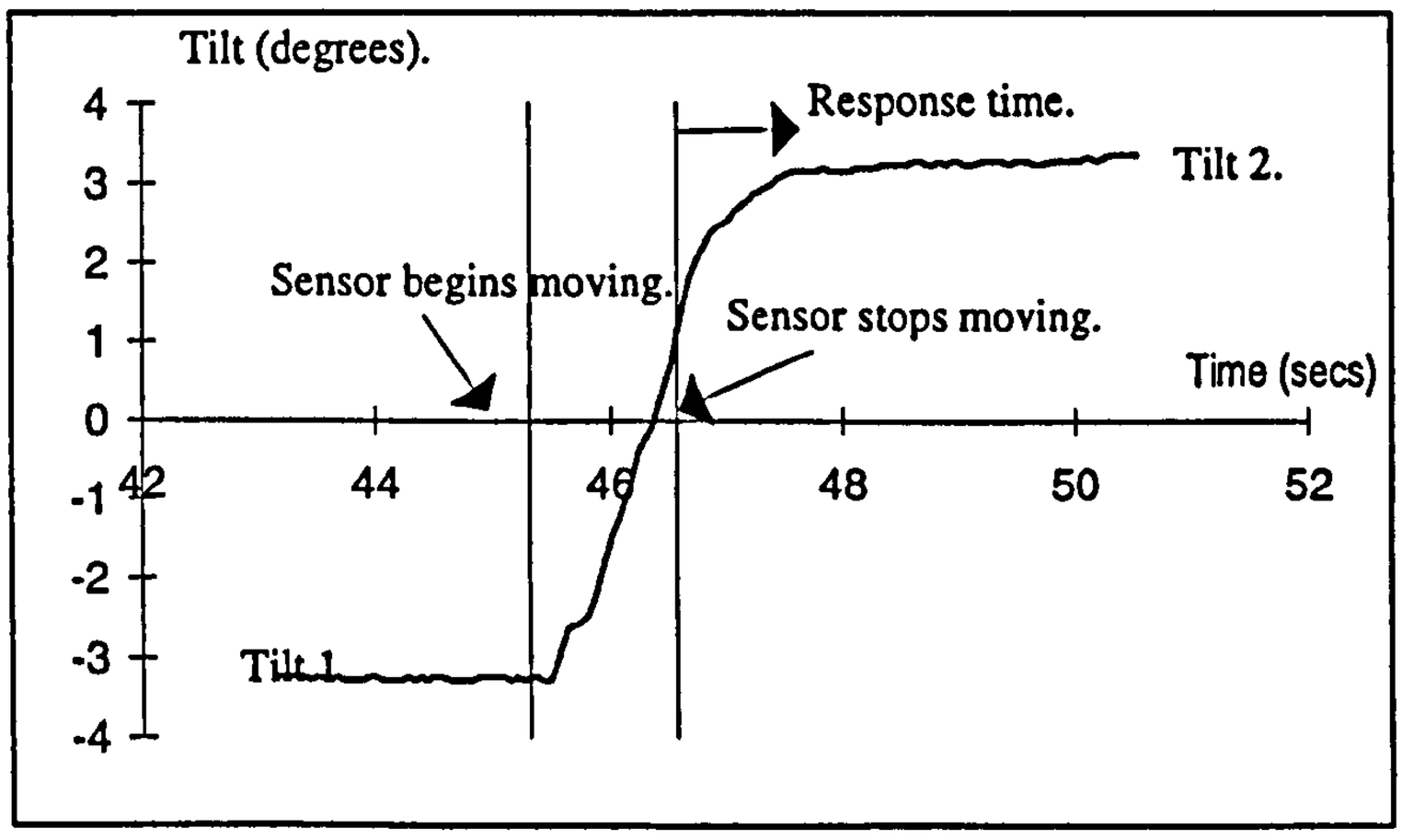

Figure 6.4 - Typical graph of tilt sensor test data [*Smith and Joy,1995*]

The series of tests that were performed showed clearly that the sensors had an internal delay of approximately 1 second, irrespective of the velocity of movement. This was corroborated by information discovered in the sensor datasheets [*Lucas, 1992*]. The *time constant*, an important variable in control theory and system design, was 0.3 seconds. This translates [*Doebelin, 1985*] to the 1 second delay discovered during the laboratory testing.

The poor tilt sensor angle recovery in the Pontefract 1994 flight and the resulting appraisal is very significant. The Lucas Accustar model had not performed to the required accuracy level, particularly in the high dynamics of poor weather conditions. Two options were apparent:

- Replace the sensors with a more suitable model
- Attempt to limit the in-flight dynamics

Since one of the primary aims of the research is to test GPS integration, with the orientation measurement being secondary, an alternative sensor was not used. Instead, the sensors were included in the further developments, with the ultimate aim to be a test of how well they would perform if the flight dynamics were more typical of production conditions (§6.7.2).

6.5 System Refinements

The Mk I system performed within the requirements of a *technology taster* to gain practical experience of the helicopter environment. However, it is clear from the performance evaluation that the GPS positioning system was not capable of reliable positioning at the centimetre level. Further developments were required to the Mk I system to improve both the performance and reliability of the GPS-camera system. The deficiencies of the Mk I system are now described as a prefix to the discussion on the Mk II system in section 6.7

6.5.1 Timing Synchronisation

One possible error in the GPS positioning system was a timing synchronisation problem with the electronic control system (§6.4.1). This arises from the delay that is introduced by the camera control box as it 'fires' the camera shutter. When this delay is not compensated, the camera instant of exposure does not coincide with the GPS position epoch and a positioning error is introduced.

The timing of the PPS signal between the GPS receiver and the camera shutter mechanism can be split into three intervals:

- GPS receiver to electronic control system
- Electronic control system to camera control box
- Camera control box to instant of exposure

The travel time of the PPS signal from the GPS receiver to the electronic control system of the Nottingham GPS-camera system is negligible because this is an electronic pulse travelling down a cable. However, if it is time to 'fire' the camera (§6.3.2), the PPS output must then travel to the camera control box. Although the travel to the camera control box is negligible, the PPS signal initiates the shutter opening mechanism. This is a mechanical device and so a time delay is introduced as this is operated. The time synchronisation delay can be defined as the time between the PPS signal starting the shutter opening mechanism and the time that the camera shutter reaches the instant of exposure (§4.2.3).

The shutter mechanism delay was not compensated for in the Mk I system. Laboratory testing of the camera (§6.6.6) showed that the shutter mechanism delay was of the order of 56 milliseconds. This corresponds to a maximum positional error of 38 centimetres at the typical helicopter ground speed of 25 kilometres per hour.

6.5.2 Reliability

During development of the Mk I system, it was found that the duration of the PPS signal was not long enough to 'fire' the camera shutter mechanism. It was necessary to incorporate the ability to lengthen this signal into the electronic control mechanism. With this capability in the system, each PPS signal that 'fired' the camera was actually a longer signal than the one that was output from the GPS receiver.

The reliability of this signal lengthening process was called into question during final laboratory testing of the Mk I system prior to the Pontefract 1994 field trial. It was found that on some occasions, the PPS signal did not 'fire' the camera shutter mechanism. Although this type of system failure did not occur during the flight, it was decided to re-evaluate the electronic control system as part of the design for the Mk II system.

6.5.3 GPS Antenna Location

The location of the GPS antenna (§6.3.4) was chosen to maintain portability of the GPS-camera system as it did not require any modification to the airframe of the helicopter. However, the performance evaluation has shown that this location may have been adversely affected by multipathing of the GPS signals and the masking of satellites by the side of the helicopter.

Changing the location of the GPS antenna is a difficult issue because of the problem of system portability. The best solution is to attach it to the camera mount so that a single unit can be fixed to the *skymount*. Since the poor performance and reliability of the Mk I antenna location may have been caused by the proximity to the side of the helicopter, it was decided to test a longer pole in the Mk II flight trial. This arrangement can be seen in Plate A.4

6.6 Mk II (Final) System

The Mk II system is the replacement to the Mk I system. Although some of the design concepts are similar, this system was developed in conjunction with the Engineering Faculty Electronics Workshop at The University of Nottingham. This allowed two important advantages over an internal development:

- Assistance in a formal design and testing procedure
- A reliable centre for all future development prospects

The purpose of this collaboration was to refine the Mk I system in order to minimise some of the problems that were clear after the Pontefract 1994 field trial and construct a robust electronic device with scope for future development.

6.6.1 Integration Overview

The integration between each of the components of the Mk II system is shown in figure 6.5.

The Mk II system uses an electronic control system (§6.6.3) which was designed along similar principles to the Mk I system. Some additional capabilities of the A/D conversion card were also used and these will be discussed in §6.6.4.

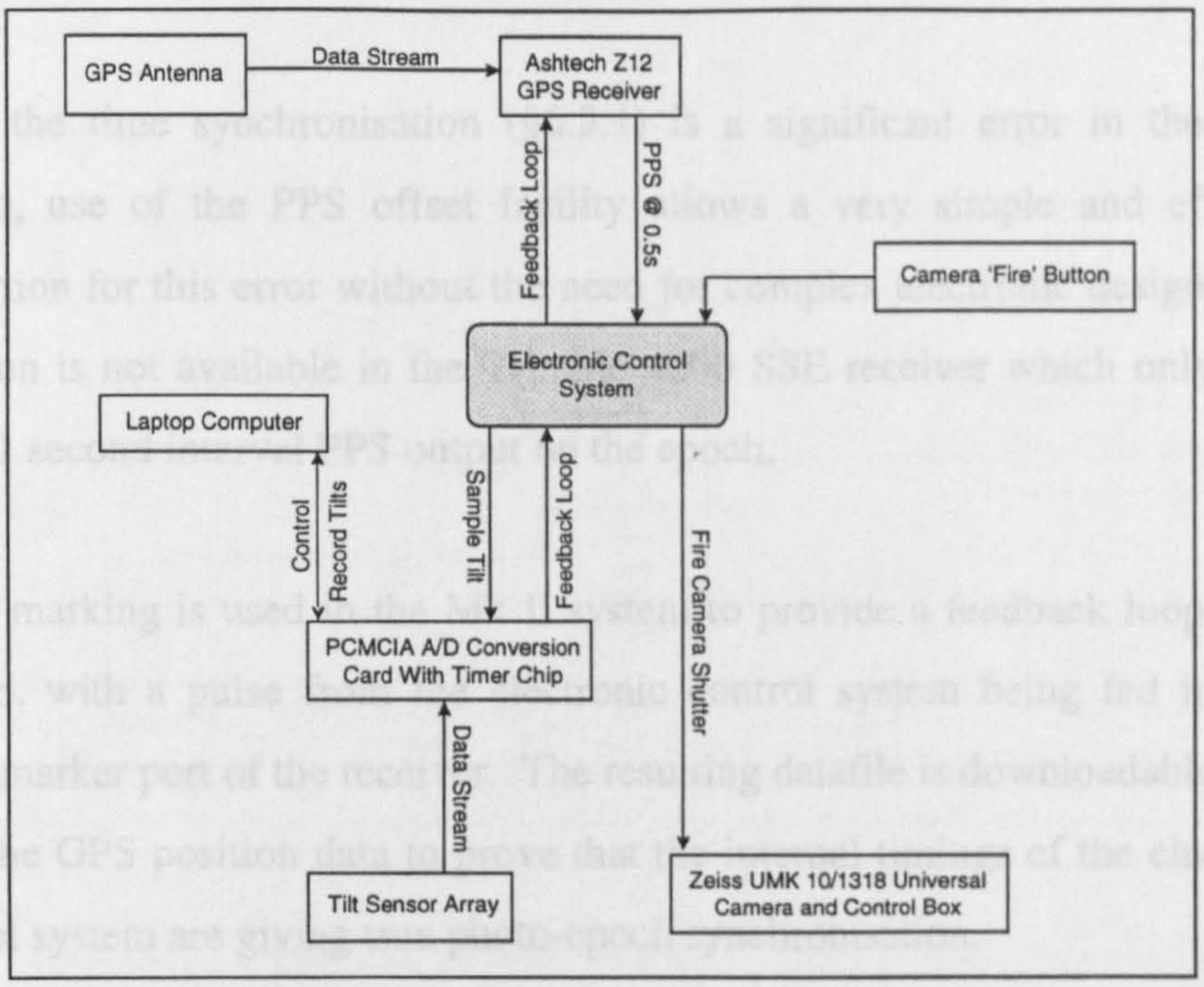

Figure 6.5 - Schematic Diagram Of the Mk II GPS-Camera System

The similarities can be seen between the schematic diagram of the Mk II GPS-camera system (figure 6.7) and the diagram of the Mk I system (figure 6.3). No additional components are used in the Mk II system, although the IBM-compatible personal computer was replaced with a IBM-compatible laptop computer in time for the Pontefract 1996 field trial (§5.3.3) because this was a more portable device.

6.6.2 Receiver Technology

The receiver used in the Mk II system is the Ashtech Z12 receiver. This has many functions which make it particularly suited to this photogrammetric application, notably [*Ashtech, 1994*]:

- PPS signal at a user defined interval (0.5s - 60s)
- PPS signal offset from GPS epoch
- Event marking

Since the time synchronisation (§6.5.1) is a significant error in the Mk I system, use of the PPS offset facility allows a very simple and effective correction for this error without the need for complex electronic design. This function is not available in the Trimble 4000 SSE receiver which only has a fixed 1 second interval PPS output on the epoch.

Event marking is used in the Mk II system to provide a feedback loop in the system, with a pulse from the electronic control system being fed into the event marker port of the receiver. The resulting datafile is downloadable along with the GPS position data to prove that the internal timings of the electronic control system are giving true photo-epoch synchronisation.

6.6.3 The Electronic Control System

The electronic control system functions along the same principles as the Mk I system. The camera 'fire' button is integrated into the control system so whilst the camera operator pushes the button when the helicopter has reached the position of the next exposure, the camera shutter mechanism is actually initiated by the PPS signal from the GPS receiver.

The principle of operation of the Mk II electronic control system is shown in Figure 6.6. One of the concerns from the Mk I system is the delay between the camera operator pressing the 'fire' button and the next PPS signal. The Trimble GPS receiver can only output the PPS signal at a 1 second interval, which means that the maximum time delay is 1 second or a forward helicopter movement of approximately 7 metres. The Ashtech Z12 GPS receiver has a programmable PPS interval and for the Mk II system this was programmed to the minimum interval of 0.5 seconds.

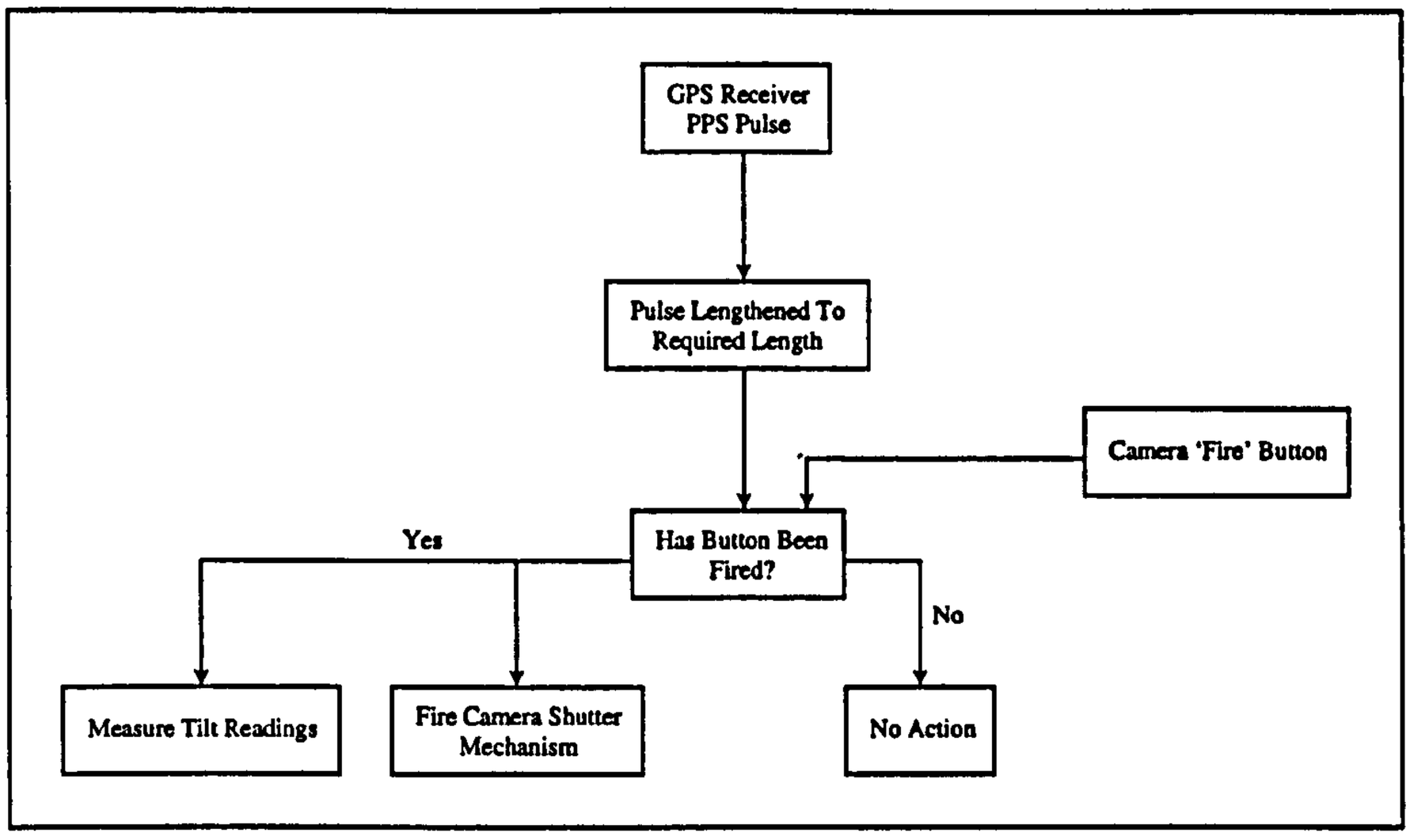

Figure 6.6 - The Electronic Control System Design Principle

Each PPS signal is lengthened by the electronic control system but no further action is taken if the camera operator has not pressed the camera 'fire' button. The electronic control system remembers if the button has been pressed since the last PPS signal. If the button has been pressed the signal is split to initiate two responses. The signal is used to initiate the camera shutter mechanism and to initiate measurement of the tilt at the instant of exposure.

The final part of the electronic control system can be seen in figure 6.7. A feedback loop is used to record the exposure time in the GPS receiver memory (§6.6.2). Since the UMK camera has no electronic feedback capability, this is achieved through the control software for measuring the tilt sensors. It is further discussed in §6.6.5.

6.6.4 The PCMCIA A/D Conversion Card

The original A/D card used in the Pontefract 1994 trial was replaced during the development of the Mk II system with a PCMCIA version suitable for use in a laptop computer. This meant that the tilt angle data collection system was

compacted to include only a sub-palm size electronic card plugged into a laptop computer. A major restriction to portability of the Mk I system was the requirement for a converted desktop computer with ISA expansion slots to integrate the A/D card.

The Computer Boards PCM-DAS16 is a data acquisition and control board for laptop computers with PCMCIA type 2 slots [*Computer Boards, 1994*]. Analog signals can be routed to the Analog to Digital convertor through upto 16 channels. The card has an on board pacer clock which can be used to trigger data acquisition and conversion.

In addition to the Analog to Digital conversion capabilities, the PCMCIA card timing chips were utilised in the Mk II development (§6.6.5) .

6.6.5 Control Software

The control software is used to control the A/D card in the Nottingham GPS-camera system. This card has other capabilities apart from the tilt sensor input channels, notably an on-board pacer clock and trigger in/out ports.

It is important to ensure that the tilt sensors are sampled at the instant of exposure. This means that the time synchronisation delay must be accounted for or the tilts will be sampled too early. The on board pacer clock and counter chips of the A/D card are configured by the software with the time delay at the start of the flight (figure 6.7).

The operation of the control software and A/D card is given in figure 6.7. The signal from the electronic control system is fed into a trigger port of the A/D card which is software configured to wait for a trigger. When this trigger is received, the counter chip counts to the time delay value and then signals the software to sample the tilt sensors. The tilts are converted into angular values

and written to a file. A message on the laptop screen informs the user that a tilt has been measured.

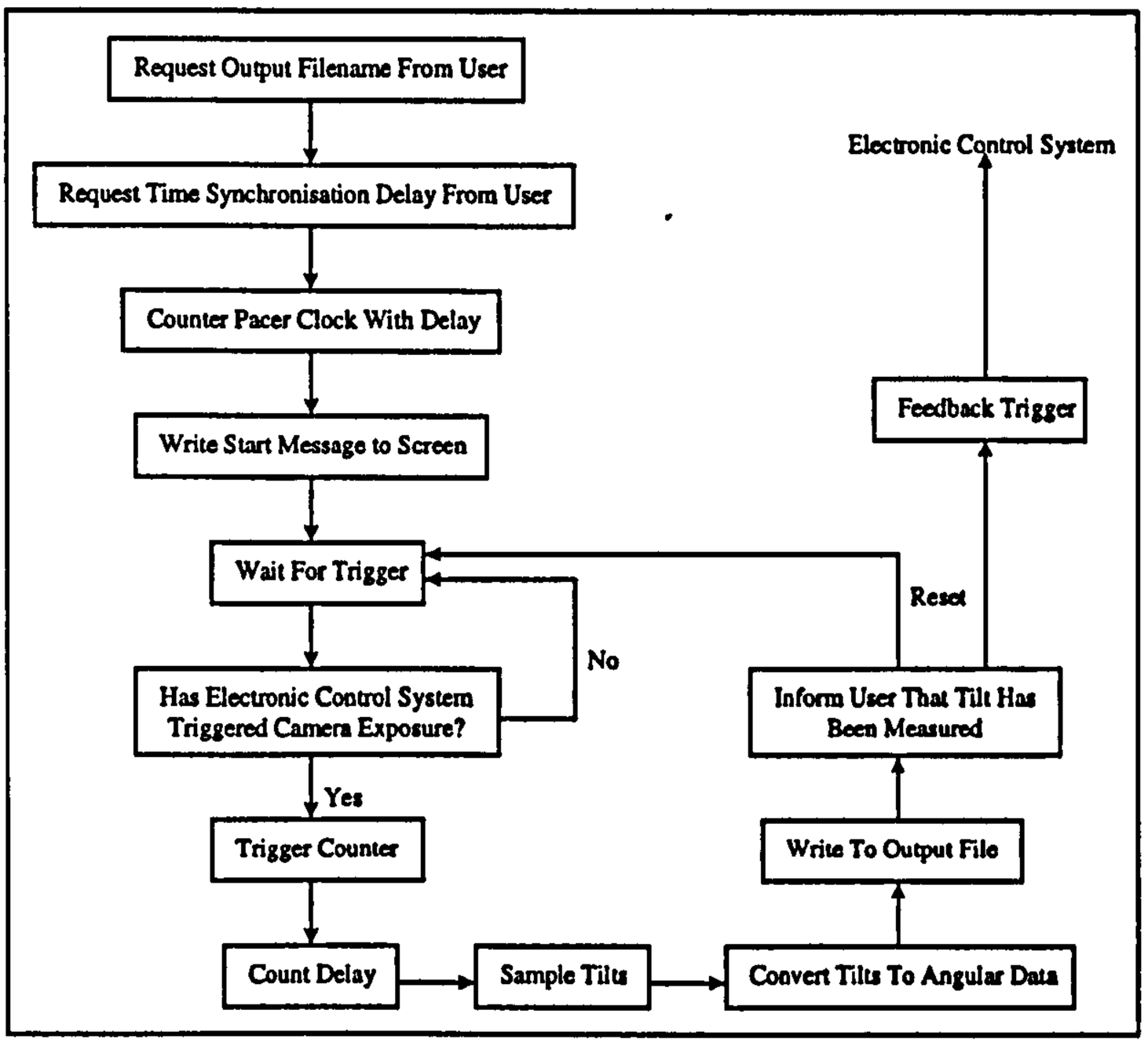

Figure 6.7 - The Control Software

The system resets after each photographic exposure and sends a return signal to the electronic control system. This forms the feedback loop into the GPS receiver to confirm that the timing of the GPS-camera system is working correctly.

6.6.6 Zeiss UMK Testing Principles

Aerial camera systems such as the **Zeiss LMK series** use a photodiode in the focal plane of the camera to measure the time offset (§6.5.1). The UMK camera used in this research has no such capability and so it is necessary to calibrate this time synchronisation.

A small bulb and battery is placed between the lens cone and the film back of the UMK to provide an illumination source from within the camera. This is shown in Plate A.5. An Opto-Schmitt trigger, which is a light sensitive diode with a response time of only 2.5μs, is placed over the outside of the lens cone as shown in plate A.6. Both the optical sensor and the switch are connected to a digital storage oscilloscope to produce the full laboratory setup.

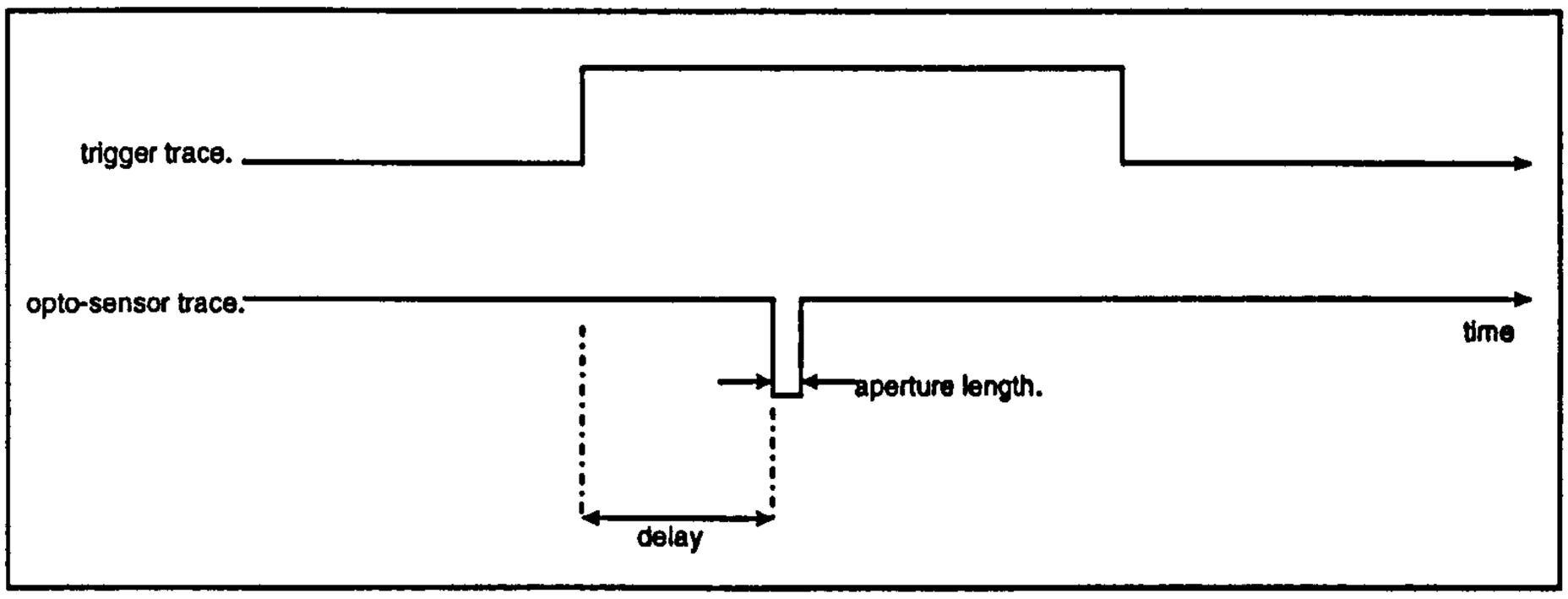

Figure 6.8 - Sample oscilloscope trace from shutter mechanism 'fire'

The principle of the testing is that when the shutter mechanism is fired, the diode registers the precise time that the beam of light is shining through the lens cone. This is then be measured against a trace of the switch activation. Figure 6.8 shows the form of this oscilloscope trace.

A potential problem with the need to calibrate a camera for the time synchronisation offset, is the repeatability of the camera shutter mechanism. If the mechanism moves at a different speed each time the shutter is opened then this time offset could not be reliably determined. The camera which was calibrated for use in the Pontefract 1996 trial had a time synchronisation offset of 56 milliseconds with a root mean square error (rmse) of 0.3 milliseconds from the laboratory tests.

6.6.7 Offset Vector Calibration

The GPS antenna-camera offset vector (§4.2.2) is fixed in magnitude because both the GPS antenna and the camera are fixed to camera mount and do not move (relatively) during the photographic flight. This approach make it possible to calibrate the offset vector for inclusion in the aerial triangulation process (§4.3.1).

The calibration setup for the Pontefract 1996 field trial can be seen in Plate A.9. The vector is calibrated by a process of theodolite angle intersection from two observation stations which have been positioning in an arbitrary local coordinate system. The observation data is processed with THINTER1, a software package originally written for the work of *Smith* [1986]. The offset vector must be defined in the fiducial coordinate system for inclusion in equation 4.1. The transformation between the arbitrary coordinate system used for the measurement and the fiducial coordinate system is achieved with 3DTRAN6 (§7.4.2) which was also written for the work of *Smith* [1986].

The calibration of the GPS antenna-camera offset vector is a straightforward process because it can be undertaken under laboratory conditions.

6.7 Medical School Performance Evaluation

The Medical School field trial was undertaken in Nottingham, UK (§5.3.2). The aim of this trial was purely to assess the performance of the Mk II GPS-camera system. Unfortunately, the camera had developed an intermittent shutter fault which meant that only two photographic exposures were suitable for analysis.

The following sub-sections discuss the performance evaluation of the system.

6.7.1 Antenna Phase Centre Coordinate Recovery

The procedure for assessing the accuracy of the GPS antenna phase centre positions has been introduced (§6.4.1). Only two exposures were suitable for this analysis because of the camera problems. The kinematic GPS data was processed using the NOTF On-The-Fly Kinematic Software and the a residual was calculated in the same manner as the Pontefract 1994 evaluation. The results are summarised in table 6.3.

Frame Number	Residual Vector (m)			Vector Magnitude Between Solutions (m)
	dX (m)	dY (m)	dZ (m)	
4_4a	0.036	0.046	0.053	0.076
4_4b	0.039	0.041	0.050	0.075
3_1a	0.048	0.016	0.030	0.058
3_1b	0.037	0.012	0.031	0.049

Table 6.3 - Residual between the GPS antenna phase centre coordinates from photogrammetric 'truth' calculation and those from NOTF

The results in table 6.3 illustrate the capability of the Mk II system, with a relative coordinate accuracy of approximately 6cm. Each exposure station is shown as a repeat truth calculation to investigate any errors inherent in the photogrammetric truth calculations. In the case of the given exposures, only the dX for frame 3_1 differs significantly. Closer examination of the photogrammetric transformations used in the calculation showed that the frame 3_1a calculation was adversely affected by poor image coordinate measurements.

6.7.2 Tilt Sensor Angle Recovery

Following the performance evaluation principles from the Pontefract 1994 trial (§6.4.2), a set of tilt sensor readings were compared against their photogrammetric truth. Table 6.4 illustrates the results.

Frame Number	Tilt Sensor - Calculated 'Truth'(°)
2_5	-0.50
3_1	+0.03
3_5	-0.68
4_1	-0.33
4_4	+0.30

Table 6.4 - Error of measured tilt in relation to photogrammetric truth for a subset of the Medical School photographic exposures

The accuracy of the sensors in this controlled terrestrial situation are seen to be approximately 0.5 degrees. This would be acceptable for initial approximations to an aerial triangulation computation.

6.7.3 Operational Performance

The electronic control system functioned well during the Medical School trial, even though the GPS-camera system reliability was affected by the camera fault. The antenna coordinate recovery results show that the GPS antenna positions can be related to the photograph exposure positions to an accuracy of only a few centimetres. This is a significant improvement on the performance of the Mk I system in the Pontefract 1994 trial.

The final stage of the development of the GPS-camera system is to test it in the true helicopter environment. However, the experiences of the Pontefract 1994 trial suggest that it is valuable to consider how the equipment will be operated. These operational enhancements are considered in the next section.

6.8 Operational Enhancements

During a photogrammetric flight, a maximum of two survey personnel can be accommodated inside the helicopter in addition to the pilot. In response to the experience of the Pontefract 1994 flight, some consideration was given to the workload of these two personnel during the photographic flight. The ergonomics of the Mk II system were tuned to allow both personnel to undertake specific tasks which would enable collection of full image and positioning datasets.

6.8.1 The Camera Operator

The tasks undertaken by the camera operator can be termed the *photographic duties*. Primarily, this involves the identification of the exposure points along a flight line and taking of the photograph. Both hands of the operator are required to hold the camera mount, particularly when the wind resistance is high. Since the tilt sensors are not suited to highly dynamic environments, this camera movement restraining is beneficial to the in-flight orientation aspects as well as minimising the photographic image movement. Any monitoring of additional components of a GPS-camera system must clearly be undertaken by the navigator.

6.8.2 The Navigator

The navigator's primary responsibility is to ensure that the pilot locates the correct photographic flight lines. When the GPS-camera system is in operation, they can undertake several additional tasks:

- Monitor the quality of the GPS dataset
- Confirm that the exposure tags are being recorded in the receiver
- Record any additional details in the flight log
- Monitor the GPS-camera system components

The additional tasks can be termed the *geodetic duties*. The feedback of the system into the GPS receiver allows the navigator to be an independent check on the performance of the camera firing system. This means that the camera operator can concentrate on the photographic work without this being detrimental to the GPS positioning aspects.

6.9 Pontefract 1996 Performance Evaluation

The data collected from the first two field trials was hampered by poor performance of the data collection system and environmental conditions. However, it served the intended purpose of indicating areas which needed further development. The data set from the Pontefract trial was extensive because the aforementioned hinderences were minimised.

The following sub-sections discuss the final performance evaluation of the Nottingham GPS-camera system.

6.9.1 Antenna Phase Centre Coordinate Recovery

The GPS data was processed with the Ashtech PRISM and PNAV commercial software suite (§4.2.4). This software provides a user friendly and intuitive interface, employs a reliable OTF algorithm [*Hansen, 1996*] and is suitable for processing a dataset with minimal cycle slips. A comparison of the performance of the NOTF software and the Ashtech Software has been performed [*Hansen, 1996*] and there is no significant difference in the coordinates derived from either.

	Rmse of Residual Vector (m)			Rmse of Vector Magnitude Between Solutions (m)
	dX (m)	dY	Z	
Pontefract 1996 Summary	0.04	0.04	0.06	0.08

Table 6.5 - Residual between the GPS antenna phase centre coordinates from photogrammetric 'truth' calculation and those from PNAV

Table 6.5 shows a summary of the antenna coordinate recovery that was performed on the Pontefract 1996 dataset. It is clear that the performance of the GPS positioning system in the helicopter environment has matched the performance that was seen in the Medical School trial (§6.7.1).

The GPS antenna was still attached to the camera mount, as in the Pontefract 1994 trial. However, the pole was nearly 2 metres in length which positioned the antenna marginally above the main fuselage of the helicopter (§6.5.3). This new position means that the GPS antenna is not restricted by the side of the helicopter and is more likely to receive signals from more GPS satellites across the whole sky. Throughout the field trial, the number of satellites which were tracked by the GPS receiver remained mostly between 5 and 7 satellites. The PDOP for the flight was usually under 3 (as compared to the PDOP of 12 during the Pontefract 1994 trial). Only short portions of 4

satellite coverage were noted and these were invariably caused by the banking of the helicopter at the ends of each photographic strip.

6.9.2 Tilt Sensor Angle Recovery

Although tilt sensor data was collected during the Pontefract 1996 field trial, it was not of primary importance to process this data and investigate the performance of the Lucas tilt sensors. Time constraints and the need to process a large amount of photographic and GPS data meant that the tilt data could not be analysed. Although the sensors did not perform well in the Pontefract 1994 trial, when the weather was poor by commercial photogrammetry standards, it is possible that the tilts could be derived to a suitable accuracy for estimating the initial photographic tilts for aerial triangulation.

6.9.3 Operational Performance

The Nottingham GPS-camera system functioned well throughout the Pontefract 1996 trial. With good flight conditions, it was possible to obtain good quality photography and extensive GPS positioning data for use in the aerial triangulation tests. The system performed well in terms of both:

- Integration accuracy
- Reliability

The accuracy of the GPS positioning system and its relation to the camera perspective centre positions is clear from the antenna coordinate recovery. The accuracy in the helicopter environment is as good as the results from the Medical School trial. The improvement in performance over the Mk I system can be attributed to both the location of the GPS antenna and the time synchronisation.

The system performed reliably throughout the trial and the camera was *fired* successfully for all of the photographic exposures. The operational enhancements to the system were essential to ensure that the ergonomics were well designed and suited to this type of work. Only minor alterations could be recommended for future work.

6.10 Summary

An in flight GPS-camera system has been developed through this research. The system is portable and can be decoupled from the camera when the GPS positioning capability is not required.

The GPS-camera system uses an electronic control system to control interaction between the GPS receiver and the photogrammetric camera. The PPS signal from the receiver is used to trigger the camera shutter mechanism. The system is modular in design to allow alternative components to be used.

An array of tilt sensors were available from another research project and they have been integrated into the system to measure the orientation of the camera.

The GPS-camera system has been tested in the helicopter through a field trial and can reliably provide GPS positions at the 5cm accuracy level. The tilt sensor system is not suitable for high accuracy orientation of the camera platform. However, the modular design provides a suitable infrastructure for implementing an alternative sensor.

Chapter 7

Software

7.1 Introduction

The aerial triangulation investigations undertaken as part of this research were achieved with computer software written by the author. The main program is a combined GPS Bundle Estimation package called TABBY. The software design approach and structure are discussed in the following sections. Several auxiliary programs were also developed in line with TABBY and these are discussed.

7.2 Software Development Considerations

There are many prominent aerial triangulation software packages, based around bundle estimation principles, which can be purchased in the commercial marketplace. However, in house development of similar software during the course of a research study can serve two important benefits:

- Allow development of specialised functionality or a new concept
- Further the understanding of an analytical solution

TABBY is the first aerial triangulation software package to be developed at the IESSG. It owes some of its input data formats to the ORINT4 package [*Smith, 1986*]. It may, in future generations of photogrammetric research, serve as a guide or framework for software development. In the timescale of the study it has not been possible to approach the functionality of a commercial package, but the more important aspects which ensure a rigorous solution have been included. The package is modular in design (containing many self-contained routines) to aid future development.

7.3 TABBY - Aerial Triangulation Software

The development of all the software discussed in this chapter was undertaken in a popular high level programming language, C. Some of the fundamental matrix manipulation routines were included from early IESSG software development in the FORTRAN 77 programming language. FORTRAN 77 is a popular language for use in mathematical research, with C being more versatile and universally accepted for general software development tasks. A hybrid software development combines the benefits of both languages.

7.3.1 Software Platform

The primary development was undertaken on a Silicon Graphics Indigo workstation. The debugging of the software code and the analytical checks (§7.3.6) were achieved through the Casevision Workshop software development suite. The implementation of the C programming language used is compliant with standards defined by the American National Standards Institute (ANSI). These standards ensure that the software is portable across different hardware platforms and software compilers.

All the software described in this chapter has been tested on SGI Irix, SUN Solaris, Digital Unix and Linux operating systems. The programs can be compiled with either an ANSI compliant compiler or the GNU compiler.

7.3.2 Photograph And Point Limitations

All aerial triangulation software packages place some limitation on the number of photograph and point unknowns which can be concurrently estimated. In the commercial marketplace, it is often the case that these restrictions are considerably beyond the user's requirements. The limitation is usually only imposed because of a built-in restriction on the main memory *grabbed* by the software for its calculations.

Main memory can be allocated to software in a static or a dynamic manner. Dynamic allocation is often more preferable in cases where the memory required for a matrix calculation will vary depending on the number of unknown parameters in the calculation. The FORTRAN 77 programming language is unable to allow dynamic allocation of main memory but this is possible with ANSI C, illustrating a significant advantage of this programming language.

The aerial triangulation software in this research was initially developed to use only static memory allocation. This maintained the clarity of the least squares solution within the software code for effective debugging and testing. However the size of a single estimation is restricted:

- 20 photographs
- 100 ground points
- 800 image point observations

After the testing phase (§7.3.6), the memory allocation was converted to the dynamic mode. This significantly enhances the capacity for a single estimation by making a 75% reduction in the maximum main memory requirement compared to a similar static estimation. The photograph and point limitations for the final version used in the aerial triangulation investigations are:

- 100 photographs
- 100 ground points
- 1000 image point observations

These limitations are deemed to be the maximum requirement to successfully process any dataset during this research.

7.3.3 Program Structure

The basic principles of the bundle estimation have already been discussed at length in chapter 3. Figure 7.1 illustrates the basic program structure used to implement the bundle estimation process in TABBY.

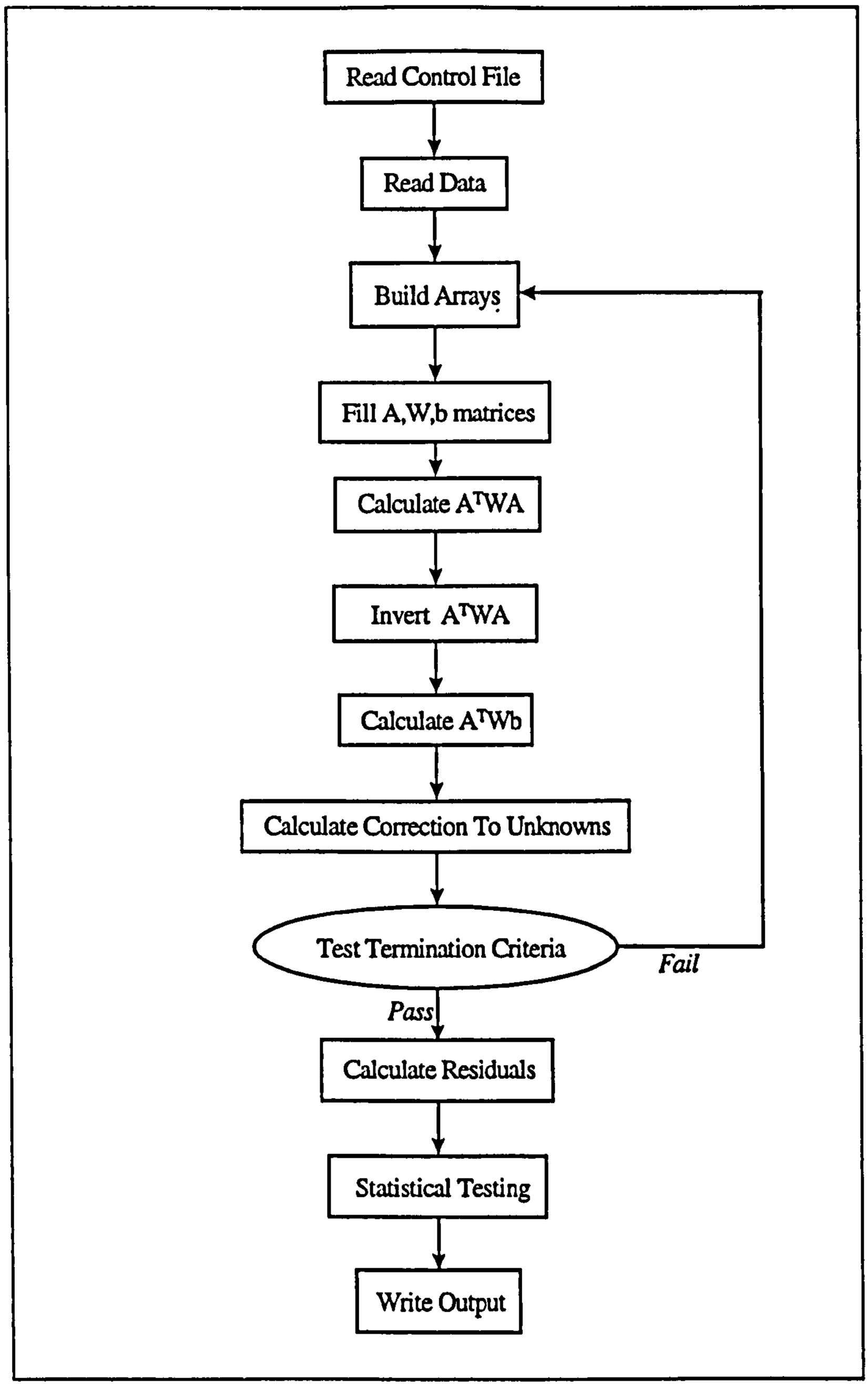

Figure 7.1 - TABBY Program Structure

The control file defines the parameters which are dynamic between successive program runs and so is read as the first task in the program. The definition of the number of points, photographs and GPS antenna positions is used to build matrix arrays which are the correct size for the estimation.

Observation equations are built up for each image point, ground point and GPS antenna coordinate to be used in the estimation and these are then used to build up the A and b matrices. This follows the linear model for observation equations which is used to obtain a least squares solution of the unknown parameters (§2.4.5).

The solution of these observation equations, which are weighted by the use of weight matrices, is a correction to each of the approximate values of the unknowns used to develop the observation equations. The least squares process is iterative so the observation equations are rebuilt with the updated approximate values and solved in the same way again (§2.4.8). The process repeats until the corrections to the unknown values are smaller than the termination criteria of the software.

Once the final corrections to the approximate values have been applied, the final parameters are output along with the residuals of the estimation and the results of appropriate statistical tests.

7.3.4 The Program Control File

The operational parameters of TABBY are altered through a simple text control file. This is shown in Figure 7.2.

The first parameter is the network ID which can be provided to prefix the names of the output files, which is important to prevent confusion over the results from successive estimations.

```
# TABBY version 3.11b Control File.
# Written by Chris Joy 1995/96.
#
# Pont96 Full Block
#
gball              ! Network ID.
520                ! Number x,y obs.
33                 ! Number of photos.
32                 ! GPS Antenna Positions
55                 ! Number of points.
1                  ! Real=1, Simulation=0;
1                  ! Combined GPS=1.
1                  ! Stochastic=1, Deterministic=0.
5.000              ! global image s.e. in microns.
0.005              ! global x ground s.e. weight in metres.
0.005              ! global y ground s.e. weight in metres.
0.002              ! global z ground s.e. weight in metres.
0.02786            ! x eccentricity.
-0.27014           ! y eccentricity.
2.11318            ! z eccentricity.
```

Figure 7.2 - Alteration of TABBY Operational Parameters With The Control File *tabby.ctl*

The number of observations, photographs, points and GPS antenna positions are defined in the control file as the next four parameters. It is historical that these quantities are defined in the control file and any incorrect definition will cause the estimation to fail. Extension of TABBY into a fully dynamic program, able to determine the size of the estimation without knowledge of these parameters, would be trivial.

Three 0-1 switches control the type of estimation. The first switch defines whether the real or simulated image observation datasets are being used. The second switch identifies the mode of operation as a traditional aerial triangulation or a GPS assisted aerial triangulation. Ground control points can be taken as fixed positions or used with a globally defined standard error by altering the third switch.

If the operation mode uses GPS antenna coordinates then the eccentricity of the antenna, in the image coordinate system, can be provided through the three final parameters in the control file.

7.3.5 The Data Files

There are four types of input file for the TABBY software. All the files are *free format* text files, which means that there is no restriction on the number of white space characters (space or tab fields) between each numerical field. The files are:

- TPOBS.IN The image point observation file
- PHOTO.IN The initial photograph orientations file
- POINT.IN The ground point file
- GPSANT.IN The GPS antenna coordinate file

The files can all be manually edited. However, the image point observation file, TPOBS.IN, can also be created from the pre-processor software discussed later in this section (§7.4.1). Further discussion of the data files is not included within the main body of this thesis. The reader is referred to Appendix B for sample file structure.

7.3.6 Analytical Testing

There are two possible approaches for testing aerial triangulation software. The first option utilises a common dataset and compares the final solution from the new software against that from a proven package. The second option is to work through the calculation stages and derive a series of intermediate solutions to compare against the software.

The software development tool, the Casevision Workshop, is able to display the value of any variable or matrix at user defined stages within the software. Given that no other established aerial triangulation package was available, the analytical testing was undertaken by the second option of benchmarking against intermediate solutions. The testing was repeated many times during the development cycle and this ensured that the software was correctly calculating the least squares solution.

7.3.7 Output Files

There are 10 different output files produced from the software. The primary file is the ground point residuals file which has an *out* suffix and includes the final adjusted ground point coordinates and their associated residual. The residual (§8.1) is an observed coordinate minus computed coordinate term with the computed term being the final ground point coordinates from the bundle estimation. The other three important files are the residual file, suffixed with *res*, the histogram file, suffixed with *his*, and the final coordinate file, suffixed with *crd*.

The residuals file and the histogram file are important for identification of outliers (§2.7.3). In addition to the observation residual, a test statistic is also calculated according to Baarda data snooping (§2.7.3).

The final coordinate file details the standard error of the derived parameters from the covariance matrices and the unit variance which is the primary indicator for the statistical analysis (§2.6.3).

The remaining files are detailed in Appendix B and include further information on the standard errors of the estimated quantities as well as summarising the final computed parameters in useful formats.

7.4 Additional Support Software

During the course of the research, it was necessary to develop several additional software packages to support the successful utilisation of the main triangulation package. Each contributes a minor additional function to the entire software suite and are described in the following sub-sections.

7.4.1 SCOOBIE - The Data Pre-Processor

The image point observations are invariably extracted from analytical plotter data files. They may be in some arbitrary order which is not suited to the required order for TABBY. The SCOOBIE pre-processor converts a file of image point observations to be ordered imagewise then pointwise.

```
#Scoobie version 1.0
#Written by Chris Joy January 1996
#
#
#
602     !Start Photo Number.
622     !Finish Photo Number.
5701    !Start Point Number.
6223    !Finish Point Number.
205     !Number of Obs.
```

Figure 7.3 - The SCOOBIE control file

The software is controlled by a simple data file with is shown in Figure 7.3. This file defines the start and finish numbering of both the photographs and the point numbers in the raw observations file. The total number of observations is also defined.

The input file of raw observations is called *rawdat.in* and is a free format text file. The program sorts the data and writes the output data to *tpobs.in*. This is

the same file naming convention used for the photogrammetric observations file in TABBY.

7.4.2 TRANSFORM - Coord. Transformation

In a GPS assisted bundle estimation, the ground points will usually be defined in a local ground coordinate system. In contrast, the GPS antenna phase centre positions output from GPS analysis software are usually given in the WGS84 global coordinate system. A prerequisite of the TABBY software is that the GPS antenna phase centre positions and ground point coordinates are defined in the same coordinate system. Therefore, one set of coordinates must be transformed in the coordinate system used by the other set before the data is entered into the Bundle estimation software.

The transformation parameters in this research are calculated with a three dimensional transformation package, 3DTRAN6, originally written for the work of *Smith* [1986]. A network of ground points defined in both the local coordinate system and the WGS84 system are entered into the software which calculated all the required parameters. The mathematical relationship between the coordinates of a point in two different systems is given equation 7.1.

$$\begin{bmatrix} x_b \\ y_b \\ z_b \end{bmatrix} = R \begin{bmatrix} x_a \\ y_a \\ z_a \end{bmatrix} + \begin{bmatrix} \Delta x \\ \Delta y \\ \Delta z \end{bmatrix} \qquad [7.1]$$

where:

$[x_b \quad y_b \quad z_b]^T$ is the coordinates of the point in coordinate system b

$[x_a \quad y_a \quad z_a]^T$ is the coordinates of the point in coordinate system a

$[\Delta x \quad \Delta y \quad \Delta z]^T$	is the datum shift from system a to system b
R	is the rotation matrix describing the axes rotation from system a to system b

This is the full 7 parameter Helmert transformation. The TRANSFORM software uses the parameters derived with 3DTRAN6 and applies them to a series of points according to equation 7.1. The operation of TRANSFORM is enabled through the definition of parameters in the control file shown in Figure 7.4.

```
# Transformation Control File
# Written by Chris Joy February 1996
#
#
#
1.000028071          !Scale Factor
0.016187860          !Omega
0.634603026          !Phi
3.141592654          !Kappa
3790808.67211        !Datum Shift X
-84217.45709         !Datum Shift Y
5111463.39582        !Datum Shift Z
33                   !Number of points.
0                    !Operation forward=0,backward=1;
```

Figure 7.4 - The TRANSFORM control file

The control file defines all seven transformation parameters for a particular test field. It also defines the number of points which are to be transformed. The final parameter is a switch which allows transformation of a series of points either way between coordinate system a and b previously discussed. The input coordinates are entered into a free format text file named *data.in*. The final transformed coordinates are written to the output file *coord.out*.

7.5 Summary

Aerial triangulation software using the principles of bundle estimation of unknown parameters has been developed as part of this research. The software can use image points observations, ground point coordinates and GPS antenna phase centre coordinates as input observation types. It has been developed for use on any variant of the Unix operating system with an ANSI C and FORTRAN 77 compiler.

Several additional programs are available to support the main triangulation software.

Chapter 8

Aerial Triangulation: Tests and Results

8.1 Introduction

The final data of a highway survey is typically provided to the client as a series of spot height strings along the various lanes of the highway or as a full topographical survey [*Boardman, 1994*], formatted into an appropriate data format for input into a computer based highway design package such as MOSS [*Stanbridge, 1987*].

In the traditional photogrammetric analysis phase of a highway survey, pairs of overlapping photographs are orientated as a *stereomodel* in a photogrammetric plotter to allow mapping of the required points. Ground control points are required to orientate this model, such that the image point measurements can be located as corresponding ground coordinates in the object space.

The primary objective of this research, and the subject of this chapter, is to investigate the potential use of both conventional aerial triangulation and GPS assisted aerial triangulation in the large scale mapping of highways. Specifically, it is important to investigate the quality of the derived coordinates of the ground points to be confident that a configuration can provide coordinates at the required accuracy. Since both the number and distribution of measured image points is fixed for each photographic overlap (§5.4.1), there are only three variables which can be altered between any two successive aerial triangulations. These are discussed in §8.2.

The primary indicator of quality used throughout the tests is the accuracy of the ground point coordinates. Specifically, a residual is derived from the discrepancy between the final estimated ground coordinates calculated in the triangulation and the computed coordinates calculated from the ground survey. An rmse value is then calculated from these residuals to give a single measure of accuracy for each axis of the ground control coordinate system.

The aerial triangulation tests are introduced in section 8.2 with an overview of the observation data and the configurations used in the triangulations. The results for the conventional aerial triangulation are given in section 8.3 and section 8.4 details the similar results for the GPS assisted aerial triangulation. Section 8.5 details some auxiliary testing that was undertaken as a result of the main testing. Further testing using minimal ground control in a GPS assisted aerial triangulation is detailed in section 8.6. The tests are further discussed in section 8.7 and section 8.8 and suggest areas for future investigation, including the investigation of coordinate precision and the application of statistical testing.

8.2 Introduction To The Tests

The aerial triangulation tests were performed in such a way that they could be compared to investigate the variation of the computed ground point coordinate accuracy. The number and distribution of image points is fixed for each photographic overlap (§5.4.1) and this means that there are only three variables which can be altered between any two successive aerial triangulations. These are:

- The block geometry (the number of photographs taken over the test field)
- The quantity and distribution of the ground control within the test field
- The use of GPS antenna phase centre positions (so called GPS assisted aerial triangulation)

Three lateral overlapping strips were taken of the Pontefract 1996 test field (§5.3.2) and these were combined into four separate photographic block configurations for the tests (§8.2.1). All the ground points were coordinated by a prior ground survey (§5.4.2) to provide a *ground truth* for the tests. This ground control is discussed in §8.2.2.

The theory of aerial triangulation using the method of bundles has been introduced (§2.4). In these tests, the observation data is introduced as weighted observation equations which relate the observations to the unknown parameters of photograph position and orientation parameters and the positions of the ground points. Three types of observation data (§5.4) are used: image point observations, ground control point observations and GPS antenna phase centre position observations. These are discussed in §8.2.3 to §8.2.5.

8.2.1 Photographic Configurations

There are four photographic configurations produced from the photography which was taken in the Pontefract 1996 field trial (§5.3.2):

- Centre Strip Only
- Two Lateral Overlapping Strips (Centre + Left)
- Two Lateral Overlapping Strips (Centre + Right)
- Full Block (Centre + Left + Right)

These configurations are used throughout this chapter to investigate the effect of additional photography on the quality of the aerial triangulation.

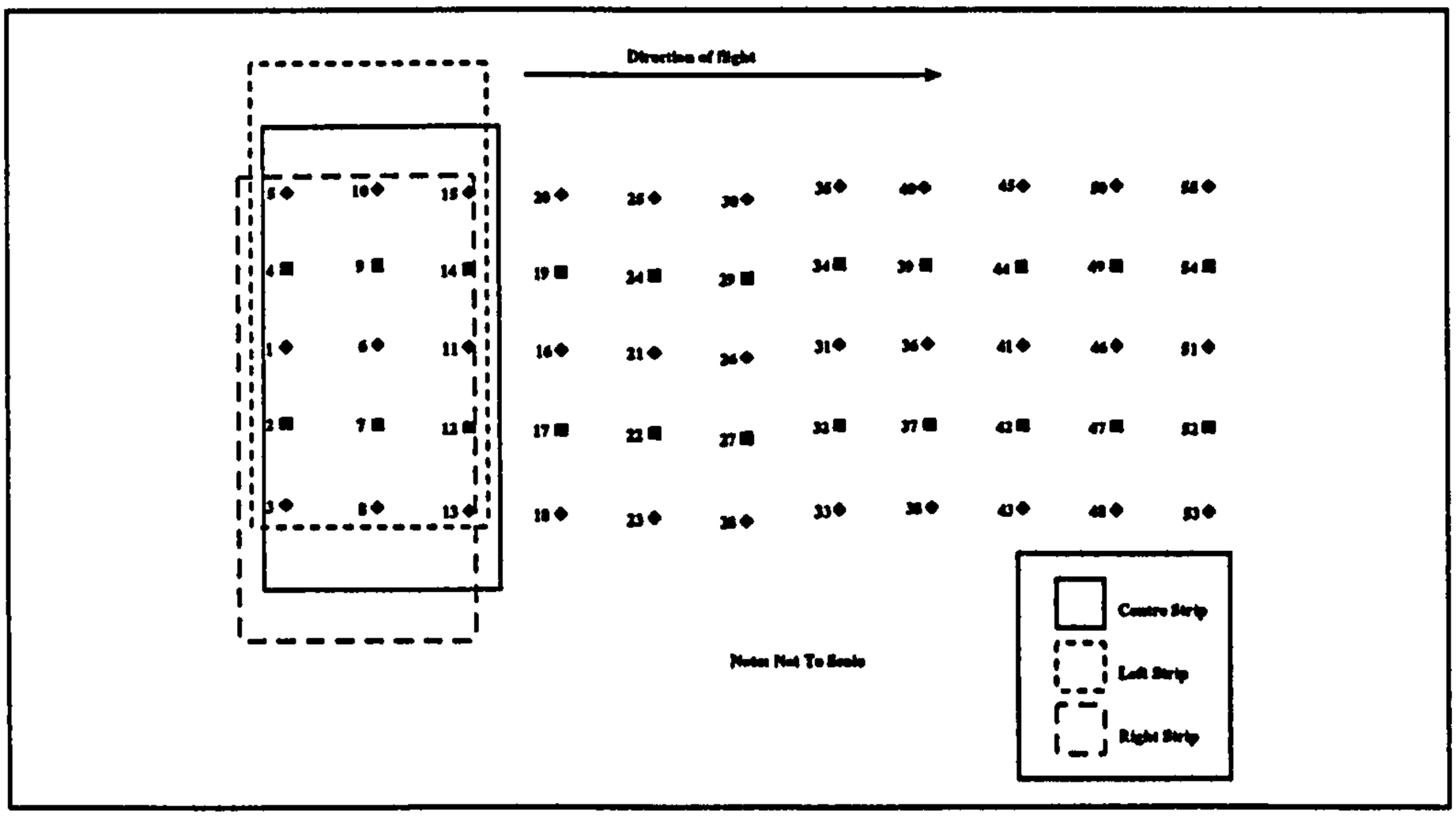

Figure 8.1 - Stereomodel Configuration Over The Test Field

The positioning of the stereomodels over the test field can be seen in figure 8.1. The two side strips are offset by 18m, so although all the ground points are imaged in each frame, they are offset to one side of the image area.

8.2.2 Ground Control Configurations

The standard ground control interval for 1:750 scale photography is 50m (§1.3). One control point is usually coordinated at the back of each hard shoulder of the highway. This means that two control points are coordinated every 50m interval of highway and this can be seen in Figure 8.2. In the tests performed in this research, three additional tie points are measured at the same interval along the test field (§5.4.1) and these are signalised points which have also been coordinated during the ground survey.

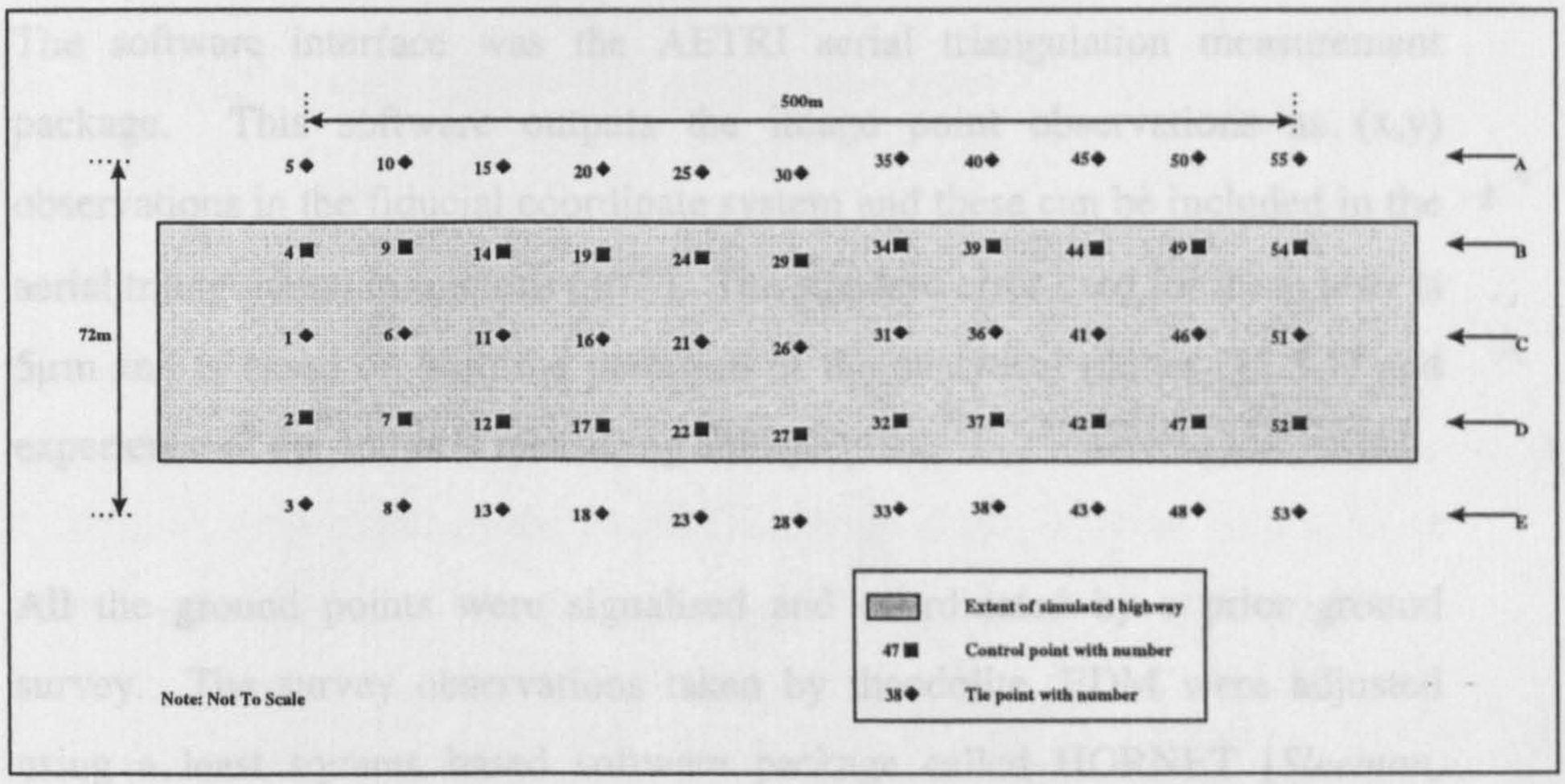

Figure 8.2 - Pontefract 1996 Ground Point Configuration

The 500m test field contains 55 ground points, with 20 points being ground control points and 35 being signalised tie points. The configuration of these points into different ground point strategies is referenced by the row in which they appear (for example, row B in figure 8.2).

8.2.3 Conventional Observation Data

The observation data used in the conventional aerial triangulation is image point observations and ground control point coordinates. The background to these observations has been given (§5.4) so this section details the methodology for introducing them as weighted observation in the aerial triangulation.

The Leica SD2000 analytical plotter at the University of Nottingham was used by the author to measure the tie points and control points on the photography. The software interface was the AETRI aerial triangulation measurement package. This software outputs the image point observations as (x,y) observations in the fiducial coordinate system and these can be included in the aerial triangulation in microns (10^{-6}). The standard error used for these tests is 5μm and is based on both the precision of the analytical plotter (§2.5.1) and experience of the author's measuring ability.

All the ground points were signalised and coordinated by a prior ground survey. The survey observations taken by theodolite, EDM were adjusted using a least squares based software package called HORNET [*Sleeman, 1992*]. The level information was calculated directly from the levelling observations with overlapping observations to provide an independent check. Both the a posteriori precision from the HORNET adjustment and the precision of the digital level instrument is used to suggest a suitable standard error for the ground control coordinates. The control point standard errors used for these tests are 0.005m in both the x and y direction, and 0.002m in height.

8.2.4 GPS Antenna Phase Centre Position Data

The GPS antenna phase centre observations were processed using the Ashtech PNAV package (§4.2.4) to produce coordinates in the WGS84 global coordinate system. The coordinates at each GPS antenna position were compared to a photogrammetrically derived 'truth' coordinate (§6.10.2) to assess both the performance of the GPS during the field trial and the suitability of the GPS antenna location. This accuracy of the GPS antenna position provided an estimate for the standard error of 0.005m in all directions.

8.2.5 Coordinate Transformation

In the aerial triangulation, the ground points are computed in an arbitrary local ground coordinate system. In contrast, the GPS antenna phase centre positions output from the PNAV software are given in the WGS84 global coordinate system. A prerequisite of the TABBY software is that both the GPS antenna phase centre positions and the ground point coordinates are defined in the same coordinate system (§7.4.2) .

The GPS antenna coordinates were transformed into the local coordinate system before being included in the aerial triangulation. The transformation was calculated with a three dimensional transformation package, 3DTRAN6 (§7.4.2) using a network of ground points defined in both the local coordinate system and the WGS84 system. The coordinate rmse of this transformation was 0.007m.

8.2.6 Ground Point Residuals

In each test, the ground point residuals (§8.1) are split into two groups. These are the tie points and the control points, whose position on the photographs has

been discussed (§5.4.1) and can be related to the ground points in figure 8.2. The tie points represent the similar observations that may be made during aerial triangulation data collection to allow a stable orientation of the photographs [*Slama, 1980*]. They are sometimes natural features on the ground, but in this research the tie points have been signalised and coordinated to provide a full assessment of aerial triangulation accuracy. It would also have been difficult to measure natural features on the grass runway and surrounding fields.

To provide a single measure of accuracy, the two types of residuals are grouped together with a root mean square error (rmse) value. This is calculated according to equation 8.1:

$$x = \sqrt{\frac{\sum_{1}^{n} v^2}{n}} \qquad [8.1]$$

where:

x	is the root mean square error of either tie point or control point residuals
v	is the residual of the ground coordinate
1....n	is the group of observations from which the rmse is to be calculated

The rmse is calculated for the residuals along each of the coordinate axes which gives upto six rmse values per aerial triangulation configuration. This assumes that both tie points and control points are included in the test.

8.3 Conventional Aerial Triangulation

The use of conventional aerial triangulation is the simplest method investigated in this research for reducing the aforementioned ground control requirement. This is because GPS antenna phase centre positions are not used

and so the GPS positioning system is not required for a photogrammetric flight. The tests described in this section investigate whether a combination of reduced ground control and varying photographic configurations can be used to compute ground point coordinates without a significant reduction in accuracy.

8.3.1 Pontefract 1996 Data Validation

The first stage of the conventional aerial triangulation tests is to validate the data as suitable for use. The validation is a way of discovering how well the photogrammetric observations fit onto the ground control points and vice-versa. It is also a way of finding and removing any gross errors in the image point observations.

It has already been described (§8.2.3) how all the ground points are actually three dimensionally coordinated control points. This is important because it provides ground point *truth* coordinates which, at this stage, can be assumed to be of a significantly higher accuracy. An aerial triangulation run was configured with the following data:

- Image point observations from all three strips of photography (full block)
- All ground points configured as 3-d control points
- Ground control precision as defined in §8.2.3
- Image point precision as defined in §8.2.3

The first stage after the aerial triangulation run is to investigate the image point observation residuals. This is calculated from equation 2.16 and is a comparison of the observed image point observations against the computed values from the triangulation. Since the expected precision of the observations was 5μm, the criteria for rejection of an observation was if the residual was greater than 15μm.

A histogram can be plotted to show the distribution of the residuals. Figure 8.3 resembles the normal distribution curve of Figure 2.3 [*Crawshaw and Chambers, 1984*].

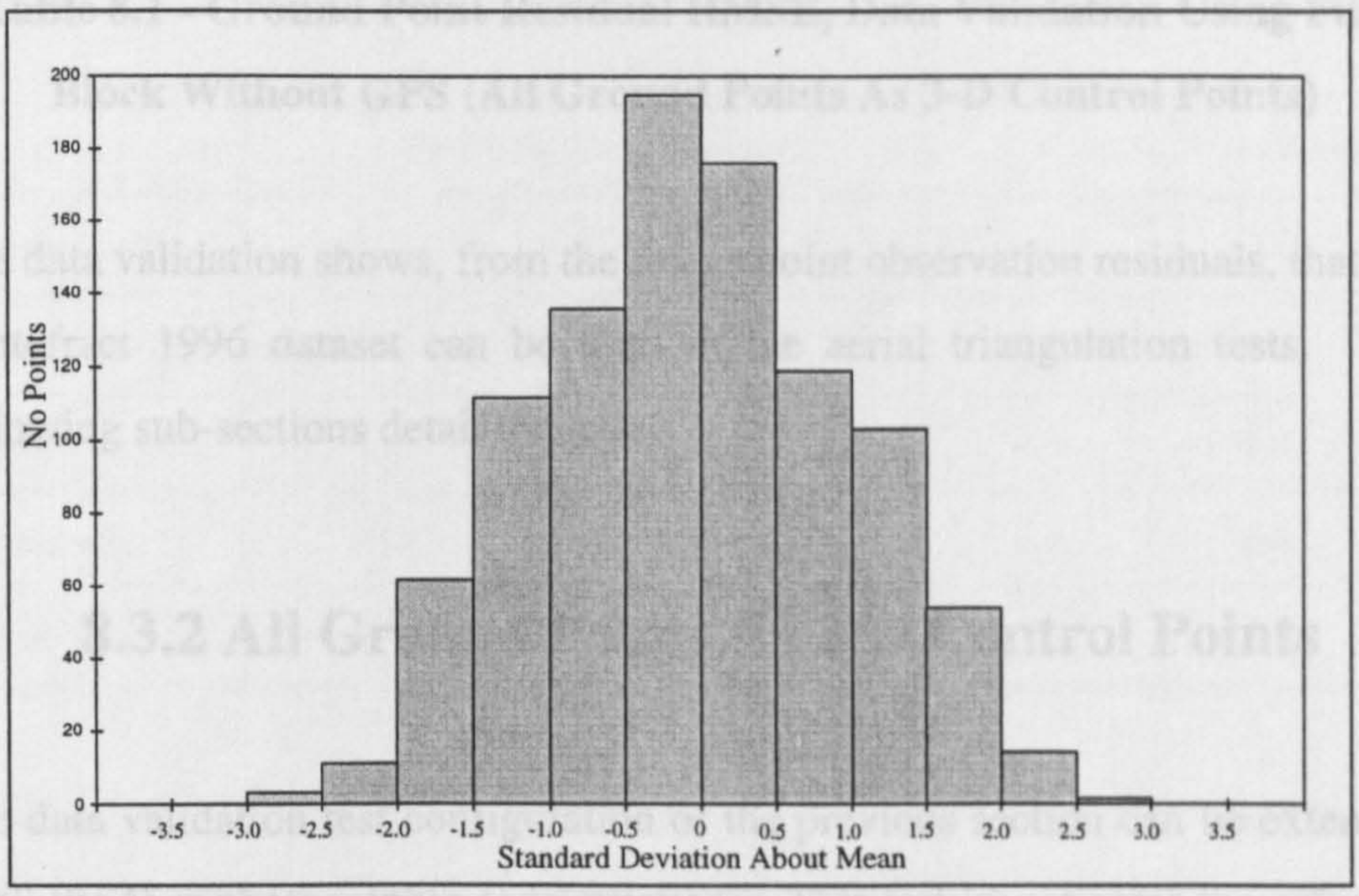

Figure 8.3 - Histogram Of Image Point Residuals For Full Block With All Points As 3-D Control

The measure of accuracy of ground point coordinate determination can be seen by calculating the ground coordinate residuals for each ground point. This residual is derived from the discrepancy between the final estimated ground coordinates calculated in the triangulation and the initial coordinates calculated from the ground survey. A root mean square error of the residuals for each ground point (§8.2.6) is calculated for each axis of the ground control coordinate system:

The residual rmse values show that the ground control residuals are greater along the x axis than along the y axis of the coordinate system. The x axis corresponds to the direction of flight, parallel to the strips of photography. The y axis is perpendicular to the direction of flight.

	Tie Point RMSE (mm)			Control Point RMSE (mm)		
Photo Config	**X**	**Y**	**Z**	**X**	**Y**	**Z**
Full Block	-	-	-	10.0	4.6	2.9

Table 8.1 - Ground Point Residual RMSE, Data Validation Using Full Block Without GPS (All Ground Points As 3-D Control Points)

The data validation shows, from the image point observation residuals, that the Pontefract 1996 dataset can be used in the aerial triangulation tests. The following sub-sections detail the tests.

8.3.2 All Ground Points As 3-D Control Points

The data validation test configuration of the previous section can be extended to all the four photographic configurations. This test investigates the effect of additional image point observations from side strips of photography on the determination of the ground point coordinates.

Table 8.2 shows residual rmse values for each of the photographic configurations. In this test, there are no tie points because all the points are control points.

The ground control point residual rmse values become marginally worse in the x and y direction (which are the two component of the plan position) when the additional strips of photography are used. This implies that the centre strip only case gives the best fit between the photogrammetric observations and the ground control points.

The ground control point height residual rmse shows a more marked change between photographic configurations. The height residual rmse is significantly increased from the centre only configuration to the full block configuration.

The high rmse residual for the full block configuration could be caused by the left strip because the ground control point height residual rmse for the centre + left photographic configuration is also relatively high. The centre + left residual rmse is significantly higher than the similar residual rmse for the centre + right photographic configuration.

	Tie Point RMSE (mm)			Control Point RMSE (mm)		
Photo Config	**X**	**Y**	**Z**	**X**	**Y**	**Z**
Centre only	-	-	-	9.8	4.2	1.5
Centre + Left	-	-	-	9.8	4.4	2.8
Centre + Right	-	-	-	9.9	4.6	2.0
Full Block	-	-	-	10.0	4.6	2.9

Table 8.2 - Ground Point Residual RMSE, 4 Photographic Configurations Without GPS (All Ground Points As 3-D Control Points)

A further pattern that can be seen in Table 8.2 is that the residual rmse along the x axis is greater than the residual rmse along the y axis and this is not affected by the different photographic configurations. This can be better illustrated by plotting the individual coordinate residuals along the x and y axes on a vector diagram. The diagrams C.1.1 to C.1.4 in Appendix C show the ground point coordinate residuals for the x and y axes separate to the height axis residuals. The x axis of the ground coordinate system is along the direction of flight and it can be seen that the residuals are greater in this direction. Whilst the magnitude of the arrows in the plot changes marginally between the four photographic configurations, the pattern displayed by the arrows remains similar. There is a clockwise rotation pattern in the residuals with the greatest residuals to be found at the outside points and particularly at the ground survey observation stations.

8.3.3 3-D Control Points At 50m Interval

The ground control points which would be coordinated along the hard shoulder of each side of a highway were established in the same way along the simulated highway of the Pontefract 1996 field trial. This corresponds to rows B and D in figure 8.2. At this scale of photography (1:750) there is a requirement for ground control points at a 50m spacing along the fictitious highway (§8.2.2). In the single model orientation procedure used traditionally by Photarc Surveys Ltd (§1.3), the 4 control points that fall in each stereomodel would be utilised. This test uses all the ground control points that would be used in single model orientation. The control points are all the points on rows B and D (figure 8.2).

Table 8.3 shows the residual rmse values for each of the photographic configurations.

	Tie Point RMSE (mm)			Control Point RMSE (mm)		
Photo Config	**X**	**Y**	**Z**	**X**	**Y**	**Z**
Centre only	11.3	5.6	6.3	8.6	3.8	2.0
Centre + Left	11.1	5.3	6.0	8.5	3.6	2.9
Centre + Right	11.1	5.6	5.4	8.4	4.0	1.9
Full Block	11.1	5.7	6.5	8.6	4.4	4.0

Table 8.3 - Ground Point Residual RMSE, 4 Photographic Configurations Without GPS (3-D Control Points At 50m Interval)

In a similar way to the residual rmse values for the ground control configuration discussed in the previous section, the residual rmse along the x axis is worse than the residual rmse along the y axis. This can be seen in the residual plots C.2.1 to C.2.4 which cover the four photographic configurations.

Table 8.3 shows that the use of additional strips of photography appears to reduce the ground point accuracy. The tie point height residual rmse value of the full block photographic configuration is worse than the centre strip only configuration. This could be influenced by the height residual rmse value of the centre + left photographic configuration which is higher than for the centre + right photographic configuration. The x and y axis residual rmse values are not significantly changed between the photographic configurations and this can also be seen in the residual plots C.2.1 to C.2.4 which show that there is only a marginal change in the direction and magnitude of the individual coordinate residuals.

The control point height residual rmse values show the same pattern as the tie points. The centre only photographic configuration produces a significantly higher accuracy than the full block configuration and this could be caused by the left strip of photography as previously discussed. A possible explanation for the poor performance of the side strips is that both the tie points (rows A, C and E) and the control points (rows B and D) fall to one side of the side strip's image area (figure 8.2). This could affect the quality of the aerial triangulation.

8.3.4 3-D Control Points At 250m Interval

It has already been explained that a highway survey requires permanent ground markers (PGM) to be installed at a 250m spacing along the carriageway (§1.3). Since these markers must be coordinated, it might be useful to utilise them as ground control points for the photogrammetry. This test investigates the effect on the aerial triangulation when 3-D ground control points are provided at a 250m interval along the test field. The points are along rows B and D (figure 8.2) of the test field which corresponds to a point at either end of the row and one in the middle.

Table 8.4 shows the residual rmse values for each of the photographic configurations.

	Tie Point RMSE (mm)			Control Point RMSE (mm)		
Photo Config	**X**	**Y**	**Z**	**X**	**Y**	**Z**
Centre only	14.4	8.8	19.0	7.5	2.9	1.2
Centre + Left	12.8	6.5	11.9	6.8	3.5	2.8
Centre + Right	11.6	6.6	13.0	7.6	1.6	1.8
Full Block	12.0	7.4	11.7	6.7	4.6	5.5

Table 8.4 - Ground Point Residual RMSE, 4 Photographic Configurations Without GPS (3-D Control Points At 250m Interval)

The phenomenon seen in the previous tests where the use of additional photography reduces the accuracy of the ground point coordinates, is reversed in this test. It has a beneficial effect on the accuracy, with the tie point height residual rmse reduced by almost half between the centre strip only photographic configuration and the full block photographic configuration. The tie point x and y axis residual rmse values are also reduced as the photographic configuration is altered. The increase in accuracy is not as sharp as in the height axis, but is several millimetres overall.

The residuals for this test are shown in residual plots C.3.1 to C.3.4. The x axis and y axis vector plots show a clockwise rotating trend centred around the two central control points. The rotation pattern is constant across the four photographic configurations but the magnitude of the residuals on some of the outside points is varied. The points within the first half of the test field have larger coordinate residuals than the second half.

The improvement in height accuracy which has been discussed from table 8.4 can be clearly seen the residual plots C.3.1 to C.3.4. The height residual bubbles are significantly larger on plot C.3.1 which represents the centre strip

only photographic configuration. Within this plot, the accuracy is worse in the first half of the test field. The use of additional photography improves the accuracy and the height bubble plots in C.3.2 to C.3.4 are similar in both pattern and magnitude of the individual residuals. The residuals in the first half of the test field are more similar to those in the second half, with the height accuracy greatest at both ends and the centre of the test field (the locations of the control points).

A comparison of the values in table 8.4 with those of table 8.3 shows that the residual rmse values for the tie points are higher than those in the 50m interval control configuration. The residual rmse on the tie points is moderately worse along the x axis and y axis. The height residual rmse is approximately double the 50m interval control values.

A poorer aerial triangulation accuracy might be expected in this test because there is not as much ground control. There is a greater reliance on the internal photogrammetric geometry. The improvement in accuracy when additional side strips are used is in contrast to the previous tests. This phenomenon could suggest that there is a problem with some of the ground control because there is less ground control in this test.

8.3.5 3-D Control Points At 500m Interval

The test field is 500m long so the maximum interval of control points is 500m. A minimum of three plan and two height control points are required to allow the transformation into the ground coordinate system, so this configuration which uses four points is the minimum number of control points that are used in the aerial triangulation tests where no additional observations (GPS antenna phase centre positions) are provided. This test investigates the effect on the aerial triangulation when the amount of ground control is reduced to the maximum interval allowed by the test field. The control points are at either end of rows B and D (figure 8.2).

Table 8.5 shows the residual rmse values for each of the photographic configurations.

	Tie Point RMSE (mm)			Control Point RMSE (mm)		
Photo Config	**X**	**Y**	**Z**	**X**	**Y**	**Z**
Centre only	19.2	8.1	64.5	6.6	6.4	1.6
Centre + Left	24.6	8.3	83.6	6.3	5.9	4.1
Centre + Right	17.5	11.8	83.7	7.4	1.4	2.9
Full Block	12.2	10.5	85.3	6.4	2.8	6.9

Table 8.5 - Ground Point Residual RMSE, 4 Photographic Configurations Without GPS (3-D Control Points At 500m Interval)

The potential problem with the left strip of photography can be seen clearly in table 8.5. The height residual rmse for both the tie points and the control points are significantly increased over the centre strip only photographic configuration. It is possible that this also has an effect on the full block photographic configuration residual rmse values. There is some degradation in x axis coordinate accuracy when the left strip of photography is used but this is not propagated into the full block rmse values because this shows an improvement in accuracy over the centre strip only photographic configuration.

There is an increase in the tie point residual rmse when additional strips of photography are included in the triangulation. Again, the use of the left strip of photography produces a higher residual rmse for the tie points, particularly along the x axis and the z axis. In this test, the higher residual rmse values is also seen along the z axis when the right strip is included in the triangulation.

The diagrams C.6.1 to C.6.4 show the individual ground point coordinate residuals for the four photographic configurations in this test. It can be seen in

the height bubble plots that the height residuals increase from a minimum at the ends where the control points are positioned, to a maximum at the centre of the test field. The higher residuals are in the first half of the test field.

The vector plots for the x and y axis residuals in diagrams C.6.1 to C.6.4 show that in addition to a varying magnitude, as seen in table 8.5, the residuals display a change in pattern between each photographic configuration. When each additional side strip of photography is used (diagrams C.6.2 and C.6.3), the higher residuals are on the same side of the test field as the additional photography. The direction of the residuals along the x axis is reversed between the two cases. The overall effect of the photography is seen in the full block configuration, shown in diagram C.6.4 where the higher residuals are down the right side and concentrated in the first half of the test field.

A comparison of the values in table 8.5 with those of table 8.3 shows that the residual rmse values for the tie points are increased over the 50m interval control configuration. The residual rmse on the tie points is double the 50m interval control values along the x axis and y axis for all but the full block photographic configuration where the residual rmse is only moderately worse than the 50m case. The height residual rmse is more than a factor of 10 times the 50m interval control values.

8.3.6 Summary

Conventional aerial triangulation has been performed with image point observations and ground control points derived from the Pontefract 1996 field trial. The data validation (§8.3.1) test shows that the coordinate accuracy is significantly worse along the x axis than the y axis and this could be attributed to the geometry of the test field. The x axis is parallel to the direction of flight for the photographic strips and the test field is much longer than it is wide.

The residual vector plots of Appendix C show that there is a systematic error trend to the plan coordinate residuals. There is little variation in this trend as additional photographic strips are included in the aerial triangulation, so this is a potential ground control coordinate problem.

The use of additional strips of photography tends to produce lower coordinate accuracy in the triangulation of the test field. There is evidence to suggest that use of the left strip of photography causes a particularly poor triangulation. This phenomenon could be a ground control coordinate problem because the use of additional photography improves the accuracy in the 250m control case (§8.3.4). The choice of ground control is also important if some of the points have been poorly coordinated.

	Tie Point RMSE (mm)			Control Point RMSE (mm)		
Control Interval (m)	**X**	**Y**	**Z**	**X**	**Y**	**Z**
50	11.3	5.6	6.3	8.6	3.8	2.0
250	14.4	8.8	19.0	7.5	2.9	1.2
500	19.2	8.1	64.5	6.6	6.4	1.6

Table 8.6 - Summary of Ground Point Residual RMSE, Varying 3-D Control interval Without GPS (Centre Strip Only)

A summary of the ground point residual rmse values for the centre strip only photographic configuration is shown in Table 8.6 for the different 3-D ground control configurations. As the ground control is reduced from the maximum configuration of 3-D control at a 50m interval, the tie point height coordinate accuracy becomes significantly worse. At the 250m control interval, the tie point height residual rmse is approximately double the 50m value. When the ground control is reduced to the maximum interval of 500m, the tie point height residual rmse is a factor of 10 times the 50m value. The residual bubble plots show clearly how the tie point height errors propagate between the

control points and this is most clear for the plots of the 500m control interval test.

The x and y axes tie point residuals are also increased as the ground control is reduced. At the 250m control interval, the tie point coordinate residuals are only moderately worse than the 50m values. When the ground control is reduced to the maximum interval of 500m, the x and y axes tie point residuals are significantly increased. In some cases, the increase is approximately double the 50m values but this is less when additional photographic strips are used in the triangulation.

The results of the conventional aerial triangulation are further discussed in §8.7.

8.4 GPS Assisted Aerial Triangulation

The inclusion of GPS antenna phase centre positions as additional observation data in the aerial triangulation should allow a greater reduction in the amount of ground control which is required. In fact, ground control may not be required if the transformation parameters between WGS84 and the local system are already known or the coordinates are required in the WGS84 system (§4.3.2).

This series of tests mainly repeats the photographic and ground control configurations of the conventional aerial triangulation tests. A test is also configured as a GPS assisted aerial triangulation without any ground control point observations (§8.4.6).

8.4.1 Pontefract 1996 Data Validation

The first stage of the conventional aerial triangulation tests in the previous section was to validate the data. The validation was a way of discovering how well the photogrammetric observations fit onto the ground control points and vice-versa. It was also a way of finding and removing any gross errors in the image point observations.

The data validation can be extended to the GPS assisted aerial triangulation tests to investigate how well the GPS antenna phase centre position observations fit to the other observations. An aerial triangulation was configured with the following data:

- Image point observations from all three strips of photography (full block)
- All ground points configured as 3-D control points
- GPS antenna phase centre positions for each exposure station
- Ground control precision as defined in §8.2.3
- Image point precision as defined in §8.2.3
- GPS antenna phase centre position precision as defined in §8.2.4

The image point observations were the same as those used in the conventional aerial triangulation tests. These had already been checked for gross errors (§8.4.1) and no image point gross errors were apparent in this validation test.

The measure of accuracy of ground point coordinate determination can be seen by calculating the ground coordinate residuals for each ground point. The rmse value of these residuals is shown in table 8.7 for each coordinate axis.

	Tie Point RMSE (mm)			Control Point RMSE (mm)		
Photo Config	**X**	**Y**	**Z**	**X**	**Y**	**Z**
Full Block	-	-	-	9.8	4.8	2.8

Table 8.7 - Ground Point Residual RMSE, Data Validation Using Full Block With GPS (All Ground Points As 3-D Control Points)

The rmse values shown the familiar pattern of the residuals being greater along the x axis than along the y axis. A comparison with the conventional aerial triangulation data validation results of table 8.1 shows that the accuracy is marginally higher at the sub-millimetre level.

A rmse value can be calculated for the residual of the GPS antenna phase centre positions from the discrepancy between their final computed positions from the triangulation and the initial values computed from the PNAV software. In this data validation test, the residuals are 0.03m along the x axis, 0.03m along the y axis and 0.03m along the height axis. These values show that the GPS positions fit well in the triangulation.

8.4.2 All Ground Points As 3-D Control Points

In the same manner as §8.3.2, the data validation test can be extended to all the four photographic configurations. This test investigates the effect of additional photography on the GPS assisted aerial triangulation and, by comparison with table 8.2, enables an investigation of the effect of the GPS observations on the computed coordinate accuracy of an aerial triangulation.

Table 8.8 shows the residual rmse values for each of the photographic configurations.

	Tie Point RMSE (mm)			Control Point RMSE (mm)		
Photo Config	**X**	**Y**	**Z**	**X**	**Y**	**Z**
Centre only	-	-	-	9.9	4.2	1.5
Centre + Left	-	-	-	9.6	4.3	2.7
Centre + Right	-	-	-	9.8	4.7	2.0
Full Block	-	-	-	9.8	4.8	2.8

Table 8.8 - Ground Point Residual RMSE, 4 Photographic Configurations With GPS (All Ground Points As 3-D Control Points)

A comparison with table 8.2 shows that the inclusion of the GPS antenna phase centre observations marginally improves the accuracy of the aerial triangulation. The residual rmse values for the control points are reduced at the sub-millimetre level along all three coordinate axes.

The trends in the control point residual rmse values follow the same pattern as the conventional aerial triangulation results of table 8.2. The use of additional strips of photography produces a marginal decrease in accuracy for the plan axes and a significant decrease in height accuracy. Again, the left strip of photography appears to produce a lower accuracy for the ground point coordinates than the right strip of photography.

The diagrams C.5.1 to C.5.4 show the individual ground point coordinate residuals and this can be compared to the plots for the conventional aerial triangulation tests (C.1.1 to C.1.4). It can be seen that the plots from the two tests follow a near-identical pattern with only a marginal change in the magnitude of some of the residuals. The same clockwise rotation pattern (§8.3.2) can be seen in the xy residual vector plots, with the greatest residuals to be found at the outside points and particularly at the ground survey observation stations.

8.4.3 3-D Control Points At 50m Interval

In the single model orientation procedure used traditionally by Photarc Surveys Ltd (§1.3), the ground control points would be established at a 50m interval along the hard shoulder of the highway. This test uses all the ground control points that would be used in single model orientation and by comparison with table 8.3 enables a comparison with a conventional aerial triangulation using only image observations and 3-D ground control points.

Table 8.9 shows the residual rmse values for each of the photographic configurations.

A comparison with table 8.3 shows that the inclusion of the GPS antenna phase centre observations only marginally improves the accuracy of the aerial triangulation. The tie point residual rmse values are reduced at the sub-millimetre level along all three coordinate axes, although there is a marginal increase in the residual along the y axis when the right strip of photography is included.

	Tie Point RMSE (mm)			Control Point RMSE (mm)		
Photo Config	**X**	**Y**	**Z**	**X**	**Y**	**Z**
Centre only	11.2	5.3	6.0	8.4	3.5	1.4
Centre + Left	11.0	5.2	5.8	8.2	3.7	3.0
Centre + Right	11.1	6.0	5.6	8.5	4.5	2.0
Full Block	10.9	6.4	6.4	8.4	5.2	4.1

Table 8.9 - Ground Point Residual RMSE, 4 Photographic Configurations With GPS (3-D Control Points At 50m Interval)

The reason for the minimal accuracy improvement in the GPS assisted aerial triangulation could be that there is a lot of ground control in this test. Since

this has a higher precision than the GPS antenna phase centre coordinates, it may have a greater effect on the triangulation.

The use of additional photography in this test shows a similar pattern to the conventional aerial triangulation test (§8.3.3). The tie point height residual rmse is increased between the centre strip only photographic configuration and the full block photographic configuration. The height residual rmse for the centre + left photographic configuration and the centre + right configuration are different and this could affect the aforementioned full block residuals.

The residuals along the x and y axes are not significantly changed between the photographic configurations, although the y axes residual rmse is slightly increased as additional photography is included. The control point residual rmse values are significantly increased along the height axis in a similar pattern to the conventional aerial triangulation test.

The diagrams C.6.1 to C.6.4 show the individual ground point coordinate residuals for the four photographic configuration in this test. The phenomenon of the coordinate residuals being greater along the x axis than the y axis can be seen in all of the vector plots. If the diagrams are compared to the diagrams for the conventional aerial triangulation using the same 50m control interval (C.2.1 to C.2.4), it can be seen that they display the same characteristics. The changes in pattern and magnitude of the residuals are similar as the photographic configuration is altered. There is only a marginal change in the magnitude of some of the individual vectors and bubbles. Again, the similarities in behaviour between this test and the conventional aerial triangulation could be caused by the large quantity of ground control.

8.4.4 3-D Control Points At 250m Interval

A highway survey requires permanent ground markers (PGM) to be installed at a 250m spacing along the carriageway (§1.3). This test investigates the effect

on GPS assisted aerial triangulation when 3-D ground control points are provided at a 250m interval along the test field. A comparison with table 8.4 enables a comparison with a conventional aerial triangulation using only image observations and 3-D ground control points.

Table 8.10 shows the residual rmse values for each of the photographic configurations.

	Tie Point RMSE (mm)			Control Point RMSE (mm)		
Photo Config	**X**	**Y**	**Z**	**X**	**Y**	**Z**
Centre only	11.6	6.6	13.5	8.4	2.1	1.5
Centre + Left	10.8	5.9	9.9	6.7	2.7	2.0
Centre + Right	11.2	5.6	13.1	8.1	3.3	2.2
Full Block	10.4	6.9	10.9	7.2	6.1	4.0

Table 8.10 - Ground Point Residual RMSE, 4 Photographic Configurations With GPS (3-D Control Points At 250m Interval)

A comparison with table 8.4 shows that the tie point residual rmse values are lower when the GPS antenna phase centre observations are included in the aerial triangulation. In the case of the centre strip only photographic configuration, the height residual rmse is reduced by several millimetres. The additional photographic strips had improved the conventional aerial triangulation and it can be seen that the benefit of the GPS observations is less significant for the full block photographic configuration. The height accuracy improvement for that configuration is only at the sub-millimetre level.

The improvement in accuracy over the conventional aerial triangulation along the y axis is at the sub-millimetre level for each photographic configuration. The improvement along the x axis is higher, with a decrease in the residual rmse value of several millimetres for the centre strip only photographic configuration.

The use of additional photography in this test shows a similar pattern to the conventional aerial triangulation test (§8.3.4). The tie point residual rmse values are marginally improved along both the x axis and the y axis. The height axis residuals are significantly improved on the tie points.

The diagrams C.7.1 to C.7.4 show the individual ground point coordinate residuals for the four photographic configuration in this test. The x axis and y axis arrow plots are similar to the plots for the conventional aerial triangulation test shown in diagrams C.3.1 to C.3.4. A clockwise rotating trend centred around the two central control points is apparent and this rotation pattern is constant across the four photographic configurations. Only the magnitude of the residuals on some of the outside points is varied between the configurations.

The improvement in tie point height coordinate residual can be seen between diagram C.7.1 and diagram C.7.4. Throughout this series of diagrams, it is clear that the height residuals are always higher in the first half of the strip and the pattern is affected by the photographic configuration.

8.4.5 3-D Control Points At 500m Interval

The test field is 500m long so the maximum interval of control points is 500m. In the conventional aerial triangulation tests, this is the minimum number of control points that are used. This test investigates the effect on the aerial triangulation when the amount of ground control is reduced to the maximum interval allowed by the test field. A comparison with table 8.5 enables a comparison with a conventional aerial triangulation using only image observations and 3-D ground control points.

Table 8.11 shows the residual rmse values for each of the photographic configurations.

	Tie Point RMSE (mm)			Control Point RMSE (mm)		
Photo Config	**X**	**Y**	**Z**	**X**	**Y**	**Z**
Centre only	24.4	8.8	21.0	6.7	2.6	1.3
Centre + Left	11.0	8.9	,18.6	6.7	2.9	2.7
Centre + Right	14.0	6.5	21.5	7.1	2.8	1.8
Full Block	10.5	10.9	20.8	6.9	5.6	4.2

Table 8.11 - Ground Point Residual RMSE, 4 Photographic Configurations With GPS (3-D Control Points At 500m Interval)

A comparison with table 8.5 shows that the height residual rmse value is significantly lower for both the tie points and the control points when the GPS antenna phase centre observations are included in the aerial triangulation. In the case of the full block photographic configuration, the improvement is by a factor of 4 for the height residual rmse value of the tie points. The improvement in the height residual rmse value for the control points is less significant but is still several millimetres.

The plan residual rmse value is generally reduced by a small amount. In the case of the full block photographic configuration, the x axis residual rmse value is reduced by a couple of millimetres when the GPS observations are included. One significant change in the x axis residuals of table 8.5 can be seen in the centre + left photographic configuration. The tie point residual is improved by a factor of 2 when the GPS observations are included.

Contrary to the conventional aerial triangulation test summarised in table 8.5, the use of additional photography marginally improves the accuracy of the GPS assisted aerial triangulation in this test. Between the centre only photographic configuration and the full block photographic configuration, the tie point residual rmse value is decreased along the x axis and marginally increased along the y axis. There is a marginal improvement in the tie point

residual rmse value along the height axis. The control point residual rmse values are marginally increased along the x axis and significantly increased along both the y axis and the height axis.

The diagrams C.8.1 to C.8.4 show the individual ground point coordinate residuals for the four photographic configurations in this test. It can be seen that the height residuals are higher in the first half of the strip for the centre only photographic strip, shown in diagram C.8.1, and this pattern is not affected by additional photographic strips.

It can be seen in the diagrams C.8.1 to C.8.4 is that the x axis residuals are always higher than the y axis residuals. This is the same phenomenon that has been seen throughout the tests. The use of additional photographic strips appears to increase the residuals along the y axis and this can also be seen in the diagrams. The increase in y axis residuals can be attributed to the clockwise rotational pattern of diagram C.8.2 to C.8.4. This pattern is similar to the conventional aerial triangulation.

8.4.6 No Ground Control Points

The ultimate reduction in ground control points for a GPS assisted aerial triangulation is to not include any control points. If the ground points are to be coordinated in the WGS84 global coordinate system, or the transformation parameters to the local coordinate system are known, the ground control points may only be required to prevent the propagation of errors that is apparent in the conventional aerial triangulation. This test shows the attainable accuracy for a triangulation where no control points are included.

Table 8.12 shows the residual rmse values for each of the photographic configurations.

	Tie Point RMSE (mm)			Control Point RMSE (mm)		
Photo Config	**X**	**Y**	**Z**	**X**	**Y**	**Z**
Centre only	30.0	21.7	40.7	-	-	-
Centre + Left	16.3	140.5	57.7	-	-	-
Centre + Right	19.6	70.1	39.4	-	-	-
Full Block	15.3	47.3	30.3	-	-	-

Table 8.12 - Ground Point Residual RMSE, 4 Photographic Configurations With GPS (No Ground Control Points)

It can be seen in table 8.12, that the ground point residual rmse values are much higher when there are no ground control points in the test field. The residual rmse values for the centre strip only configuration are increased by a factor of 3 in the x axis and by a factor of 4 in both the y axis and height axis from the test results in table 8.2 (where the ground control is at a 50m interval and no GPS observations are included).

Although no ground control points are included in this test, the GPS antenna phase centre position observations are coordinated in the local coordinate system (§8.2.5). It could be expected that these would act as control points at the exposure station and so would affect the ground point coordinate accuracy. The GPS antenna residual rmse values are 0.03m along the x axis, 0.025m along the y direction and 0.03m along the height axis. These values are similar to the residual rmse values for the centre strip only photographic configuration.

When the photographic configuration is changed to include the left strip of photography, the residual rmse values are significantly altered. The residual rmse value along the x axis is reduced but the residual rmse value along the height direction is increased. The most noticeable increase is along the y axes which increases by a factor of 7 over the centre strip only photographic configuration. This suggests that there is a larger discrepancy between the

photogrammetric observations and the ground survey. This could be because the additional observations of the left strip strengthen the photogrammetric geometry to the ground position, suggesting that the ground survey is poor. However, it may also suggest that some of the photogrammetric observations in the left strip are poor and are falsely influencing the photogrammetric geometry.

The diagrams C.9.1 to C.9.4 show the individual ground point coordinate residuals for the four photographic configurations in this test. The centre strip only photographic configuration is shown in diagram C.9.1 and it can be seen that the residuals are poorer in the first half of the test field, particularly along the x axes and the height axes. The second half of the strip displays much lower coordinate residuals.

The negative effect of the left strip of photography can be seen in diagram C.9.2. The residuals along the y axes are significantly increased with every point being pulled towards the left side of the test field. In contrast, the height residuals are significantly increased along the right side of the test field. The residuals for the centre + right photographic configuration are shown in diagram C.9.3 and this reverses the pattern of the centre + left photographic configuration. The y axes are increased towards the right side of the test field, to a lesser degree than in diagram C.9.2. The height residuals are greater along the left side of the test field and the points in the first half of the strip generally display a higher height residual.

The overall effect of the additional strips of photography can be seen in diagram C.9.4. The x and y axis residuals are higher in the second half of the strip where they are pulled towards the left side of the test field. This pattern follows that which could be expected from the vector sum of the residuals in diagrams C.9.2 and C.9.3 where the effect of the side strips are clearly shown. The height axis residuals appear to follow the same principle.

8.4.7 Summary

GPS assisted aerial triangulation has been performed with image point observations, ground control points and GPS antenna phase centre coordinates derived from the Pontefract 1996 field trial. The tests show that the coordinate accuracy is significantly worse along the x coordinate accuracy than along the y axes. This is the same pattern as seen in the conventional aerial triangulation tests, and can be seen in the residual diagrams associated with the GPS assisted aerial triangulation tests.

The tests where the control is dense (the 50m control point interval and the extended data validation test) show that there is only a marginal benefit to the ground point coordinate accuracy when the GPS antenna phase centre positions are included in the triangulation (Tables 8.13 and 8.6). However, when the control is reduced to the 250m interval, an improvement in accuracy is apparent. The height residual rmse value on the tie points is reduced by several millimetres and the residual along the x axis is similarly improved.

	Tie Point RMSE (mm)			Control Point RMSE (mm)		
Control Interval (m)	**X**	**Y**	**Z**	**X**	**Y**	**Z**
50	11.2	5.3	6.0	8.4	3.5	1.4
250	11.6	6.6	13.5	8.4	2.1	1.5
500	24.4	8.8	21.0	6.7	2.6	1.3
no control	30.0	21.7	40.7	-	-	-

Table 8.13 - Summary of Ground Point Residual RMSE, Varying 3-D Control interval With GPS (Centre Strip Only)

When the control interval is increased to 500m, the benefit of GPS antenna phase centre positions is clear, with a factor of 4 times improvement in the tie point height residuals. There is less improvement along the x and y axes from

the use of the GPS observations as this is more dependent on the photographic configuration.

The use of additional strips of photography tends to produce a lower coordinate accuracy in the triangulation of the test field. This is a similar phenomenon to that seen in the conventional aerial triangulation tests. The problems with these additional strips of photography are investigated in the next section.

8.5 Border Ground Control

It has been seen in the tests (§8.3) that the use of additional strips of photography has produced a poorer accuracy of the ground point coordinates over the centre strip only configuration. It is possible that, because the block covers a much wider area, the positioning of the control down the hard shoulder of the fictitious highway is not suitable. This could potentially cause problems with stability of the photographs in the side strips and, therefore, adversely affect the ground point coordinates.

The standard configuration of ground control for highway mapping is along the hard shoulder of the highway (rows B and D in figure 8.2). However, a test was set up with 3-D control points at a 50 metre interval along the borders of the test field (rows A and E in figure 8.2) to test how this positioning effects the accuracy of the aerial triangulation.

8.5.1 Conventional Aerial Triangulation

The test was conducted as a conventional aerial triangulation in a similar manner to the tests described in §8.3. Table 8.14 shows the root mean square

error (rmse) of the ground point residuals for each of the control point configurations.

	Tie Point RMSE (mm)			Control Point RMSE (mm)		
Photo Config	**X**	**Y**	**Z**	**X**	**Y**	**Z**
Centre only	7.5	3.7	5.2	12.9	5.9	1.4
Centre + Left	7.6	3.8	5.8	12.8	5.9	2.7
Centre + Right	7.3	3.8	4.5	12.9	6.2	1.4
Full Block	7.5	3.9	5.2	12.9	6.2	2.3

Table 8.14 - Ground Point Residual RMSE, 4 Photographic Configurations Without GPS (Border 3-D Control Points At 50m Interval)

A comparison with table 8.3, where the ground control is positioned at a 50 metre interval along rows B and D, shows the effect that this border ground control has on the accuracy of the ground point coordinate determination. The tie point residual rmse value is reduced by almost a half along both the x and y axes. It is also reduced along the height axis by a smaller amount.

The control point rmse value, in contrast, is increased along both the x and y axis. However, it is marginally reduced along the height axis. These trends could suggest that the position of the control does not significantly affect the plan residuals overall because the border points will tend to have a higher residual. In this case, the border points are the control points and in table 8.3 they are tie points. Whilst the plan residuals are not affected, it appears that the height residuals of the ground points are improved by positioning the control along the borders.

The use of additional photography has a minimal effect on the residual rmse values along the x and y axes. This can also be seen in the diagrams C.10.1 to C.10.4 which are the individual residual plots for this test. The diagrams show

that there is no significant variation in both the magnitude and direction of the plan residuals between photographic configurations. The largest residuals are on the control points which are along the edges of the test field.

The height residual rmse values are affected by the photographic configuration. The use of the left strip increases the tie point height residual but the use of the right strip reduces the residual. This can be seen in diagrams C.10.2 and C.10.3 and is caused by only a few poor points. The residuals pattern is similar between the two plots. The full block configuration, shown in diagram C.10.4, shows that same pattern as the two strip cases with higher residuals in the centre of the test field.

8.6 Minimal Ground Control

When the ground control is reduced to only a few points or removed completely, the ground point coordinate accuracy may not be suitable for the highest quality highway profiling of ±5mm rmse. However, there are occasions when a client only requires spot levels at ±20mm rmse (table 1.1). It may also be the case that provision of ground control for the mapping is difficult and so only a handful of points can be surveyed.

In this series of tests, only minimal ground control is used to investigate if the ground point coordinate accuracy can be improved over the no ground control case (§8.4.6). Since the number of points is below the requirement for a 3-D transformation between coordinate systems (§8.3.5), the assumption is made that the transformation parameters between WGS84 and the local coordinate system are already available or that the mapping is required in the WGS84 coordinate system. All the tests are a GPS assisted aerial triangulation using the centre strip only photographic configuration. There is no comparison of the effect of additional photography.

8.6.1 One Height Control Point

The least amount of ground control in a GPS assisted aerial triangulation might be a single height control point which could be available anywhere across the test field. For the purpose of this test, the height control point was positioned in four different locations to investigate how this affects the accuracy of the ground point coordinates. The four points are at the one end of the test field at points 2 and 4 and in the middle of the test field at points 27 and 29 (figure 8.2).

Table 8.15 shows the root mean square error (rmse) of the ground point residuals for each of the control point configurations.

	Tie Point RMSE (mm)			Control Point RMSE (mm)		
Control Location.	**X**	**Y**	**Z**	**X**	**Y**	**Z**
At Position 2	30.1	71.9	44.2	-	-	0.01
At Position 4	30.3	141.5	64.0	-	-	0.01
At Position 27	30.0	164.3	62.1	-	-	0.01
At Position 29	28.9	246.6	92.0	-	-	0.02

Table 8.15 - Ground Point Residual RMSE, One Height Control Point Only With GPS (Centre Strip Only)

It is clear from table 8.15 that the accuracy of the height control point is very high. This means that the triangulation has been very tightly controlled by the height control point, which might be expected because there is only one control point for the photogrammetric observations to fit on. With no redundancy in the control, the choice of ground control point may significantly affect the accuracy of the ground point coordinates.

The residual rmse values for the tie points show that the accuracy is significantly affected by the choice of height control point. This variation in the rmse value is most noticeable along the y axis and the height axis of the coordinate system. The tie point y axis residual rmse value multiplies by a factor of upto 3 between control configurations and the tie point height residual rmse is increased by a factor of 2.

The effect of the single height control point position on the individual coordinate residuals can be seen in the diagrams C.11.1 to C.11.4 where each configuration is plotted. The xy vector plots show that when the height control point is at one end of the test field, the residuals are pulled along the y axis to one side. When the control point is at position 2, the residuals are greater in the first half of the strip than in the second half. However, when the point is moved to position 4, the residuals in the second half of the test field increase to give a uniform pattern across the whole test field. The uniform pattern of residuals is also seen when the control point is located at positions 27 and 29 in the middle of the test field. The lowest xy residuals from table 8.15 are when the height control point is at location 2 and this appears, from diagram C.11.1, to be attributed to the lower residuals in the second half of the test field.

The height bubble plots show that when the control point is at position 2, the residuals are relatively low and are greater in the first half of the strip than the second half. When the control point is changed, the residuals tend towards a pattern of greater residuals along the outside of the test field. There is still the phenomenon of the residuals being greater in the first half of the strip.

A comparison can be made between table 8.15 and the residual rmse values for the no ground control configuration in table 8.12. The inclusion of the single height control point actually causes a decrease in accuracy over the no ground control configuration. This could be an indication of the negative effect of a single height control point on the internal photogrammetric geometry.

However, it is also possible that the accuracy in table 8.15 is affected by problems in the ground control point coordinates.

8.6.2 Two Height Control Points

It has been seen in the previous test that using a single control point does not control the propagation of errors across the ground point coordinates. The next increment of control quantity might be to use two height control points in the triangulation. This test investigates whether an additional height control point at the opposite end of the test field would be beneficial. The two points are at positions 2 and 54 and at positions 4 and 52 (figure 8.2).

Table 8.16 shows the root mean square error (rmse) of the ground point residuals for each of the control point configurations.

	Tie Point RMSE (mm)			Control Point RMSE (mm)		
Control Location.	**X**	**Y**	**Z**	**X**	**Y**	**Z**
At Positions 2 and 54	30.1	74.4	45.1	-	-	0.0
At Positions 4 and 52	30.0	73.9	47.1	-	-	0.1

Table 8.16 - Ground Point Residual RMSE, Two Height Control Points Only With GPS (Centre Strip Only)

It can be seen from table 8.16 that the triangulation is accurately fitted to the control points, with the height residual rmse at the sub-millimetre level. This is the same phenomenon that was seen in the previous test where the triangulation is tightly controlled when there is minimal ground control across the test field.

A comparison can be made between the accuracy of this triangulation using two height control points and the triangulation of the previous test which only

uses one point. The tie point residual rmse values are similar in magnitude to the values in table 8.15 for the single height control point at position 2. This perhaps suggests that if the single ground control point contains no error in its coordinates, then the use of the additional point in this test is not beneficial. If the values in table 8.16 for the height control at positions 4 and 52 are compared to the single height control point at position 4 in table 8.15, there is a significant difference. The second height control point used in this test is seen to improve the residual rmse value along both the y and height axes.

The residual rmse values for the two control configurations used in this test are similar. This can be seen in more detail in diagrams C.12.1 and C.12.2 which are the individual residual plots for this test. Both the magnitude and direction of the residuals are mirrored between the two configurations. There is a marginal increase in some of the height residuals when the control is at positions 4 and 52.

8.6.3 One 3-D Control Point

The use of height control only has a negative effect on ground point coordinate accuracy as compared to the no ground case for GPS assisted aerial triangulation (§8.4.6). An alternative might be to use 3-D control points. For the purpose of this test, a single 3-D ground control point is used to investigate the effect on ground point coordinate accuracy. The 3-D point is positioned in four different locations to see the effects of control point choice. The four points are at the one end of the test field in positions 2 and 4 and in the middle of the test field in positions 27 and 29.

Table 8.17 shows the root mean square error (rmse) of the ground point residuals for each of the control point configurations.

	Tie Point RMSE (mm)			Control Point RMSE (mm)		
Control Location.	**X**	**Y**	**Z**	**X**	**Y**	**Z**
At Position 2	22.7	36.5	26.6	1.3	0.2	0.1
At Position 4	23.0	42.6	28.8	1.2	0.1	0.1
At Position 27	9.8	21.1	29.0	21.8	4.8	2.9
At Position 29	10.6	16.9	30.1	6.3	1.0	1.0

Table 8.17 - Ground Point Residual RMSE, One 3-D Control Point Only With GPS (Centre Strip Only)

It is clear from table 8.17 that the accuracy of the 3-D control point is very high. As before, this might be expected with no redundancy of control points. The rmse residual values for the tie points show that the accuracy is significantly affected by the choice of 3-D control point. The residual rmse value along the y axis varies by a factor of almost 3 between control configurations. The residual along the x axis is affected by a factor of 2 between a control point at the end of the test field (points 2 or 4) and one in the middle of the test field (points 27 and 29). The height residual is changed by a couple of millimetres between control configurations.

The variation in ground coordinate accuracy between control configurations can be seen in diagrams C.13.1 to C.13.4, the individual coordinate residual plots. When the control point is at one end of the test field (diagrams C.13.1 and C.13.2), the higher plan residuals are at the other end of the test field. This might be expected because there is no ground control at that end. The height residuals are balanced between both halves of the test field, with the greater residuals in the middle.

When the 3-D control point is positioned in the middle of the test field (diagrams C.13.3 and C.13.4), the higher plan residuals are at the two ends of the test field and the rest of the points have a low residual. This might be

expected because there is no control at either end of the test field and the control point splits the test field in half. The height residuals are higher in the first half of the test field.

A comparison can be made between table 8.17 and table 8.12. The inclusion of the single 3-D control point increases the accuracy of the ground points. The improvement is most noticeable along the height axis where the residual rmse value is reduced by over 10 millimetres. There is an improvement in plan residuals, but this is only the case along the y axis when the control point is positioned in the middle of the test field.

8.6.4 Two 3-D Control Points

It has been seen in the previous test that the ground point residuals increase with distance away from the control point. This phenomenon was also seen when a single height control point was used (§8.6.1). The next increment of control quantity might be to use two 3-D control points at either end of the test field. This test investigates whether this additional 3-D control point is beneficial to the accuracy of the ground point coordinates. The two points are at positions 2 and 54 and at positions 4 and 52 (figure 8.2).

Table 8.18 shows the root mean square error (rmse) of the ground point residuals for each of the control point configurations.

	Tie Point RMSE (mm)			Control Point RMSE (mm)		
Control Location.	**X**	**Y**	**Z**	**X**	**Y**	**Z**
At Positions 2 and 54	25.6	9.2	21.1	1.0	1.0	0.1
At Positions 4 and 52	23.8	7.7	22.5	0.9	0.8	0.1

Table 8.18 - Ground Point Residual RMSE, Two 3-D Control Points Only With GPS (Centre Strip Only)

A comparison can be made between the accuracy of this triangulation using two 3-D control points and the triangulation of the previous test which uses only one 3-D control point. The residual rmse values in table 8.18 are significantly lower than the values in table 8.17. The improvement in accuracy is most marked along the y axis where the residual is lower by a factor of 2. The height residual rmse value is lower by several millimetres.

The residual rmse values for the two control configurations used in this test are similar. This can be seen in more detail in diagrams C.14.1 and C.14.2 which are the individual residual plots for this test. Both the magnitude and direction of the residuals are similar between the two configurations.

A comparison can be made between table 8.17 and table 8.12. The inclusion of the two 3-D control points increases the accuracy of the ground points. The improvement is most noticeable along both the y axis and the height axis. The y axis residual rmse value is lower by a factor of 2 and the height axis residual rmse value is lower by a similar amount. There is an improvement in the x axis residual of several millimetres.

8.6.5 Summary

GPS assisted aerial triangulation has been performed on the centre strip of photography from the Pontefract 1996 field trial using a minimal amount of ground control. The results can be compared to the GPS assisted aerial triangulation where no ground control points are used to establish if there is any improvement in accuracy of the ground point coordinates.

The tests where only a single height control point is used, show that the location of the ground control point has a significant effect on the accuracy of the aerial triangulation. The residuals are actually worse than the no ground control case which may suggest that the height control points were poorly

coordinated in the ground survey. Alternatively, it may suggest that the use of a single height control point de-stabilises the aerial triangulation because the photogrammetric geometry is tightly constrained to a single height point.

The use of two height points does not significantly alter the accuracy of the aerial triangulation. The results suggest that the second control point only affects the ground point coordinate accuracy if the accuracy of the triangulation with the single point is relatively high.

When a single 3-D control point is used, there is a significant improvement in accuracy over the single height control case. This suggests that there is a benefit when plan control is included. An improvement in accuracy is also seen when a second 3-D control point is introduced. In comparison to the no ground control case, the improvement in accuracy is by upto a factor of 2 in both the y axis and the height axis. Since the y axis represents the width of the test field (which is relatively low compared to the length), this may suggest that the 3-D control helps to constrain the photogrammetric geometry across the test field.

8.7 Discussion

The aim of this chapter is to investigate the potential of both conventional aerial triangulation and GPS assisted aerial triangulation for reducing the ground control requirement in highway mapping. Several tests have been conducted using both different photographic and ground control configurations.

To summarise the individual tests, it is important to consider how the accuracy of the aerial triangulation relates to the needs of the client. The highest height requirement is ± 5mm rmse but this can be reduced to + 20mm rmse for some applications. The plan residual requirement is less strict and is constrained

only by the mapping scale. It is acceptable to provide the plan position of ground points to ±20mm [*Boardman, 1996*].

It has been found [*Boardman, 1994*] that using a single model orientation procedure with control at a 50m interval, provides ground point height coordinates at ± 5mm. It has also been found [*Smith and Joy, 1995*] that this can be attained by aerial triangulation processing of the data. Although the tie point residual rmse is 6mm in the Pontefract 1996 trial (§8.3.5), this could be attributed to ground survey problems. Many of the test suggest that there is some problem with the ground coordinates calculated from the ground survey. This is further discussed in §8.8.

If the ground control is reduced to a 250m interval, the height residual rmse is much greater than the ± 5mm requirement. The plan residuals are still acceptable. Even when the GPS antenna phase centre positions are included in the aerial triangulation, the height residual rmse does not reach ± 5mm rmse. These tests suggest that whilst the plan control can be reduced to 250m (the interval for PGMs), the height control requirement cannot be reduced if the ± 5mm rmse is required by the client. Full 3-D control points at a 250m meets the mapping requirement at ± 15mm rmse and at ± 10mm if GPS antenna phase centre positions are included.

The use of GPS antenna phase centre positions is not significantly beneficial when there is a large amount of control across the test field. This might be expected because the control has a higher precision than the GPS positions. However, when the control is reduced to a 250m or 500m interval, there is a clear benefit to acquiring the GPS positions and including them in the aerial triangulation. The benefit at 250m has been discussed above and at 500m the tie point height residuals are reduced by a factor of 4 to within the requirement for mapping at ±20mm rmse. This would be the minimum amount of control to allow the transformation between WGS84 and the mapping system to be calculated. The extra effort involved in acquiring the GPS positions may be

offset by the significant improvement in the coordinate residuals despite a reduction in the ground control.

Other applications such as railway mapping or mapping of inaccessible areas may benefit from the potential to reduce the ground control requirement in aerial triangulation. The maximum reduction is to not include any ground control points. This is only possible when the GPS positions are included. The tie point residual rmse is approximately 40mm depending on the photographic configuration. It is also notable that this configuration produces higher accuracy ground point coordinates than when no GPS is used and the control is reduced to a 500m interval. This is because there is one full aerial control point per photograph instead of only 2 ground points per 500m interval. This again suggests that GPS is beneficial to the aerial triangulation when the ground control is reduced and that the improvement in coordinate residuals is significant.

It has been seen in the tests that the use of additional side strips of photography has tended to produce higher coordinate residuals as compared to the use of only the centre strip. This is potentially a problem caused by the location of both the control points and the tie points on the photographs. Whilst the centre strip has points located across its whole width, the two side strips are offset from the centre. This means that there are no tie points in the outside corners of the photographs. The test described in §8.5.1 shows that if the control points are positioned at the tie point locations, the additional photography is seen to improve the coordinate residuals. This is what might normally be expected because there are more photogrammetric observations intersecting at a point. This test suggests that the use of additional side strips of photography in highway mapping is hindered by the location of the control points because they are not evenly spaced across the width of photography.

Finally, a series of tests were performed to investigate the variation in coordinate residuals when only one or two control points are included in the GPS assisted triangulation. It can be seen that the use of height points only

causes a negative effect on the residuals. This is perhaps because the use of a height control points de-stabilises the aerial triangulation. When 3-D control points are included, there is some improvement over the no ground control configuration. This is particularly so when the control is positioning at either end of the test field. These tests suggest that if minimal control is used, it should be 3-D points

8.8 Further Investigations

During the Pontefract 1996 data validation tests, the unit variance (§2.6.3) was calculated. This is a capability of the TABBY aerial triangulation package. It was found that this unit variance was significantly different to unity which has an implication on the statistical testing of the dataset (§2.6.3). Potential reasons for the unit variance deviating from unity are:

- the observations are not weighted correctly
- there is an error in the functional model

Consideration was given to the weighting of the aerial triangulation observations but it was felt that these truly reflected what could be expected.

The other option is an error in the functional model. Specifically, it is feasible that the site restrictions during the ground survey (§5.2.3) had caused some of the ground point to be poorly coordinated. This has been seen in the aerial triangulation tests where there is a large coordinate discrepancy on some points. The individual residual plots in Appendix C also show that they display systematic patterns.

Whilst the accuracy of the derived ground coordinate values is a most useful measure of the quality of an aerial triangulation, it may still be helpful to extract the precision measures from the covariance matrices. It would be

important to further investigate the systematic errors in the ground control and attempt to remove the effects. This may cause the unit variance to calculate near to unity and enable a meaningful investigation of internal precision of the aerial triangulation tests.

Chapter 9

Conclusions And Suggestions For Future Work

9.1 Introduction

The primary aim of this thesis was to investigate the potential of both conventional aerial triangulation and GPS assisted aerial triangulation for reducing the ground control requirement in large scale photogrammetric mapping of highways. The theory and algorithms for the integration of GPS and aerial triangulation have been described and a GPS-camera system has been developed. Field trials were conducted to assess the performance of the system and to acquire appropriate photography for a series of aerial triangulation tests. The aerial triangulation data was processed with software written for this research.

Based on the investigations described in this research, the following conclusions can be drawn.

9.2 Integrated GPS-camera system

(1) The integration of a photogrammetric camera and a GPS positioning system has been successfully achieved. The system was based around an existing photogrammetric camera system which has been operated by Photarc Surveys Ltd for commercial highway mapping work. The system integration is provided by a dedicated electronic control system which was shown to be a reliable and robust solution during the final field trial.

(2) The GPS-camera system is modular in design and this makes the system more adaptable. The GPS positioning components and electronic control system can be detached from the camera system when they are not required. The ergonomics of the system components have been shown to be suited to its use in future commercial work without any further developments.

(3) The GPS antenna must be attached to the camera mount to maintain portability of the system. This also negates the requirement for any Civil Aviation Authority (CAA) approval process because the equipment is not directly attached to the fuselage of the helicopter.

(4) The location of the GPS antenna is an important consideration for operational performance and reliability of the positioning system. If the antenna is located near to the camera mount then a significant number of GPS satellites are masked by the helicopter fuselage. This has a negative effect on the quality of positioning which can be as poor as 30 centimetres. When the GPS antenna is attached to the end of a

long vertical pole, the quality of positioning is improved to 5 centimetres. The experience of the field trials show that reliability is also improved.

(5) The photographic exposures cannot be related to the GPS positions by the process of time interpolation. This is because the camera is not able to output a 'instant of exposure' pulse and the motion of the helicopter is not as linear as a fixed wing aircraft. Instead, the PPS signal from a suitable GPS receiver can be used to control the camera exposures. This approach has been implemented and proven as an accurate method of exposure control and identification.

(6) The camera-antenna offset vector must be calculated so that the GPS antenna positions can contribute to a GPS assisted aerial triangulation. This vector is constant throughout the flight because the camera is fixed in its mount which is, in turn, directly attached to the GPS antenna. Therefore, in flight measurement is not necessary as the vector can be pre-calibrated in the laboratory.

(7) An array of tilt sensors that were integrated into the GPS-camera system with additional hardware and software were not suited to high accuracy in flight orientation of the camera platform. However, the modular design of the system means that alternative sensors could be implemented.

9.3 Aerial Triangulation

(8) Conventional aerial triangulation using weighted image point observations and ground control points can satisfy the ± 5mm rmse requirement for highway mapping. The height control must be positioned at a 50m interval.

(9) GPS assisted aerial triangulation using the conventional data plus weighted GPS antenna phase centre coordinates does not improve the accuracy of the aerial triangulation when full control at a 50m interval is used. This is because the ground control has a higher precision than the antenna positions.

(10) The quality of the antenna phase centre positions has been shown to be 5 centimetres in the Pontefract 1996 field trial. The use of these positions in a GPS assisted aerial triangulation is beneficial to the accuracy of the ground points. With 3-D ground control at a 250 metre interval, the triangulation can satisfy the ± 10mm rmse requirement for highway mapping.

(11) It is not beneficial to use additional side strips of photography in highway mapping unless the control points or tie points are positioned in the corners of the photographs. The standard distribution of ground points appears to de-stabilise the aerial triangulation.

9.4 Suggestions For Future Work

The following areas are suggested for future work in the field of GPS assisted helicopter photogrammetry and its application to highway profiling.

(1) The Nottingham GPS-camera system has been successfully tested in the helicopter environment. The electronic control system has been shown to be reliable and robust. However, if the GPS-camera system was to be used on commercial contracts, it may be necessary to give further consideration to the ergonomics and robustness of the system. Specifically, it may be necessary to redesign the antenna pole to make it more robust for repeated use.

(2) During the research, an array of tilt sensors were tested to see if they could accurately orientate the sensor platform. This area was not fully explored because it was not of primary concern. The use of orientation sensors should be investigated further. The integration framework is already available from the developments made in this research.

(3) The aerial triangulation investigations were only analysed by comparison of the ground point coordinate residuals. This measure was the best method for providing a true comparison of the capabilities of the technique for coordinating ground points. However, it would be possible to investigate the internal precision of the aerial triangulation tests and so this should be investigated.

(4) The main field trials were undertaken on a grass runway where there were few natural features and the ground points were signalised. It is important to test the GPS-camera system and the aerial triangulation process on a true highway mapping trial. This would provide further data on the performance of the system which could be used in the commercial marketplace to further acceptance of this non-contact large scale mapping technique.

References

Ackermann, F and Schade, H, 1993, Application Of GPS For Aerial Triangulation. *Photogrammetric Engineering And Remote Sensing, Vol. 59 No.11, November 1993, pp 1625-1632.*

Ackermann, F, 1986, The Use Of Camera Orientation Data In Photogrammetry - A Review. *Proceedings Of ISPRS Symposium: Progress In Imaging Sensors, Stuttgart, September 1986, pp 93-99.*

Ackermann, F, 1992a, GPS Application In Photogrammetry. *Proceedings Of ISPRS Congress Commission III, Washington, 1992, pp 97-101.*

Ackermann, F, 1992b, Kinematic GPS Control For Photogrammetry. *Photogrammetric Record, 14(80), October 1992, pp 261-276.*

Ackermann, F, 1992c, Operational Rules And Accuracy Models For GPS-Aerotriangulation. *Proceedings Of ISPRS Congress Commission III, Washington, 1992, pp 691-700.*

Ackermann, F, 1992d, Prospects Of Kinematic GPS For Aerial Triangulation. *ITC Journal 1992-94 pp 326-337.*

Ackermann, F, 1994, Practical Experience With GPS Supported Aerial Triangulation. *Photogrammetric Record 14(84,. October 199, pp 861-874.*

Ashtech, 1994, Z-12 Receiver Operating Manual. *Ashtech Inc, Sunnyvale, California, USA.*

Beamson, G A, 1995, Precise Height Determination Of Tide Gauges Using GPS. *PhD Thesis, The University of Nottingham, UK.*

Becker, R D and Barriere, J P, 1993, Airborne GPS For Photo Navigation And Photogrammetry: An Integrated Approach. *Photogrammetric Engineering And Remote Sensing, Vol. 59 No. 11, November 1993, pp 1659-1665.*

Bennett, M, 1989, The Clear Cone Survey System. *Municipal Engineer, Vol 6, pp 281-288.*

Biggs, P H, Pearce, C J and Westcott, T J, 1989, GPS Navigation For Large-Scale Photography. *Photogrammetric Engineering And Remote Sensing, Vol. 55 No 12, December 1989, pp 1737-1741.*

Bingley, R M, 1993, GPS Data Processing. *Lecture Notes, Sixth International Seminar on the Global Positioning System, The University of Nottingham, UK.*

Boardman, J C, 1994, High Precision Levelling of Motorways by Low Level Helicopter Survey, Photogrammetric Record, *14(84), October 1994, pp 925-942.*

Boardman, J C, 1994, Personal Communication. *Technical Director, Photarc Surveys Ltd.*

Boardman, J C, 1996, Personal Communication. *Technical Director, Photarc Surveys Ltd.*

BRF, 1997, British Road Federation - Road Fact 97. *British Road Federation, Old Kent Road, London.*

Burnside, C D, 1985, Mapping From Aerial Photographs. *Mackays.* ISBN 0-00-383036-5

Colomina, I, 1993, A Note On The Analytics Of Aerial Triangulation With GPS Aerial Control. *Photogrammetric Engineering And Remote Sensing, Vol. 59 No 11, November 1993, pp 1619-1624.*

Computer Boards Inc, 1991, CIO-AD16Jr User's Manual, *Computer Boards Inc, Mansfield, USA.*

Computer Boards Inc, 1994, PCM-DAS16 User's Manual, *Computer Boards Inc, Mansfield, USA.*

Crawshaw, J and Chambers, J, 1984, A Concise Course In A-Level Statistics. *Stanley Thornes Ltd.* ISBN 0-85950-378-X

Cross, P A, 1972, The Effect Of Errors In Weights. *Survey Review, 21(165), pp 319-325.*

Cross, P A, 1982, A Priori And A Posteriori Analyses Letter. *Survey Review, 26(204), pp303-304.*

Cross, P A, 1983, Advanced Least Squares Applied To Positioning Fixing. *University Of East London Working Paper No 6, London, UK.* ISBN 0-907382-06-1

Cross, P A, and Cooper, M A R, 1988, Statistical Concepts And Their Application In Photogrammetry And Surveying. *Photogrammetric Record, 12(71), April 1988, pp 637-663.*

Curry, S and Schuckman, K, 1993, Practical Considerations For The Use Of Airborne GPS For Photogrammetry. *Photogrammetric Engineering And Remote Sensing, Vol. 59 No. 11, November 1993, pp 1611-1617.*

Department of Transport, 1996, Manual of Contract Documents For Highway Works - Volume 5. *HMSO, April 1996.*

Diete, N, 1990, LMK-2000: A New Aerial Survey Camera System. *Jena Review 3 pp135-138.*

Dodson, A H, Hill, C J and Shardlow, P J, 1993, The Effects of Propagation Errors on GPS Measurements. *Lecture Notes, Sixth International Seminar on the Global Positioning System, The University of Nottingham, UK.*

Doebelin, E, 1985, Control System Principles And Design. *Wiley and Sons.* ISBN unavailable.

El-Hakim, S F, 1981, A Practical Study Of Gross-Error Detection In Bundle Adjustment. *The Canadian Surveyor, Vol. 35 No. 4, December 1981, pp 373-386.*

Friess, P, 1991, Aerotriangulation With GPS - Methods, Experience, Expectations. *Proceedings Of The 43rd Photogrammetric Week, 1991, Stuggart, Germany, pp 43-49.*

Ghosh, S K, 1975, Phototriangulation. *Lexington Books.* ISBN 0-669-98210-5.

Ghosh, S K, 1988, Analytical Photogrammetry. 2nd Ed.. *Pergammon Press.* ISBN 0-08-036103-x.

Granshaw, S I, 1980, Bundle Adjustment Methods In Engineering Photogrammetry. *Photogrammetric Record, 10(56), October 1980, pp 181-207.*

Grün, A, 1982, The Accuracy Potential Of The Modern Bundle Block Adjustment In Aerial Photogrammetry. *Photogrammetric Engineering And Remote Sensing, Vol. 48 No. 1, January 1982, pp 45-54.*

Grün, A, Cocard, M and Kahle, H G, 1993, Photogrammetry And Kinematic GPS: Results Of A High Accuracy Test. *Photogrammetric Engineering And Remote Sensing, Vol. 59 No. 11, November 1993, pp 1643-1650.*

Hansen, P and Joy, C I H, 1995, High Precision Highway Profiles Using Helicopter Borne 'On-The-Fly' GPS. *Proceedings Of ION GPS-95, The 8th International Technical Meeting Of The Satellite Division Of The Institute Of Navigation, September 1995, Palm Springs, California, USA, Vol. 1, pp 291-298.*

Hansen, P, 1996, On the Fly Ambiguity Resolution for GPS. *PhD Thesis, The University of Nottingham, UK.*

Hardwick, C D, and Liu, J, 1995, Characterization of Phase and Multipath Errors for an Aircraft Antenna. *Proc. of the 8th International Technical Meeting of the Satellite Division of the Institute of Navigation, ION-95, Palm Springs, California, USA. Volume 1 pp 491-506.*

Hayes, M R, and Taylor, P J, 1993, A Review of the Accident Risks Associated With Major Roadworks on All-Purpose Dual Carriageway Roads *TRL Project Report PR37.* ISSN 0968-4093

Highways Agency, 1996a, Annual Report 1995-96, *HMSO.* ISBN 0-11-551842-8.

Highways Agency, 1996b, The Road User's Charter - Getting The Best Out of England's Main Roads. *HMSO.*

Hubbard, L C M, 1995, Atmospheric Water Vapour Effects on GPS Measurements. *PhD Thesis, The University of Nottingham, UK.*

Ibrahim, A M, 1995, Reliability Analysis of Combined GPS-Aerial Triangulation System. *PhD Thesis, The University of Newcastle Upon Tyne, UK.*

IESSG, 1997, Internal Presentation Material. *Institute of Engineering Surveying and Space Geodesy, The University of Nottingham, UK.*

Jackson, F, 1996, A Clear Alternative For Highway Levelling. *Surveying World, Volume 4 No. 5, July/August 1996.*

Jacobsen, K, 1982, Attempt At Obtaining The Best Possible Accuracy In Bundle Block Adjustment. *Photogrammetria, 37, pp 219-235.*

Jacobsen, K, 1991, Trends In Photogrammetry. *Proceedings Of ACSM/ASPRS Conference, Baltimore, 1991, Vol. 5, pp 208-217.*

Jacobsen, K, 1993, Experiences In GPS Photogrammetry. *Photogrammetric Engineering And Remote Sensing, Vol. 59 No. 11, November 1993, pp 1651-1658.*

Kinlyside, D, 1988, Some Aspects On Using GPS For Airborne Photogrammetric Control, *Australian Journal Of Geodesy, Photogrammetry And Surveying, No. 49, December 1998, pp 55-72.*

Klose, H, 1990, The New Gyro-Stabilised Mount For LMK Aerial Survey Cameras. *Jena Review 3, pp 138-141.*

Krück, E, 1996, Advanced Combined Bundle Block Adjustment With Kinematic GPS Data. *Proceedings Of ISPRS Congress, Vienna, Austria, 9-19 July 1996.*

Krück, E, 1997, Personal Communication. *Director And Software Developer, GIP, mbH.*

Leica AG, 1996, Leica Ascot Aerial Visionics System, *Product Literature, Switzerland.*

Leick, A, 1995, GPS Satellite Surveying. 2nd Edition. ISBN 0-471-306266.

Lowe, D, 1994, Personal Communication. *Research Assitant, IESSG, The University of Nottingham, UK.*

Lucas, J R and Mader, G L, 1989, Recent Advances In Kinematic GPS Photogrammetry. *Journal Of Surveying Engineering, Vol. 115, No. 1, February 1989, pp 78-92.*

Lucas, J R, 1987, Aerotriangulation Without Ground Control. *Photogrammetric Engineering And Remote Sensing, Vol. 53 No 3, March 1987, pp 311-314.*

Lucas Control Systems, 1992, Schaevitz Electronic Clinometers. *Product Literature.*

Merchant, D C, 1993, GPS Controlled Aerial Photogrammetry. *Photogrammetric Engineering And Remote Sensing, Vol. 59 No. 11, November 1993, pp 1633-1636.*

Mikhail, E M, 1976, Observations And Least Squares. *IEP - A Dun-Donnelly Publisher, New York.* ISBN 0-7002-2481-5

Moffitt, F H, 1980, Photogrammetry. *Harper & Row Publisher, New York.* ISBN 0-700-22517-X

Moore, T, 1993, Differential GPS. *Lecture Notes, Sixth International Seminar on the Global Positioning System, The University of Nottingham, UK.*

NovAtel, 1995, Novatel's Multipath Elimination Technologies. *GPS World, June 1995, page 67.*

Roberts, G W, 1997, Real Time on the Fly Kinematic GPS. *PhD Thesis, The University of Nottingham, UK.*

Schut, G H, 1967, Formation of Strips From Independent Models. *Proceedings of the Semi-Annual Convention of the American Society of Photogrammetry and Remote Sensing, St. Louis, Missouri, October 1967.*

Scott, P, 1994, Personal Communication. *Owner and Pilot, Heliscott Ltd.*

Shardlow, P J, 1990, Multipath: An Investigation. *MSc Thesis, The University of Nottingham, UK.*

Shardlow, P J, 1994, Propagation Effects on Precise GPS Heighting. *PhD Thesis, The University of Nottingham, UK.*

Slama, 1980, Manual Of Photogrammetry. *American Society Of Photogrammetry.* ISBN 0-937294-01-2

Sleeman, T W, Least Squares Adjustment of horizontal Surveying Networks. *Msc Thesis, The University of Nottingham, UK.*

Smith, M J, 1986, Photogrammetric Techniques For Archaeological Mapping Using Oblique Non-Metric Photography. *Phd Thesis, University College London.*

Smith, M J, and Joy, C I H, 1995, Preliminary Investigations Into Developments In Using Helicopter Photography For Highway Surveying. *Photogrammetric Record, 15(85) April 1995, pp 77-84.*

Smith, M J, and Joy, C I H, 1995, Developments in an integrated in-flight positioning and orientation system for helicopter photography, *Integrated sensor orientation, theory, algorithms and systems, 274-283, Wichmann, Germany.*

Smith, M J , and Joy, C I H and Boardman, J C, 1996a, The use of helicopter photography for highway surveying, *ASPRS/ACSM Annual Convention and Exhibition, 2, 116-124, Baltimore, USA.*

Smith, M J, and Joy, C I H, 1996b, Advances In GPS-Assisted Helicopter Photogrammetry And Its Application To High Precision Highway Profiling. *ISPRS Congress, Vienna, Austria.*

Stanbridge, R, 1987, Close-Range Photogrammetric Techniques, *Land and Mineral Surveyor, Vol 5, April 1987, pp 178-184.*

Stanbridge, R, 1993, Highway levelling - by Helicopter!. *Engineering Surveying Showcase 1993, p22.*

Stanbridge, R, 1996, Brits In Chopper Jam!. *Engineering Surveying Showcase 1996, pp44-45.*

Stirling, D M, Chandler, J H and Clark, J S, 1992. Monitoring One of Europe's Largest Retaining Walls Using Oblique Aerial Photography. *Proceedings Of ISPRS Congress Commission V, Washington, 1992, pp 701-708.*

Sylvander, R, 1991, Kinematic GPS Measurements With Special Emphasis On Applications In Swedish Forestry. *Proceedings Of IGARSS '91 Remote Sensing: Global Monitoring For Earth Management, Vol.3, pp 1523-1526.*

Trimble Navigation, 1992, 4000 SSE Geodetic System Surveyor / 4000 SSE Geodetic Surveyor Operation Manual.

Tsakiri, M, 1995, GPS and DR for Land Vehicle Navigation. *PhD Thesis, The University of Nottingham, UK.*

Voss, G, 1973, The UMK 10/1318 Universal Photogrammetric System of VEB Carl Zeiss Jena. *Jena Review, Special Fair issue 1973, pp 63-67.*

Voss, G, 1980, The UMK 10/1318 Universal Measuring Camera and its ten year history. *Jena Review, 1/1980, pp 14-16.*

Walsh, D M A, 1994, Kinematic GPS Ambiguity Resolution. *PhD Thesis, The University of Nottingham, UK.*

Wickens, E, 1994, Personal Communication. *Sales Manager, Carl Zeiss UK Ltd.*

Wolf, P R, 1983, Elements Of Photogrammetry. *McGraw-Hill Inc., Singapore.* ISBN 0-07-Y66637-7

Appendix A

Plates

A.1 Introduction

This Appendix is a collection of plates which show interesting aspects of the research programme. They include detail on the field test sites and the Nottingham GPS-Camera system. The plates are collected at this point in the thesis so as not to disrupt the flow of information given in the main chapters.

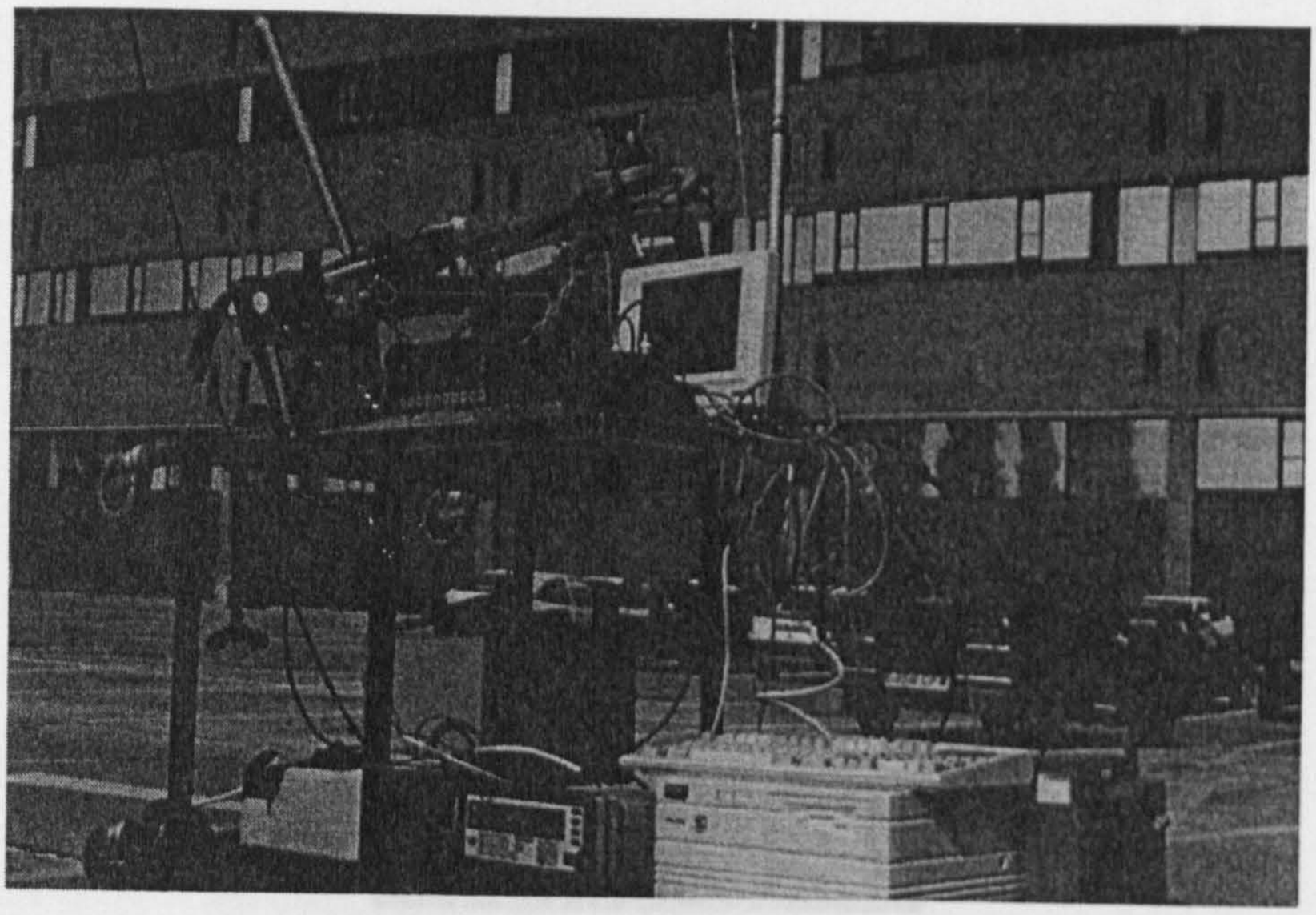

Plate A.1 -The Camera Mount In The Medical School Trial

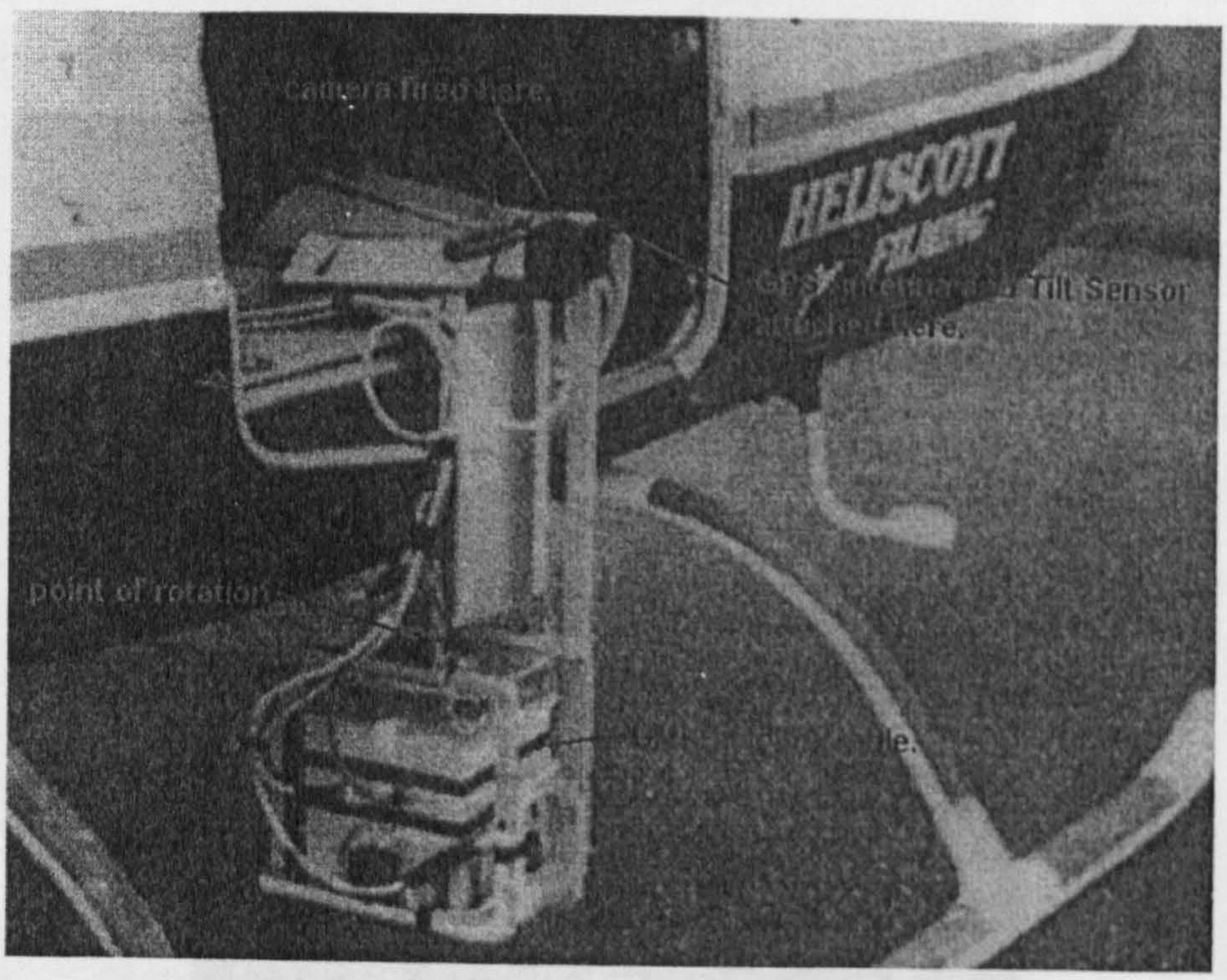

Plate A.2 -The Original Camera Mount

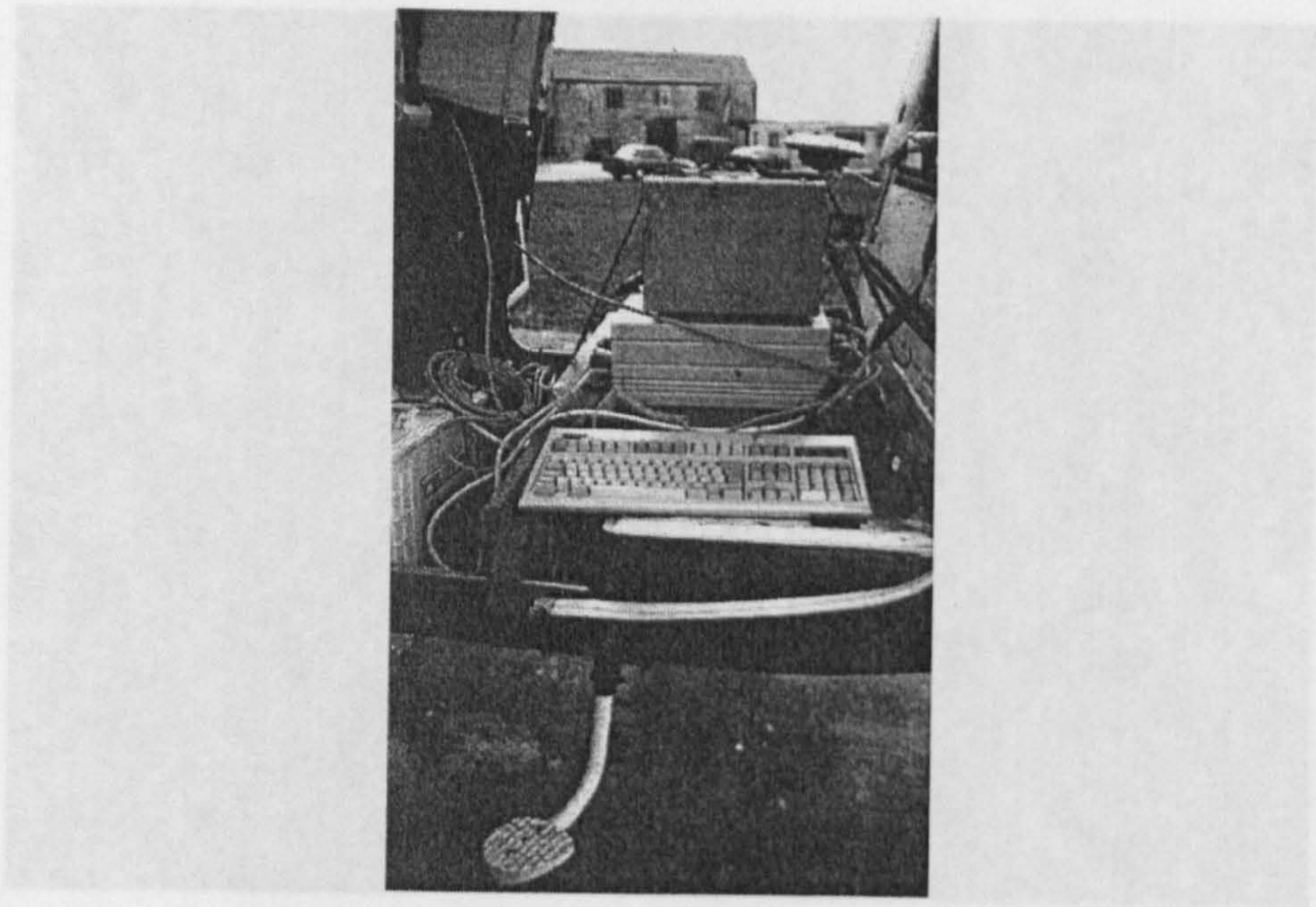

Plate A.3 -The Mk I GPS-Camera System On The Helicopter

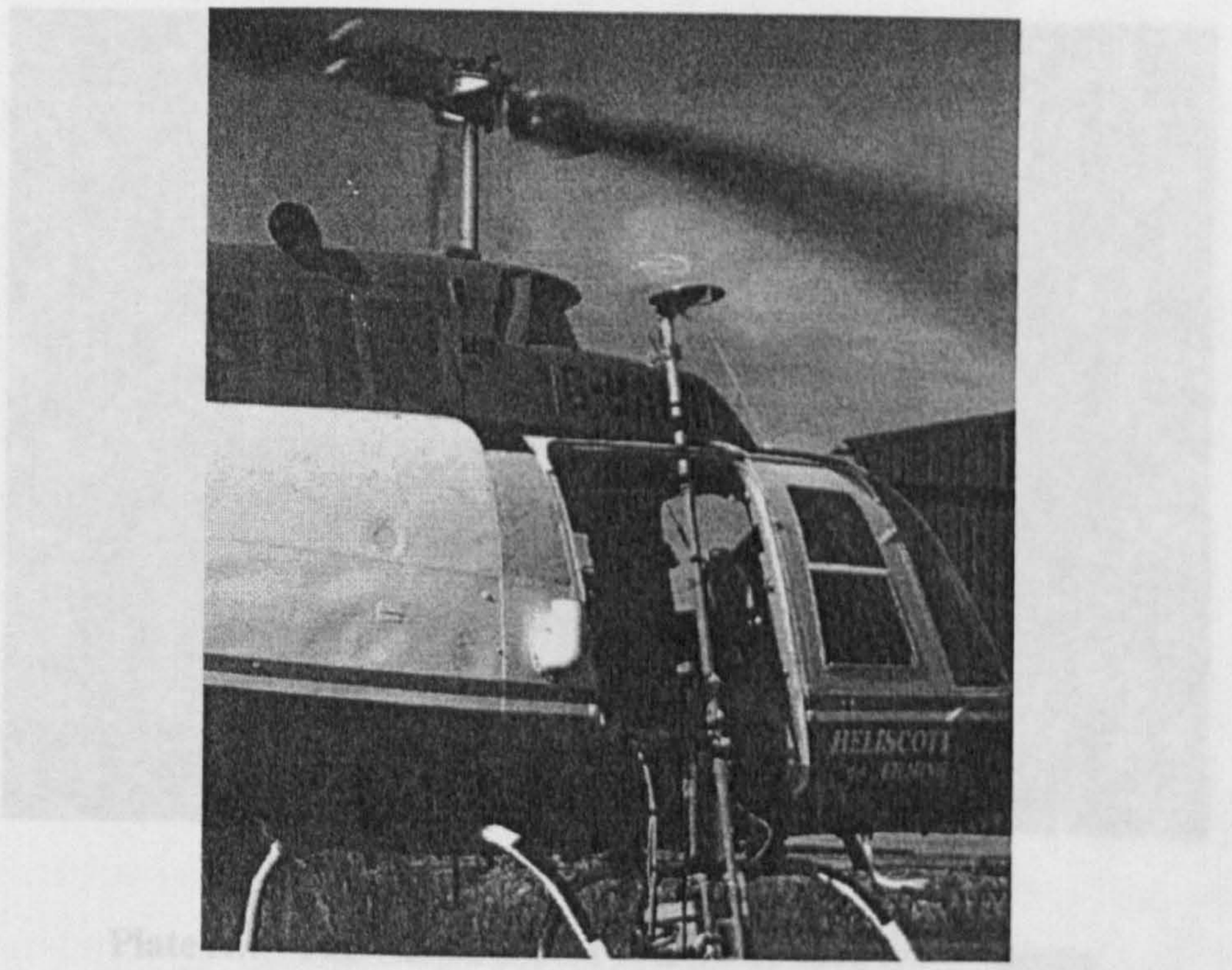

Plate A.4 -The Mk II Camera System On The Helicopter

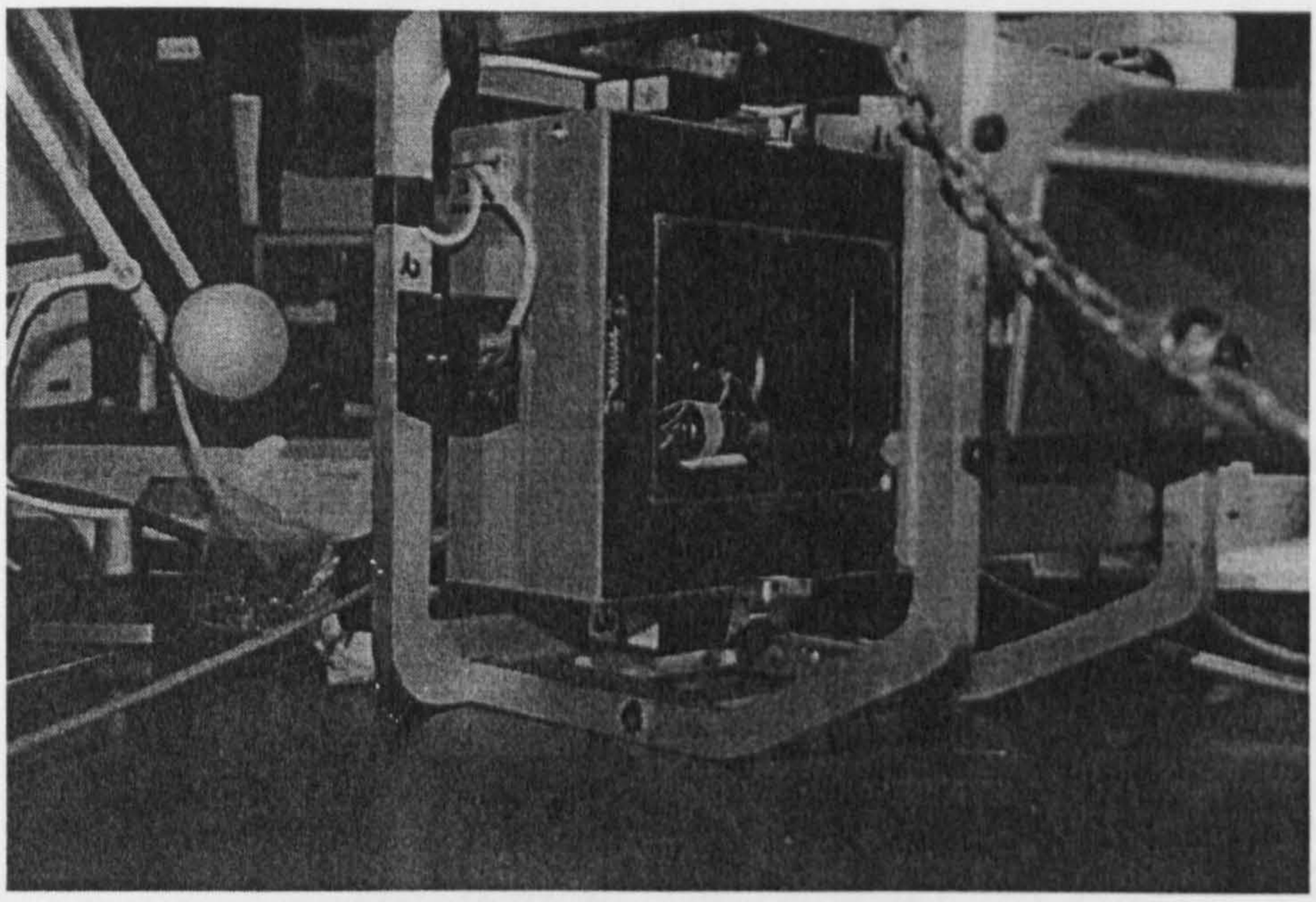

Plate A.5 -The Camera Test Setup Showing Bulb

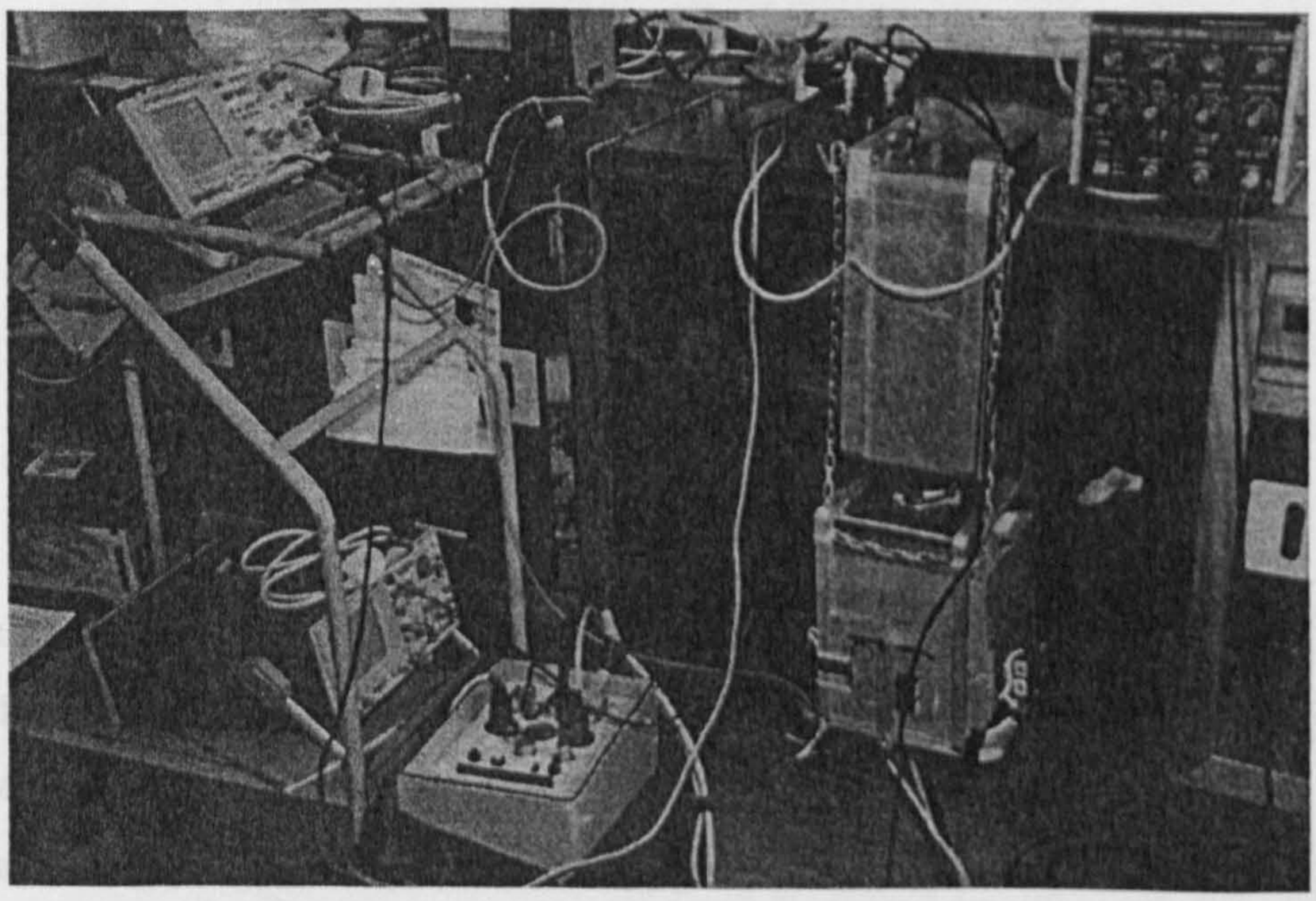

Plate A.6 -The Camera Test Setup Showing Oscilloscope

Appendix B

TABBY Input And Output File Structure

B.1 Introduction

This chapter is to be read in conjunction with the discussion on the TABBY software package in Chapter 7. TABBY is the Aerial Triangulation software used throughout this research programme and implements the principles of bundle estimation. This Appendix details the input files which are required to the software and the output files which are produced. Some of the files have been edited to curtail any unnecessary length of this Appendix.

B.2 Program Control File *tabby.ctl*

```
# TABBY version 3.11b Control File.
# Written by Chris Joy 1995/96.
#
# Pont96 Full Block
#
gball              ! Network ID.
520                ! Number x,y obs.
33                 ! Number of photos.
32                 ! GPS Antenna Positions
55                 ! Number of points.
1                  ! Real=1, Simulation=0;
1                  ! Combined GPS=1.
1                  ! Stochastic=1, Deterministic=0.
5.000              ! global image s.e. in microns.
0.005              ! global x ground coord s.e. in metres.
0.005              ! global y ground coord s.e. in metres.
0.002              ! global z ground coord s.e. in metres.
0.02786            ! x eccentricity.
-0.27014           ! y eccentricity.
2.11318            ! z eccentricity.
```

The control file is a simplistic method of defining the mode of operation of the aerial triangulation software. It is also essential for providing certain parameters to the estimation. This file is further discussed in chapter 7.

B.3 Image Point Observation File *tpobs.in*

```
Photo Point X Obs.       Y Obs.       S.e.
19    2     -8377.5000   57246.5000   1.000
19    3     -9014.5000   38424.5000   1.000
19    4     -11161.7000  -17298.0000  1.000
19    5     -11765.5000  -35848.3000  1.000
19    6     -72272.5000  12931.8000   1.000
19    8     -71455.5000  41047.0000   1.000
20    2     53177.5000   54521.0000   1.000
20    3     54476.5000   35128.2000   1.000
20    4     59415.0000   -24884.5000  1.000
20    5     61091.5000   -45767.3000  1.000
20    6     -9804.2000   2357.3000    1.000
```

The image point observation file contains the (x,y) coordinates in microns of each point in the fiducial coordinate system. The final coumn is a standard

error parameter which is not currently implemented in the software but is a legacy value from the ORINT4 software developed by the author's project supervisor.

The creation of the image point observation file must produce an ordered file. A file of random image point observations should be re-ordered into a numerical order by photograph number and then ground point number as shown.

B.4 Ground Point Coordinate File *point.in*

Point	Code	Final Xa	Final Ya	Final Za
(m)				
2	0	1030.0243	840.1338	99.9923
3	3	1018.0107	840.1195	100.1982
4	3	982.0424	840.1254	101.9284
5	0	970.0735	840.0738	102.3430
6	0	1000.0055	880.0775	101.5067
7	0	1029.9862	880.0605	100.7563
8	3	1017.9843	880.0767	100.9824
9	3	981.9567	880.0697	101.7495
10	0	969.9906	880.0646	102.0459
11	0	1000.0061	920.0343	101.5529
12	0	1030.0004	920.0653	100.5178
13	3	1017.9921	920.0588	100.7953
14	3	982.0373	920.0249	101.7973
15	0	970.0489	920.0451	102.0761
16	0	999.9817	960.0225	101.2218
17	0	1029.9723	960.0400	100.3837
18	3	1017.9633	960.0373	100.6279
19	3	981.9127	960.0069	101.7452
20	0	970.0120	960.0130	102.1688

The ground point coordinate file contains both the coordinates of the control points and the approximate coordinates of the tie points. The different points are distinguished by a point code:

- 0 tie point
- 1 height control point
- 2 plan control point
- 3 three dimensional control point

The point numbering system does not have to be sequential but cannot contain alphanumeric characters. The points must be listed in the *point.in* file in a numerical order since the image point observations are automatically re-ordered in a similar manner.

B.5 Photograph Initial Orientation File

photo.in

```
photo no     w                  phi                k (approx photo rot"s,rads)
              Xo                 Yo                 Zo (approx PC,m)     pd
       (mic)
       19    -0.004655186       -0.040500248       4.674725289
               996.034546         833.062298         165.417402        99480.000
       20    -0.040786234        0.014832683       4.760379386
               997.389659         871.728782         161.680207        99480.000
       21    -0.010135150       -0.038632178       4.696682242
               998.724747         914.926608         164.932782        99480.000
       22    -0.040990806       -0.034364915       4.696178616
              1000.345812         964.917508         163.273469        99480.000
       23    -0.004617449       -0.011423952       4.739158886
              1001.162745         995.791150         164.630408        99480.000
       24    -0.074075070       -0.025340763       4.723526104
              1018.732257         832.408968         161.315595        99480.000
       25    -0.067187547       -0.004484970       4.723255437
              1016.541238         871.725056         158.441613        99480.000
       26    -0.075879805       -0.055436758       4.663185325
              1016.146029         909.981334         163.944852        99480.000
       27    -0.079920627       -0.018618499       4.699160307
              1014.024176         951.140383         163.965963        99480.000
       28    -0.030575815       -0.026250099       4.650080928
              1014.494464         992.169692         160.225107        99480.000
```

The photograph initial orientation file contains approximate orientation values for the aerial triangulation process. Each photograph has a two line entry in this file to allow definition of position and orientation of the photograph perspective centre as well as the principal distance of the camera. The positional units are generally metres and the principal distance is given in microns (since the image point observations are generally given in microns).

B.6 GPS Antenna Coordinate File *gpsant.in*

```
TABBY Antenna Coordinate File
Photo X      Y      Z (m)
19     996.1068    833.1463    165.4960    0.095 0.095 0.095
20     997.5221    871.8844    161.8073    0.095 0.095 0.095
21     998.8565    915.0649    165.0750    0.095 0.095 0.095
22     1000.323    964.8966    163.2742    0.095 0.095 0.095
23     1001.285    995.9152    164.7892    0.095 0.095 0.095
24     1018.722    832.4290    161.3258    0.095 0.095 0.095
25     1016.493    871.6611    158.3650    0.095 0.095 0.095
26     1016.158    909.9810    163.9654    0.095 0.095 0.095
27     1014.030    951.1446    163.9911    0.095 0.095 0.095
28     1014.343    992.0179    160.1009    0.095 0.095 0.095
34     976.7289    827.3732    165.3658    0.095 0.095 0.095
35     977.1575    875.7218    159.8350    0.095 0.095 0.095
36     976.1434    911.7005    161.0651    0.095 0.095 0.095
37     977.7336    957.0579    161.7941    0.095 0.095 0.095
38     978.1521    991.7891    164.3612    0.095 0.095 0.095
```

The GPS antenna coordinate file contains the coordinates of the antenna phase centre at the instant of exposure for each photograph in the estimation. It is obviously only included for a combined GPS triangulation. The coordinates of the antenna phase centre are given in the ground control coordinate system, which implies that they must be transformaed from WGS84 by some prior process. The standard error of the coordinates, from the GPS processing phase, is also given in this file and used for weighting the observations in the functional model.

B.7 Final Coordinate File ****.*crd*

TABBY version 1.96 Coordinate File

*******Variances scaled by unit variance= 0.9998152*******
*******FTEST PASS - Statistical Base Valid*******

Photograph Exterior Orientation Elements

Photo	Omega	Phi	Kappa	se(w)	se(p)	se(k)
19	-0.004155	-0.040937	4.675017	1.214E-04	1.316E-04	5.989E-05
20	-0.040312	0.014690	4.760599	6.286E-05	8.231E-05	3.575E-05
21	-0.010280	-0.038325	4.696754	5.602E-05	8.115E-05	3.274E-05
22	-0.041263	-0.034060	4.696052	5.910E-05	8.024E-05	3.641E-05
35	-0.027843	0.001696	4.684531	1.290E-04	1.629E-04	4.945E-05
36	-0.082088	-0.022836	4.701903	6.344E-05	1.332E-04	3.931E-05
37	-0.040877	0.002122	4.696315	7.077E-05	1.497E-04	4.196E-05
38	-0.043894	0.004424	4.712434	2.365E-04	2.125E-04	6.251E-05
Average s.e.				2.085E-04	1.491E-04	4.912E-05

Photo	Xo	Yo	Zo	se(Xo)	se(Yo)	se(Zo)
19	996.055946	833.095449	165.445095	1.053E-02	8.538E-03	6.437E-03
20	997.399286	871.761622	161.684527	5.770E-03	5.105E-03	3.014E-03
21	998.706404	914.914847	164.924912	5.711E-03	4.915E-03	2.364E-03
22	1000.325840	964.899056	163.276740	5.729E-03	4.924E-03	2.767E-03
35	977.010552	875.574905	159.688061	1.018E-02	8.131E-03	6.436E-03
36	975.882106	911.439153	160.803817	8.286E-03	5.325E-03	3.162E-03
37	977.676009	957.000292	161.736491	9.424E-03	5.785E-03	3.242E-03
38	978.208142	991.845056	164.417163	1.414E-02	1.624E-02	7.303E-03
Average s.e.				1.002E-02	1.328E-02	1.006E-02

Point Coordinates

Point	X	Y	Z	se(X)	se(Y)	se(Z)
2	1030.0254	840.1328	99.9964	4.906E-03	3.897E-03	6.577E-03
3	1018.0089	840.1192	100.2081	3.155E-03	3.186E-03	1.909E-03
8	1017.9864	880.0778	100.9768	2.227E-03	2.365E-03	1.752E-03
9	981.9577	880.0706	101.7479	2.254E-03	2.359E-03	1.732E-03
22	1030.0144	1000.0171	100.7875	3.843E-03	3.741E-03	5.274E-03
23	1017.9808	1000.0155	100.9822	3.069E-03	3.135E-03	1.890E-03
24	981.9768	1000.0175	101.9402	3.068E-03	3.135E-03	1.882E-03
25	969.9935	999.9885	102.3207	3.704E-03	3.699E-03	4.807E-03
Average Unknown Point Standard Errors				2.904E-03	2.864E-03	3.660E-03
Average Control Point Standard Errors				2.533E-03	2.629E-03	1.778E-03

The final coordinate file is the primary output file from the estimation. At the top of the file is the details on the value of sigma zero and whether this passes

the f-test. The rest of the file details the final coordinates and associated standard error of each unknown parameter. The standard errors are also averaged on a category basis to give a single measure of precision to the estimation.

B.8 Residual File ****.*res*

TABBY version 3.11 Residual File

Photo	Point	X Obs.	Y Obs	vx	vy	vx/sigX	vy/sigY
19	2	-8377.5000	57246.5000	0.000	0.015	0.010	0.010
19	3	-9014.5000	38424.5000	-1.316	-0.328	-0.730	-0.168
19	4	-11161.7000	-17298.0000	0.514	-2.951	0.232	-1.481
19	5	-11765.5000	-35848.3000	0.166	1.246	0.086	0.695
19	6	-72272.5000	12931.8000	0.491	6.972	0.217	2.529
YY							
19	8	-71455.5000	41047.0000	-0.980	-2.531	-0.566	-1.203
19	9	-72749.2000	-15007.7000	0.731	-1.017	0.303	-0.369
19	10	-73214.5000	-33377.5000	0.401	-1.424	0.219	-0.617
20	2	53177.5000	54521.0000	0.001	-0.015	0.010	-0.010
20	3	54476.5000	35128.2000	3.800	-1.923	2.182	-0.871
X							
20	4	59415.0000	-24884.5000	0.122	3.062	0.075	1.590
20	5	61091.5000	-45767.3000	-0.330	-1.744	-0.612	-1.101
20	6	-9804.2000	2357.3000	2.215	0.648	0.737	0.217
20	6	-9798.8000	2354.0000	-3.185	3.948	-1.060	1.324
20	8	-11048.5000	31467.2000	3.471	-5.461	1.195	-1.831
20	8	-11039.2000	31463.5000	-5.829	-1.761	-2.007	-0.590
X							
20	9	-8449.5000	-27512.0000	3.487	2.077	1.162	0.697
20	9	-8447.0000	-27511.5000	0.987	1.577	0.329	0.529
20	10	-7562.2000	-47693.7000	1.395	-3.186	0.482	-1.128
20	10	-7556.5000	-47699.0000	-4.305	2.114	-1.488	0.748
20	11	-73470.5000	-830.0000	-4.574	5.418	-2.013	1.847
X							
20	12	-74006.8000	46071.7000	-1.200	-1.077	-0.610	-0.439

The residual file follows a similar format to the image point observations file. The image points are listed in numerical order by photograph then point and give an indication of how good the observation was in terms of the estimation. The residual between the observed coordinate and the calculated point is given for both the x and y coordinates. The final two colums are a statistic calculated according to the principles of Baarda data snooping.

B.9 Covariance Matrix File ****.*cov*

The covariance matrix is the inverse of the normal matrix and is calculated during the estimation process. It is reproduced in this file to enable examination of any off-diagonal parameters they may be of interest.

B.10 Residual Statistics File ****.*his*

```
Photo. Obs. Residual Information File

      Std Deviation:              2.624
      Std Error Sample Mean:      0.147

      Residual Histogram Data:

            Under 3.5 sig :          0
         -3.5 -> -3.0 sig :          0
         -3.0 -> -2.5 sig :          1
         -2.5 -> -2.0 sig :          4
         -2.0 -> -1.5 sig :         17
         -1.5 -> -1.0 sig :         29
         -1.0 -> -0.5 sig :         49
         -0.5 -> 0.0 sig :          65
         0.0 -> 0.5 sig :           60
         0.5 -> 1.0 sig :           38
         1.0 -> 1.5 sig :           30
         1.5 -> 2.0 sig :           21
         2.0 -> 2.5 sig :           5
         2.5 -> 3.0 sig :           1
         3.0 -> 3.5 sig :           0
           Over 3.5 sig :           0
```

The statistics file contains an analysis of the image point observation residuals. A histogram of the residuals is calculated to assist the identification of outliers in the data.

B.11 Ground Point Residual File ****.*out*

		Ground Coordinate Residuals					
		Point X Resid	Y Resid	Z Resid			
1	3	1000.0033	1000.0075	99.9994	-0.0033	-0.0075	0.0016
2	3	999.7199	982.3785	100.1352	-0.0073	-0.0115	0.0078
3	3	999.4383	963.4450	99.9549	-0.0131	-0.0108	0.0011
4	3	1000.3215	1018.3491	99.9059	0.0003	-0.0060	-0.0029
5	3	1000.5492	1036.0563	99.6327	0.0067	-0.0065	-0.0017
46	3	1451.4404	1000.1795	101.1816	-0.0040	0.0010	-0.0036
47	3	1451.2749	981.5663	101.5196	-0.0074	-0.0000	0.0004
48	3	1451.0970	962.0294	101.8022	-0.0103	0.0060	-0.0042
49	3	1451.6048	1018.9180	101.1314	0.0036	-0.0024	0.0006
50	3	1451.7158	1037.6400	101.0868	0.0022	-0.0003	0.0032
51	3	1501.8486	1000.0012	102.9747	0.0045	-0.0012	0.0013
52	3	1501.7315	981.2889	102.9534	-0.0061	0.0010	0.0026
53	3	1501.5949	961.6990	102.7972	-0.0092	0.0073	-0.0022
54	3	1501.9736	1018.7526	103.1353	0.0087	-0.0010	0.0027
55	3	1502.1378	1037.5108	103.1366	0.0102	0.0019	-0.0006
Unknown Point RMSE					NaN	NaN	NaN
Control Point RMSE					9.811E-03	4.795E-03	2.766E-03

The ground point residual file displays the final estimated coordinates of the points with a measure of accuracy. The accuracy is calculated as a residual between the ground surveyed coordinates of the point and the final estimated coordinates. The ground point residual is one of the major indicators of bundle estimation preformance in this research. The file also contains a root mean square error of the residuals across the entire test field.

B.12 GPS Antenna Residual File ****.*gps*

GPS Antenna Coordinate Residuals

Photo				X Resid	Y Resid	Z Resid
24	992.4426	1000.5638	180.1383	0.0287	-0.0005	0.0641
25	1042.5253	1001.5948	181.4894	0.0302	-0.0209	0.0210
26	1095.6523	1000.4910	183.0498	0.0299	-0.0007	0.0225
27	1141.4484	1000.5464	186.0589	0.0152	-0.0047	0.0205
28	1190.0758	1001.6349	188.2518	0.0192	0.0005	0.0254
30	1292.1812	1002.8300	182.9338	0.0617	0.0608	0.0550
60	1191.7766	1018.9296	182.0405	0.0027	-0.0061	-0.0134
61	1241.4591	1016.8927	182.4814	-0.0142	0.0040	-0.0077
62	1299.4121	1017.1959	181.7598	0.0137	-0.0128	0.0154
63	1341.0246	1017.6307	186.5561	0.0156	-0.0021	-0.0060
64	1390.5111	1017.3674	187.5396	0.0041	-0.0024	-0.0042
65	1445.1702	1015.0398	184.1772	-0.0221	-0.0544	0.0261
66	1493.0810	1021.6002	189.9867	0.0172	-0.0298	-0.0050
GPS Antenna RMSE				3.287E-02	3.080E-02	3.023E-02

The GPS antenna coordinate residual file takes a similar form to the previous file. It displays the final coordinates of the GPS antenna at each exposure, calculated from the observation equation. The measure of accuracy is calculated as a residual between the observed (pre-estimation) coordinates and the final estimated coordinates. The file also contains a root measure square error of the residuals across all the GPS antenna positions in the bundle estimation.

B.13 Photograph Final Orientation File

****.*pho*

The photograph final orientation file contains the orientation parameters for each of the photographs entered into the estimation. It follows the precise format of the photograph initial orientation file, *photo.in*.

B.14 Ground Point Coordinate File ****.*con*

The ground point coordinate file contains the final estimated coordinates of each of the points entered into the estimation. It follows the precise format of the ground point coordinate file used in the estimation, *point.in*.

B.15 GPS Antenna Coordinate File ****.*ant*

The GPS antenna coordinate file contains the final estimated coordinates of each of the GPS antenna phase centres entered into the estimation. It follows the precise format of the GPS antenna coordainte file used in the estimation, *gpsant.in*.

Appendix C

Aerial Triangulation:

Ground Point Residual Plots

C.1 Introduction

This chapter is to be used in conjunction with the aerial triangulation tests described in chapter 8. The diagrams show a plot of the individual ground point coordinate residuals for a specified aerial triangulation test configuration. Each diagram is split between a vector plot of the x and y axes residuals and a bubble plot of the height axis residuals. The ground point configuration is given overleaf.

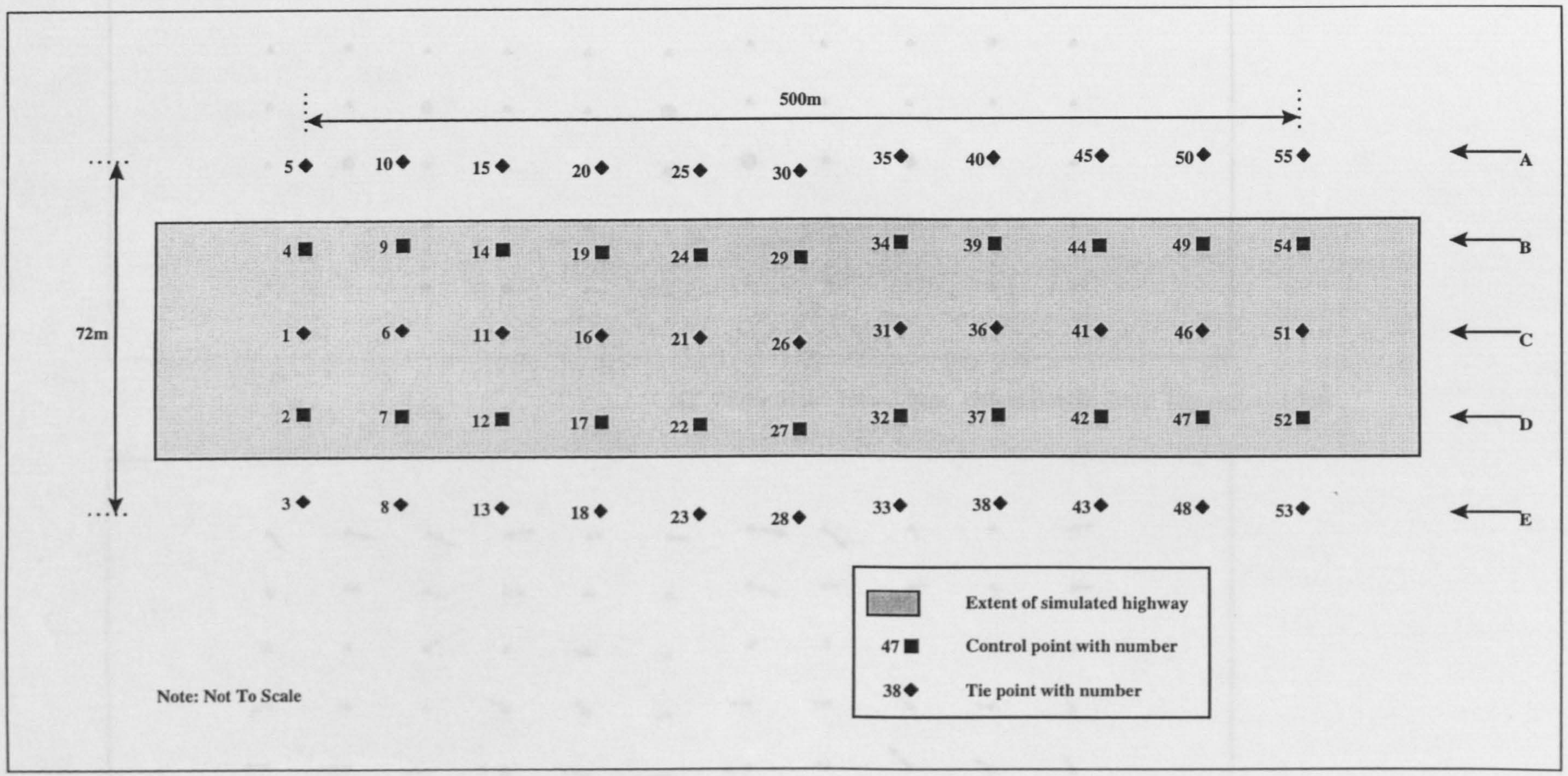
500m
72m
5 10 15 20 25 30 35 40 45 50 55
A
4 9 14 19 24 29 34 39 44 49 54
B
1 6 11 16 21 26 31 36 41 46 51
C
2 7 12 17 22 27 32 37 42 47 52
D
3 8 13 18 23 28 33 38 43 48 53
E
Extent of simulated highway
47 Control point with number
38 Tie point with number
Note: Not To Scale

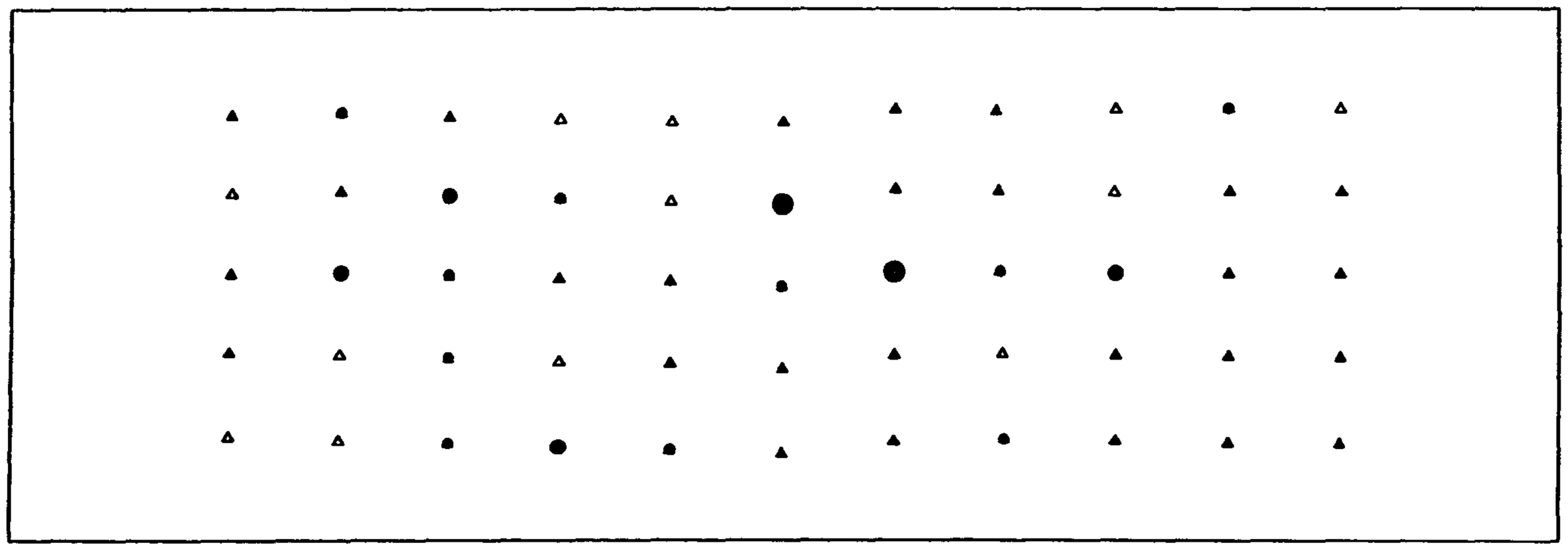

XY Vector Scale: 1cm=3.5cm Height Bubble Scale: 1cm radius=3.5cm

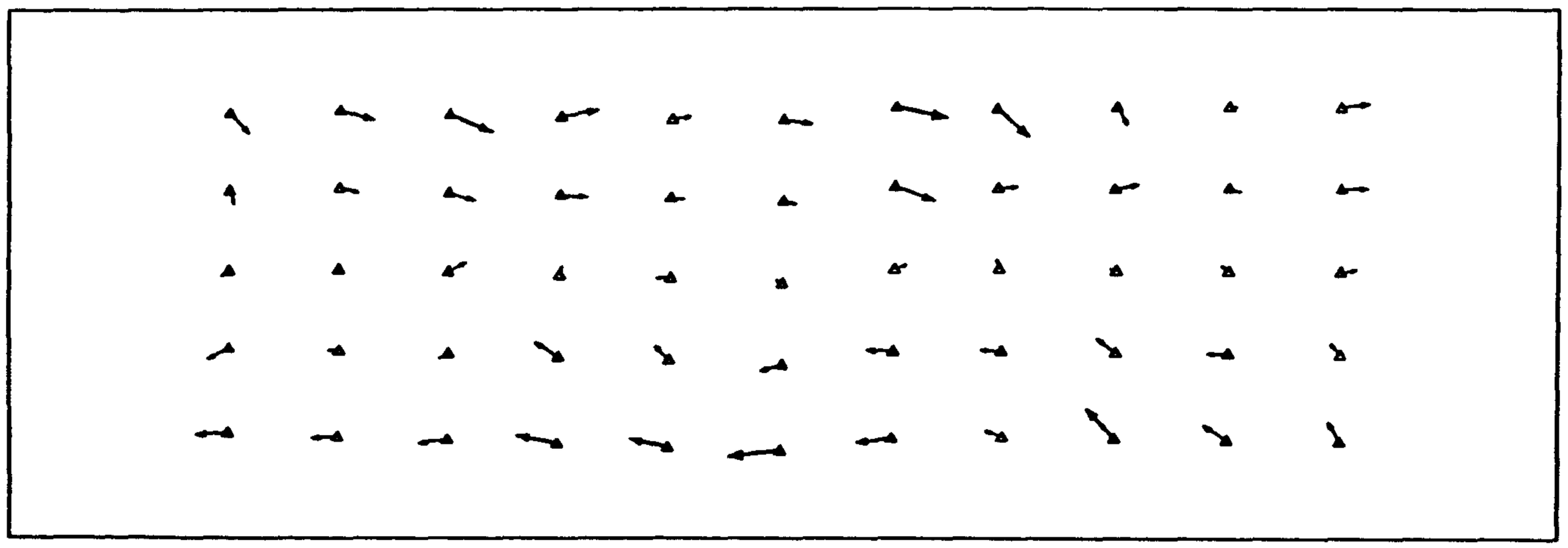

Figure C.1.1 - XY Vector Residual Plot and Height Bubble Residual Plot
(Centre Strip, No GPS, All Points As Ground Control)

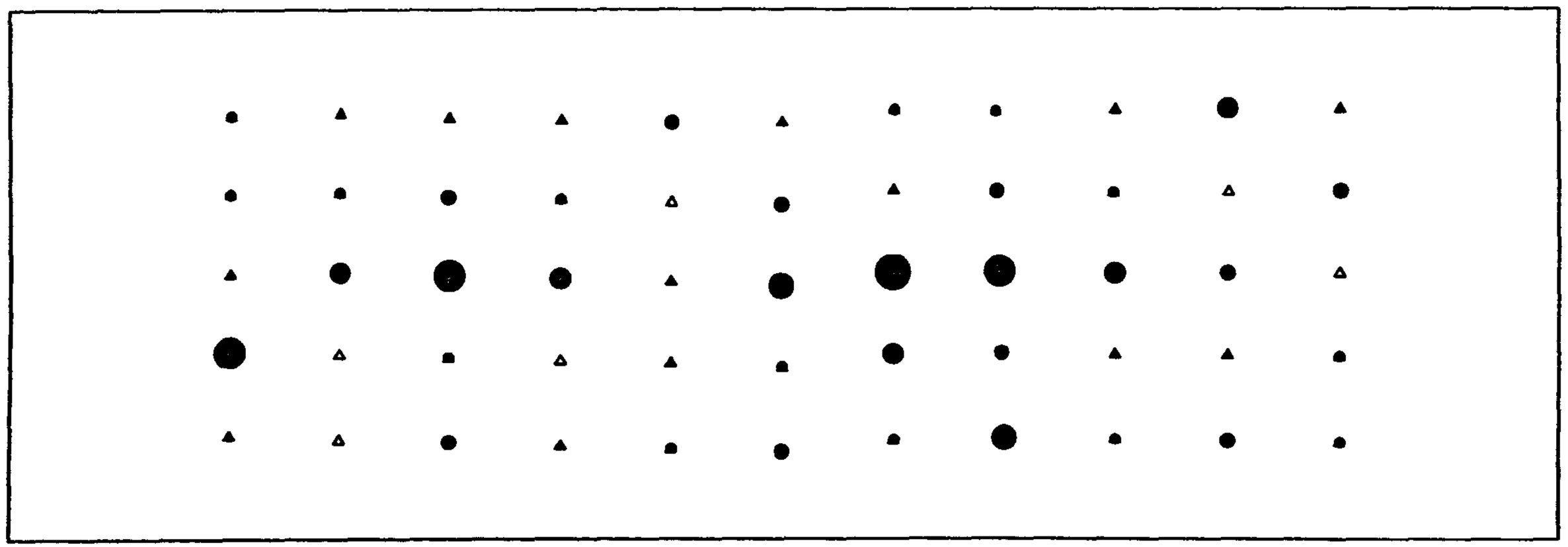

XY Vector Scale: 1cm=3.5cm Height Bubble Scale: 1cm radius=3.5cm

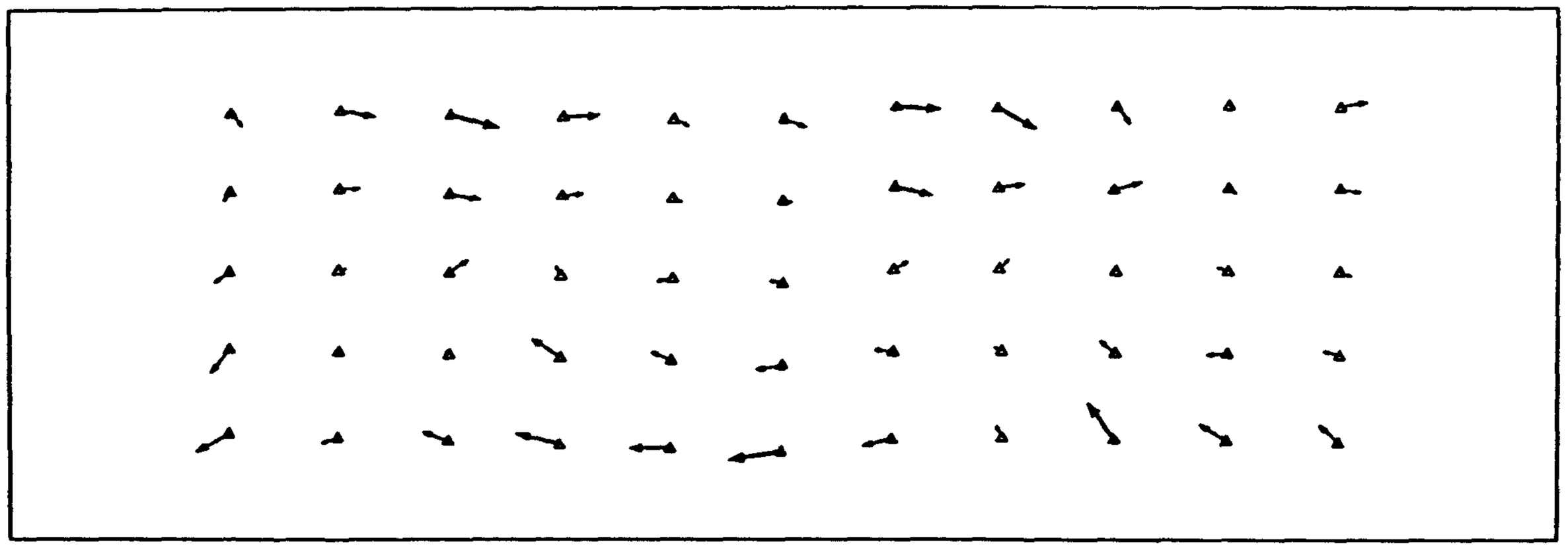

Figure C.1.2 - XY Vector Residual Plot and Height Bubble Residual Plot
(Centre + Left, No GPS, All Points As Ground Control)

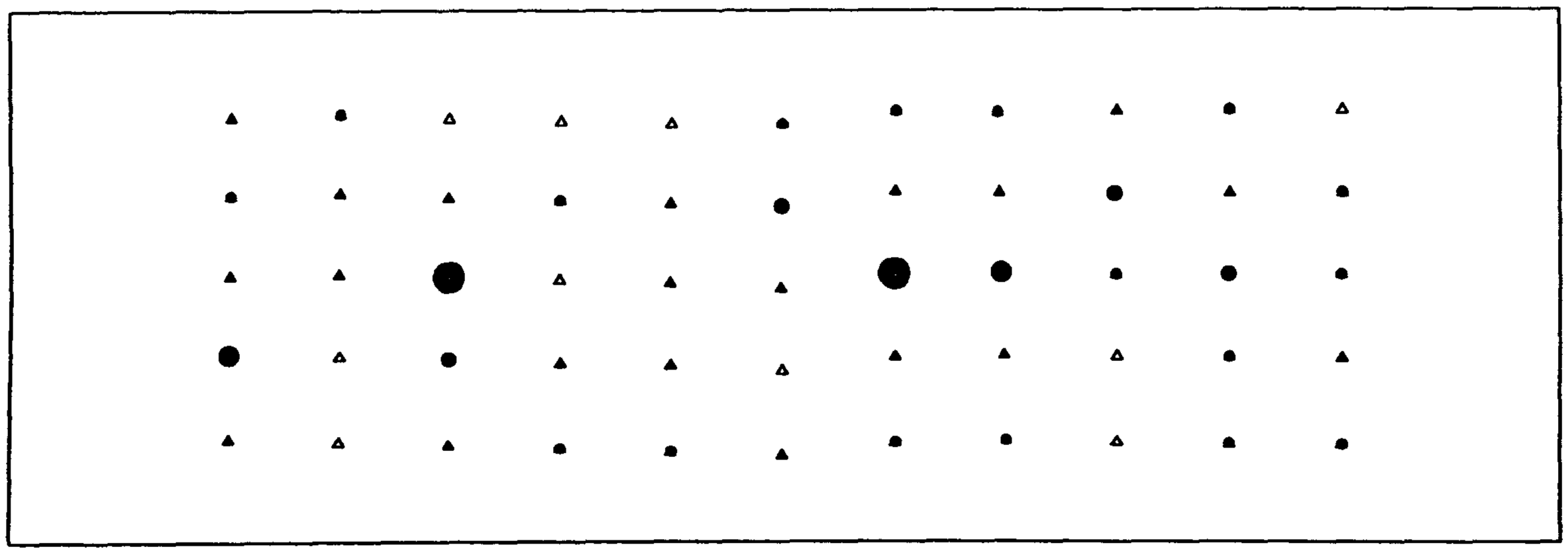

XY Vector Scale: 1cm=3.5cm Height Bubble Scale: 1cm radius=3.5cm

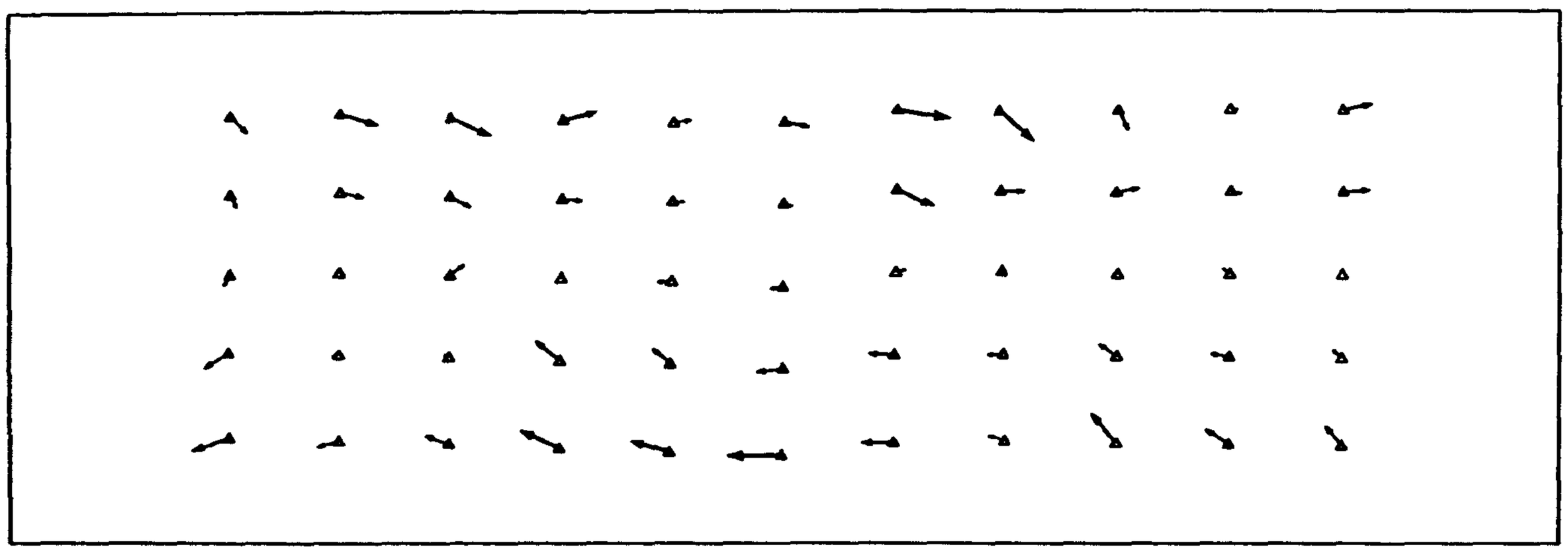

Figure C.1.3 - XY Vector Residual Plot and Height Bubble Residual Plot
(Centre + Right, No GPS, All Points As Ground Control)

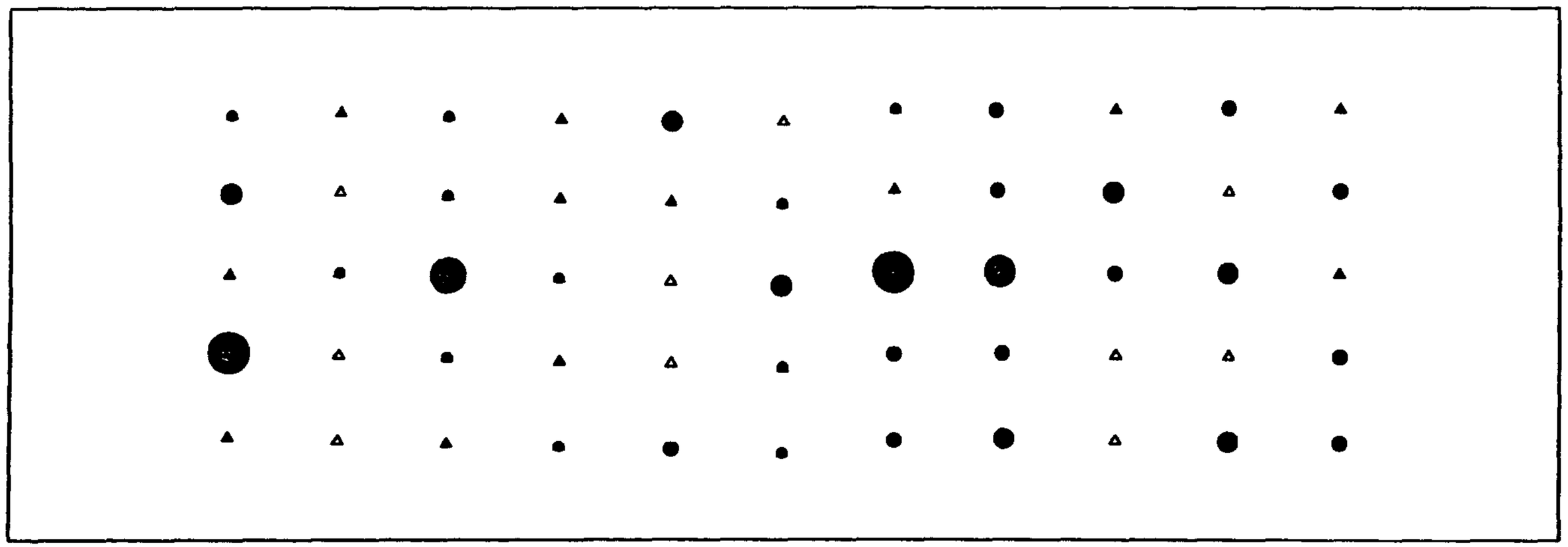

XY Vector Scale: 1cm=3.5cm Height Bubble Scale: 1cm radius=3.5cm

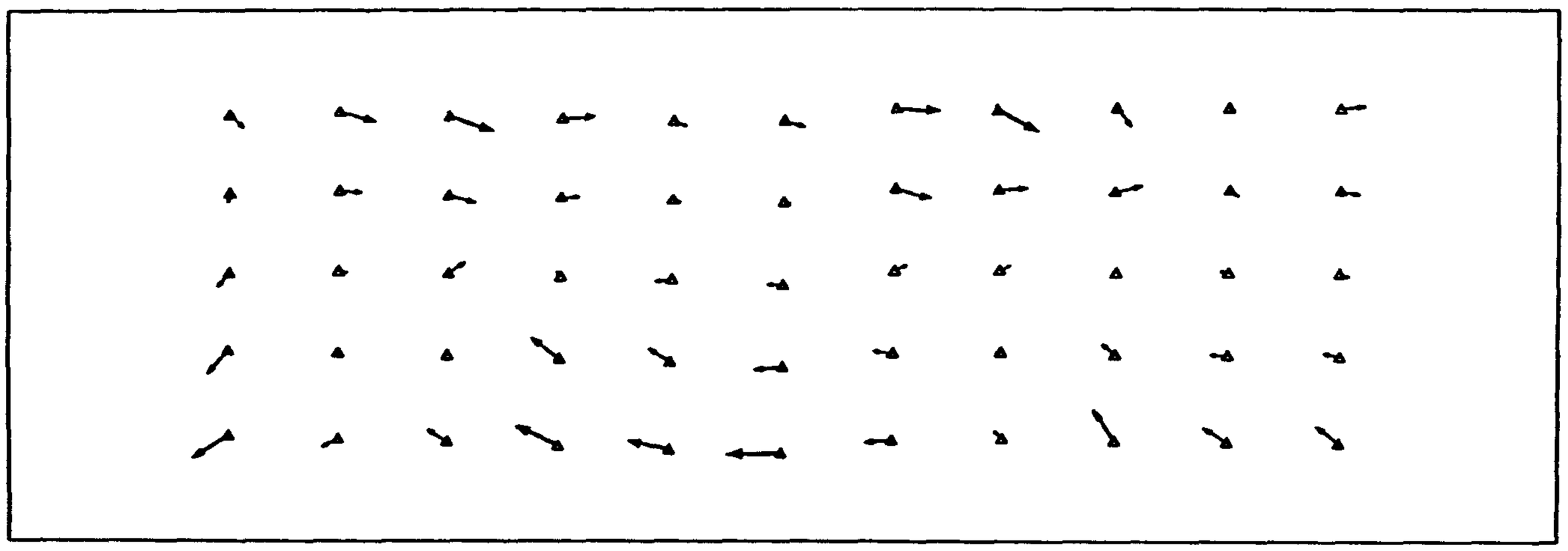

Figure C.1.4 - XY Vector Residual Plot and Height Bubble Residual Plot
(Full Block, No GPS, All Points As Ground Control)

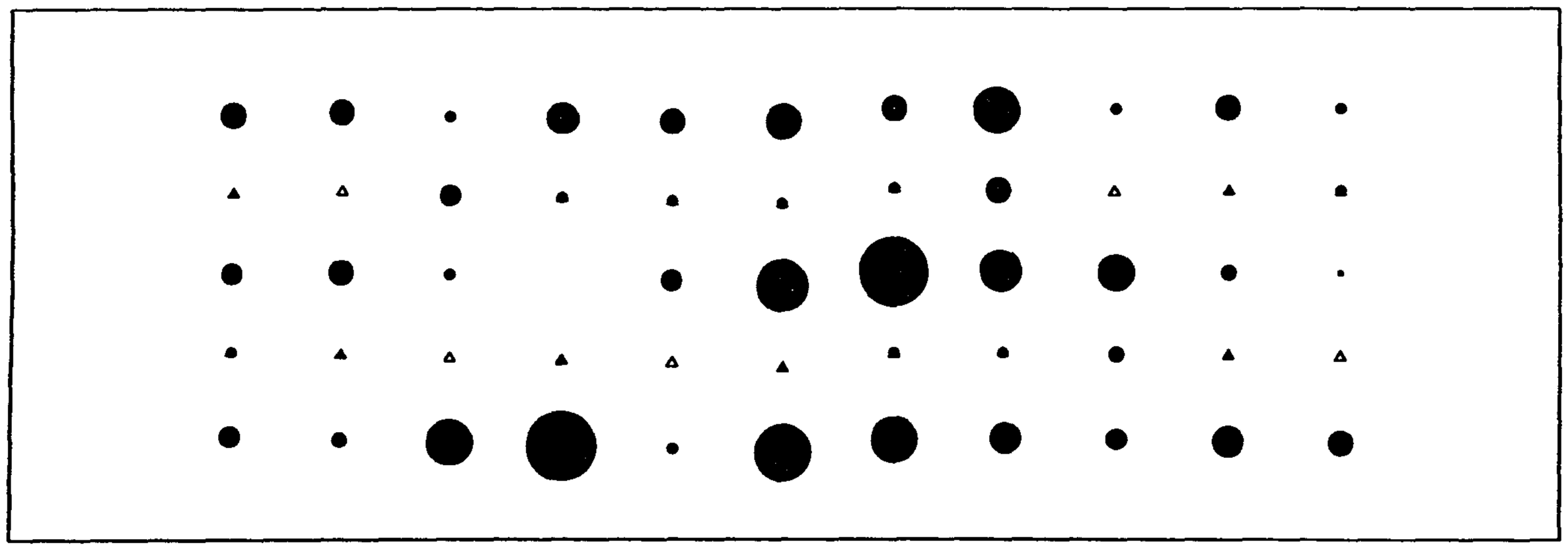

XY Vector Scale: 1cm=3.5cm Height Bubble Scale: 1cm radius=3.5cm

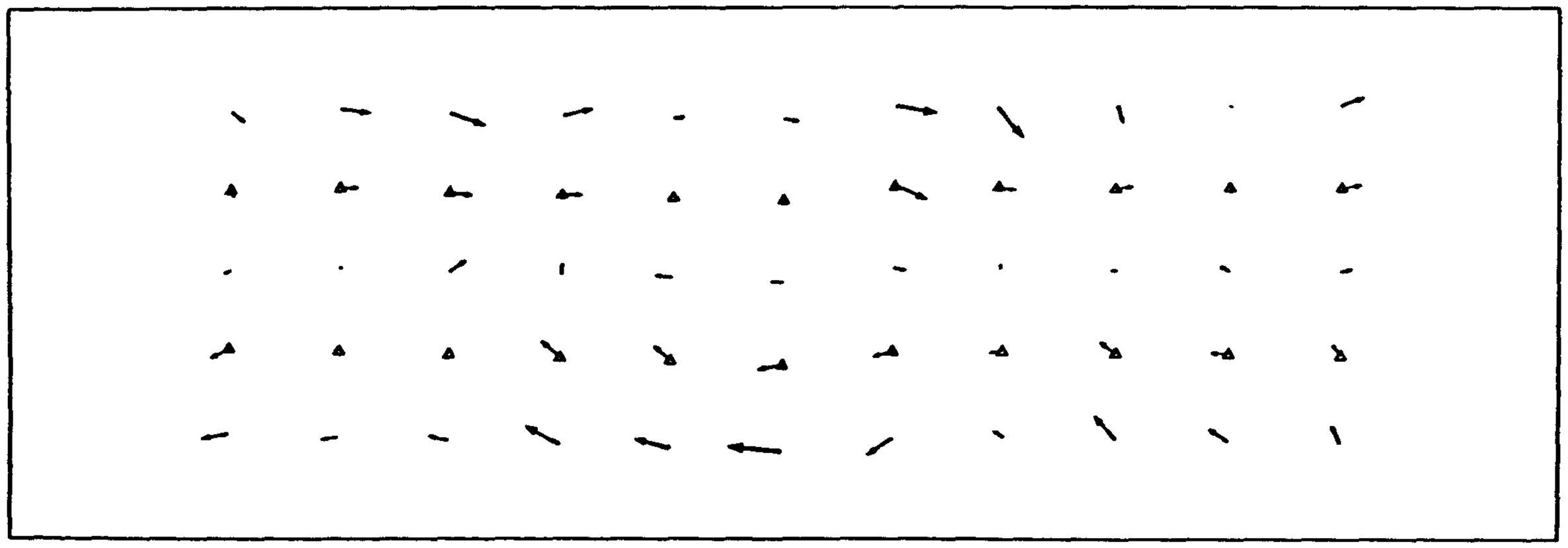

Figure C.2.1 - XY Vector Residual Plot and Height Bubble Residual Plot
(Centre Strip, No GPS, 3-D Control Points At 50m Interval)

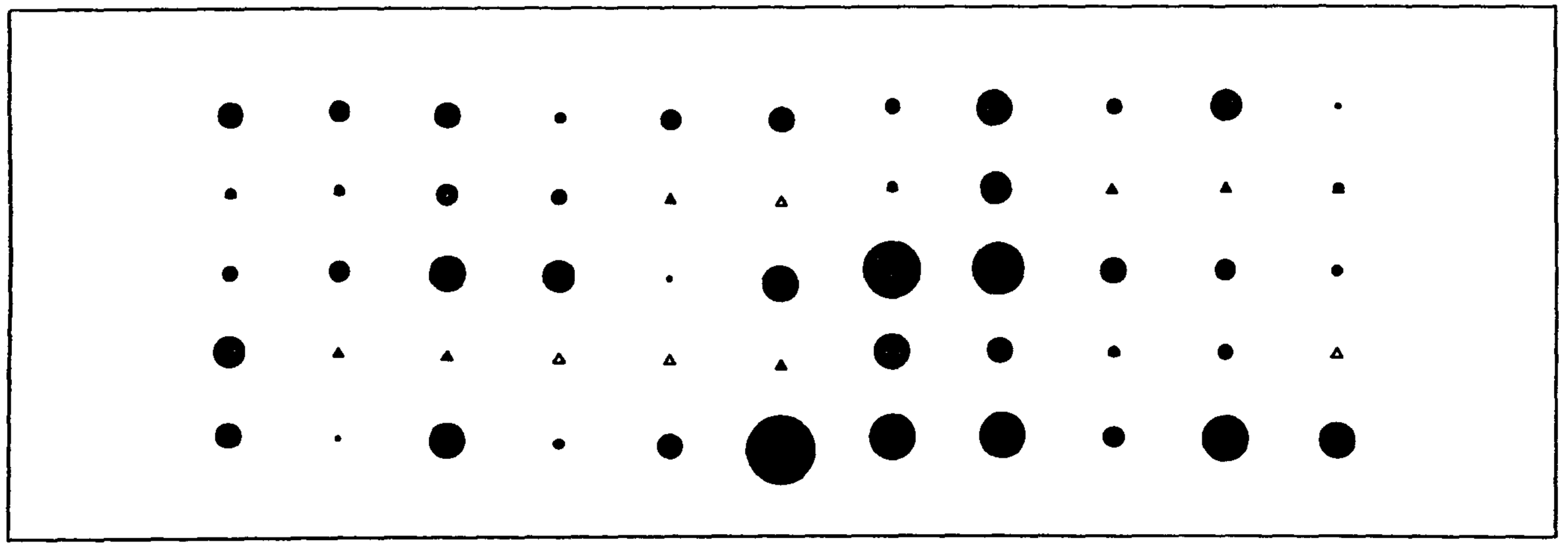

XY Vector Scale: 1cm=3.5cm Height Bubble Scale: 1cm radius=3.5cm

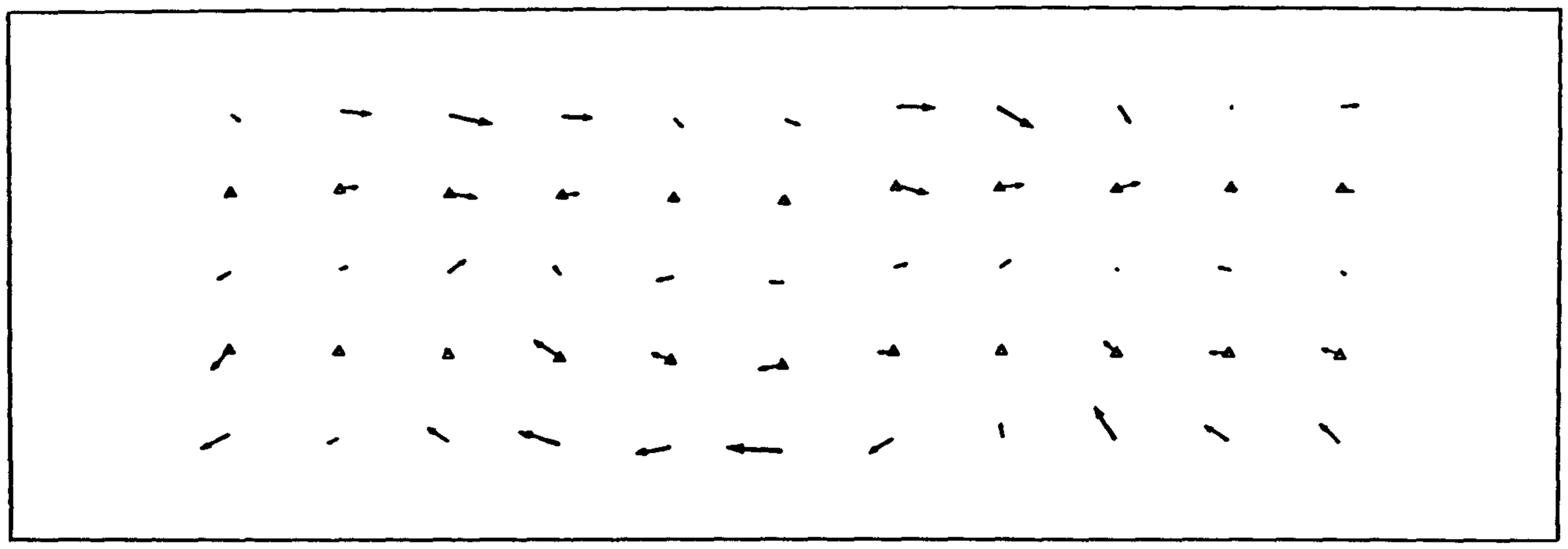

Figure C.2.2 - XY Vector Residual Plot and Height Bubble Residual Plot
(Centre + Left, No GPS, 3-D Control Points At 50m Interval)

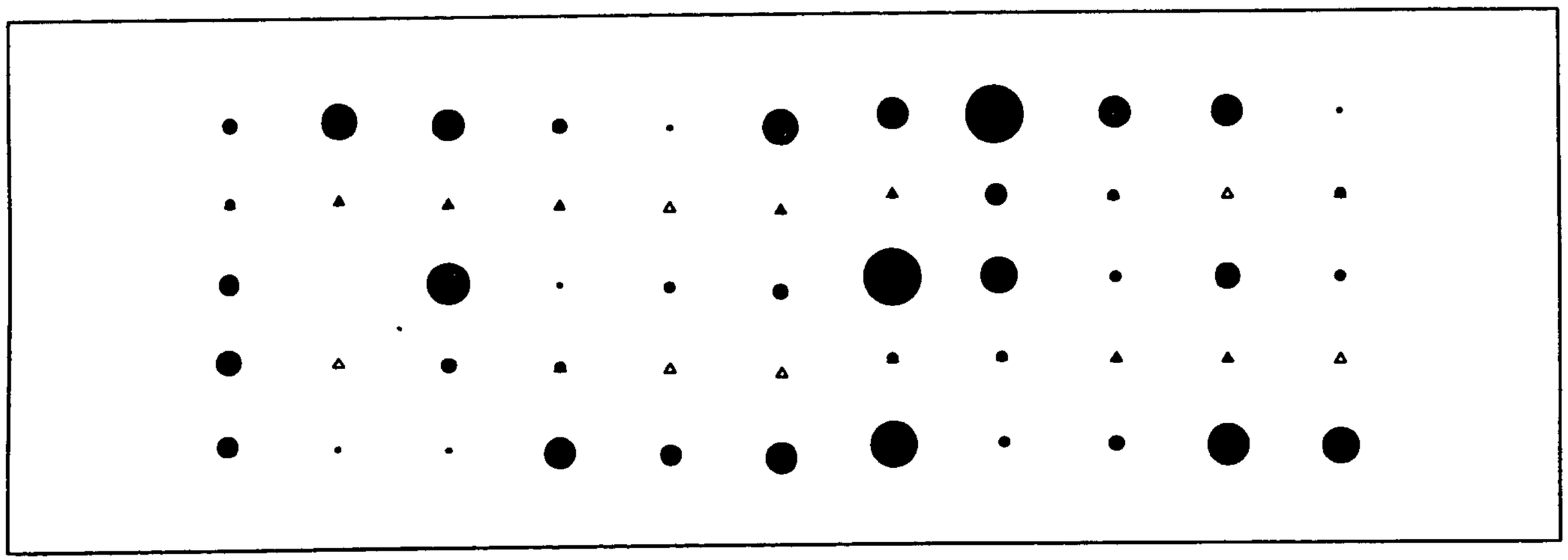

XY Vector Scale: 1cm=3.5cm Height Bubble Scale: 1cm radius=3.5cm

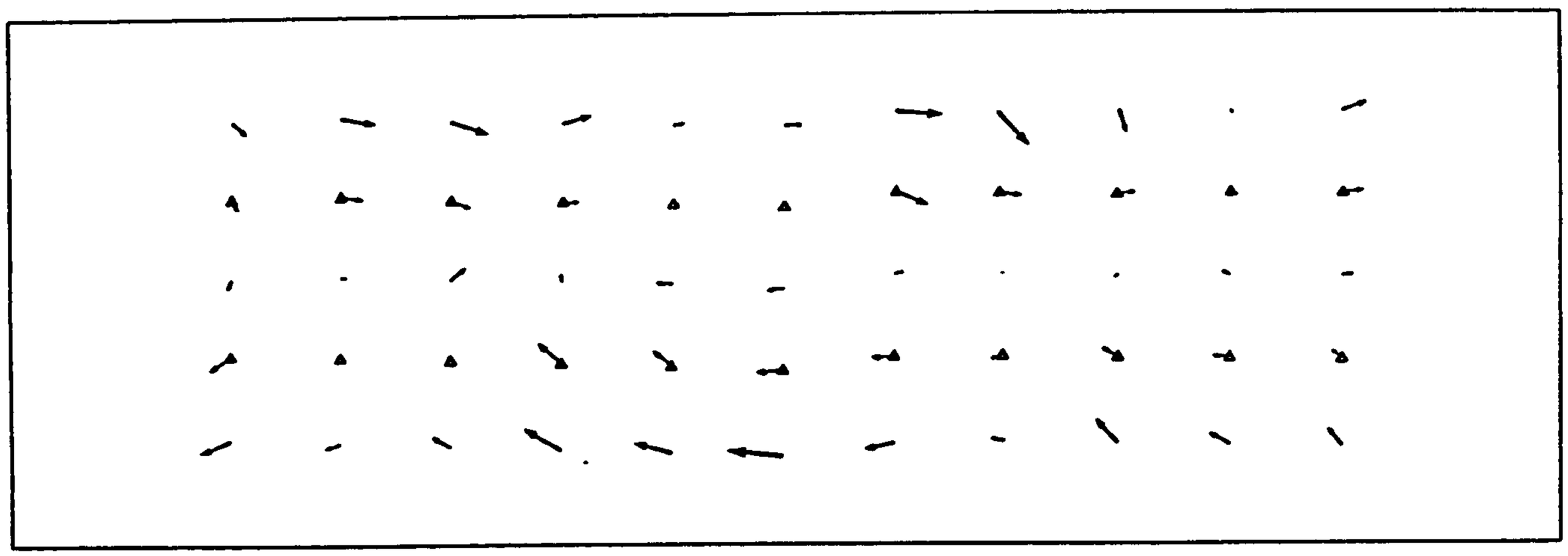

Figure C.2.3 - XY Vector Residual Plot and Height Bubble Residual Plot
(Centre + Right, No GPS, 3-D Control Points At 50m Interval)

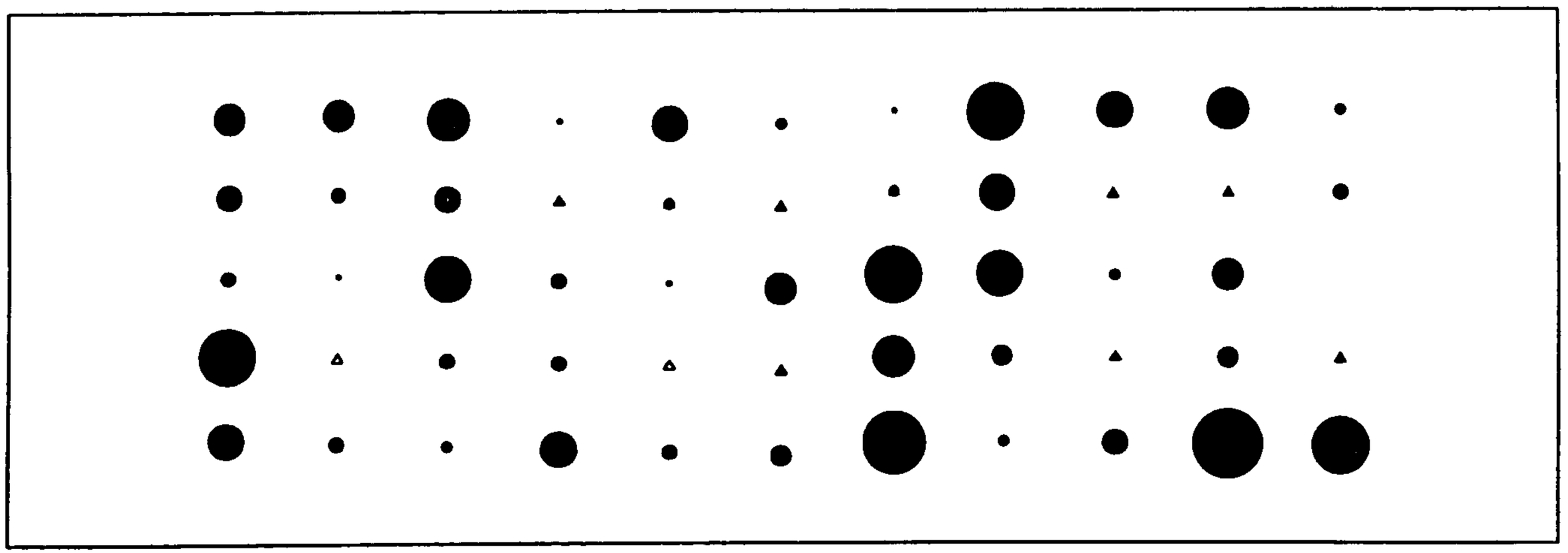

XY Vector Scale: 1cm=3.5cm Height Bubble Scale: 1cm radius=3.5cm

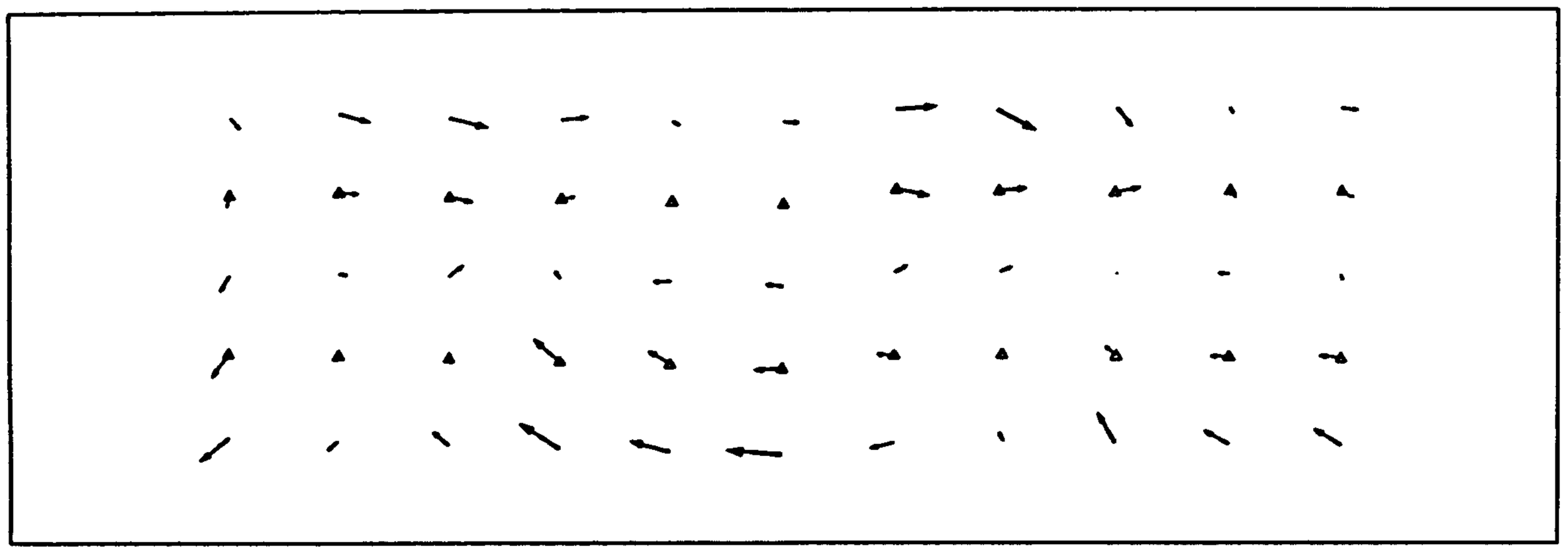

Figure C.2.4 - XY Vector Residual Plot and Height Bubble Residual Plot
(Full Block, No GPS, 3-D Control Points At 50m Interval)

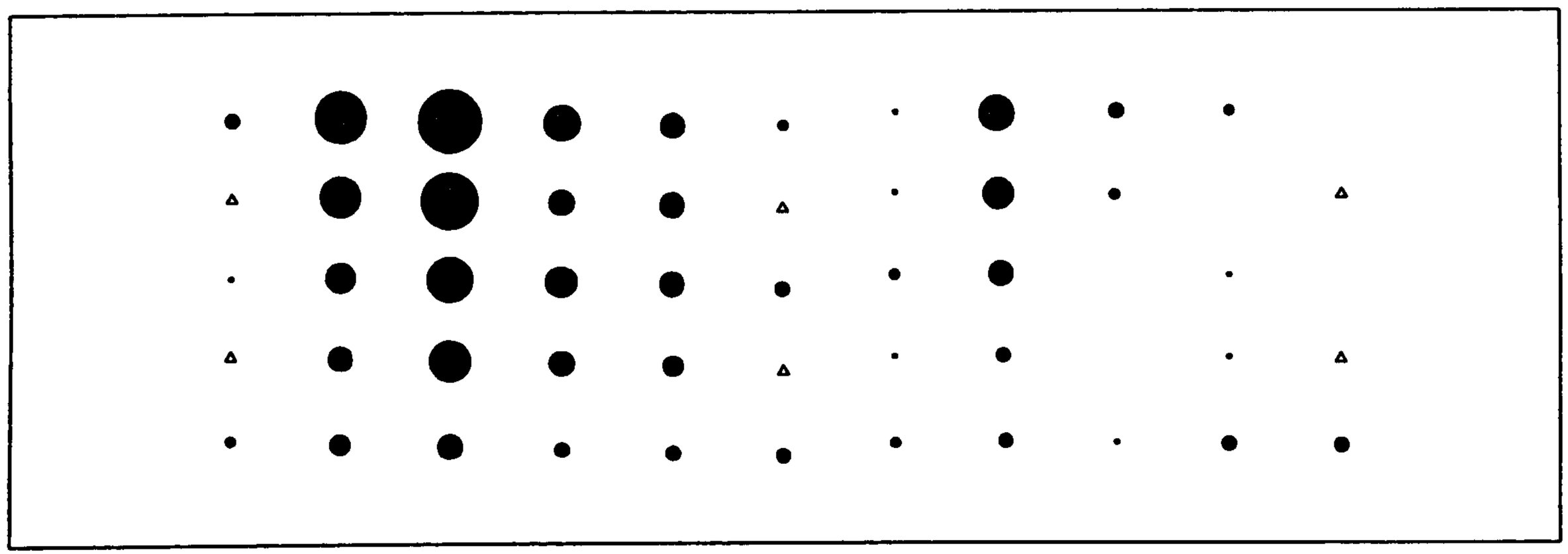

XY Vector Scale: 1cm=3.5cm Height Bubble Scale: 1cm radius=14cm

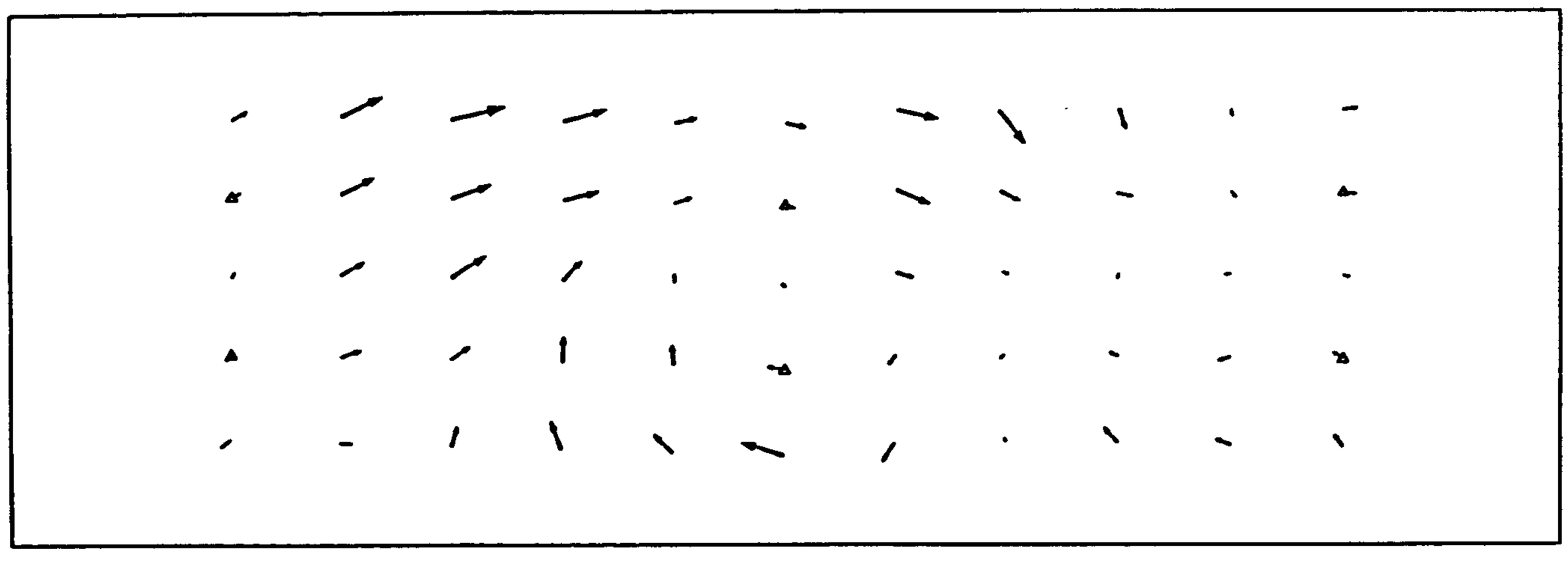

Figure C.3.1 - XY Vector Residual Plot and Height Bubble Residual Plot
(Centre Strip, No GPS, 3-D Control At A 250m Interval)

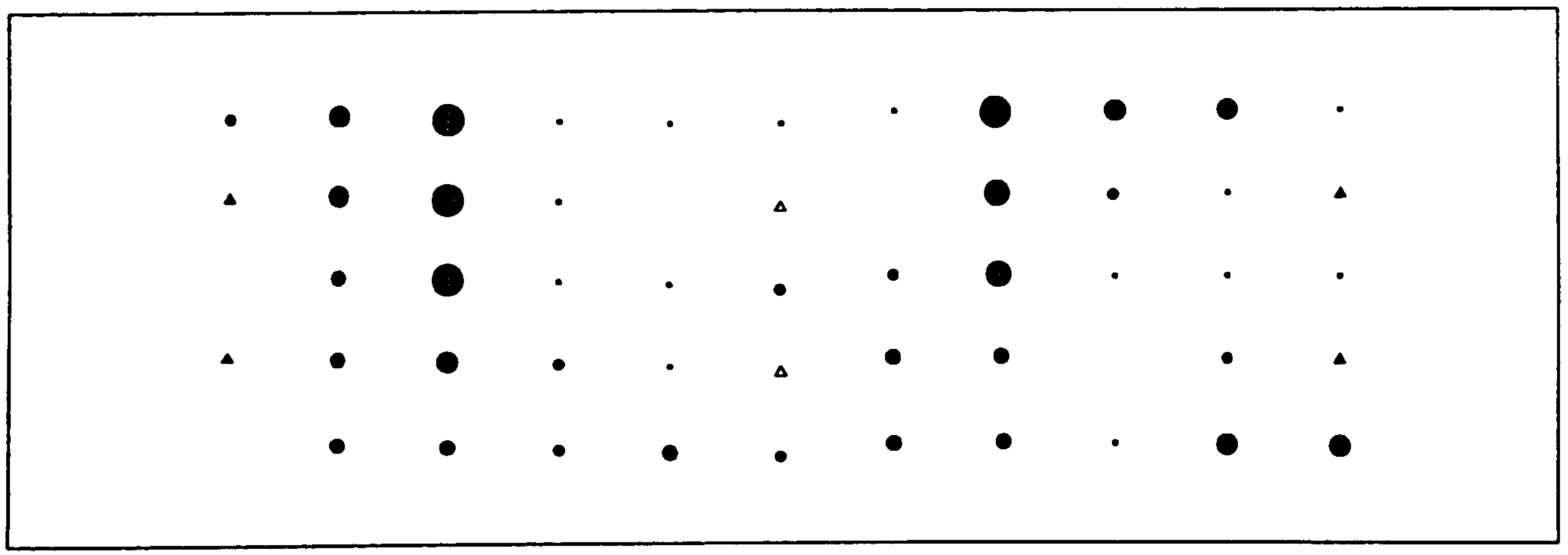

XY Vector Scale: 1cm=3.5cm Height Bubble Scale: 1cm radius=14cm

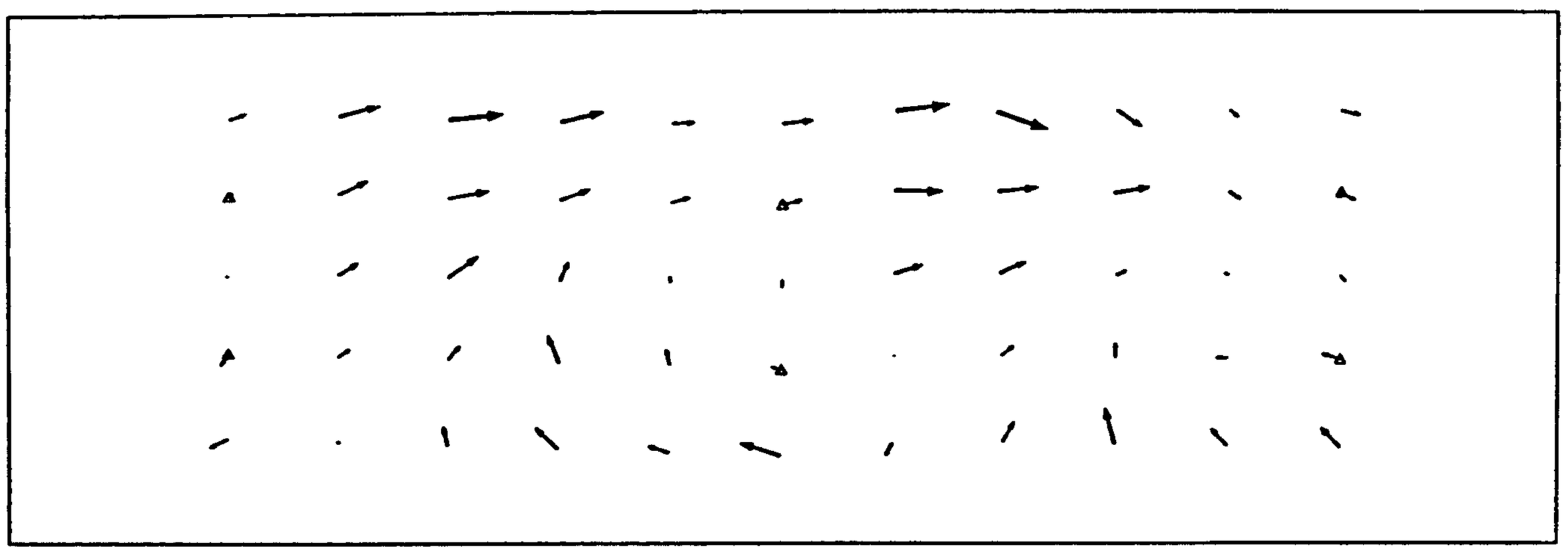

Figure C.3.2 - XY Vector Residual Plot and Height Bubble Residual Plot
(Centre + Left, No GPS, 3-D Control At A 250m Interval)

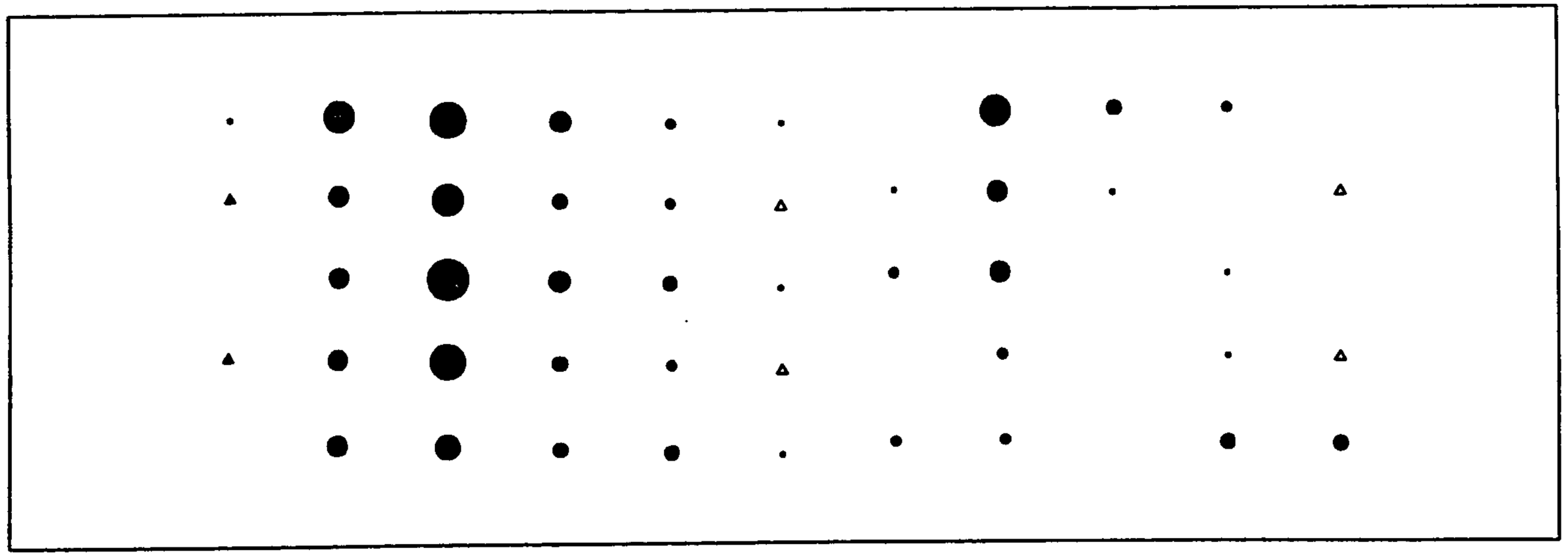

XY Vector Scale: 1cm=3.5cm Height Bubble Scale: 1cm radius=14cm

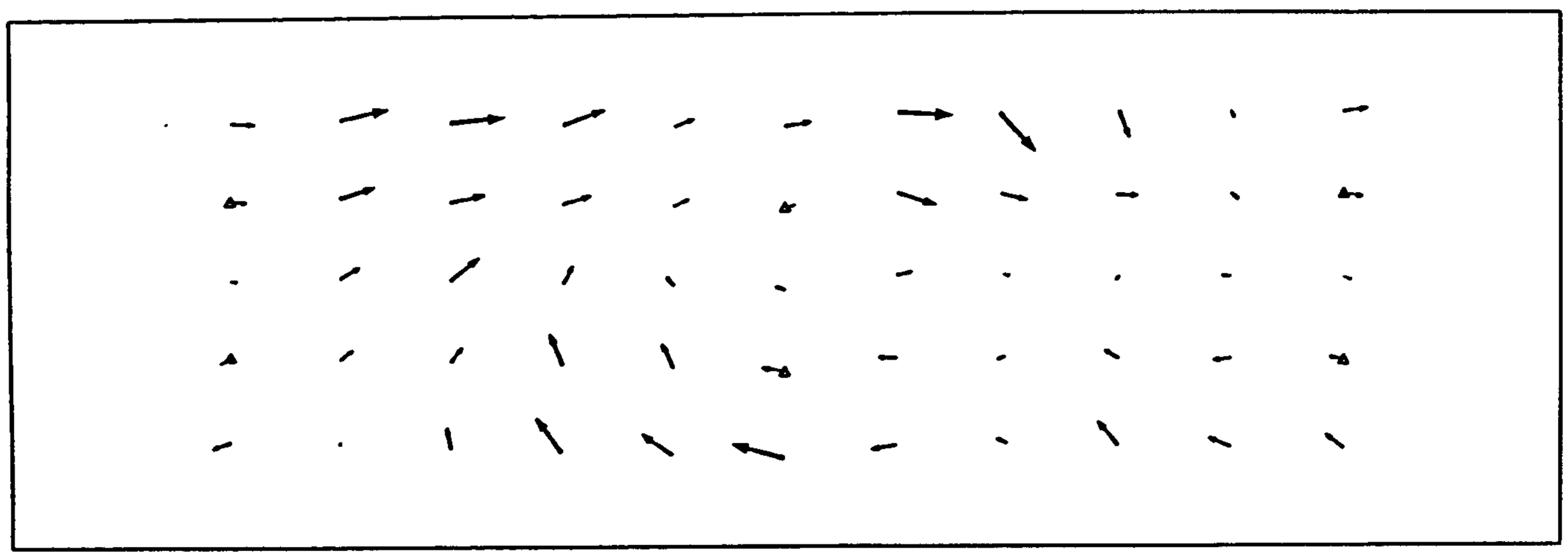

Figure C.3.3 - XY Vector Residual Plot and Height Bubble Residual Plot
(Centre + Right, No GPS, 3-D Control At A 250m Interval)

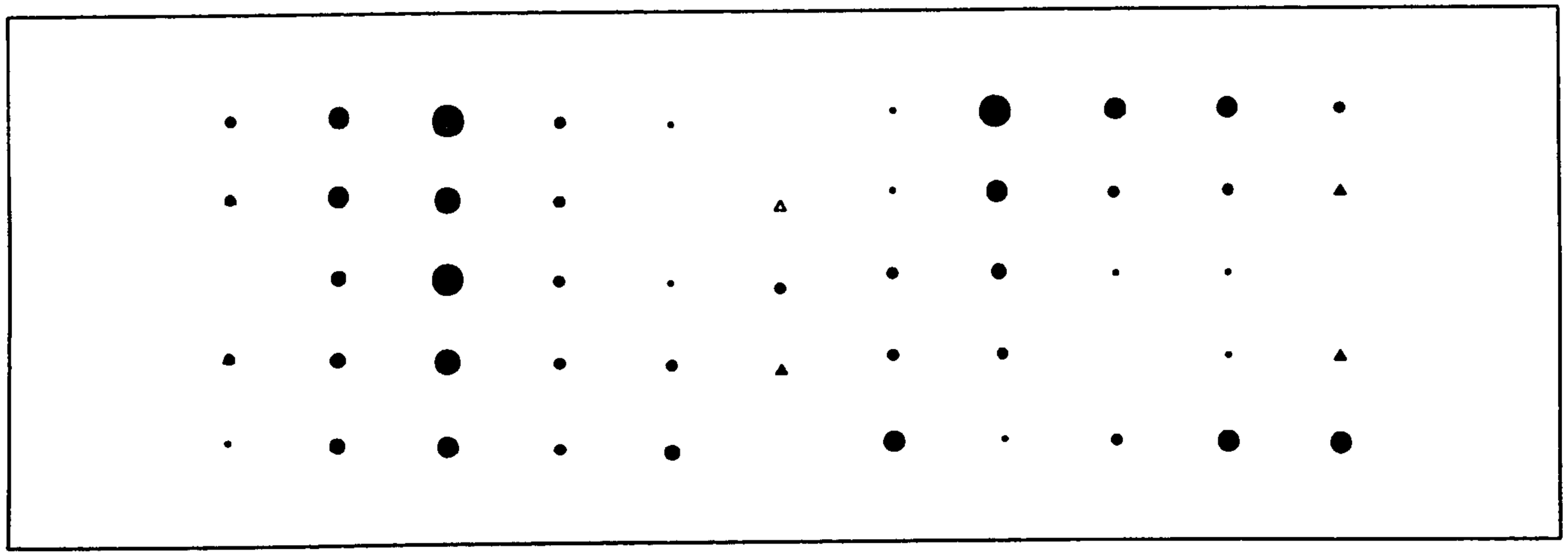

XY Vector Scale: 1cm=3.5cm Height Bubble Scale: 1cm radius=14cm

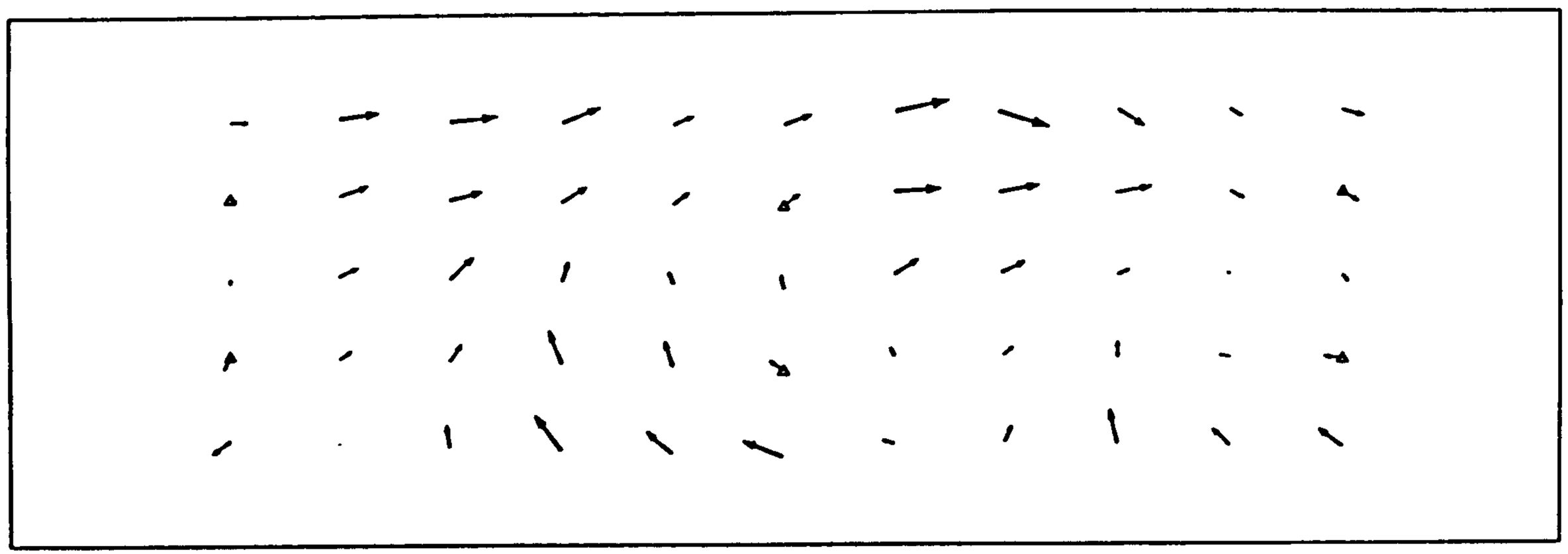

Figure C.3.4 - XY Vector Residual Plot and Height Bubble Residual Plot
(Full Block, No GPS, 3-D Control At A 250m Interval)

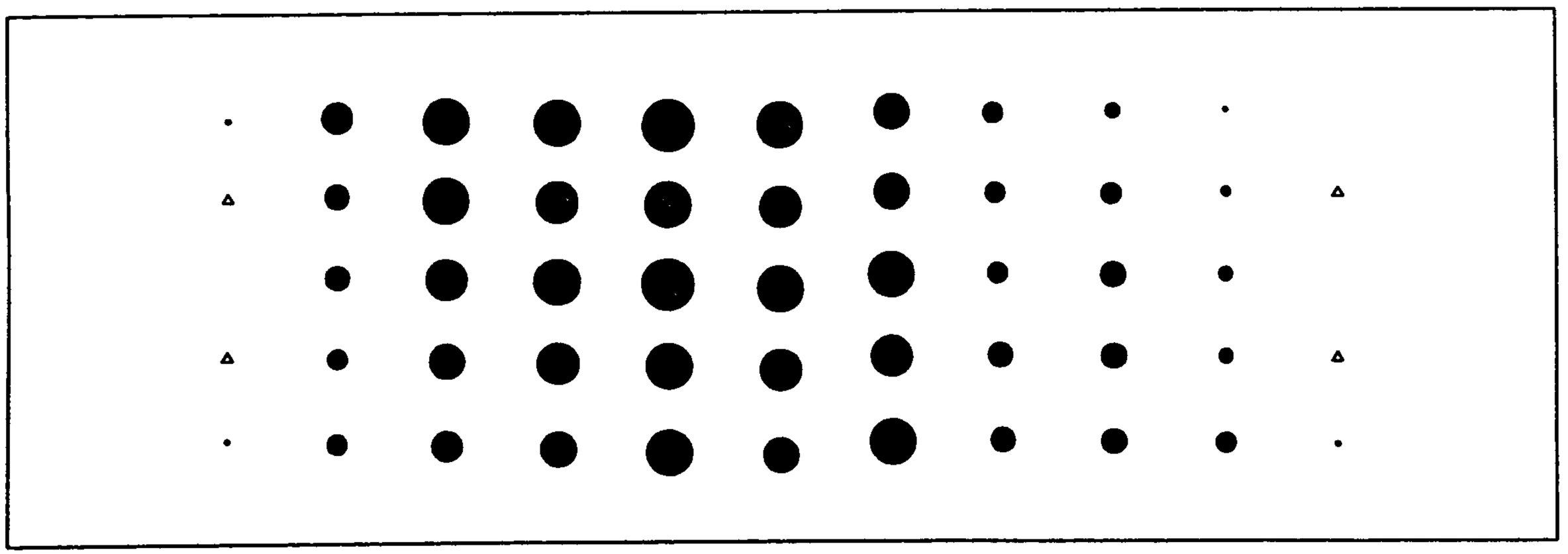

XY Vector Scale: 1cm=7cm Height Bubble Scale: 1cm radius=35cm

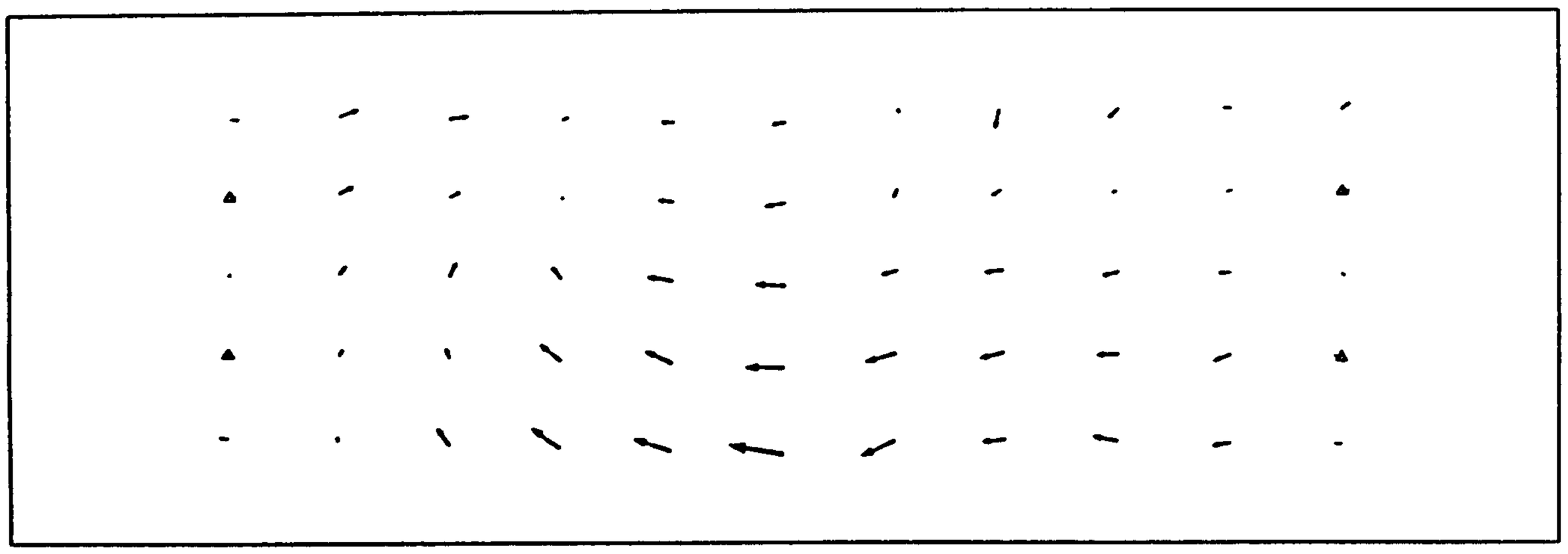

Figure C.4.1 - XY Vector Residual Plot and Height Bubble Residual Plot
(Centre Strip, No GPS, 3-D Control At A 500m Interval)

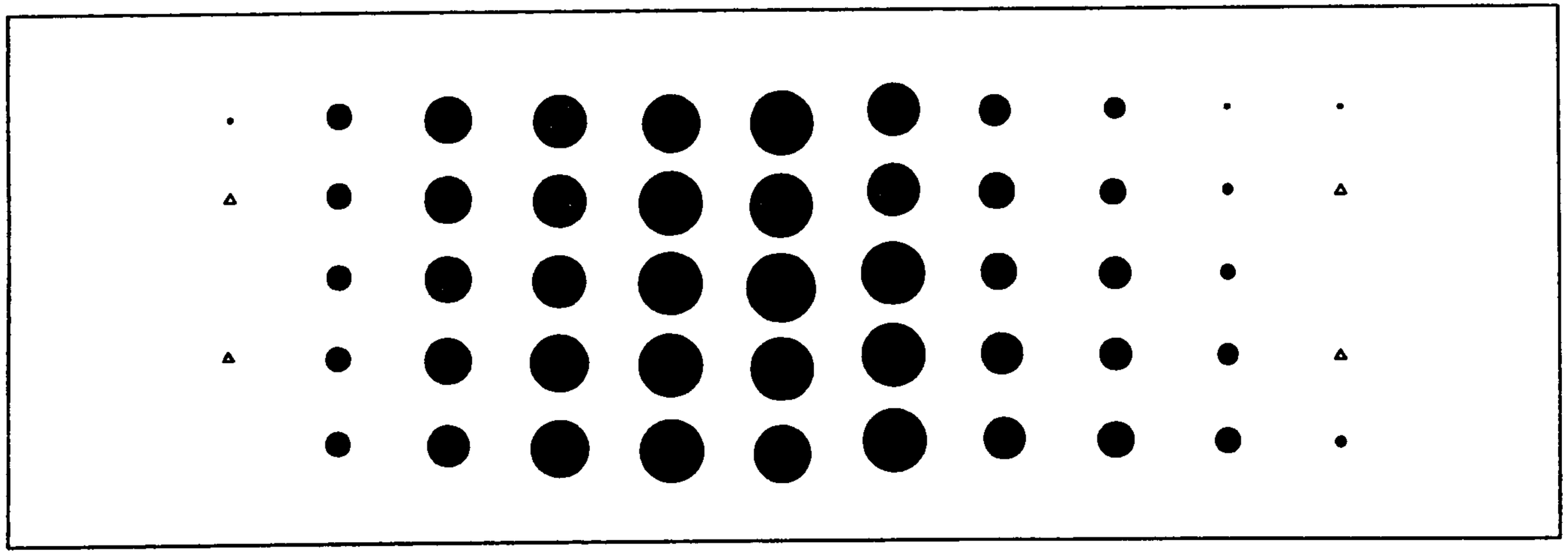

XY Vector Scale: 1cm=7cm Height Bubble Scale: 1cm radius=35cm

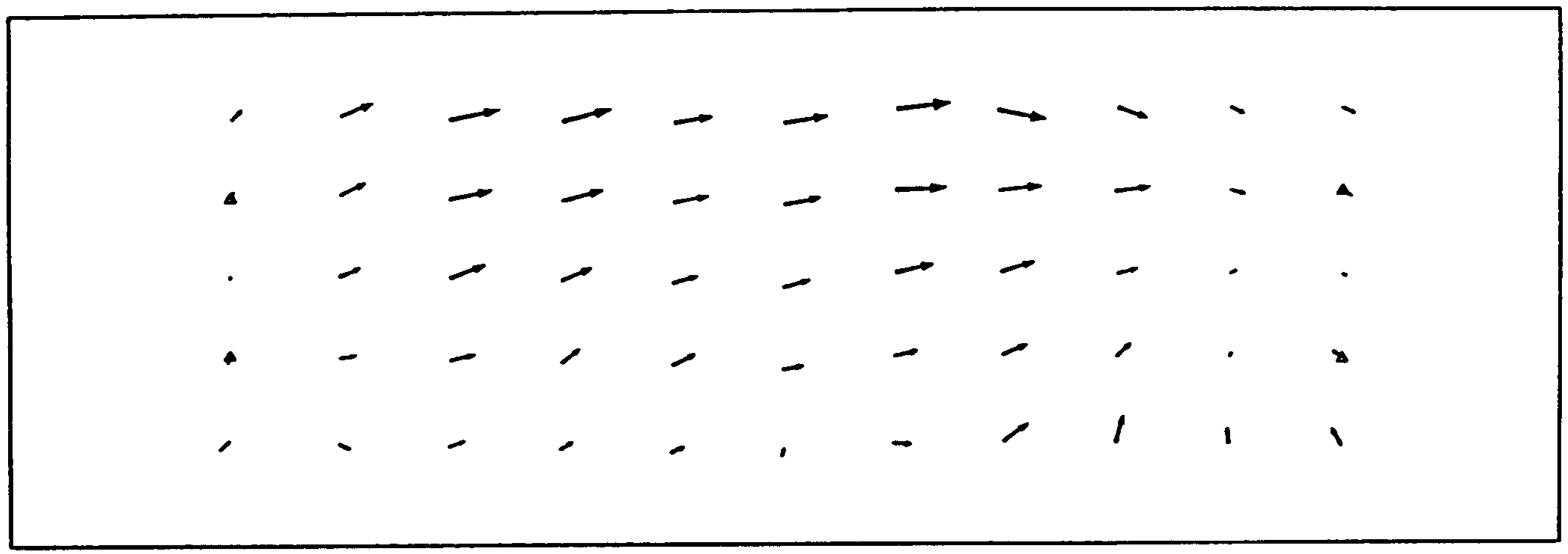

Figure C.4.2 - XY Vector Residual Plot and Height Bubble Residual Plot
(Centre + Left, No GPS, 3-D Control At A 500m Interval)

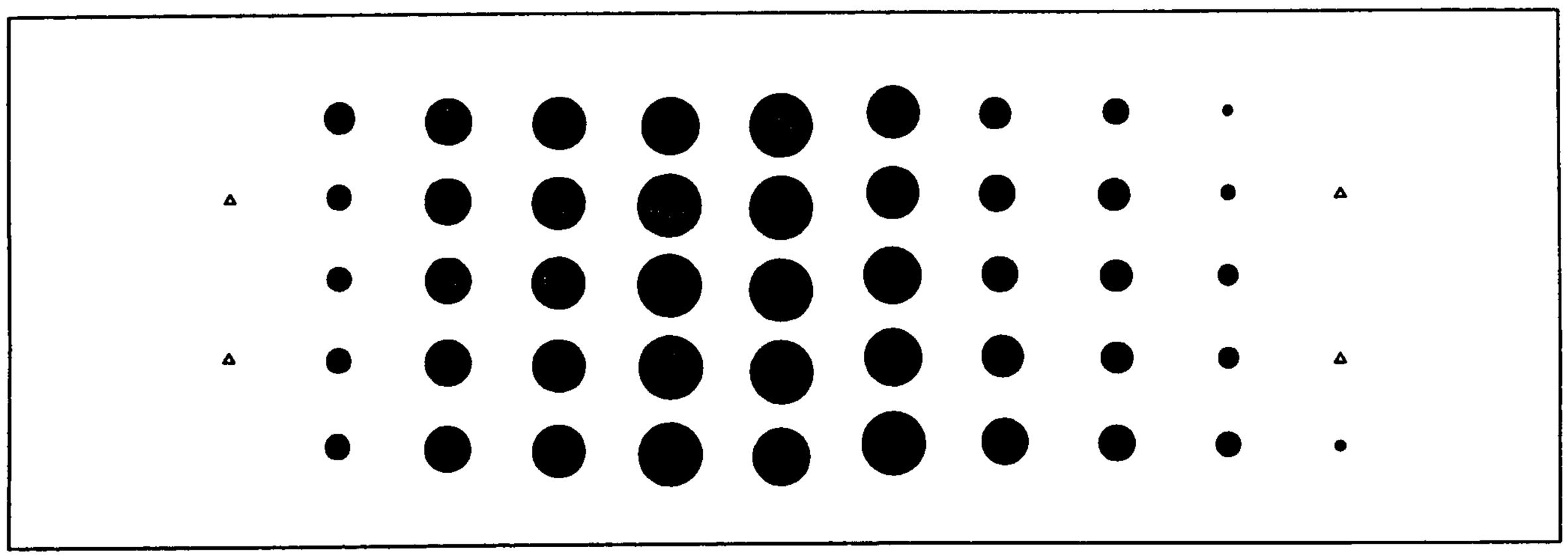

XY Vector Scale: 1cm=7cm Height Bubble Scale: 1cm radius=35cm

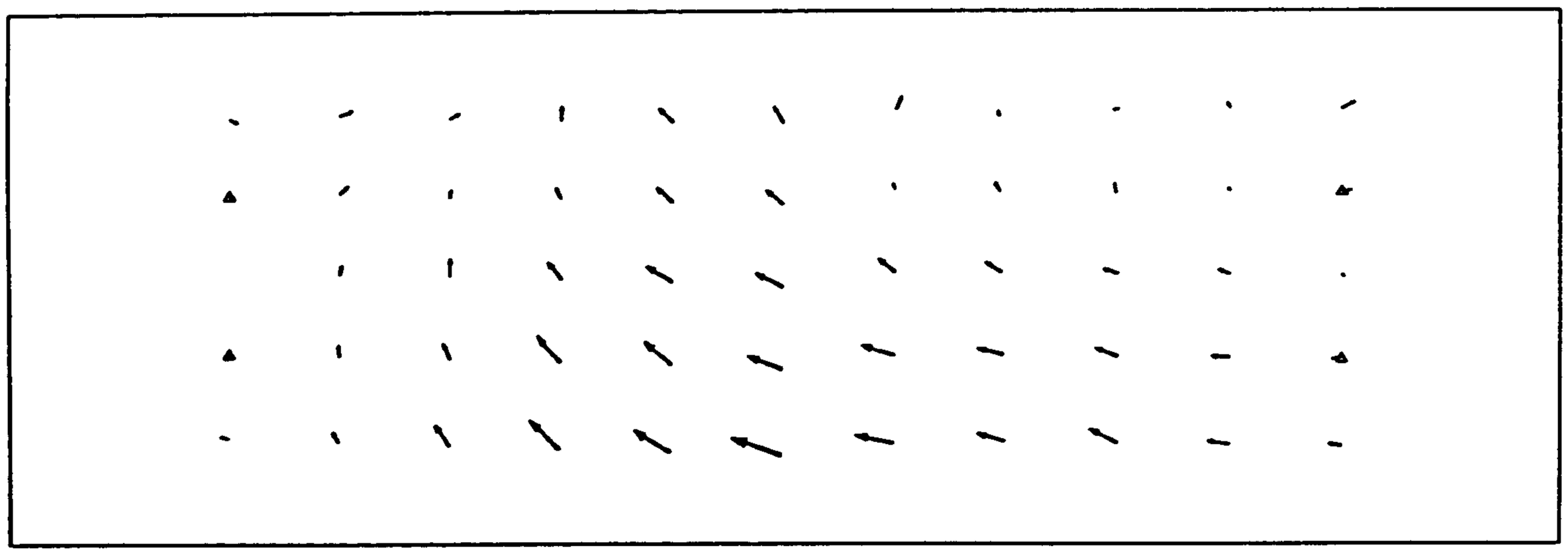

Figure C.4.3 - XY Vector Residual Plot and Height Bubble Residual Plot
(Centre + Right, No GPS, 3-D Control At A 500m Interval)

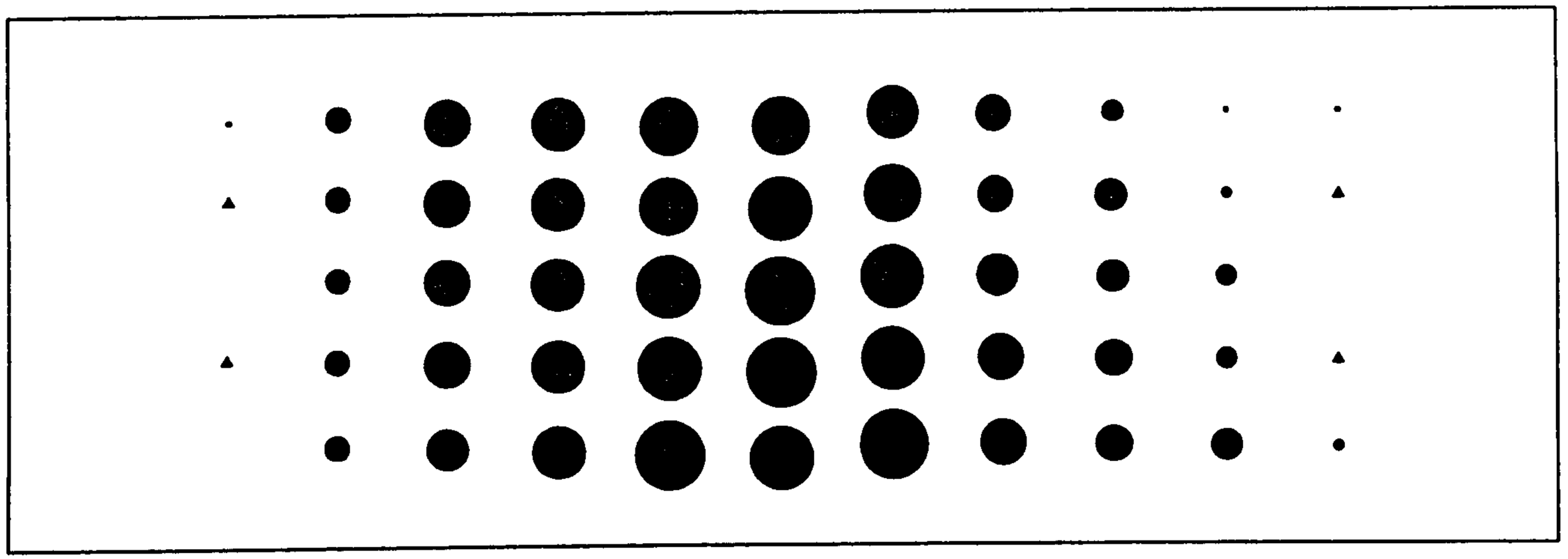

XY Vector Scale: 1cm=7cm Height Bubble Scale: 1cm radius=35cm

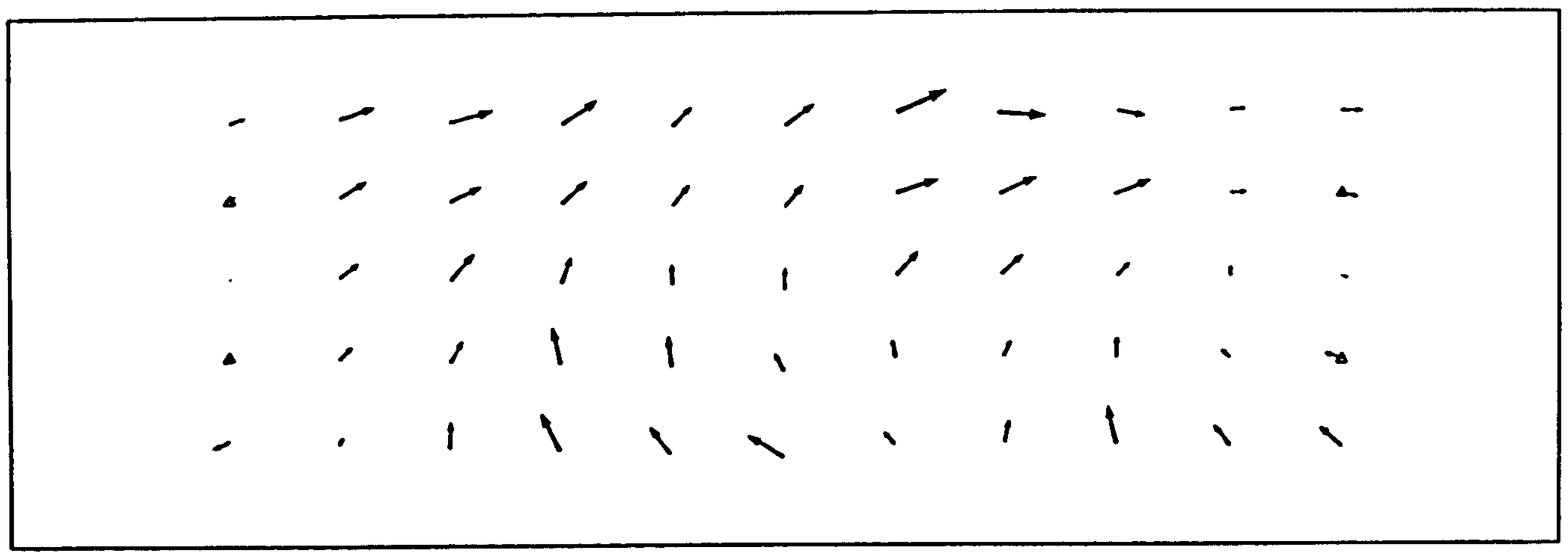

Figure C.4.4 - XY Vector Residual Plot and Height Bubble Residual Plot
(Full Block, No GPS, 3-D Control At A 500m Interval)

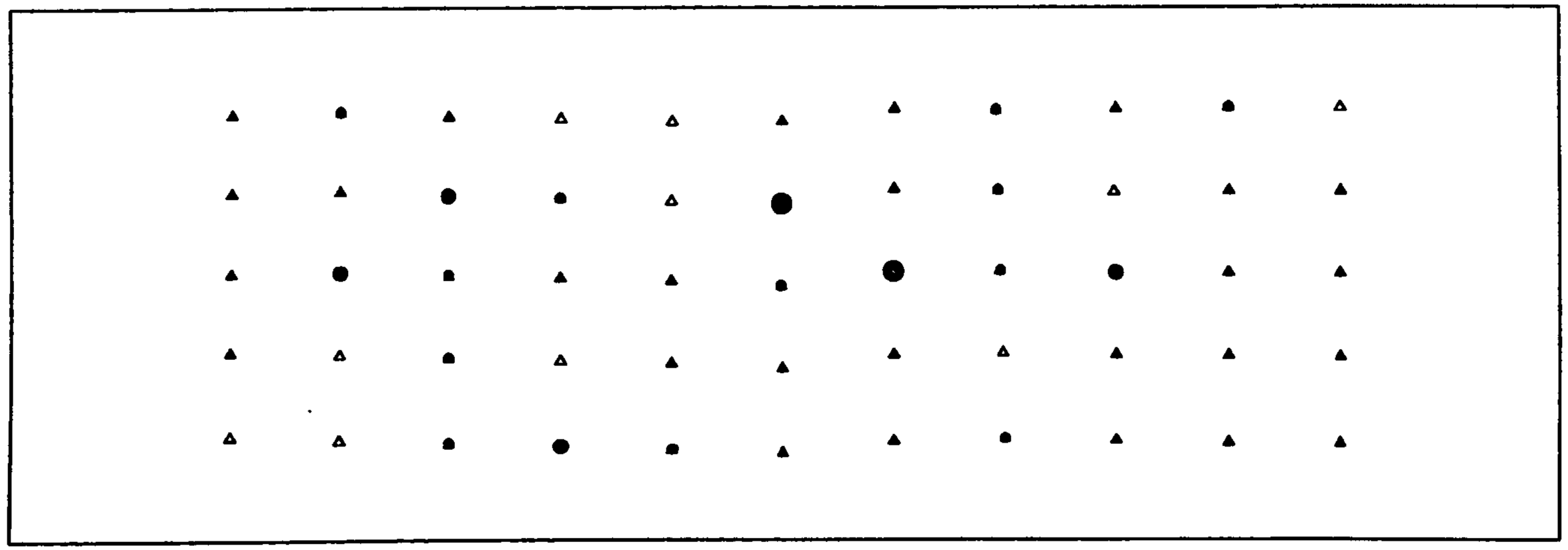

XY Vector Scale: 1cm=3.5cm Height Bubble Scale: 1cm radius=3.5cm

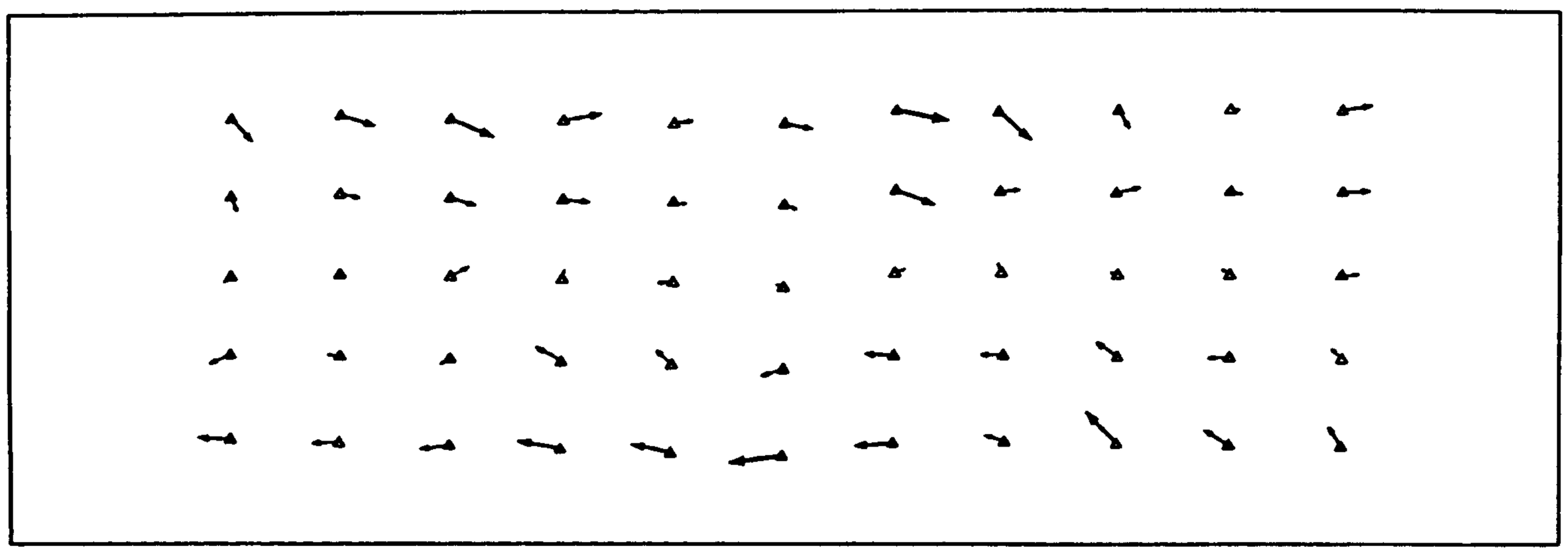

Figure C.5.1 - XY Vector Residual Plot and Height Bubble Residual Plot
(Centre Strip, With GPS, All Points As Ground Control)

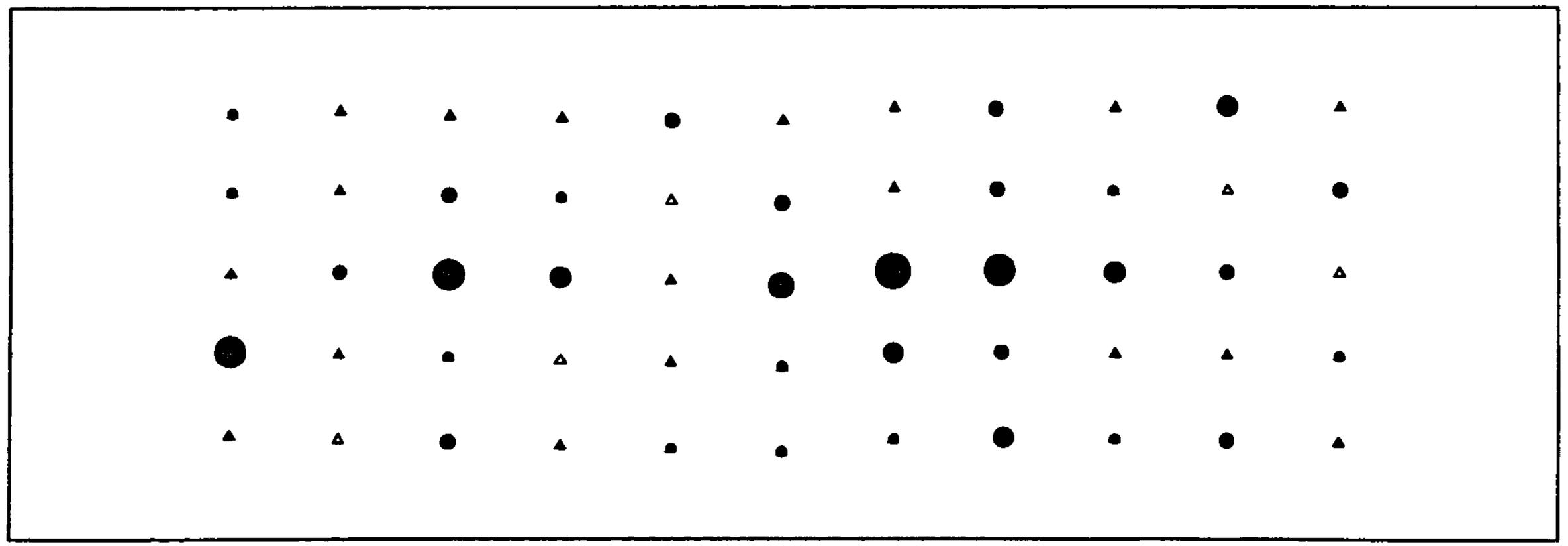

XY Vector Scale: 1cm=3.5cm Height Bubble Scale: 1cm radius=3.5cm

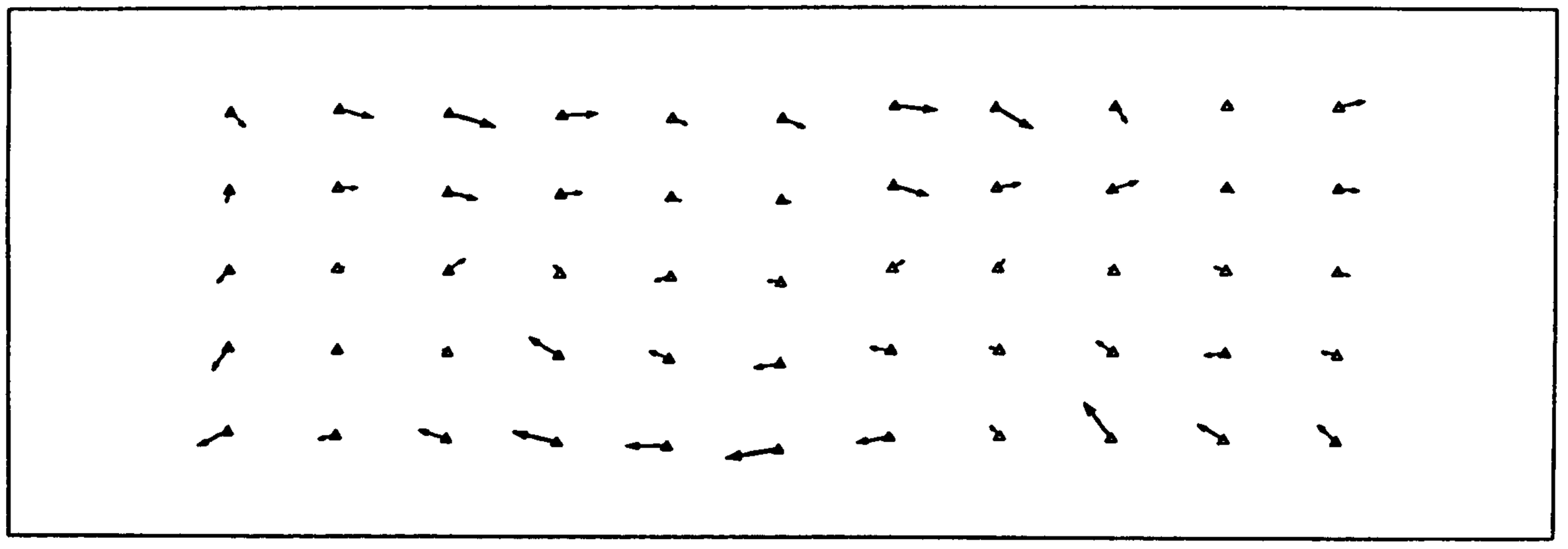

Figure C.5.2 - XY Vector Residual Plot and Height Bubble Residual Plot
(Centre + Left, With GPS, All Points As Ground Control)

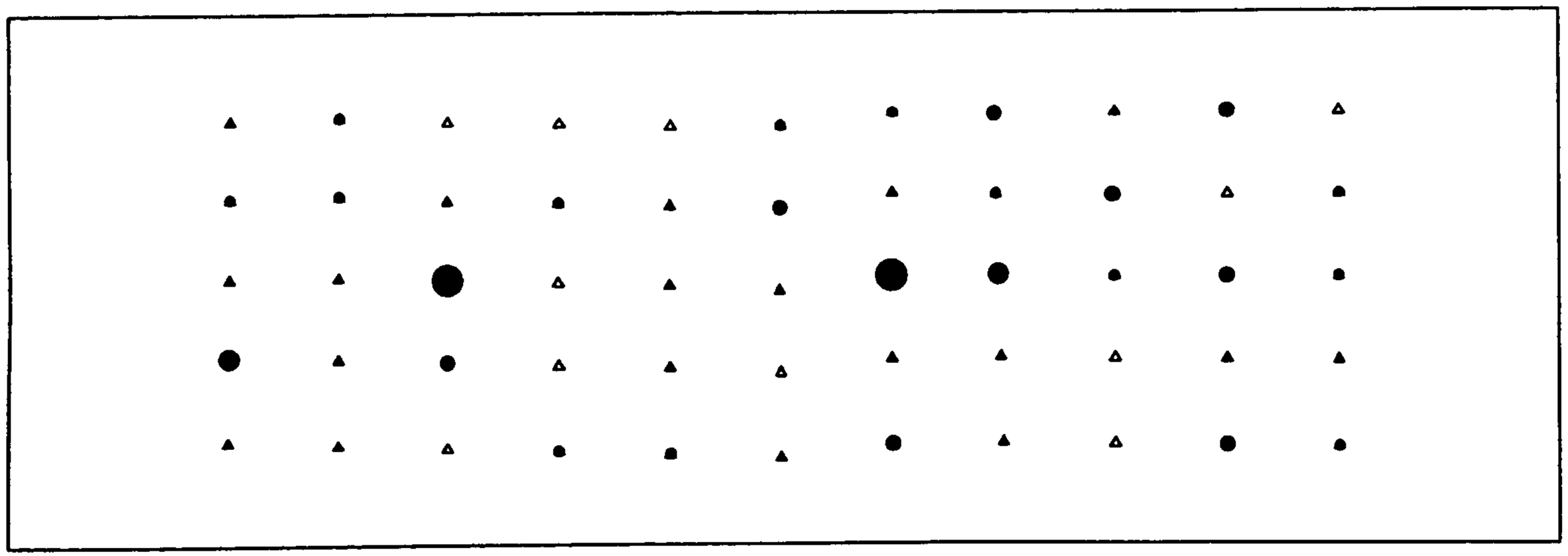

XY Vector Scale: 1cm=3.5cm Height Bubble Scale: 1cm radius=3.5cm

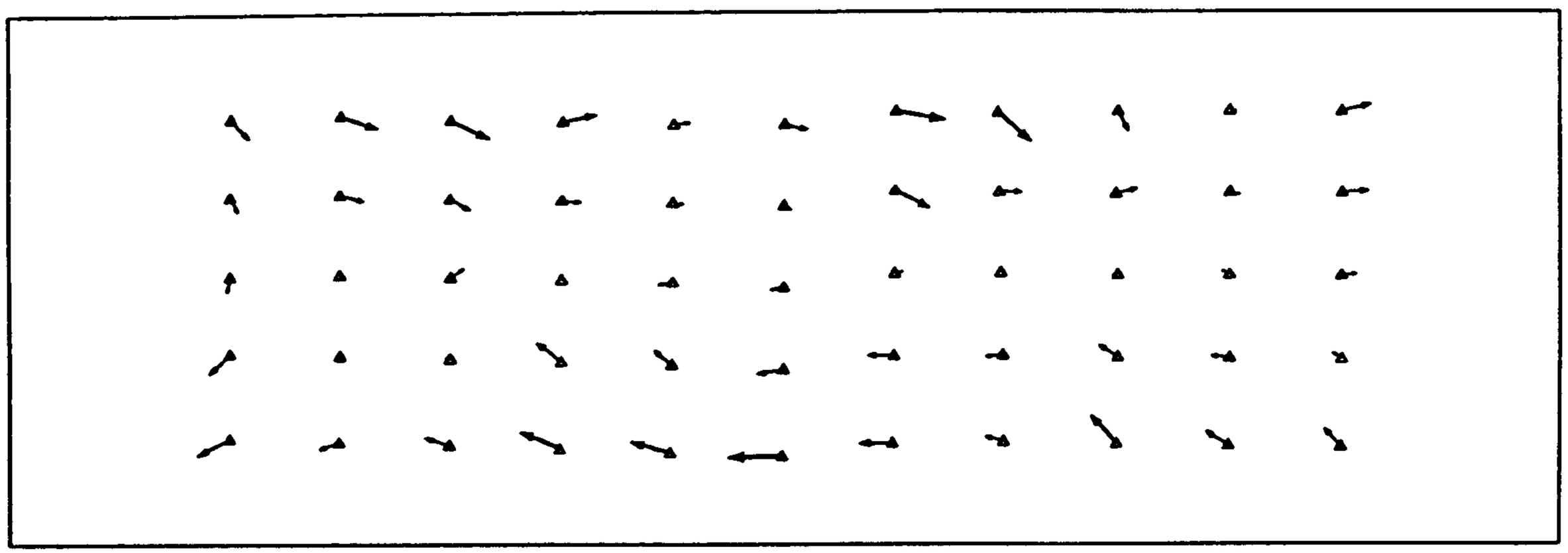

Figure C.5.3 - XY Vector Residual Plot and Height Bubble Residual Plot
(Centre + Right, With GPS, All Points As Ground Control)

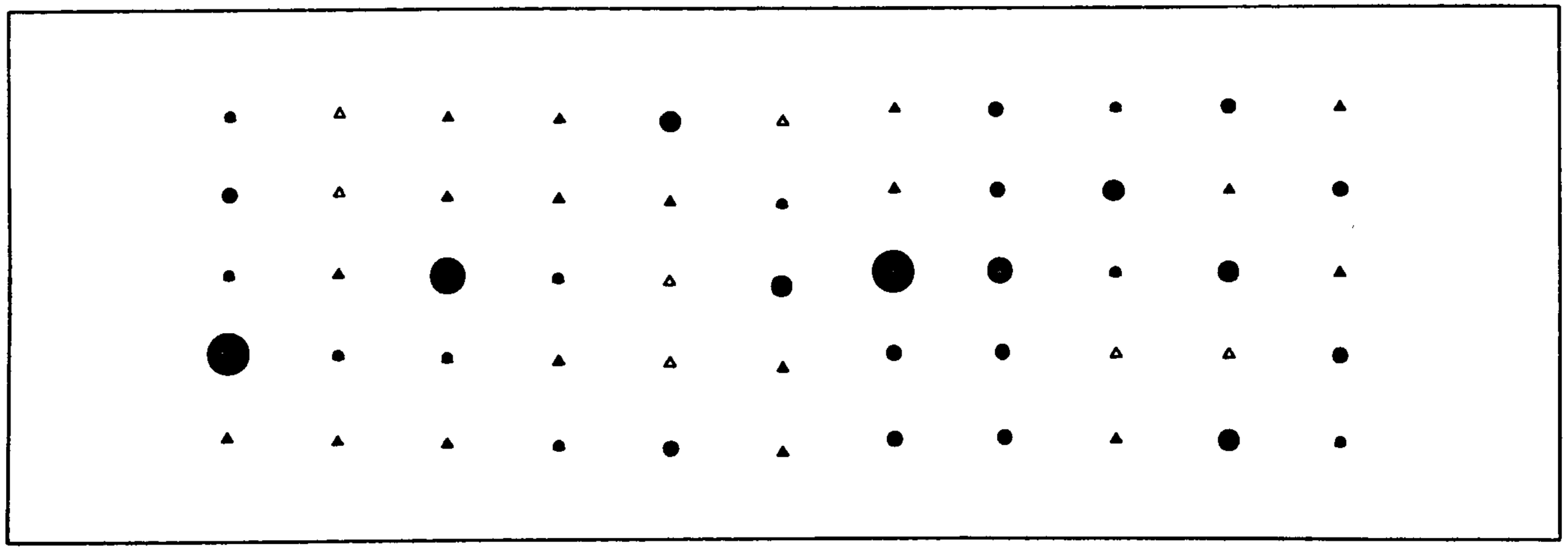

XY Vector Scale: 1cm=3.5cm Height Bubble Scale: 1cm radius=3.5cm

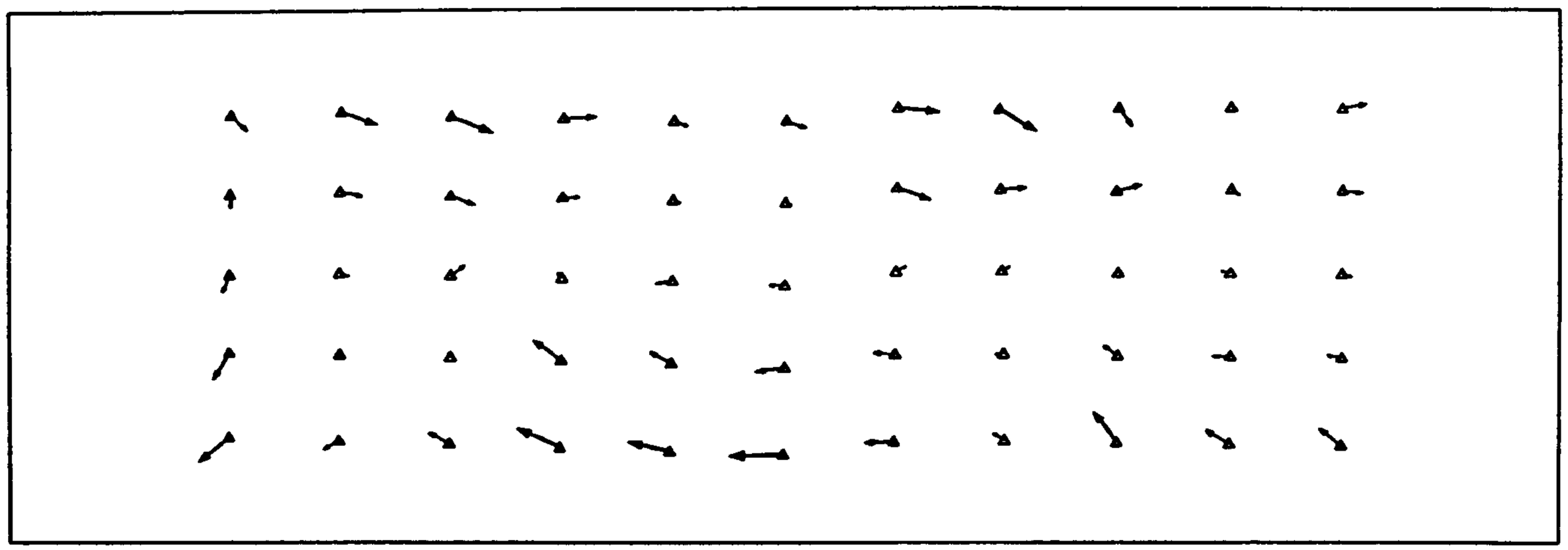

Figure C.5.4 - XY Vector Residual Plot and Height Bubble Residual Plot
(Full Block, With GPS, All Points As Ground Control)

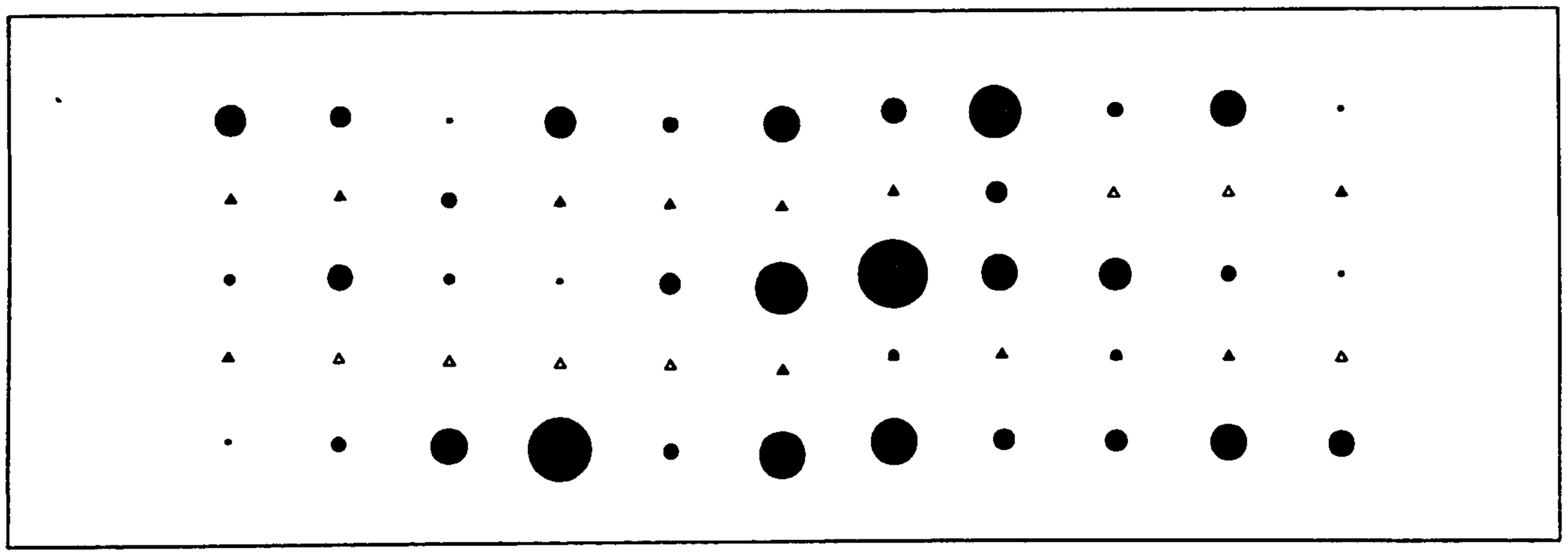

XY Vector Scale: 1cm=3.5cm Height Bubble Scale: 1cm radius=3.5cm

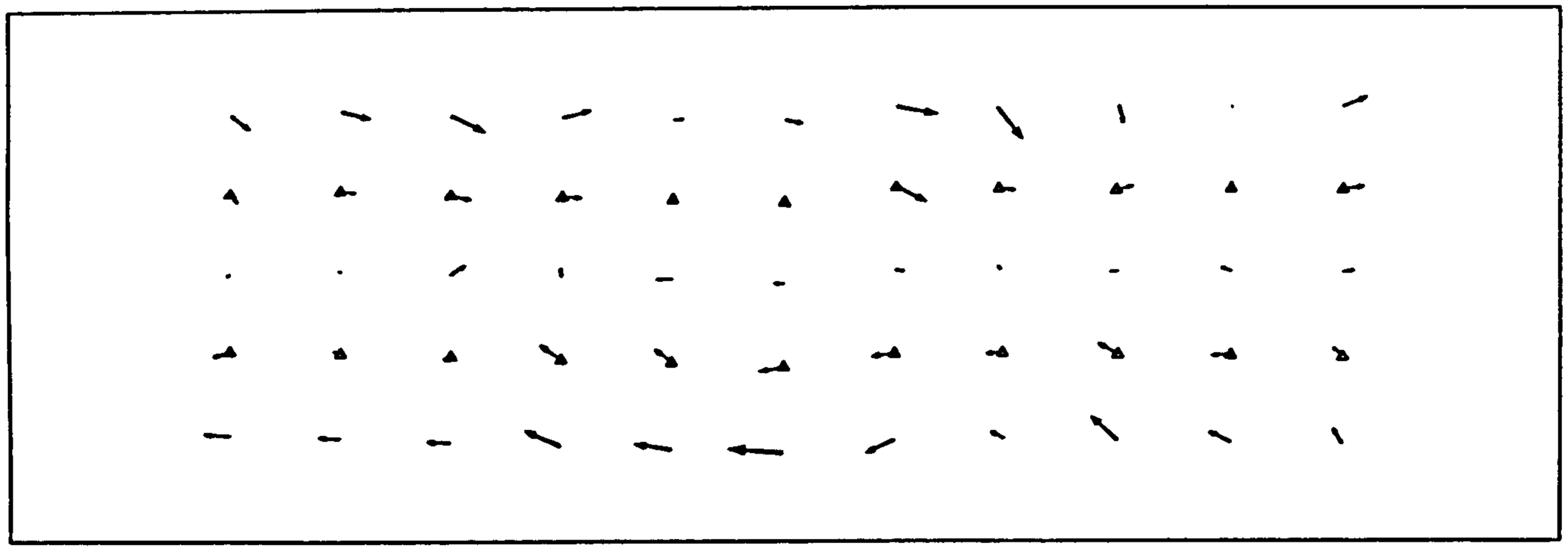

Figure C.6.1 - XY Vector Residual Plot and Height Bubble Residual Plot
(Centre Strip, With GPS, 3-D Control Points At 50m Interval)

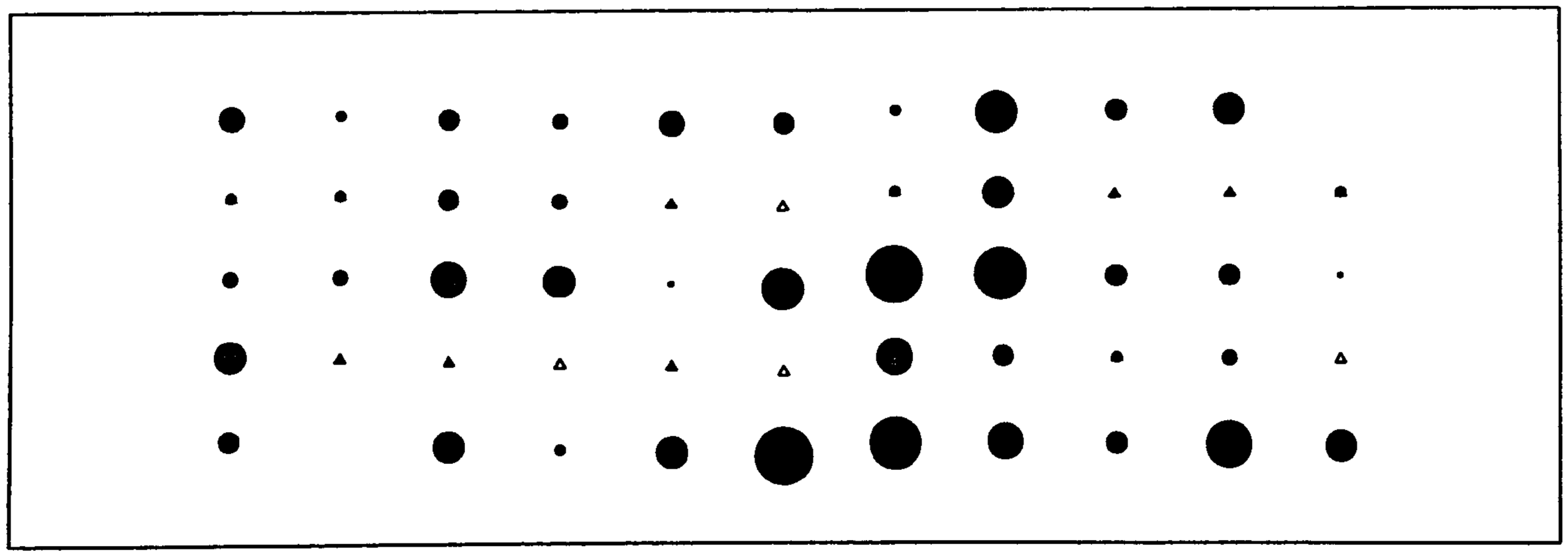

XY Vector Scale: 1cm=3.5cm Height Bubble Scale: 1cm radius=3.5cm

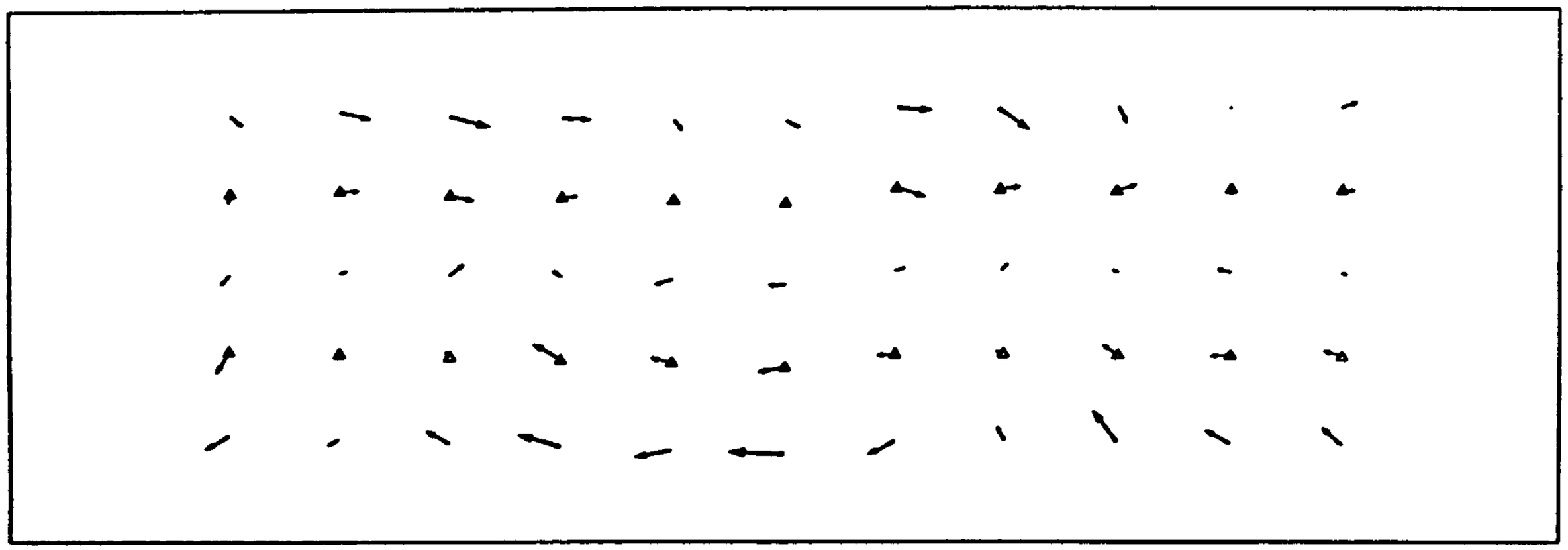

Figure C.6.2 - XY Vector Residual Plot and Height Bubble Residual Plot
(Centre + Left, With GPS, 3-D Control Points At 50m Interval)

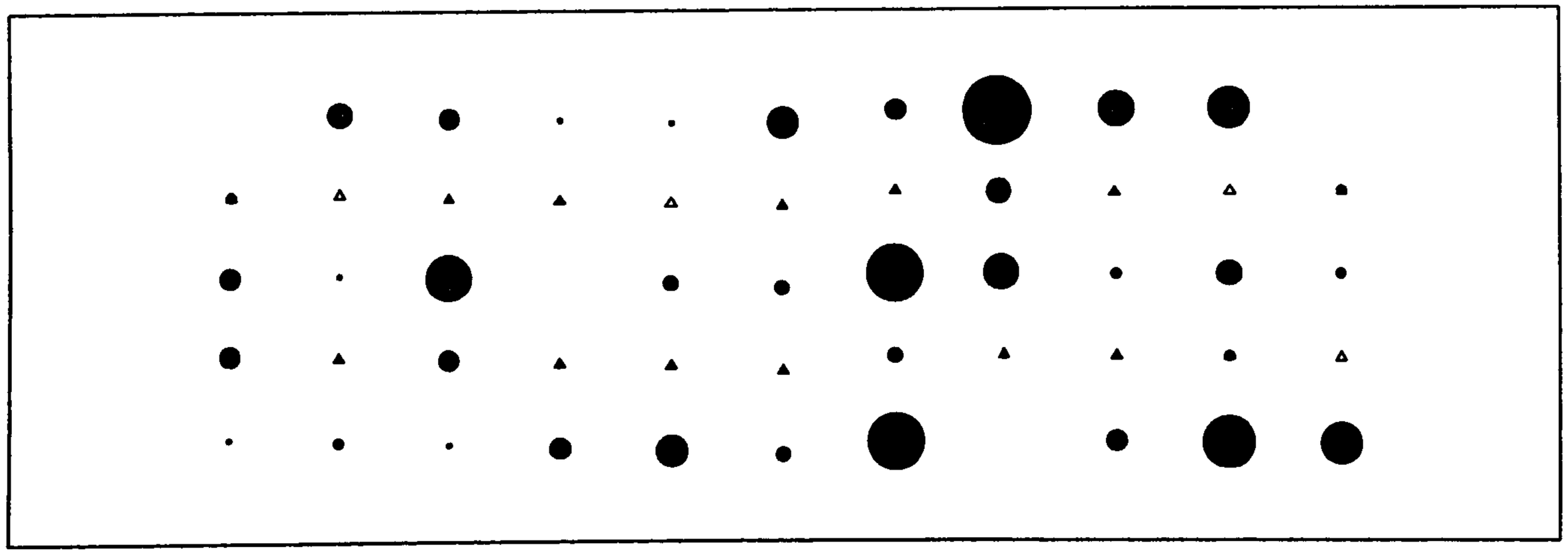

XY Vector Scale: 1cm=3.5cm Height Bubble Scale: 1cm radius=3.5cm

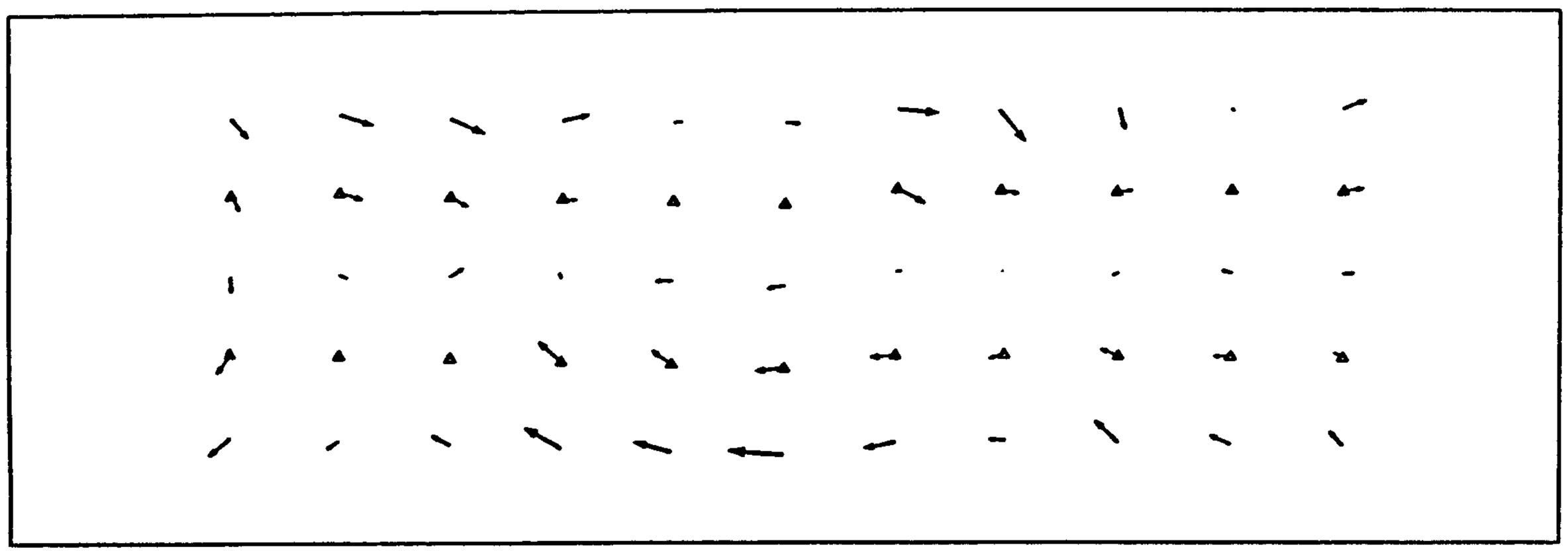

Figure C.6.3 - XY Vector Residual Plot and Height Bubble Residual Plot
(Centre + Right, With GPS, 3-D Control Points At 50m Interval)

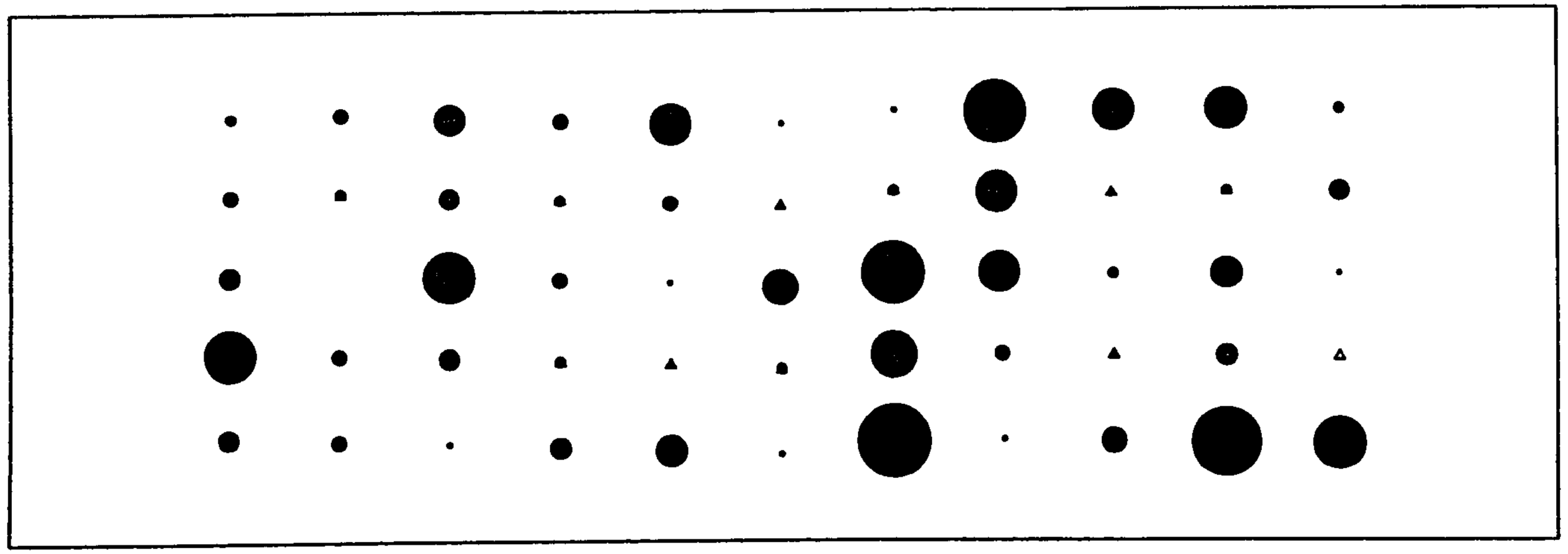

XY Vector Scale: 1cm=3.5cm Height Bubble Scale: 1cm radius=3.5cm

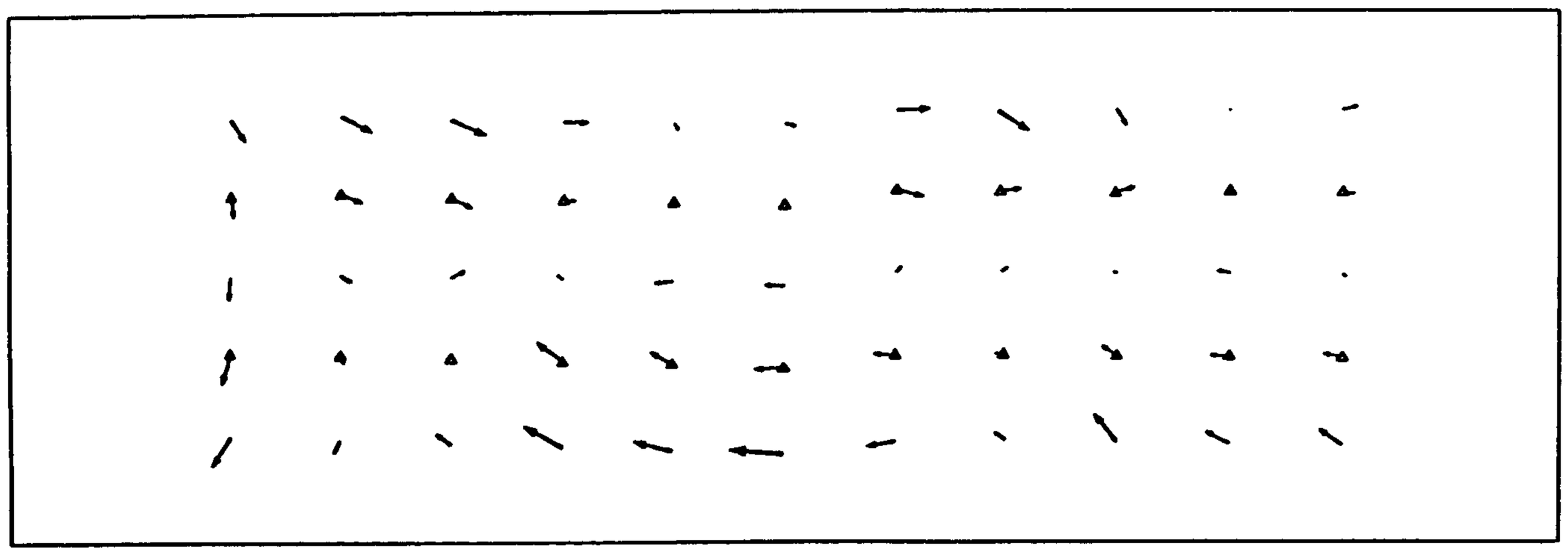

Figure C.6.4 - XY Vector Residual Plot and Height Bubble Residual Plot
(Full Block, With GPS, 3-D Control Points At 50m Interval)

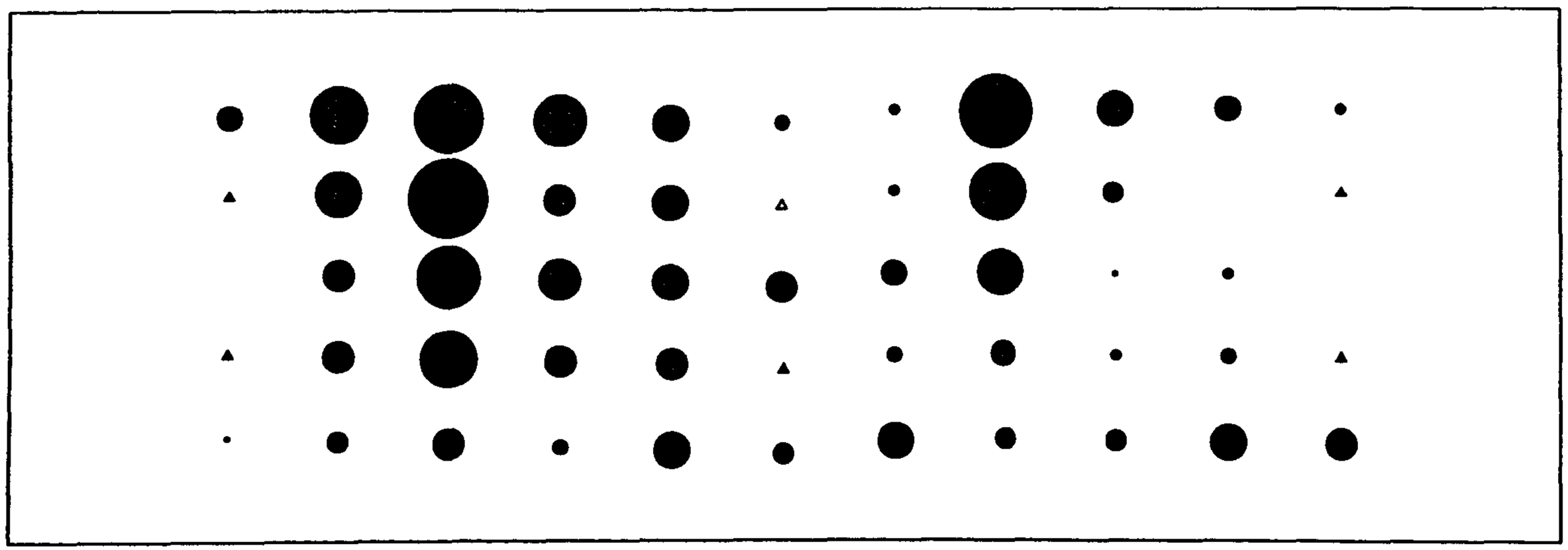

XY Vector Scale: 1cm=3.5cm Height Bubble Scale: 1cm radius=7cm

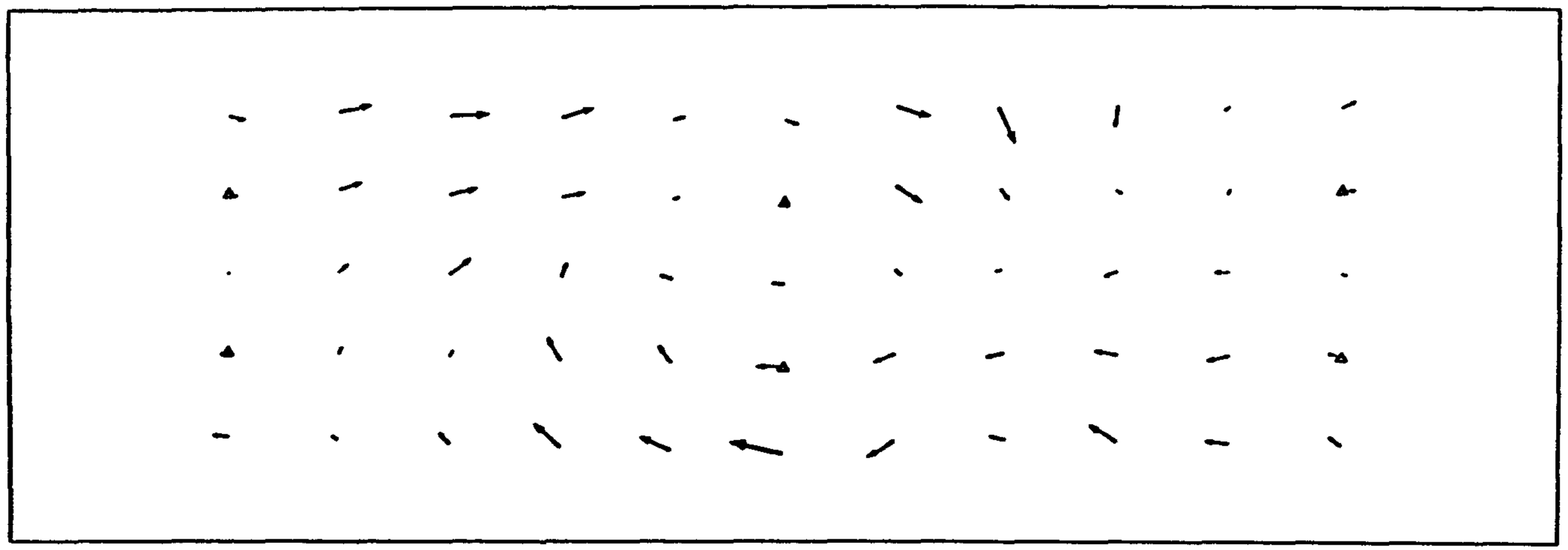

Figure C.7.1 - XY Vector Residual Plot and Height Bubble Residual Plot
(Centre Strip, With GPS, 3-D Control Points At 250m Interval)

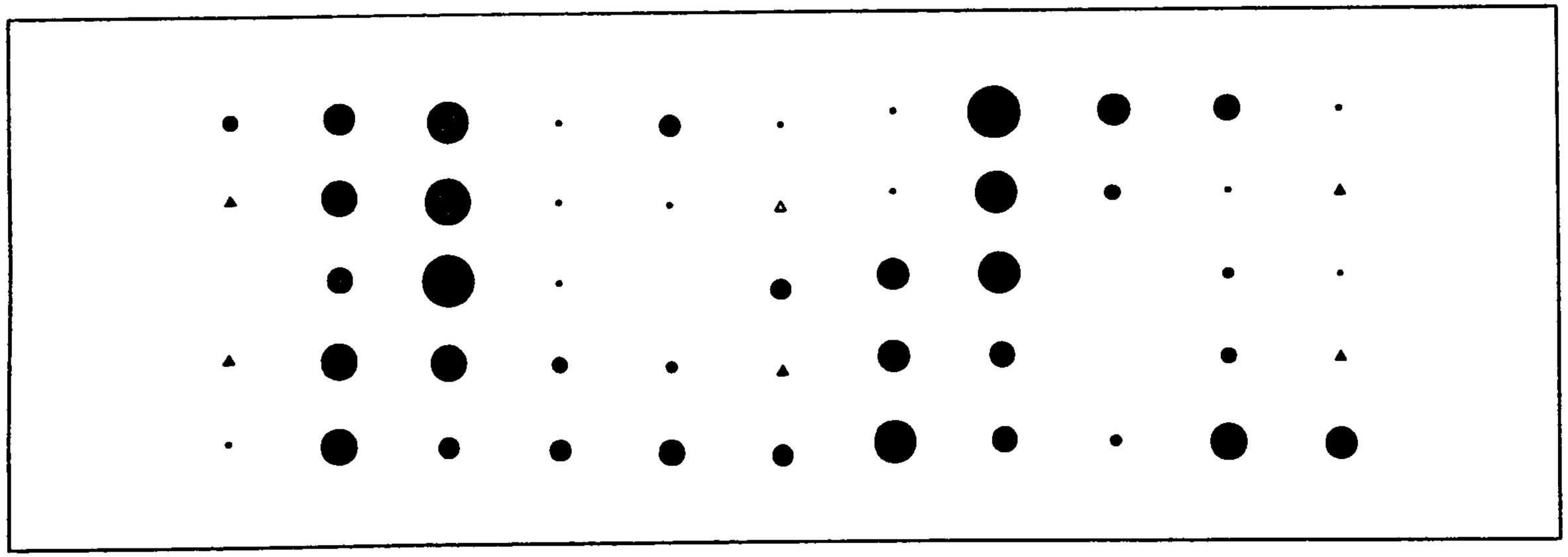

XY Vector Scale: 1cm=3.5cm Height Bubble Scale: 1cm radius=7cm

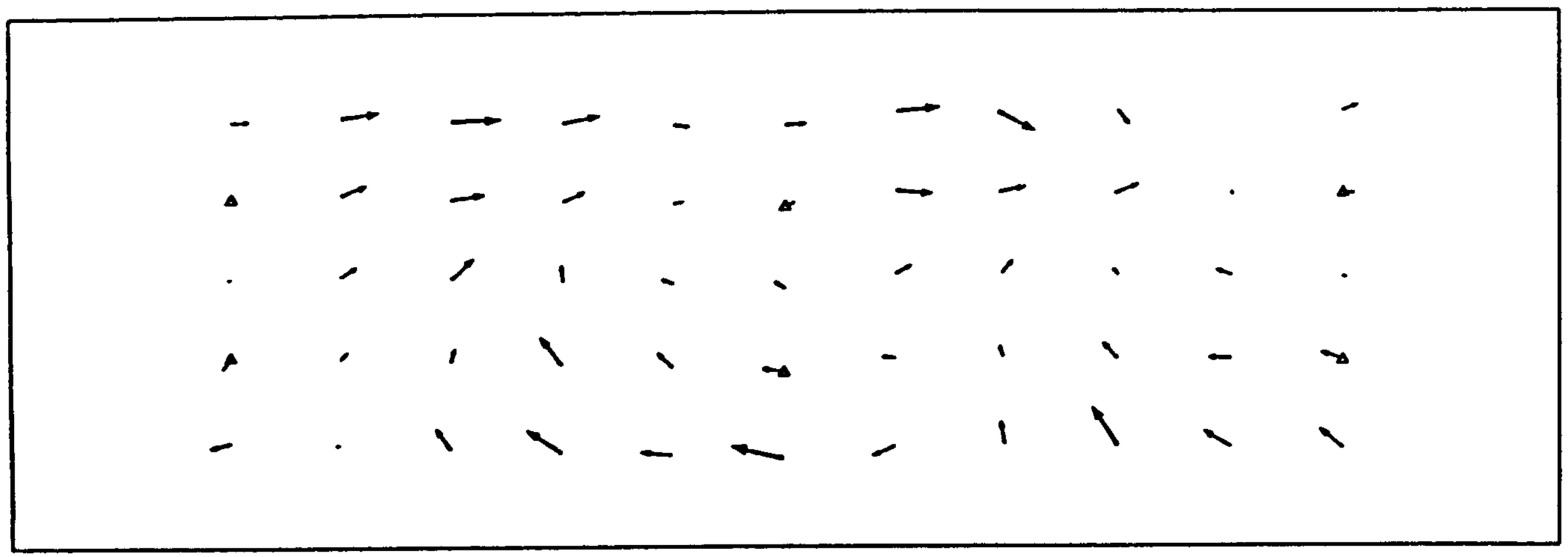

Figure C.7.2 - XY Vector Residual Plot and Height Bubble Residual Plot
(Centre + Left, With GPS, 3-D Control Points At 250m Interval)

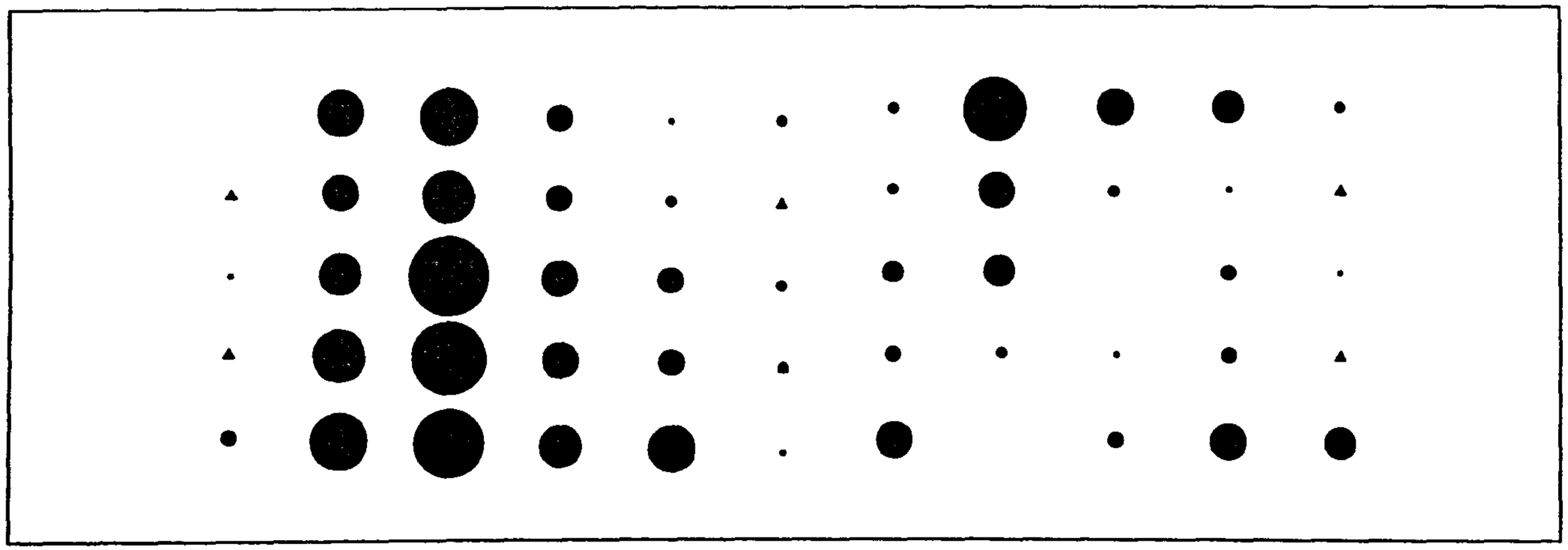

XY Vector Scale: 1cm=3.5cm Height Bubble Scale: 1cm radius=7cm

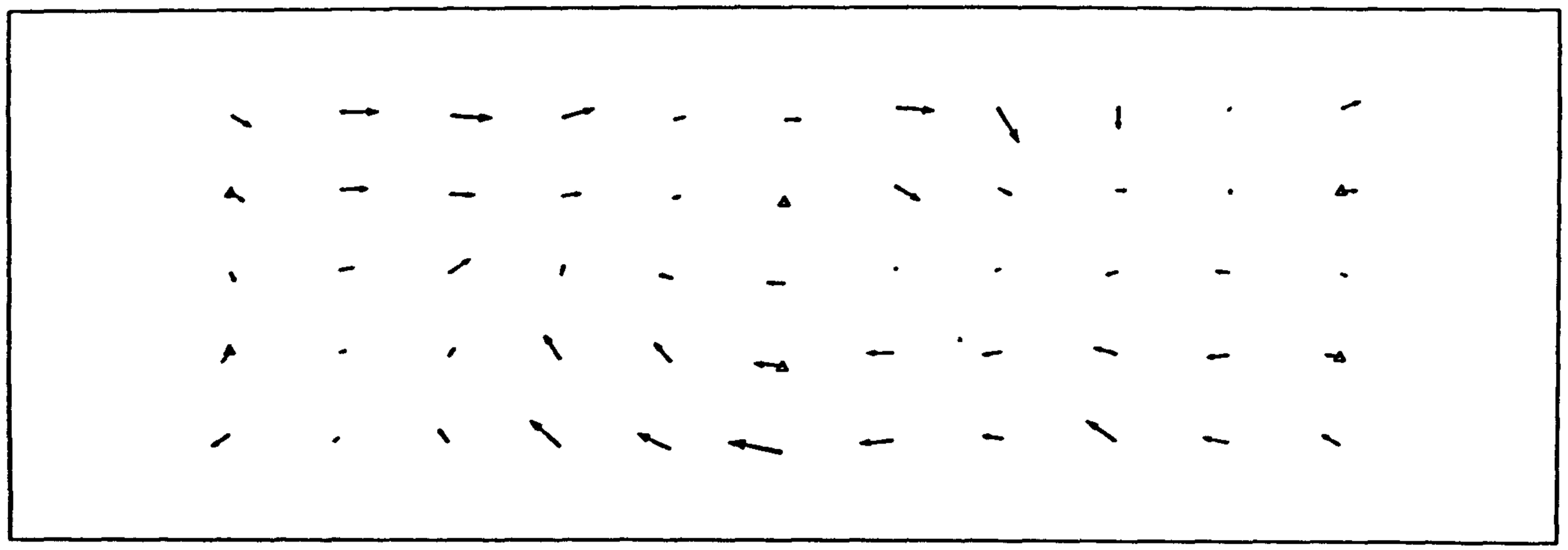

Figure C.7.3 - XY Vector Residual Plot and Height Bubble Residual Plot
(Centre + Right, With GPS, 3-D Control Points At 250m Interval)

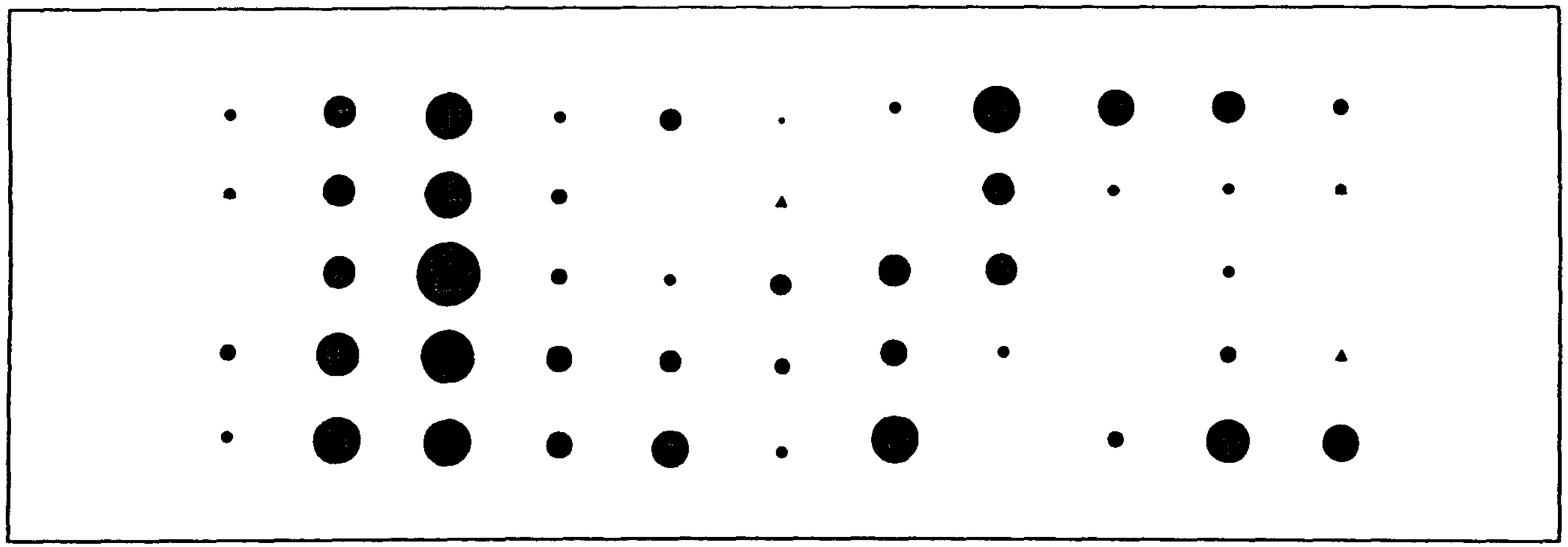

XY Vector Scale: 1cm=3.5cm Height Bubble Scale: 1cm radius=7cm

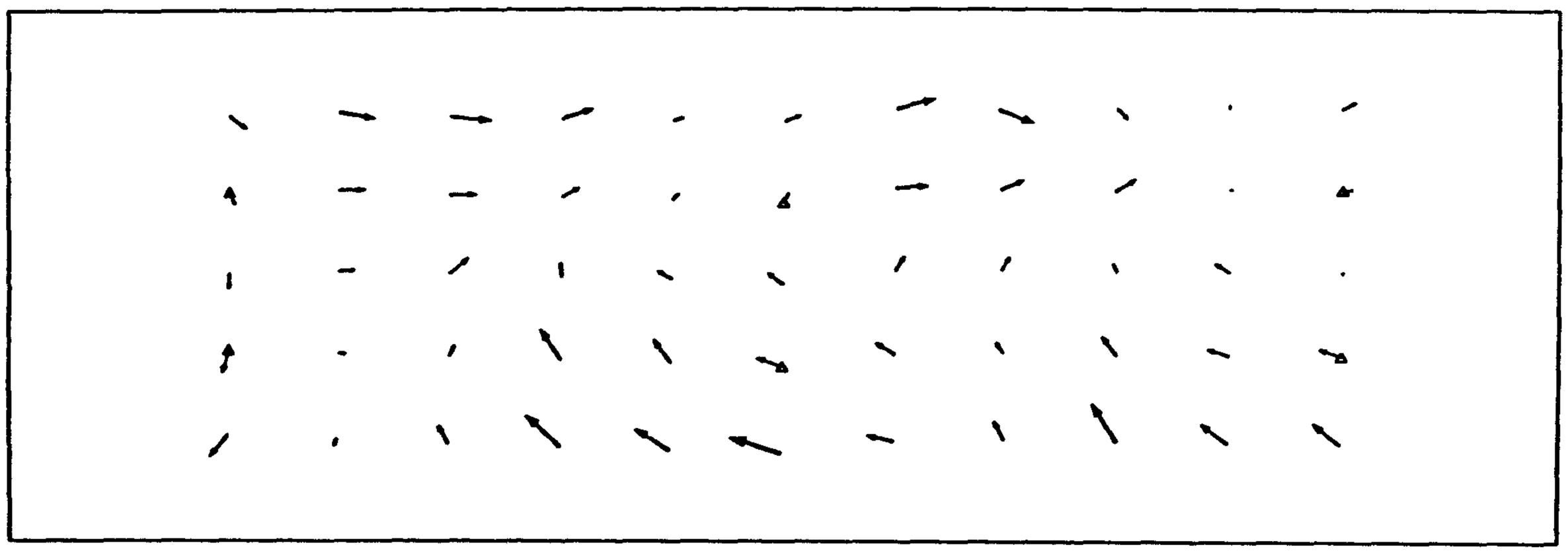

Figure C.7.4 - XY Vector Residual Plot and Height Bubble Residual Plot
(Full Block, With GPS, 3-D Control Points At 250m Interval)

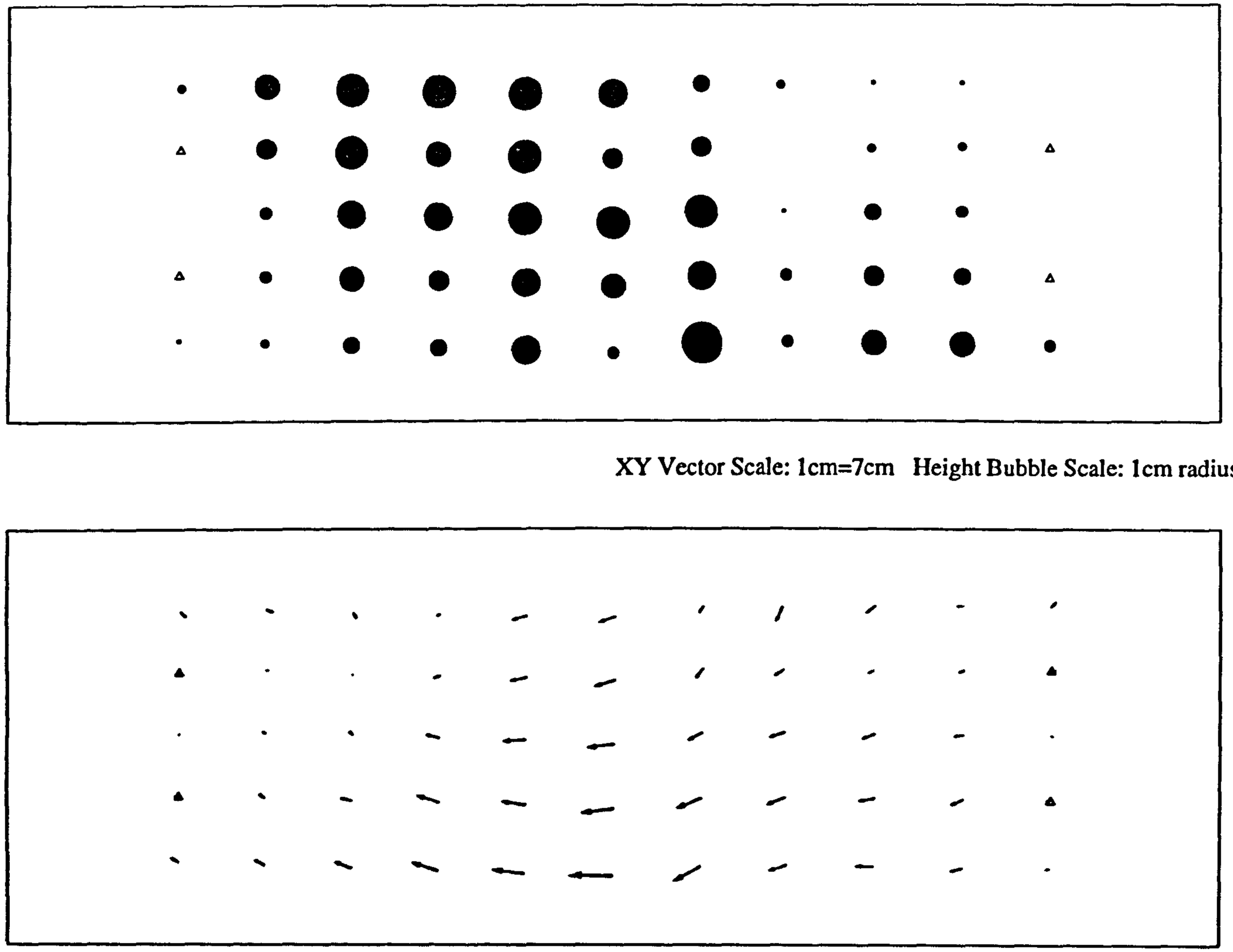

XY Vector Scale: 1cm=7cm Height Bubble Scale: 1cm radius=14cm

Figure C.8.1 - XY Vector Residual Plot and Height Bubble Residual Plot
(Centre Strip, With GPS, 3-D Control Points At 500m Interval)

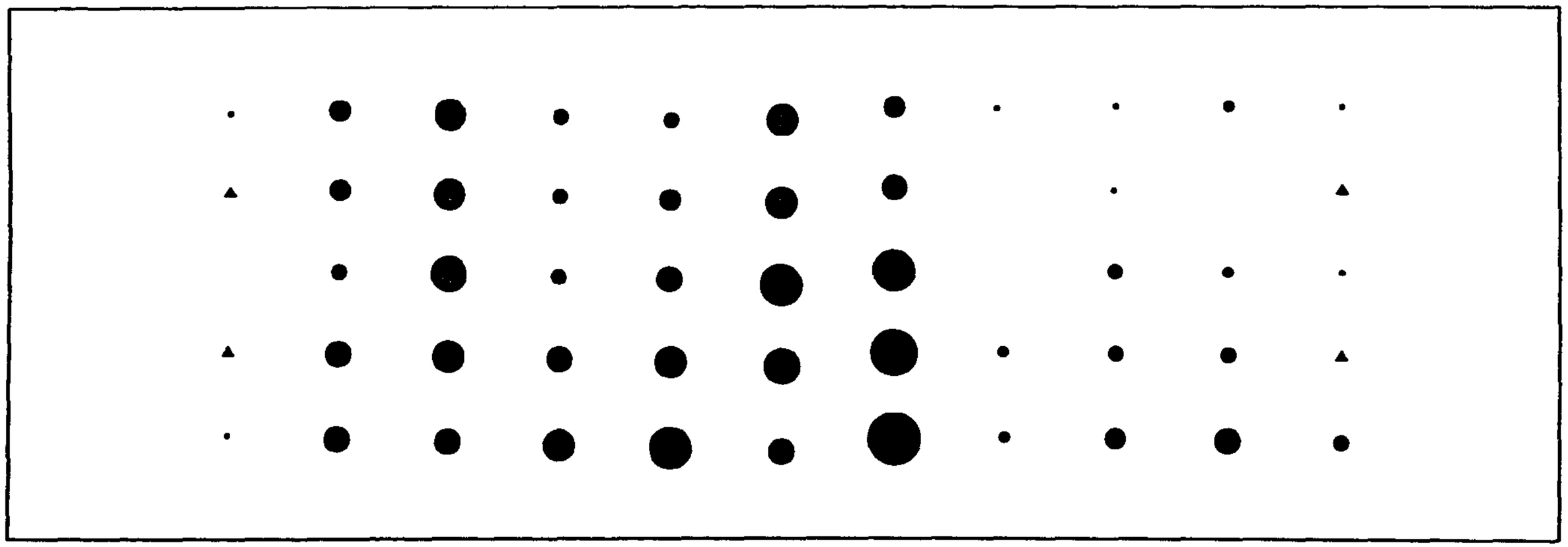

XY Vector Scale: 1cm=3.5cm Height Bubble Scale: 1cm radius=14cm

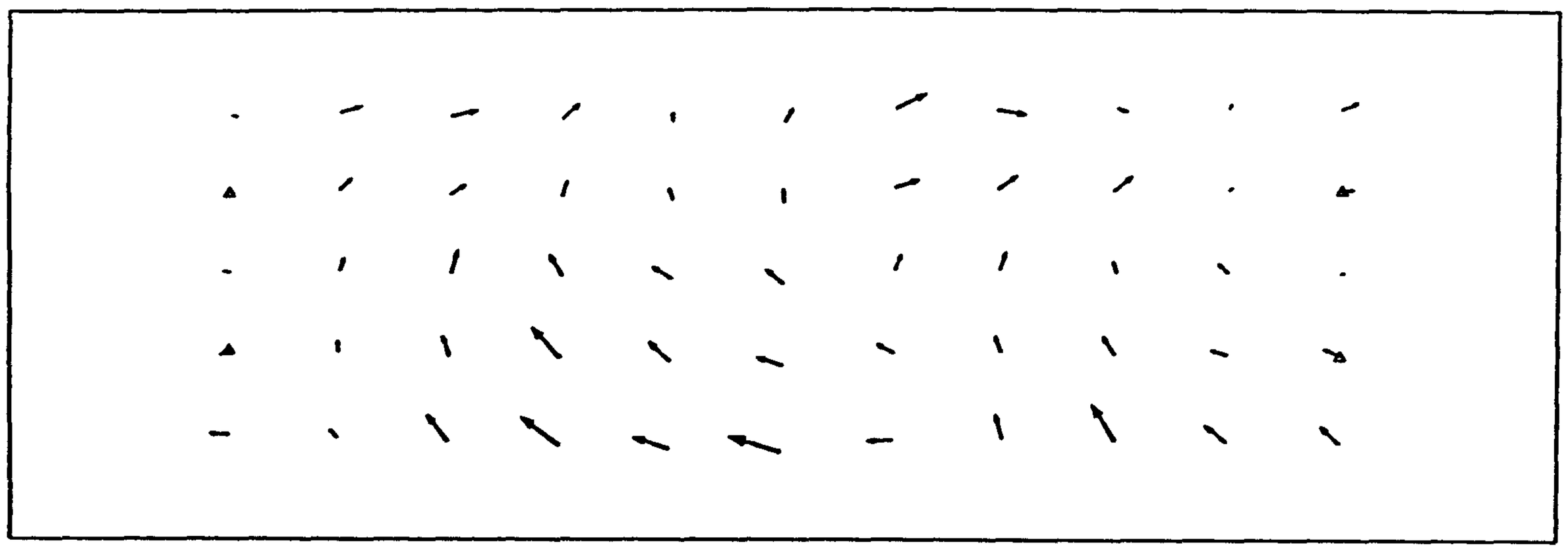

Figure C.8.2 - XY Vector Residual Plot and Height Bubble Residual Plot
(Centre + Left, With GPS, 3-D Control Points At 500m Interval)

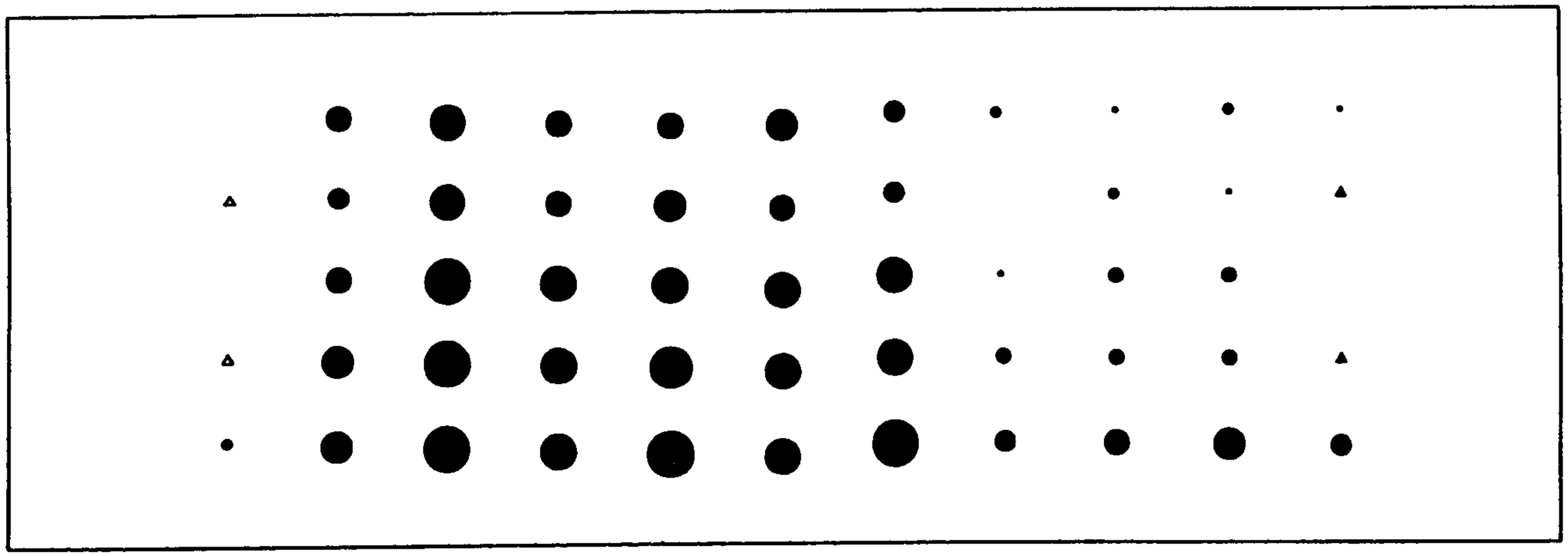

XY Vector Scale: 1cm=3.5cm Height Bubble Scale: 1cm radius=14cm

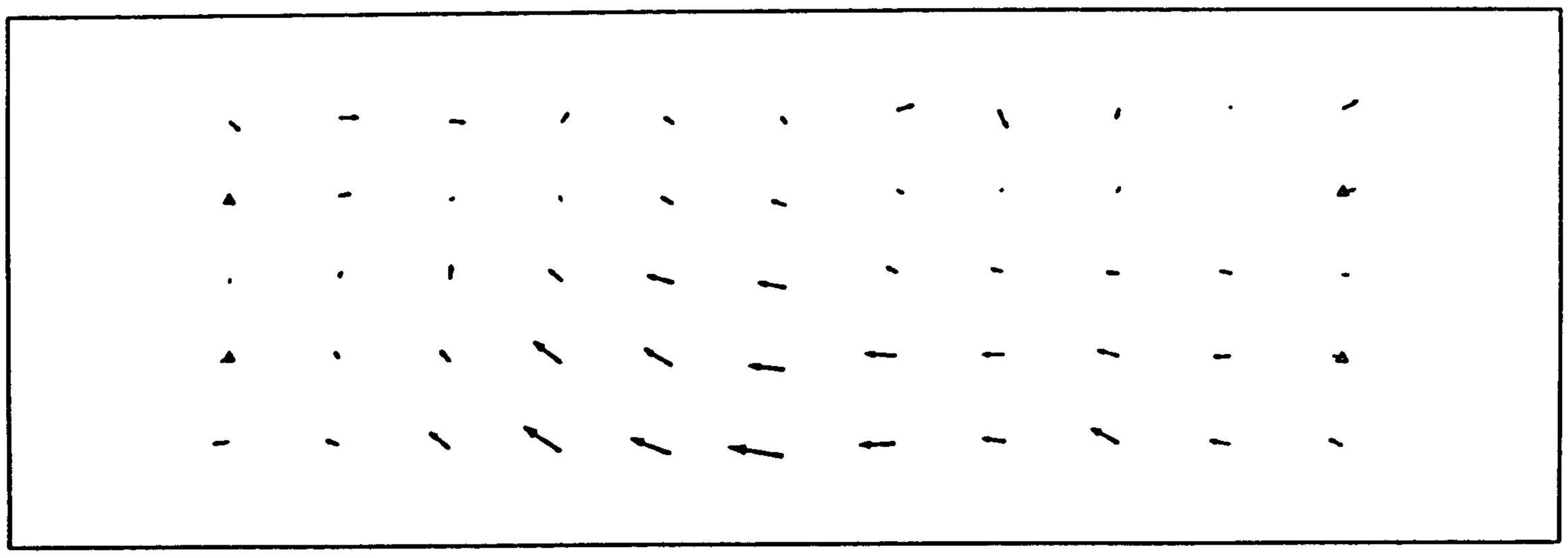

Figure C.8.3 - XY Vector Residual Plot and Height Bubble Residual Plot
(Centre + Right, With GPS, 3-D Control Points At 500m Interval)

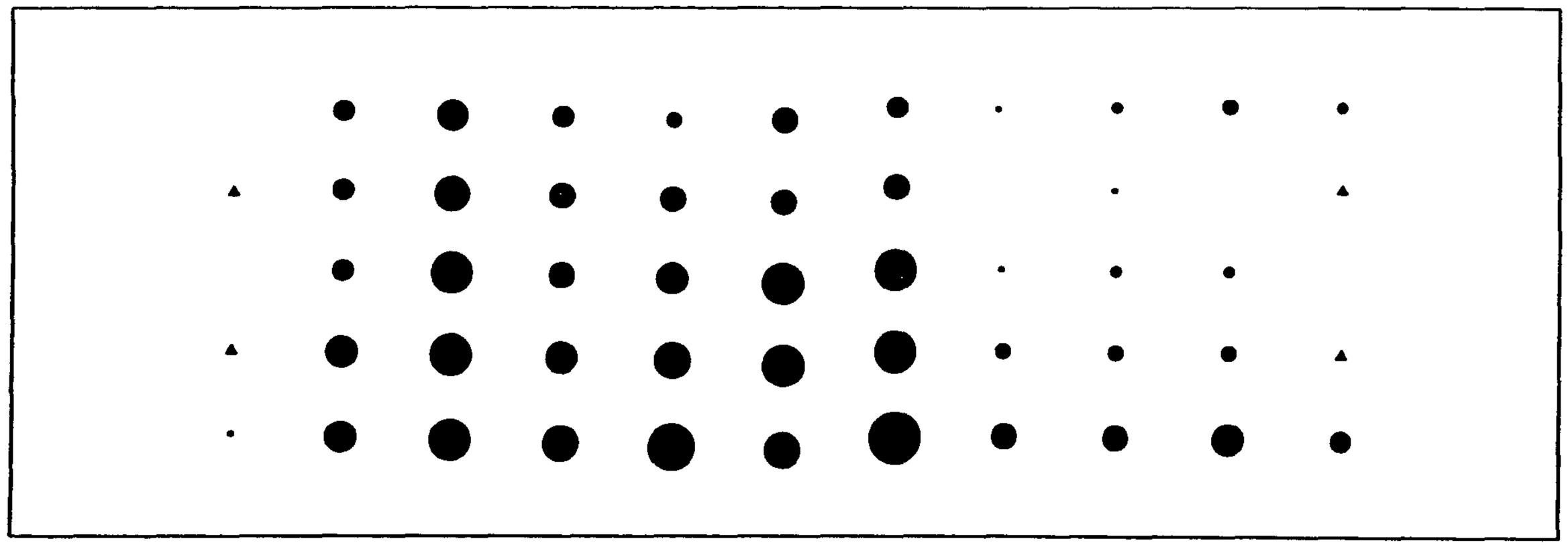

XY Vector Scale: 1cm=3.5cm Height Bubble Scale: 1cm radius=14cm

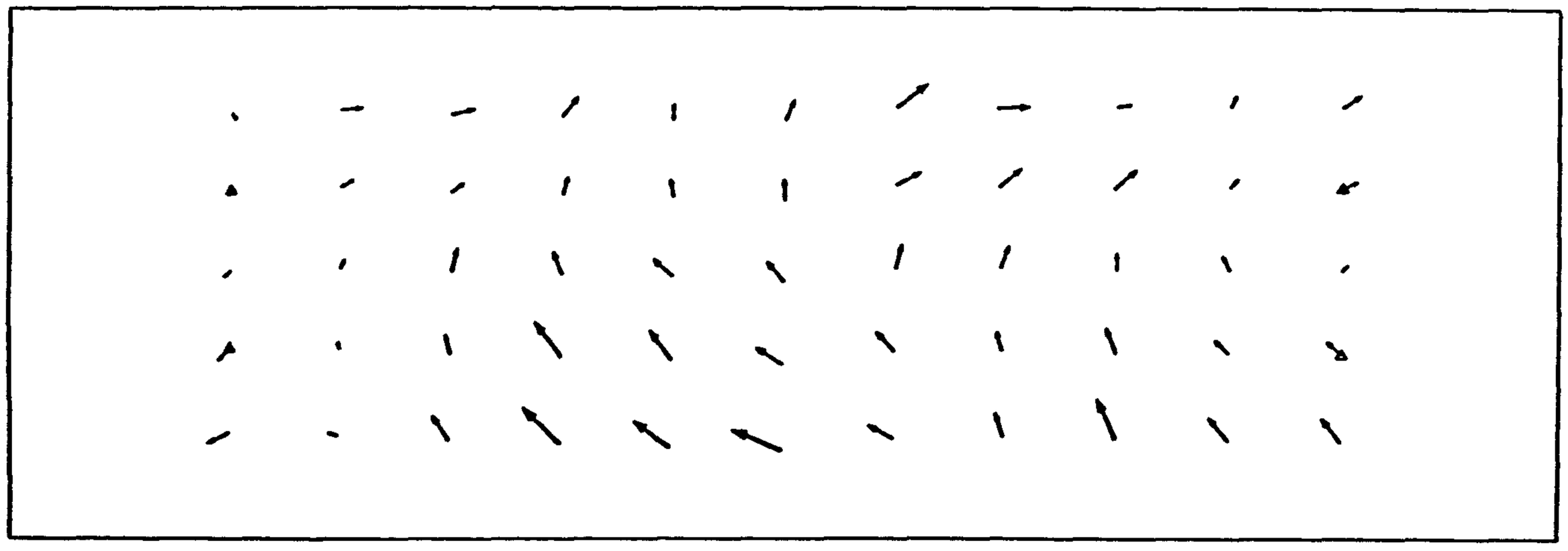

Figure C.8.4 - XY Vector Residual Plot and Height Bubble Residual Plot
(Full Block, With GPS, 3-D Control Points At 500m Interval)

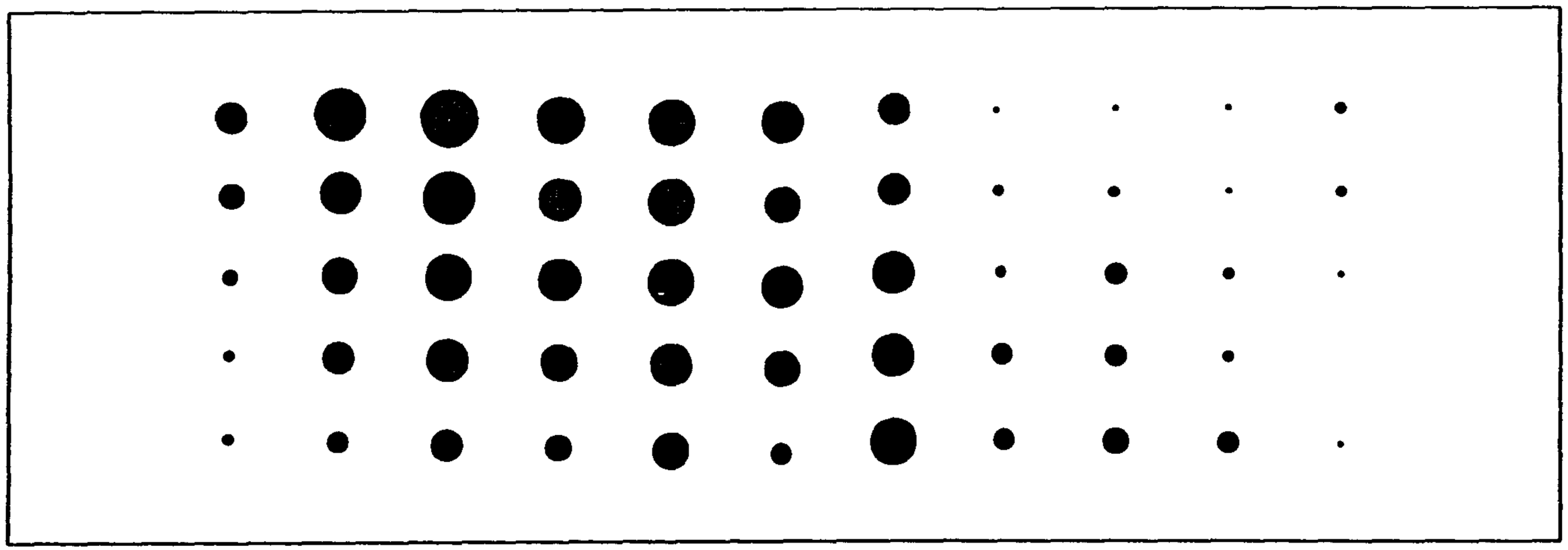

XY Vector Scale: 1cm=7cm Height Bubble Scale: 1cm radius=23cm

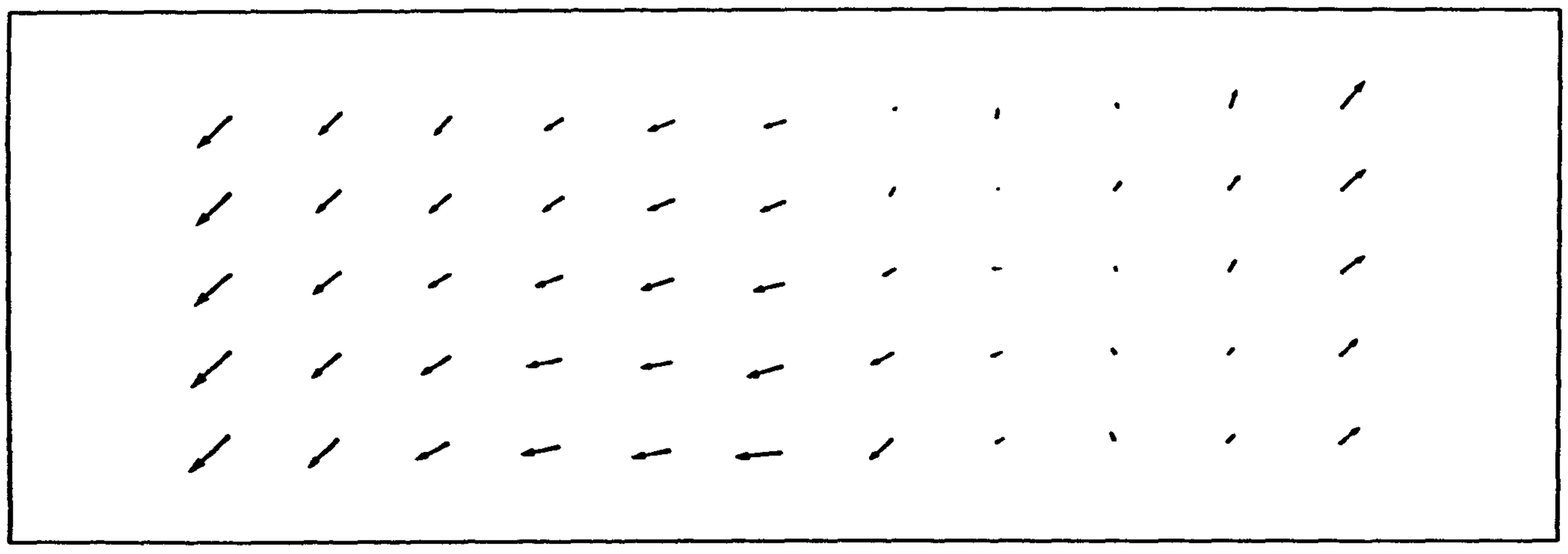

Figure C.9.1 - XY Vector Residual Plot and Height Bubble Residual Plot
(Centre Strip, With GPS, No 3-D Control Points)

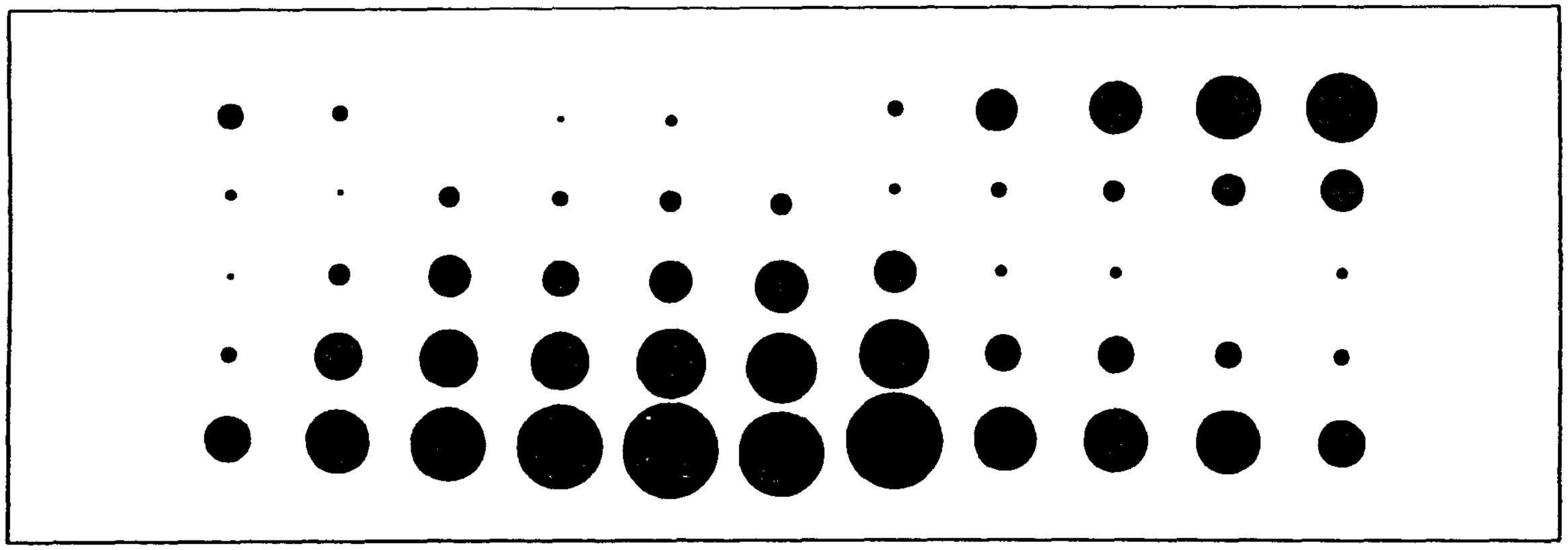

XY Vector Scale: 1cm=14cm Height Bubble Scale: 1cm radius=23cm

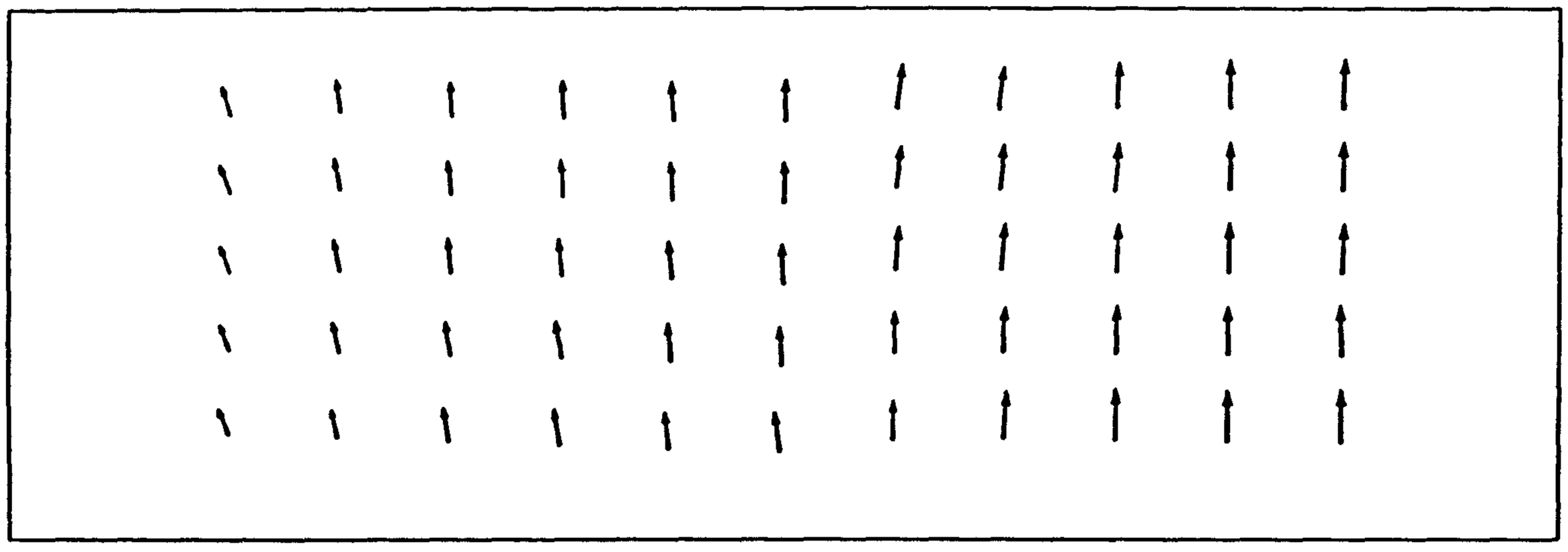

Figure C.9.2 - XY Vector Residual Plot and Height Bubble Residual Plot
(Centre + Left, With GPS, No 3-D Control Points)

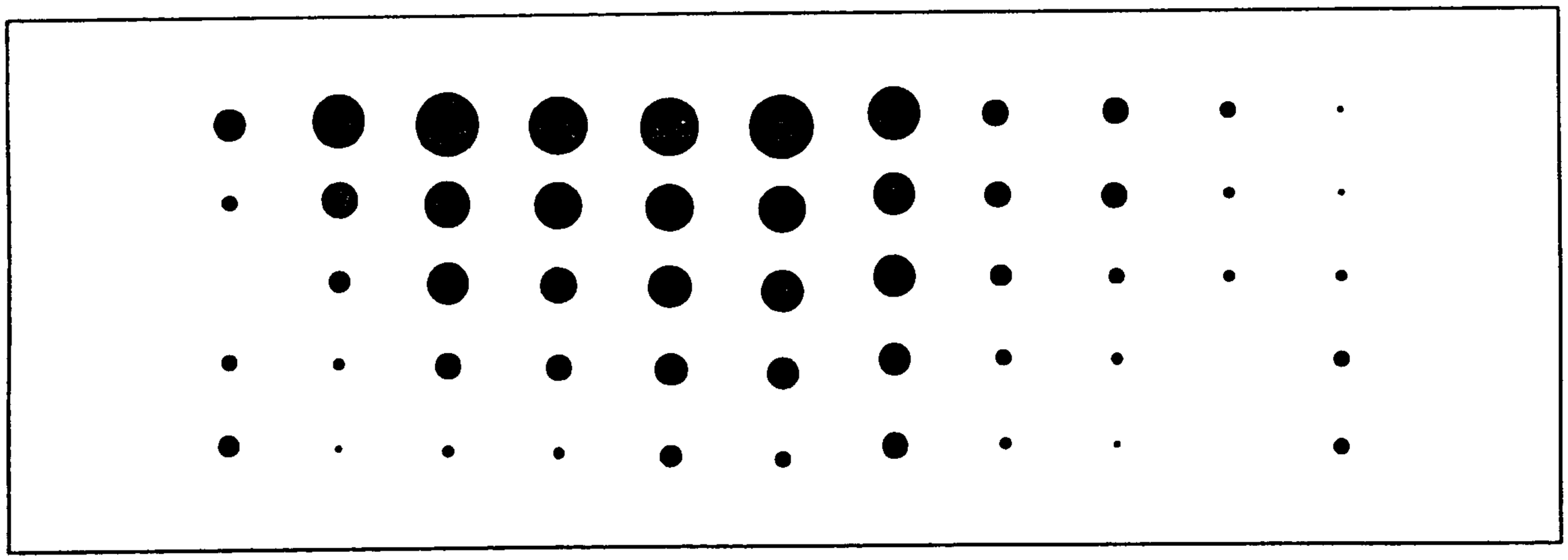

XY Vector Scale: 1cm=14cm Height Bubble Scale: 1cm radius=23cm

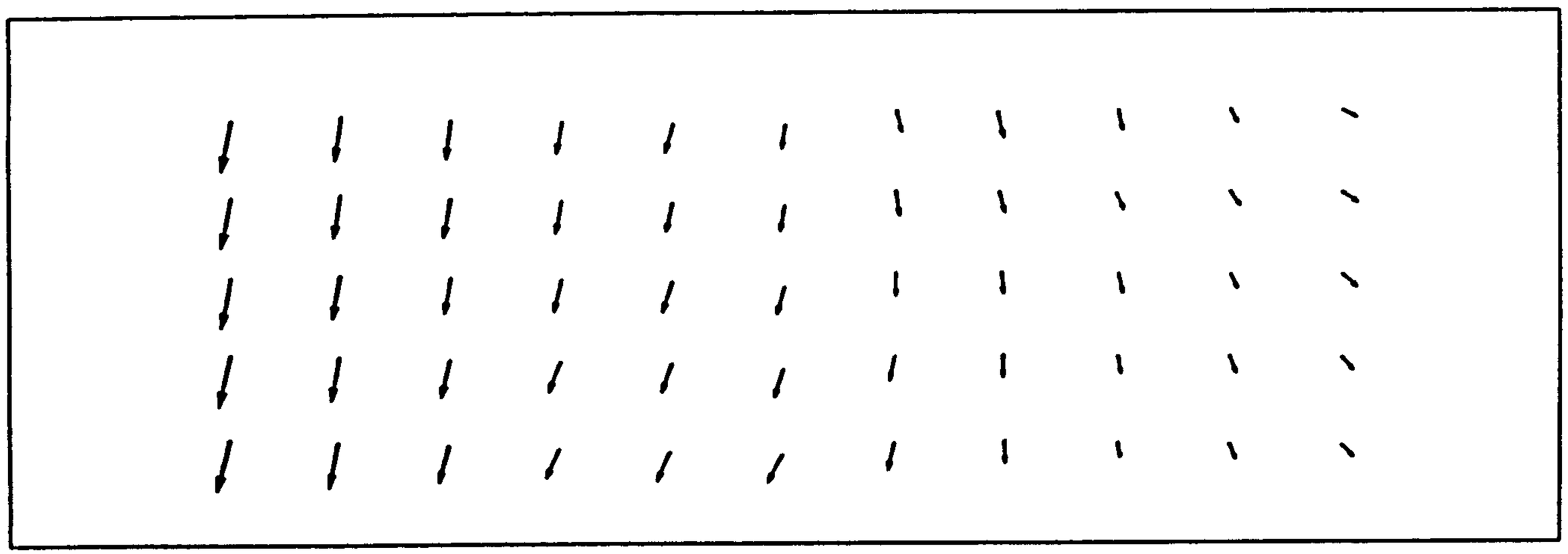

Figure C.9.3 - XY Vector Residual Plot and Height Bubble Residual Plot
(Centre + Right, With GPS, No 3-D Control Points)

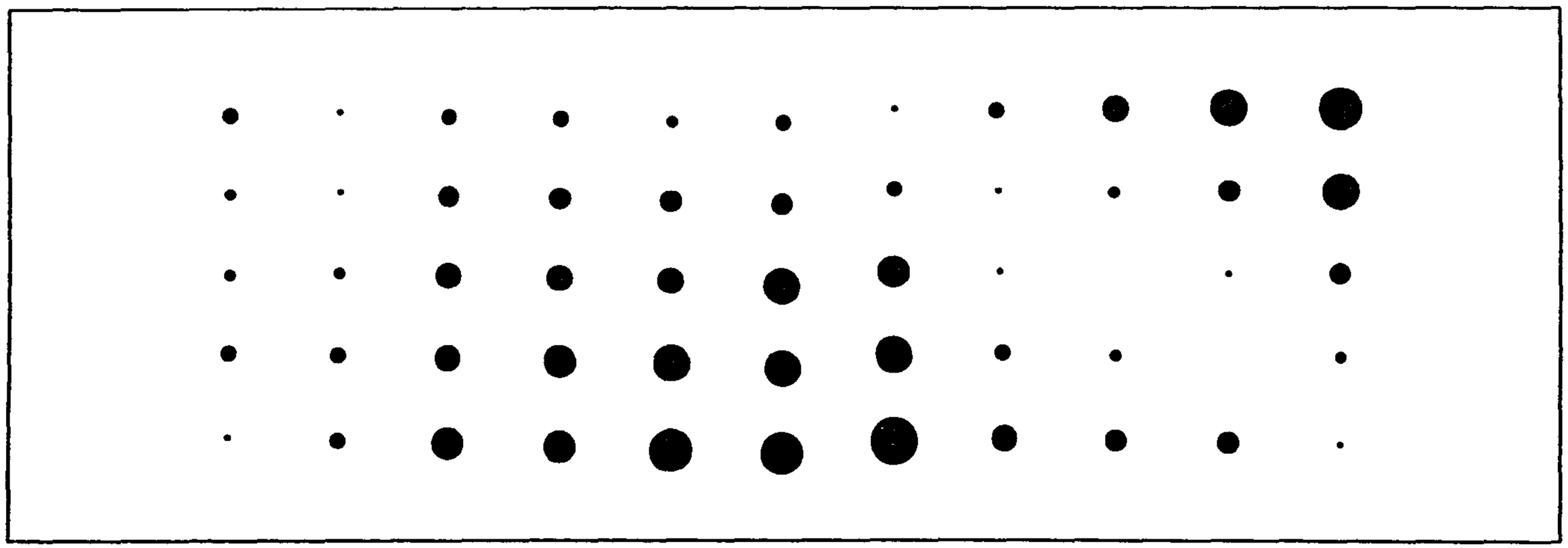

XY Vector Scale: 1cm=7cm Height Bubble Scale: 1cm radius=23cm

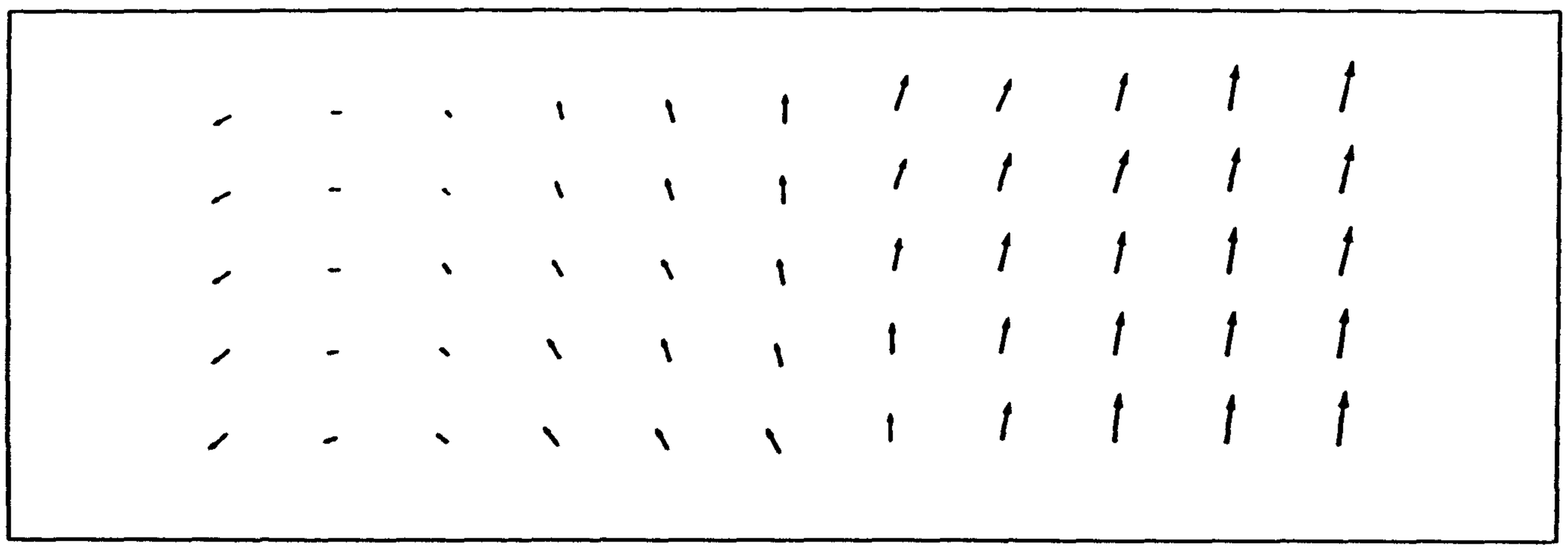

Figure C.9.4 - XY Vector Residual Plot and Height Bubble Residual Plot
(Full Block, With GPS, No 3-D Control Points)

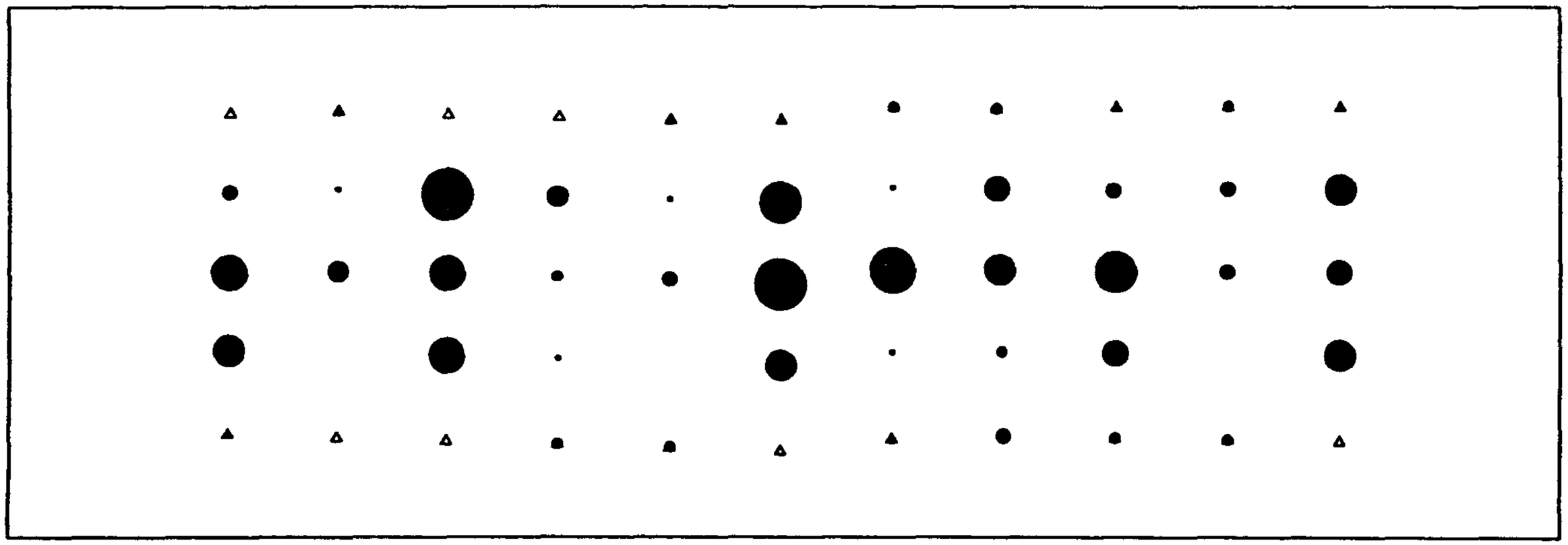

XY Vector Scale: 1cm=3.5cm Height Bubble Scale: 1cm radius=3.5cm

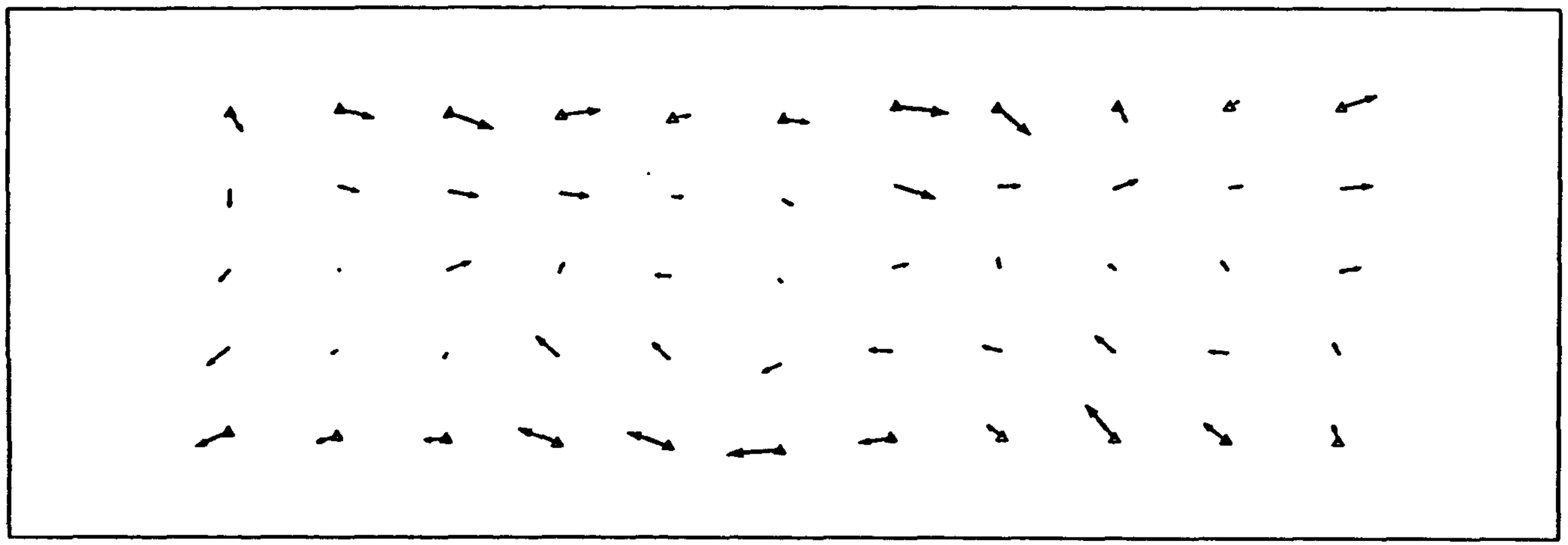

Figure C.10.1 - XY Vector Residual Plot and Height Bubble Residual Plot
(Centre Strip, No GPS, Outside 3-D Control Points At 50m Interval)

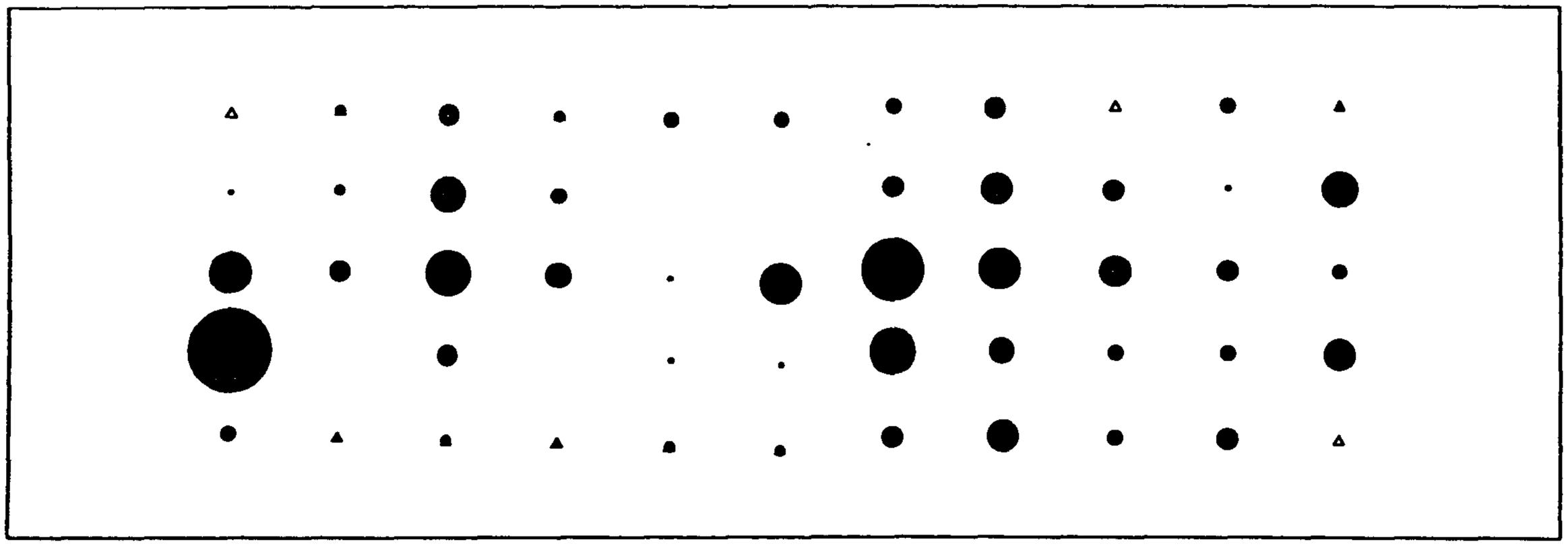

XY Vector Scale: 1cm=3.5cm Height Bubble Scale: 1cm radius=3.5cm

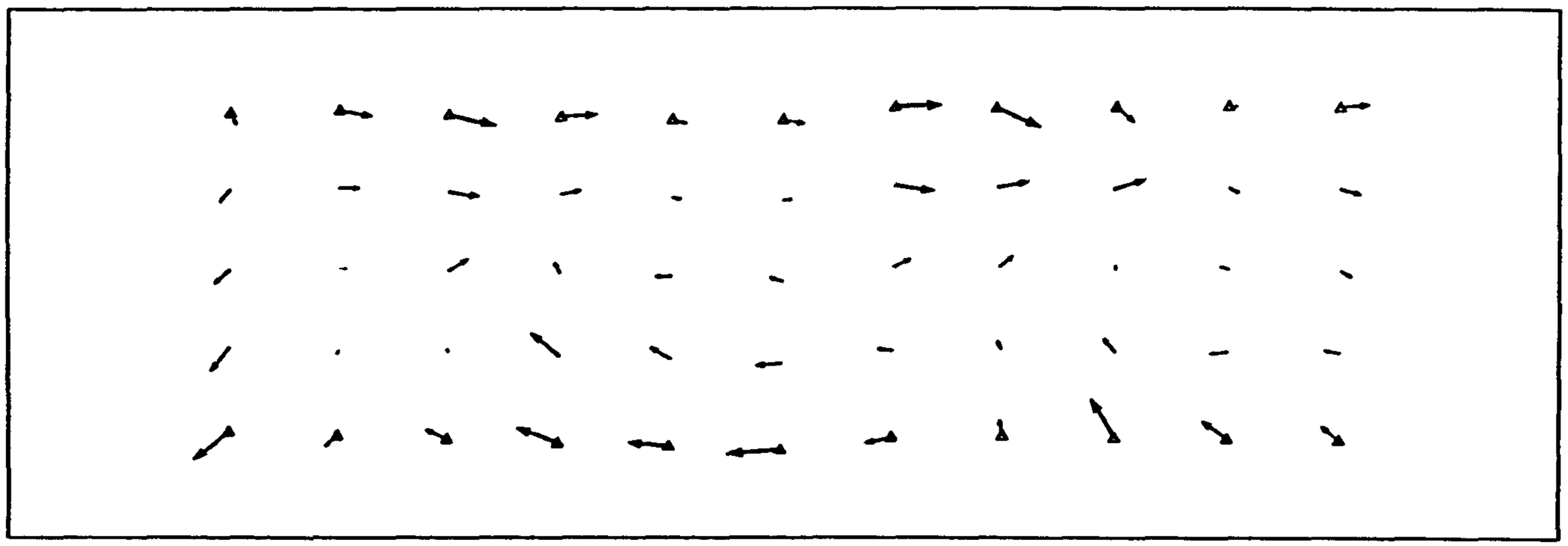

Figure C.10.2 - XY Vector Residual Plot and Height Bubble Residual Plot
(Centre + Left, No GPS, Outside 3-D Control Points At 50m Interval)

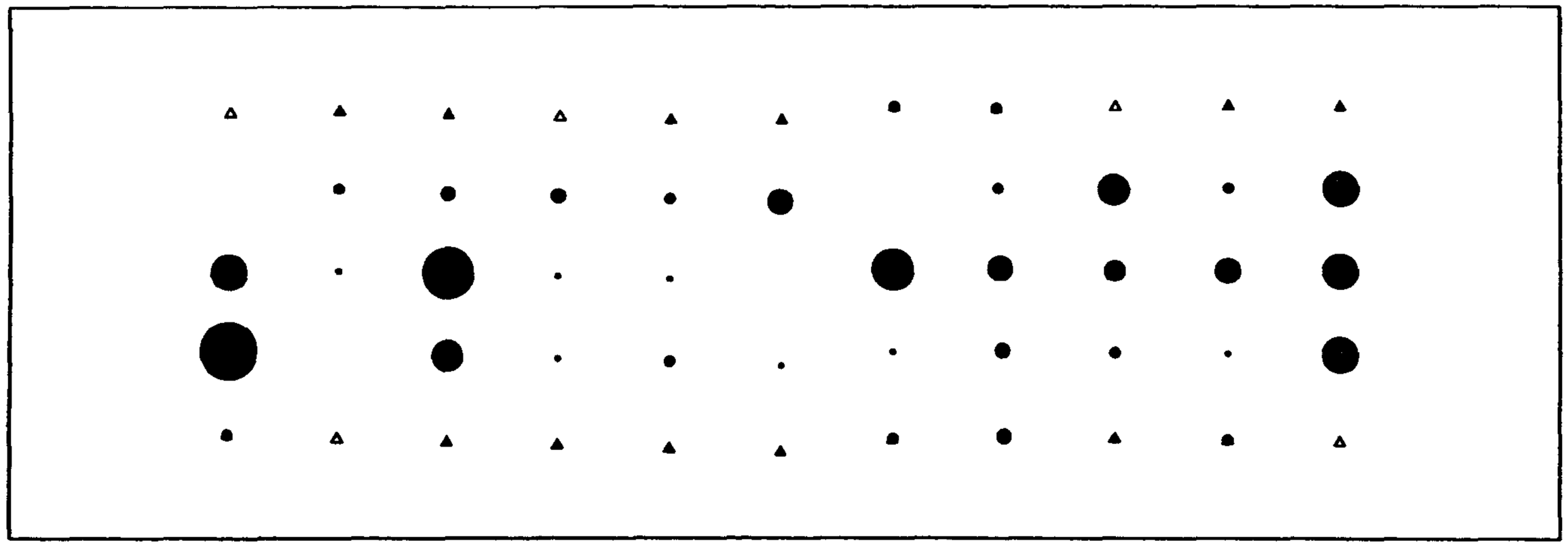

XY Vector Scale: 1cm=3.5cm Height Bubble Scale: 1cm radius=3.5cm

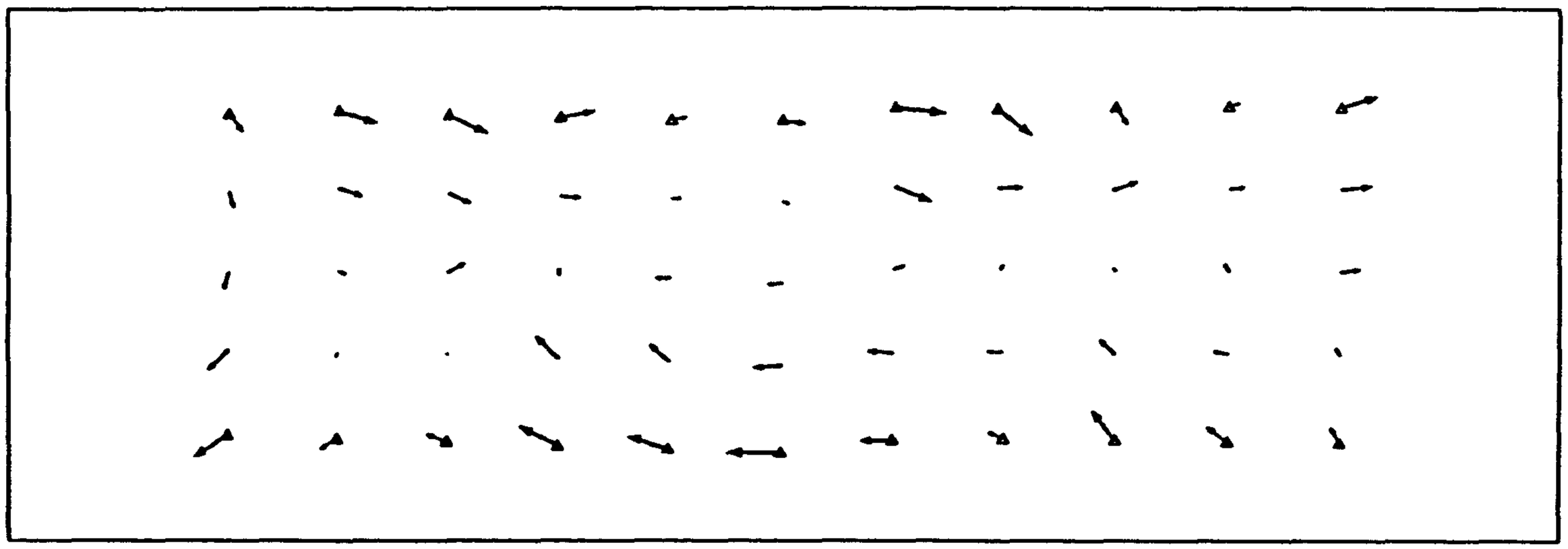

Figure C.10.3 - XY Vector Residual Plot and Height Bubble Residual Plot
(Centre + Right, No GPS, Outside 3-D Control Points At 50m Interval)

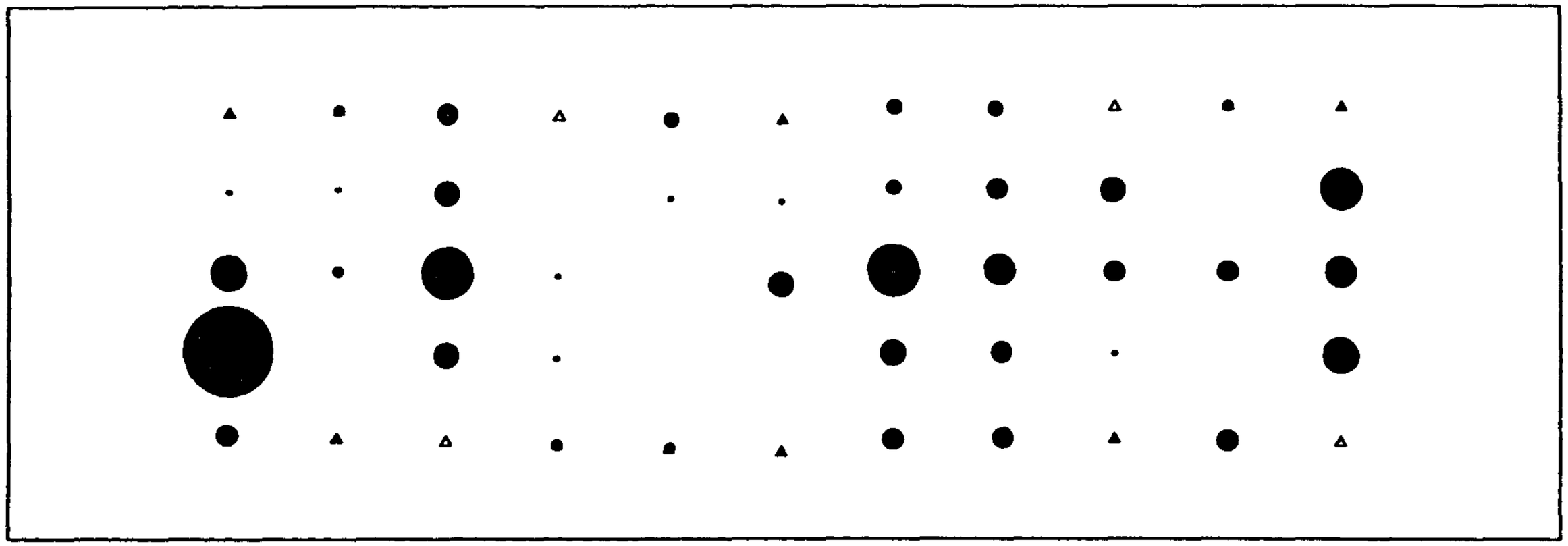

XY Vector Scale: 1cm=3.5cm Height Bubble Scale: 1cm radius=3.5cm

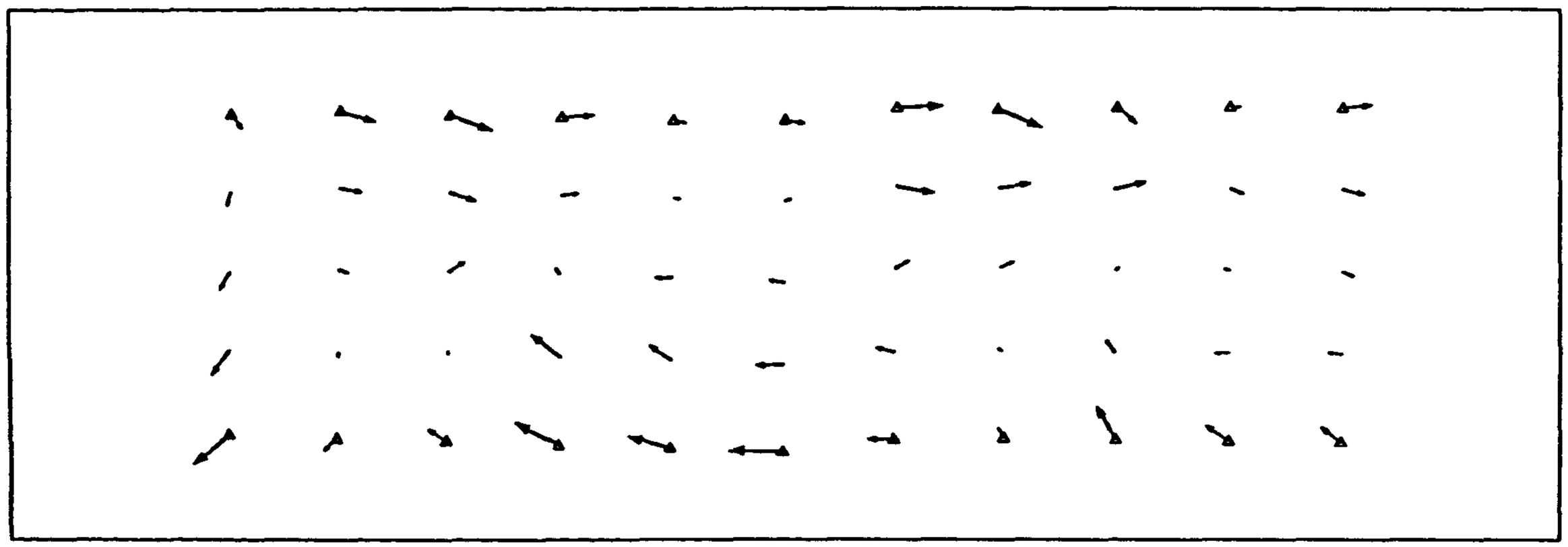

Figure C.10.4 - XY Vector Residual Plot and Height Bubble Residual Plot
(Full Block, No GPS, Outside 3-D Control Points At 50m Interval)

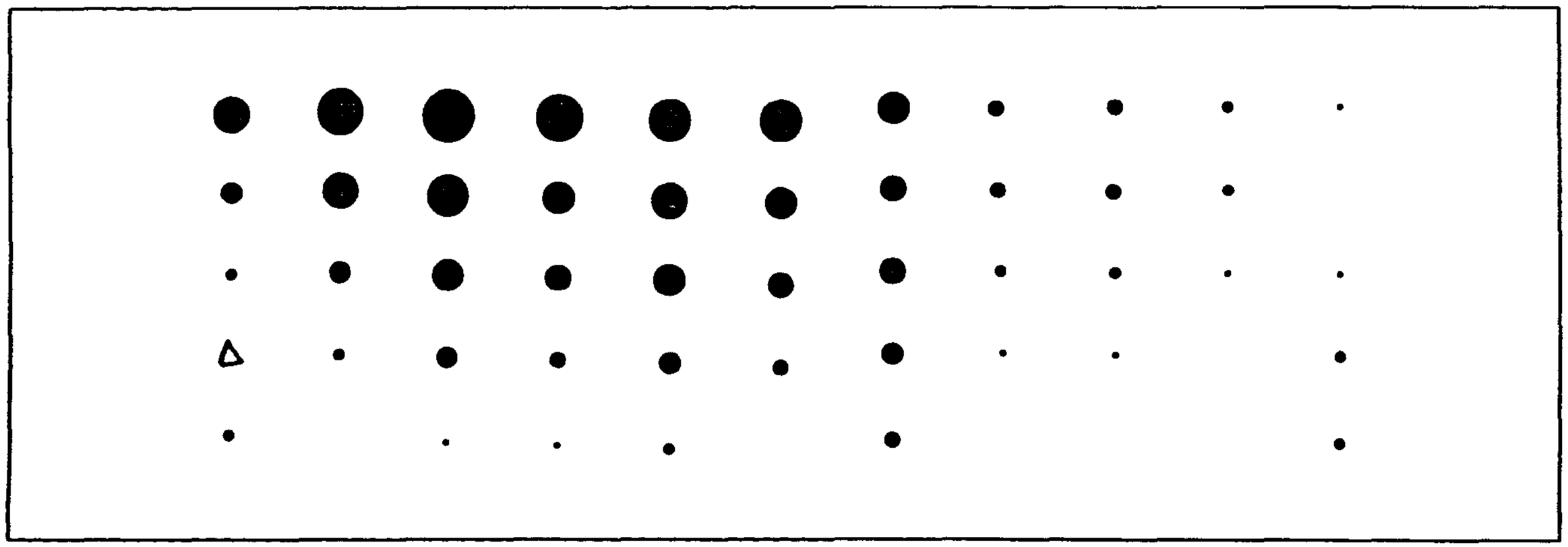

XY Vector Scale: 1cm=14cm Height Bubble Scale: 1cm radius=35cm

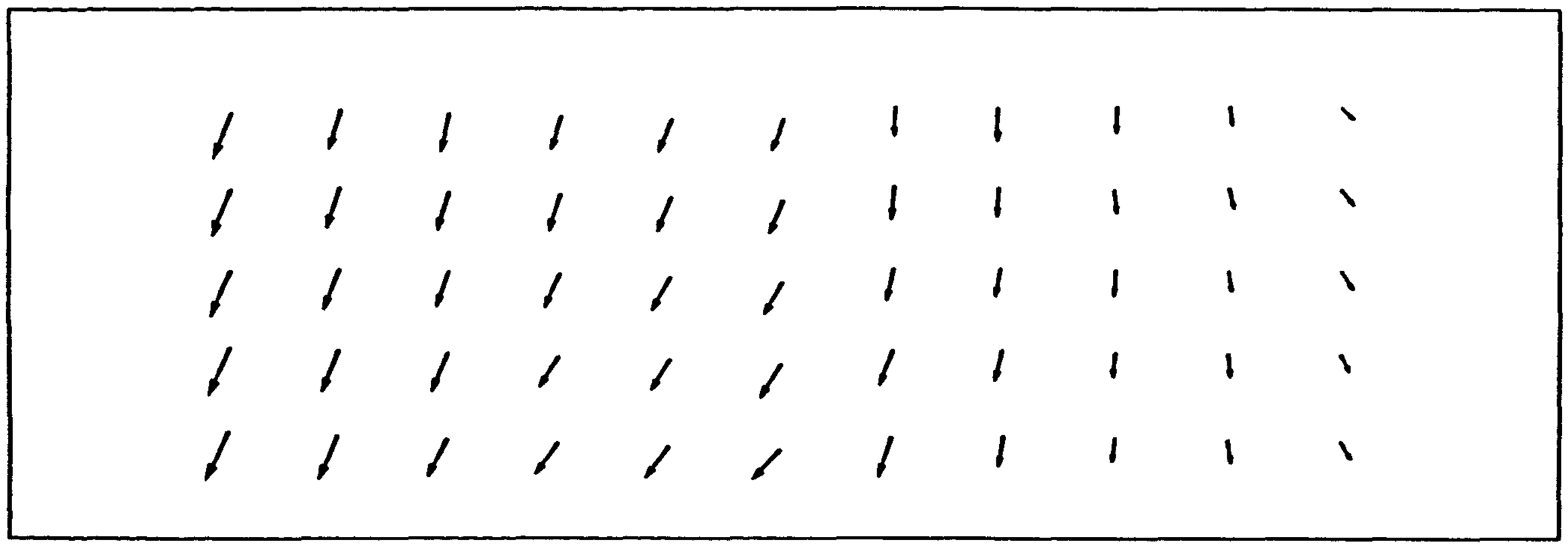

Figure C.11.1 - XY Vector Residual Plot and Height Bubble Residual Plot
(Centre Strip, With GPS, One Height Control Point At Point 2)

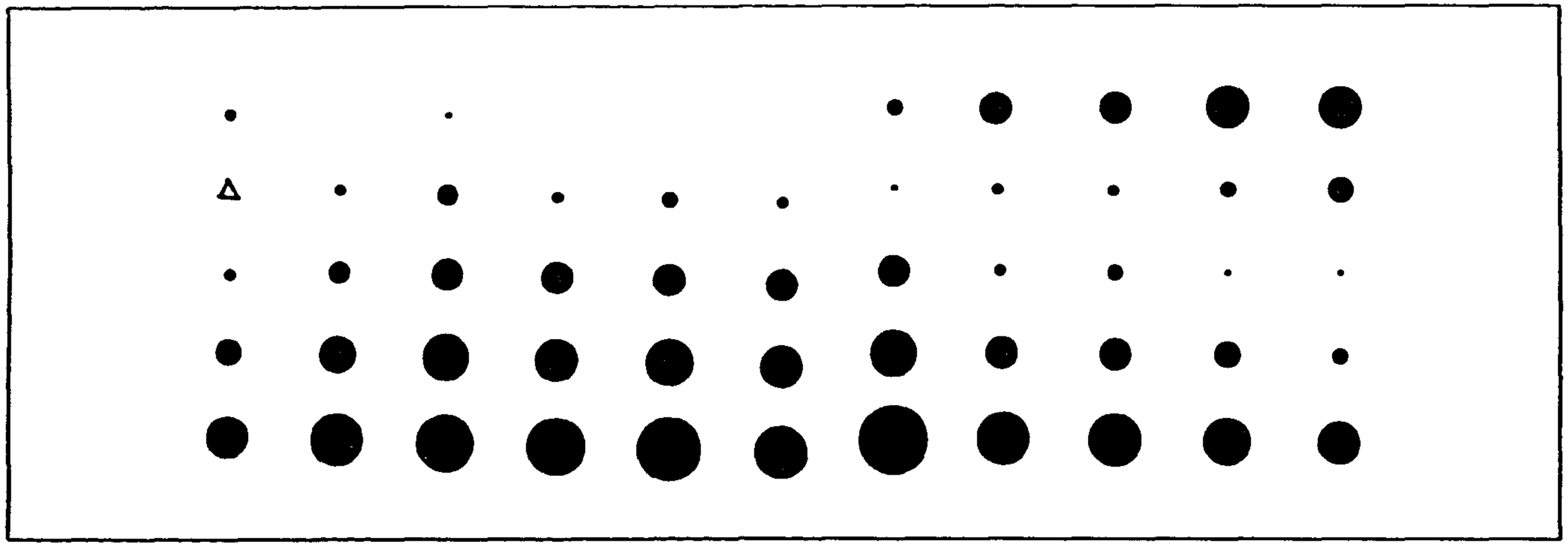

XY Vector Scale: 1cm=14cm Height Bubble Scale: 1cm radius=35cm

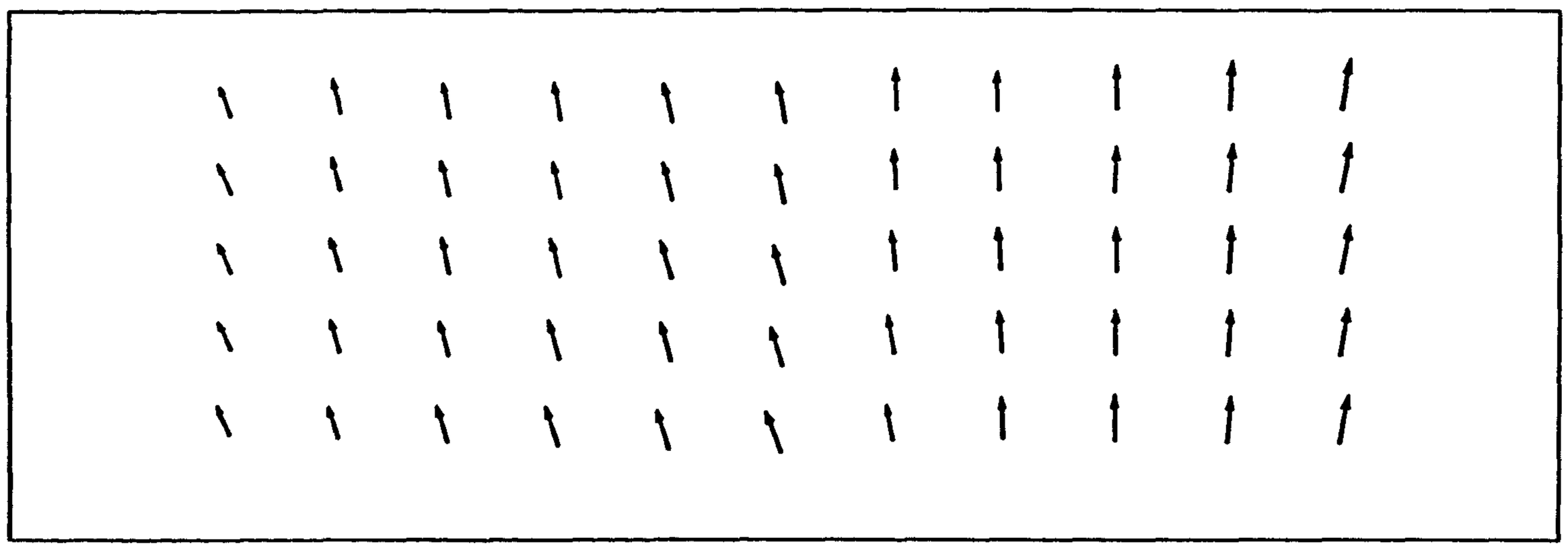

Figure C.11.2 - XY Vector Residual Plot and Height Bubble Residual Plot
(Centre Strip, With GPS, One Height Control Point At Point 4)

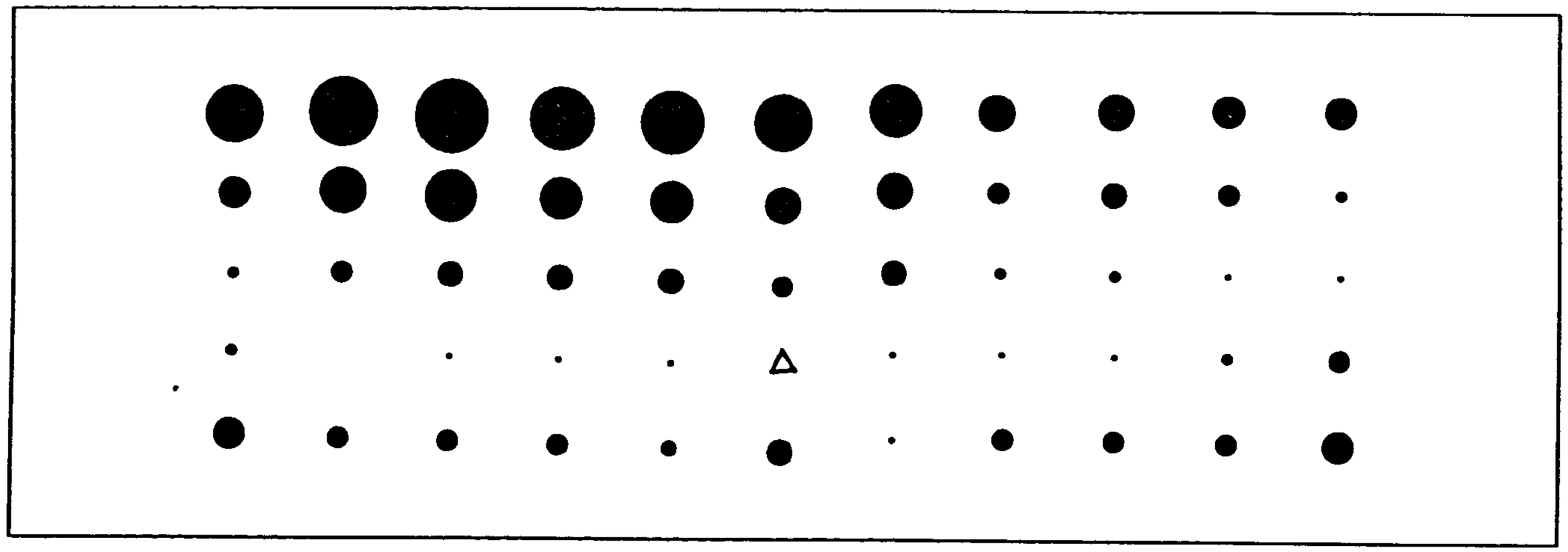

XY Vector Scale: 1cm=35cm Height Bubble Scale: 1cm radius=35cm

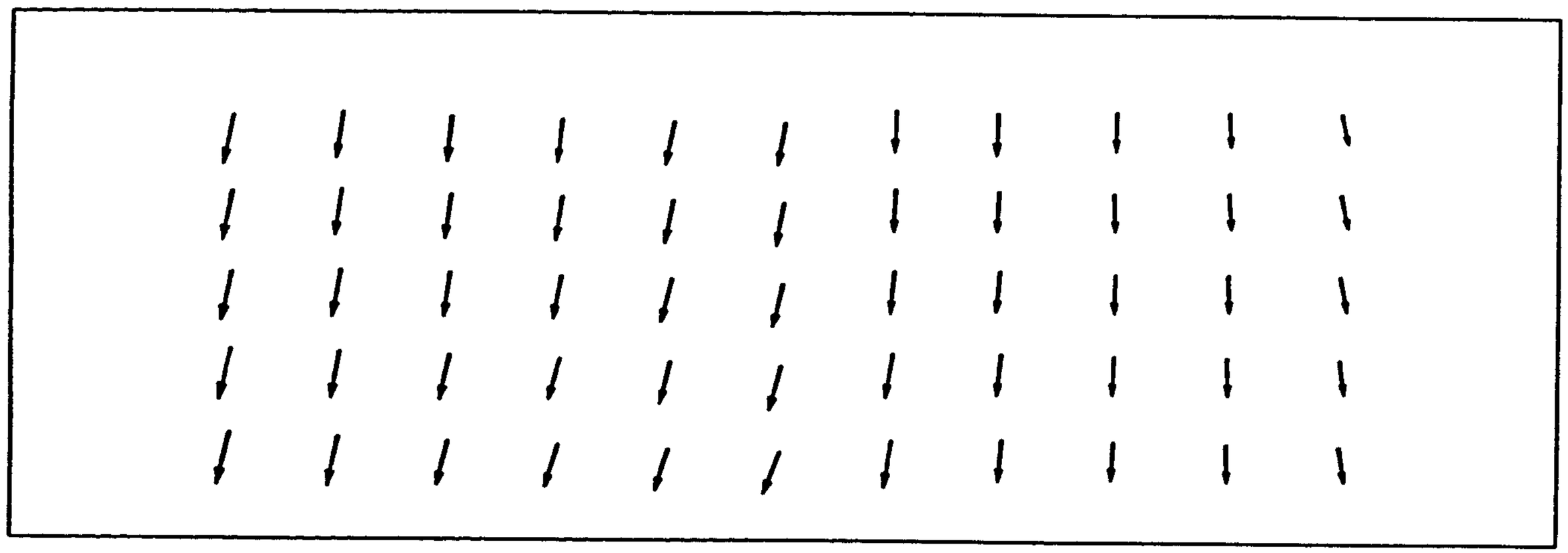

Figure C.11.3 - XY Vector Residual Plot and Height Bubble Residual Plot
(Centre Strip, With GPS, One Height Control Point At Point 27)

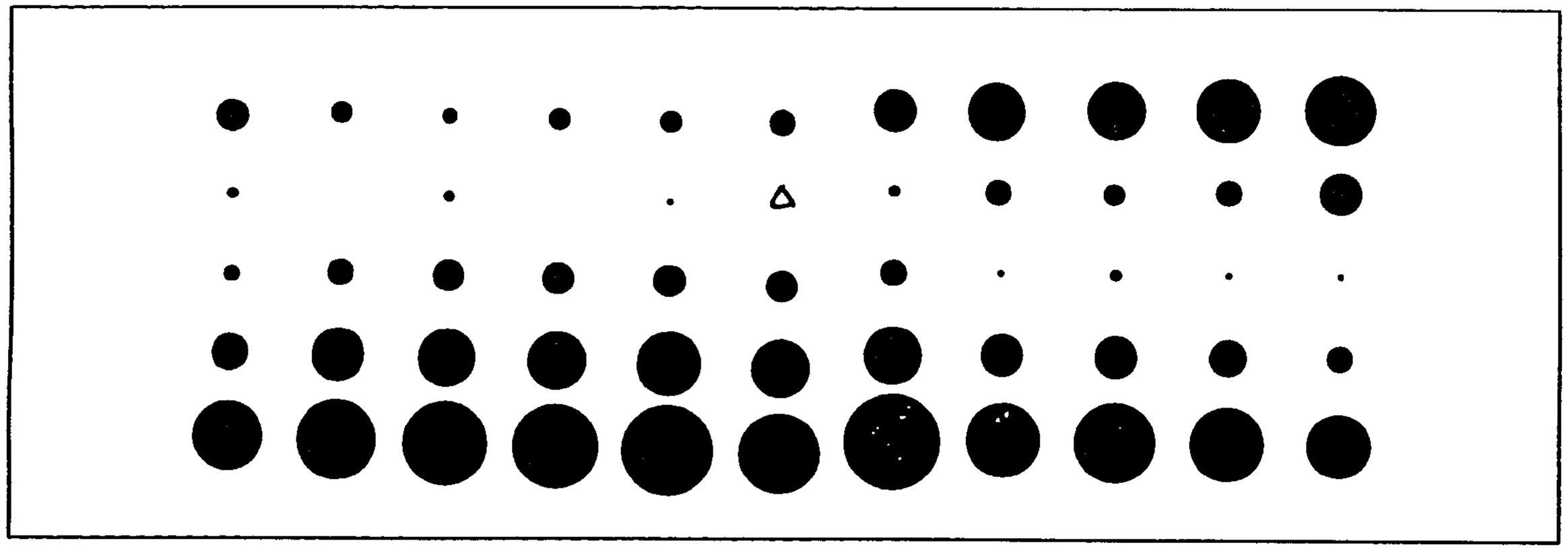

XY Vector Scale: 1cm=35cm Height Bubble Scale: 1cm radius=35cm

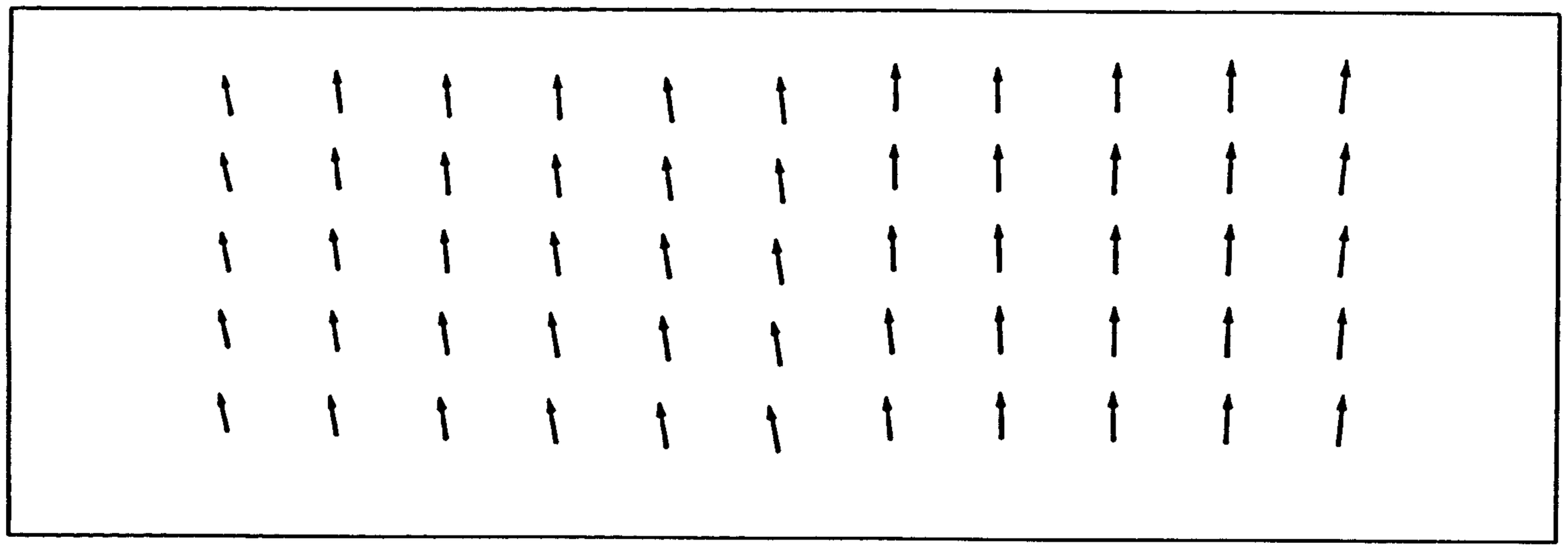

Figure C.11.4 - XY Vector Residual Plot and Height Bubble Residual Plot
(Centre Strip, With GPS, One Height Control Point At Point 29)

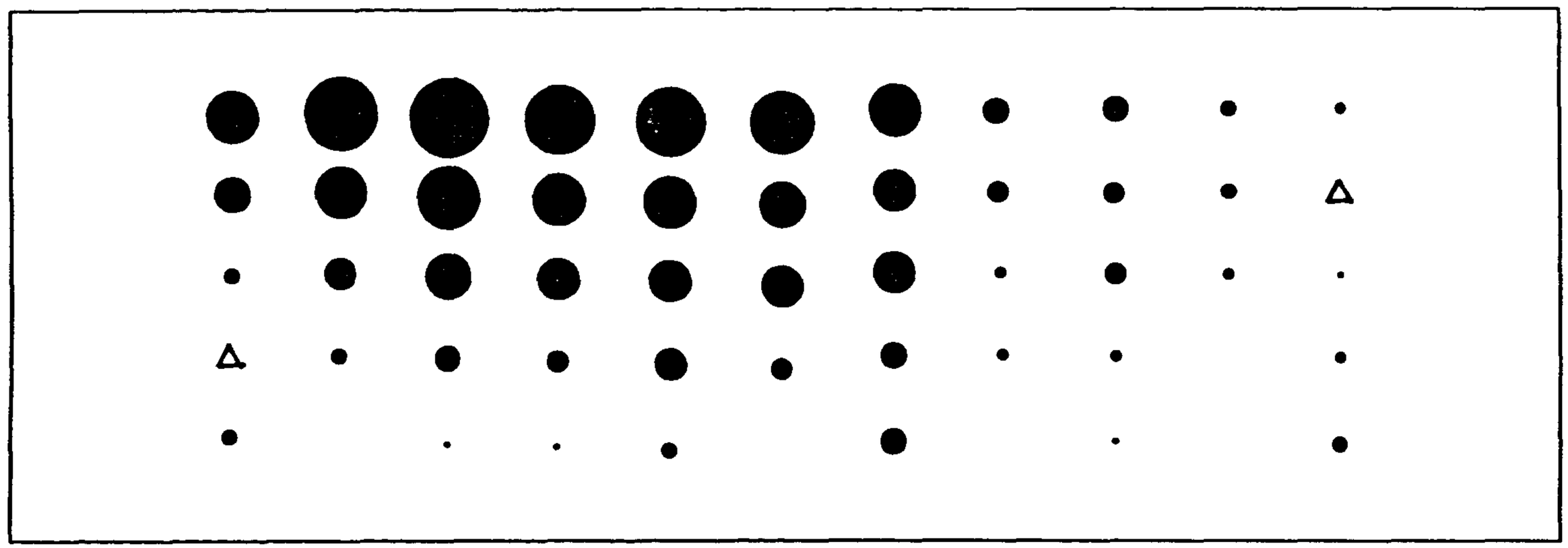

XY Vector Scale: 1cm=14cm Height Bubble Scale: 1cm radius=23cm

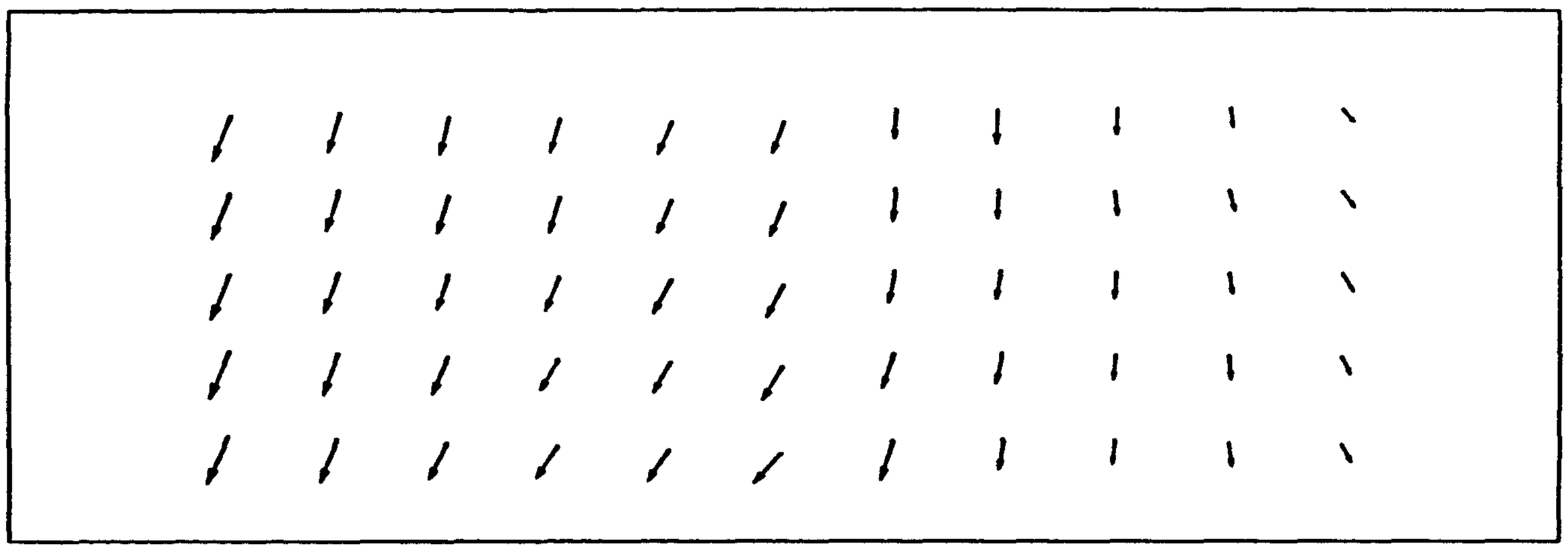

Figure C.12.1 - XY Vector Residual Plot and Height Bubble Residual Plot
(Centre Strip, With GPS, Two Height Control Points At Points 2 And 54)

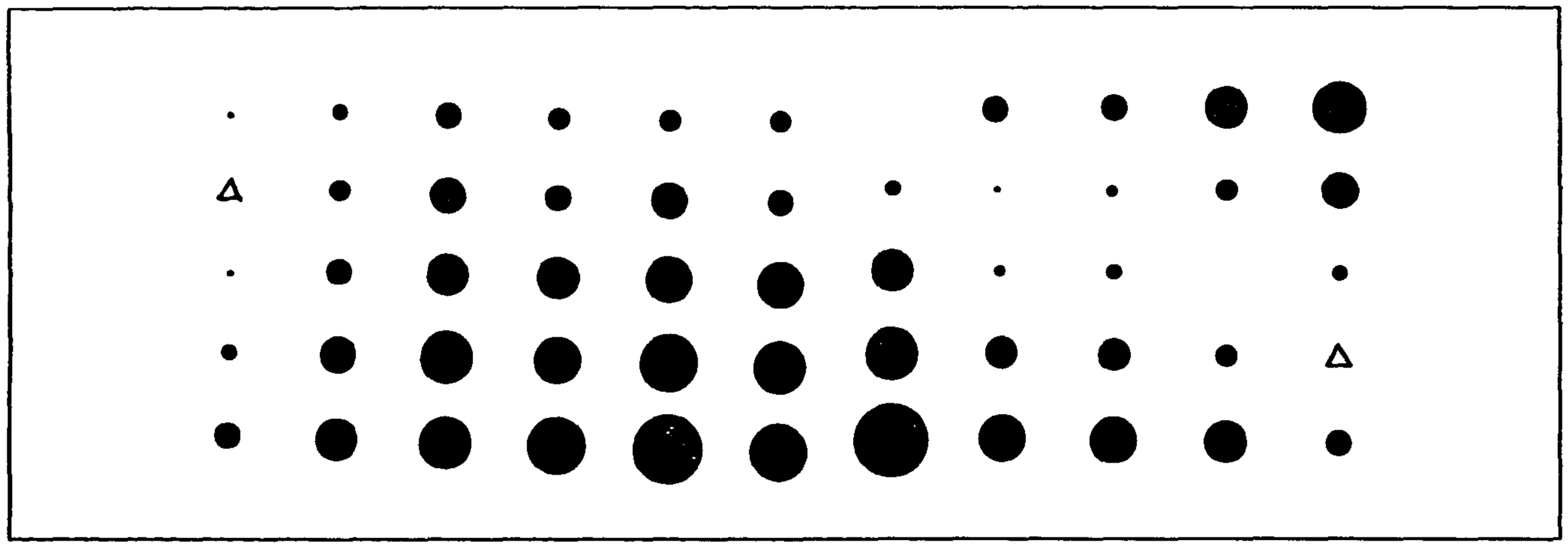

XY Vector Scale: 1cm=14cm Height Bubble Scale: 1cm radius=23cm

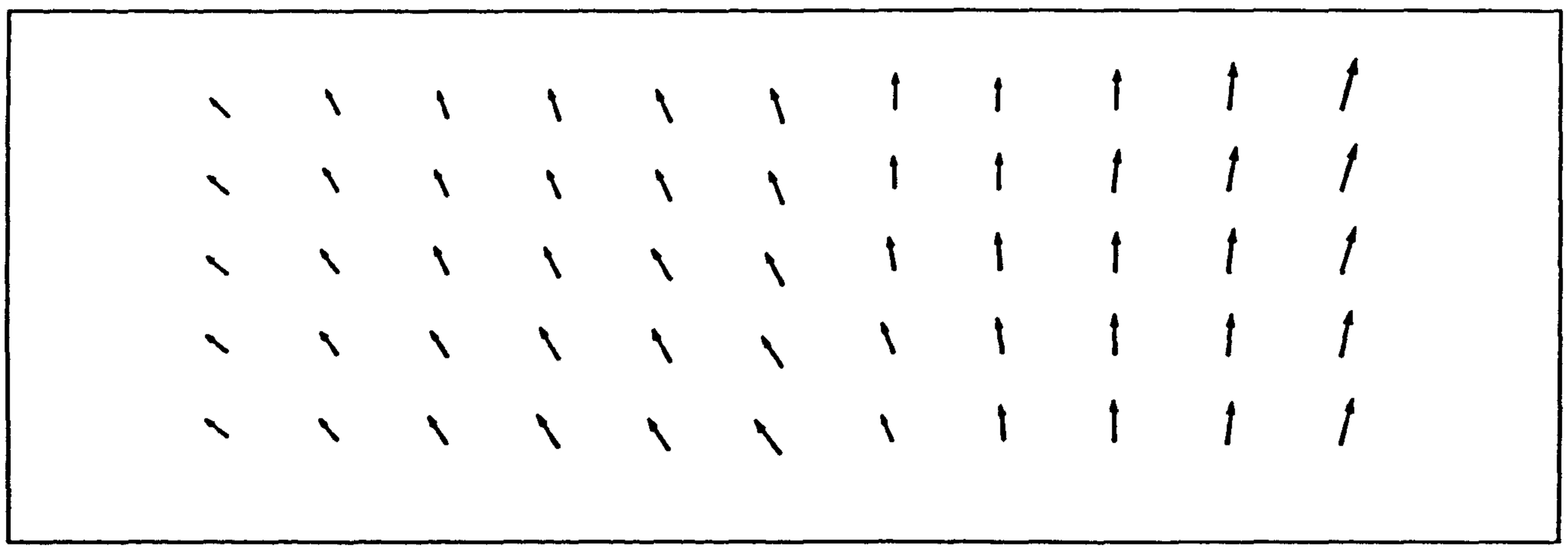

Figure C.12.2 - XY Vector Residual Plot and Height Bubble Residual Plot
(Centre Strip, With GPS, Two Height Control Points At Points 4 And 52)

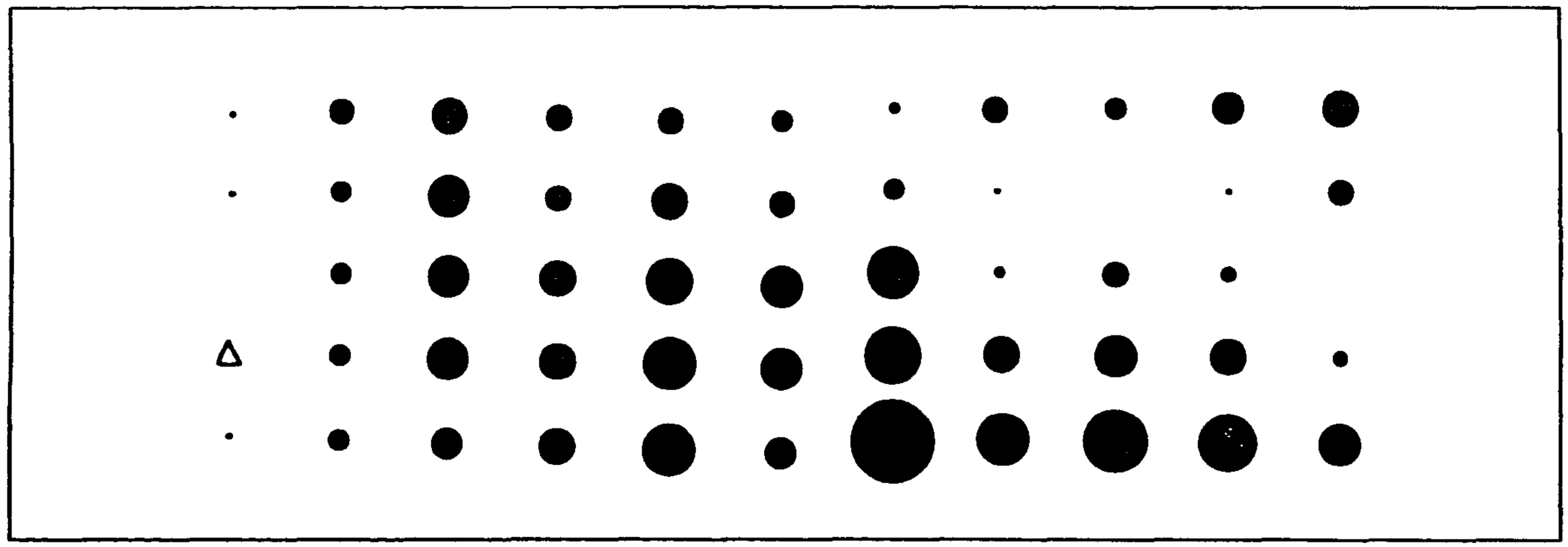

XY Vector Scale: 1cm=7cm Height Bubble Scale: 1cm radius=14cm

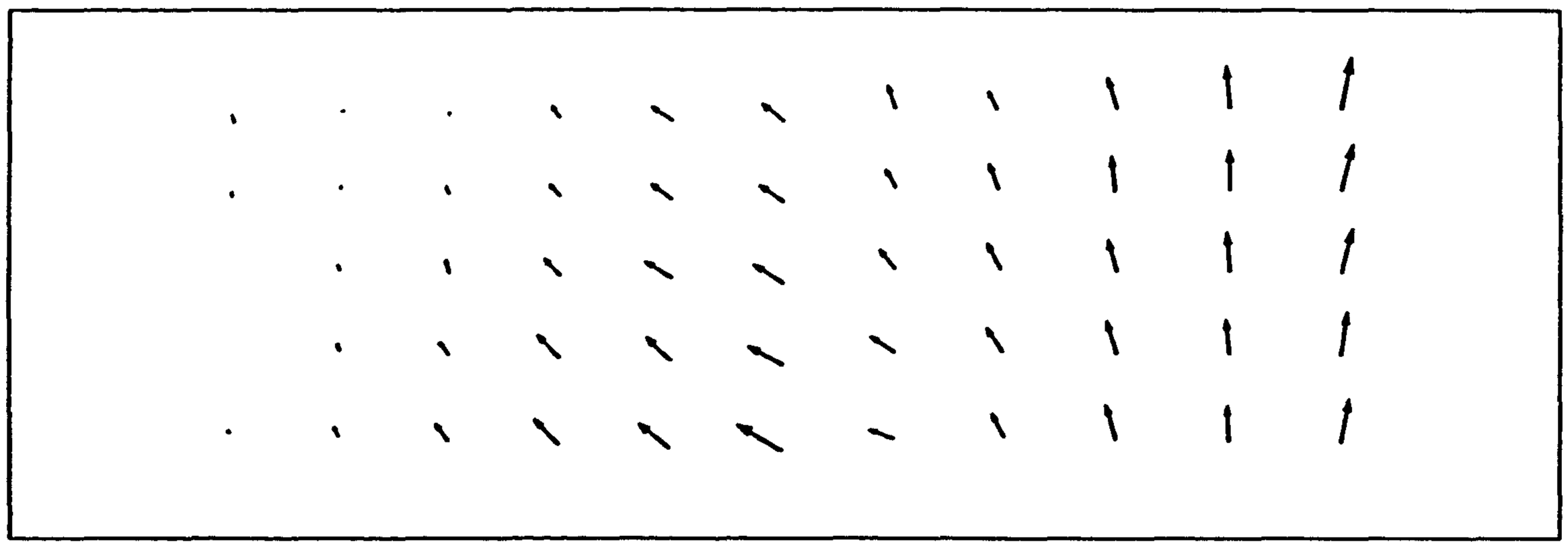

Figure C.13.1 - XY Vector Residual Plot and Height Bubble Residual Plot
(Centre Strip, With GPS, One 3-D Control Point At Point 2)

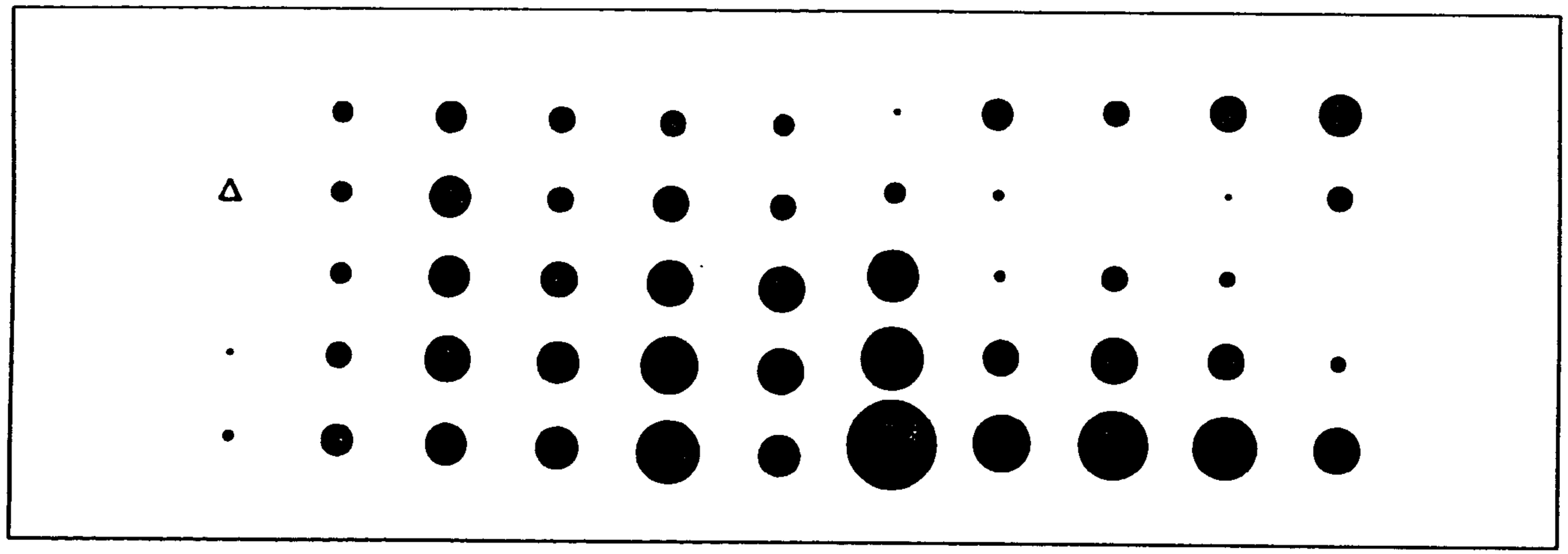

XY Vector Scale: 1cm=7cm Height Bubble Scale: 1cm radius=14cm

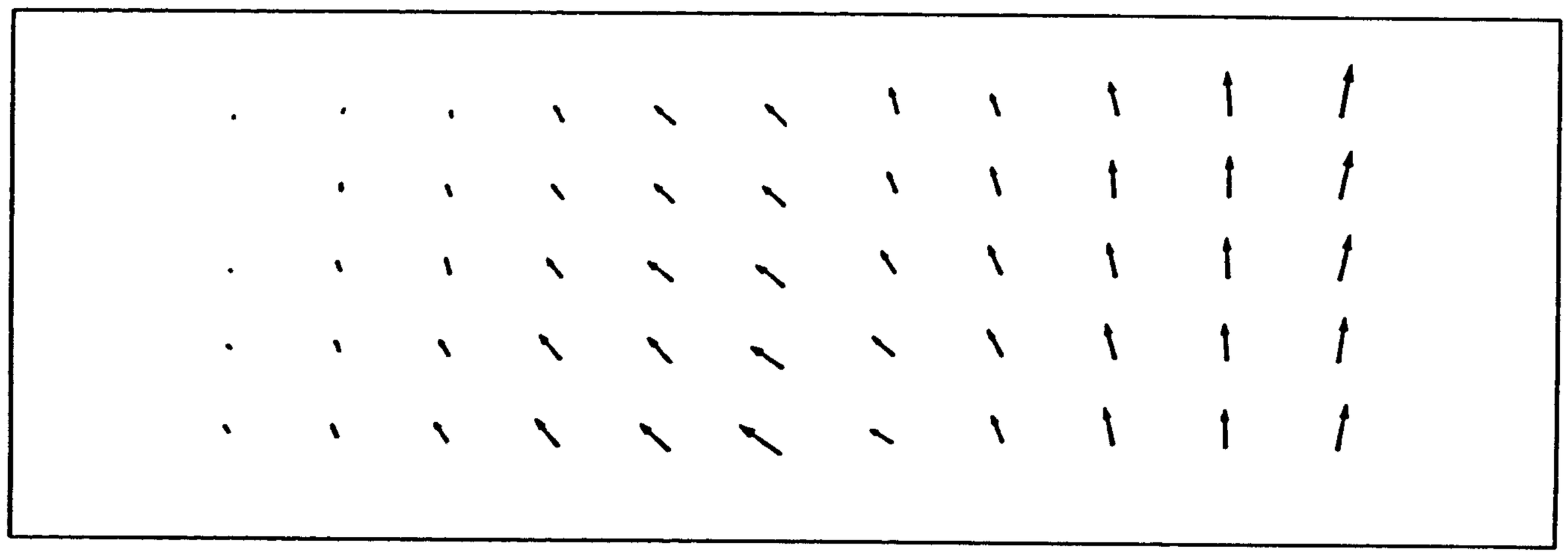

Figure C.13.2 - XY Vector Residual Plot and Height Bubble Residual Plot
(Centre Strip, With GPS, One 3-D Control Point At Point 4)

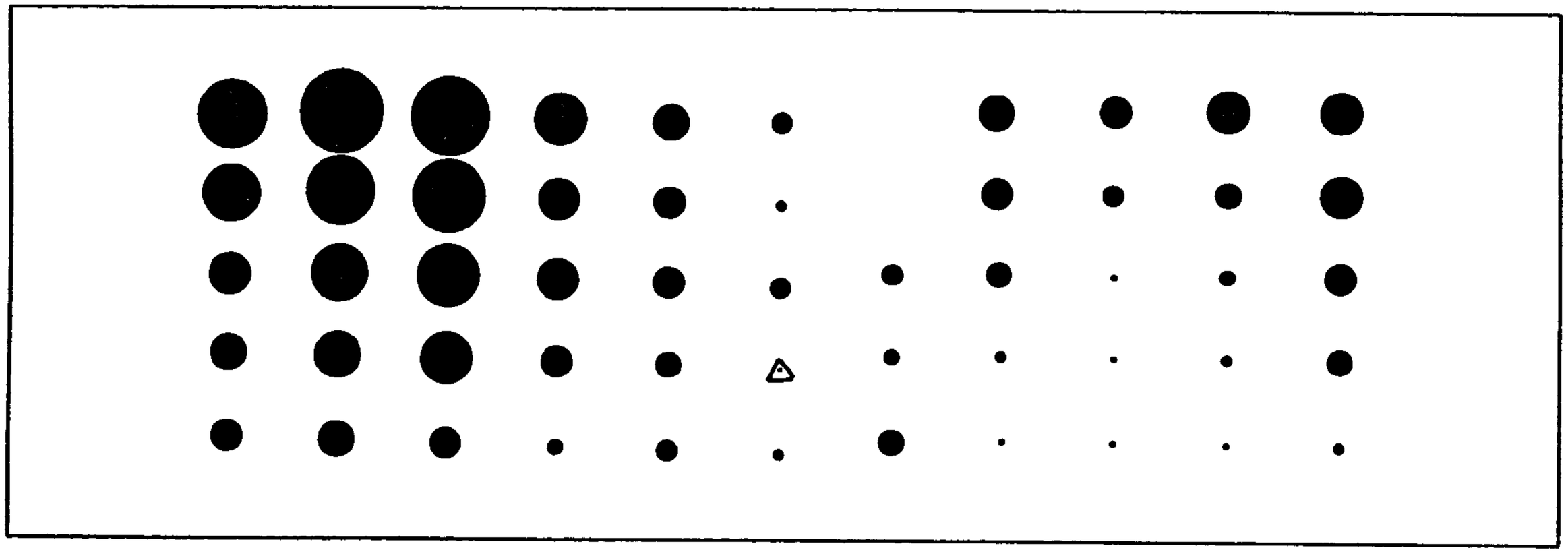

XY Vector Scale: 1cm=7cm Height Bubble Scale: 1cm radius=14cm

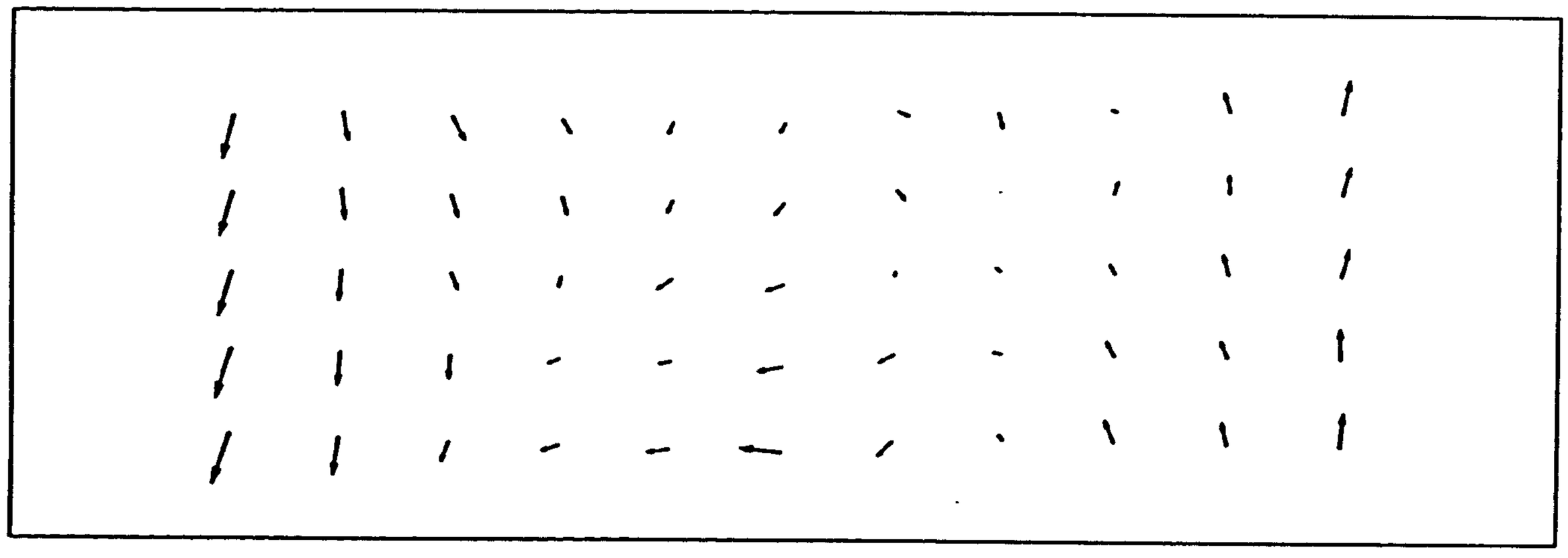

Figure C.13.3 - XY Vector Residual Plot and Height Bubble Residual Plot
(Centre Strip, With GPS, One 3-D Control Point At Point 27)

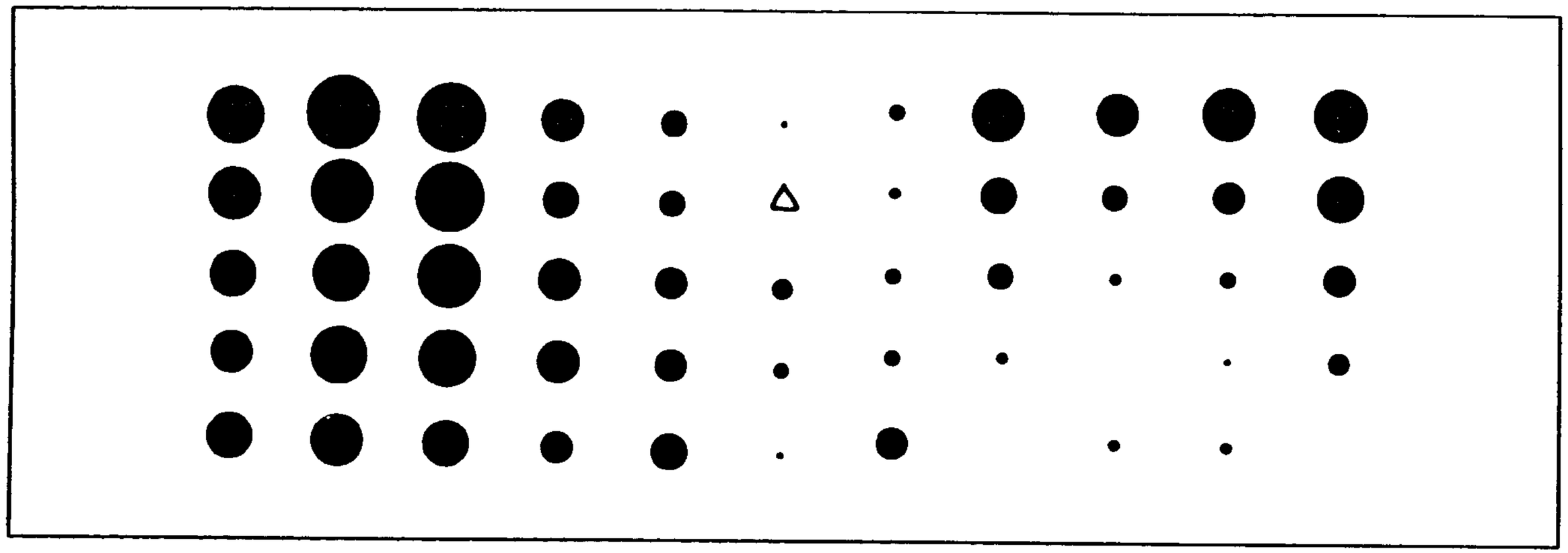

XY Vector Scale: 1cm=7cm Height Bubble Scale: 1cm radius=14cm

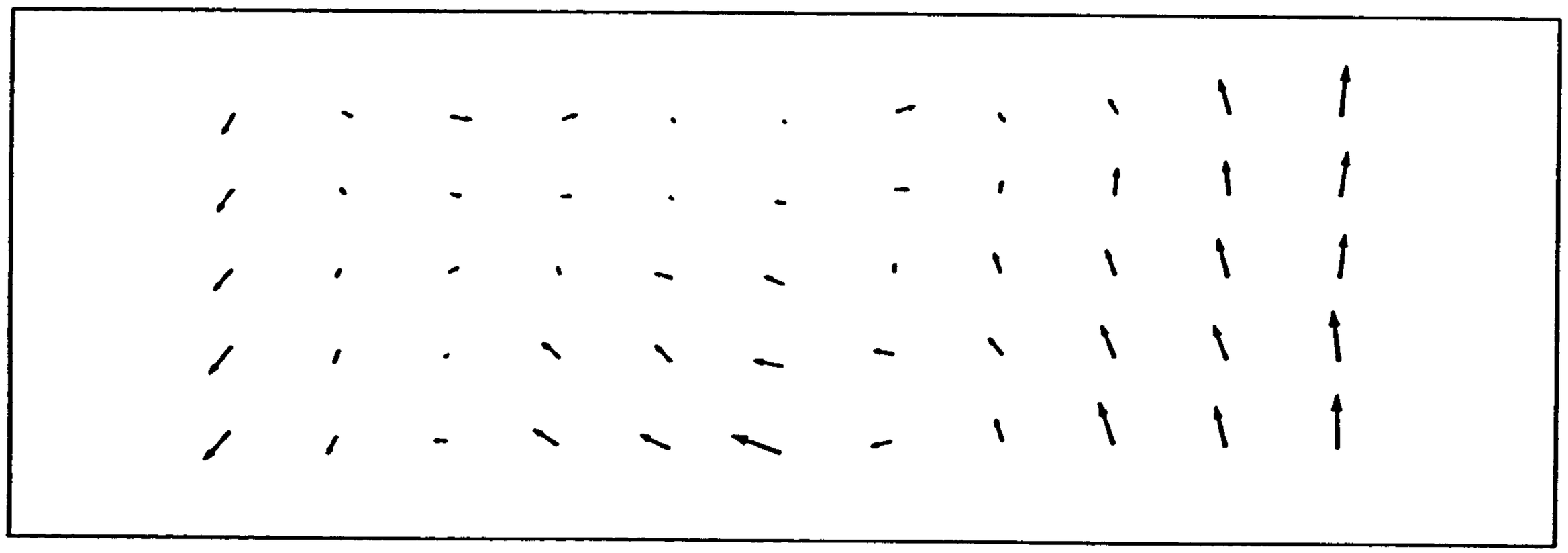

Figure C.13.4 - XY Vector Residual Plot and Height Bubble Residual Plot
(Centre Strip, With GPS, One 3-D Control Point At Point 29)

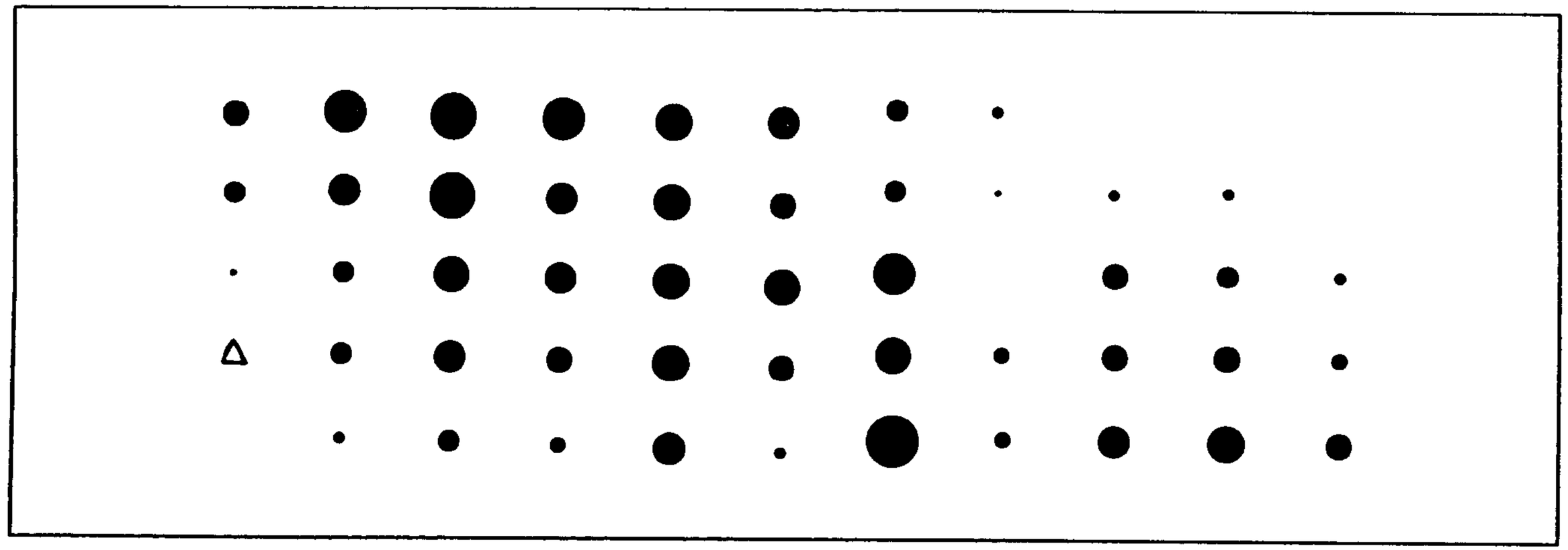

XY Vector Scale: 1cm=3.5cm Height Bubble Scale: 1cm radius=14cm

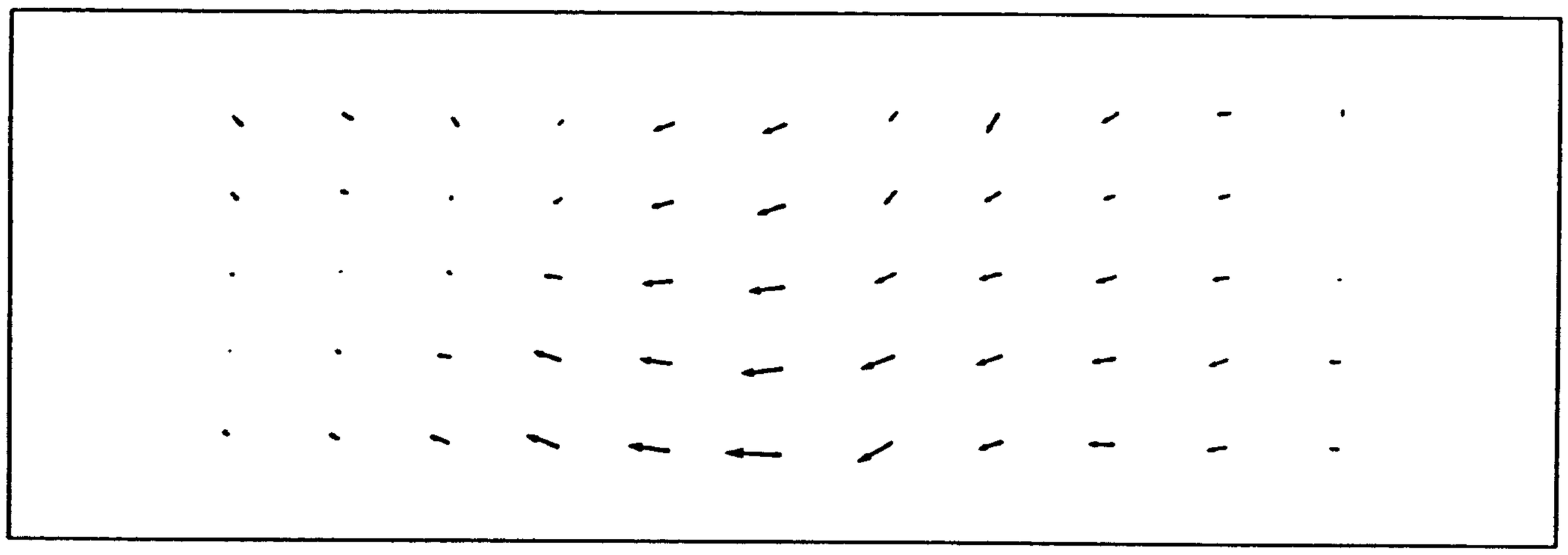

Figure C.14.1 - XY Vector Residual Plot and Height Bubble Residual Plot
(Centre Strip, With GPS, Two 3-D Control Points At Point 2 and 54)

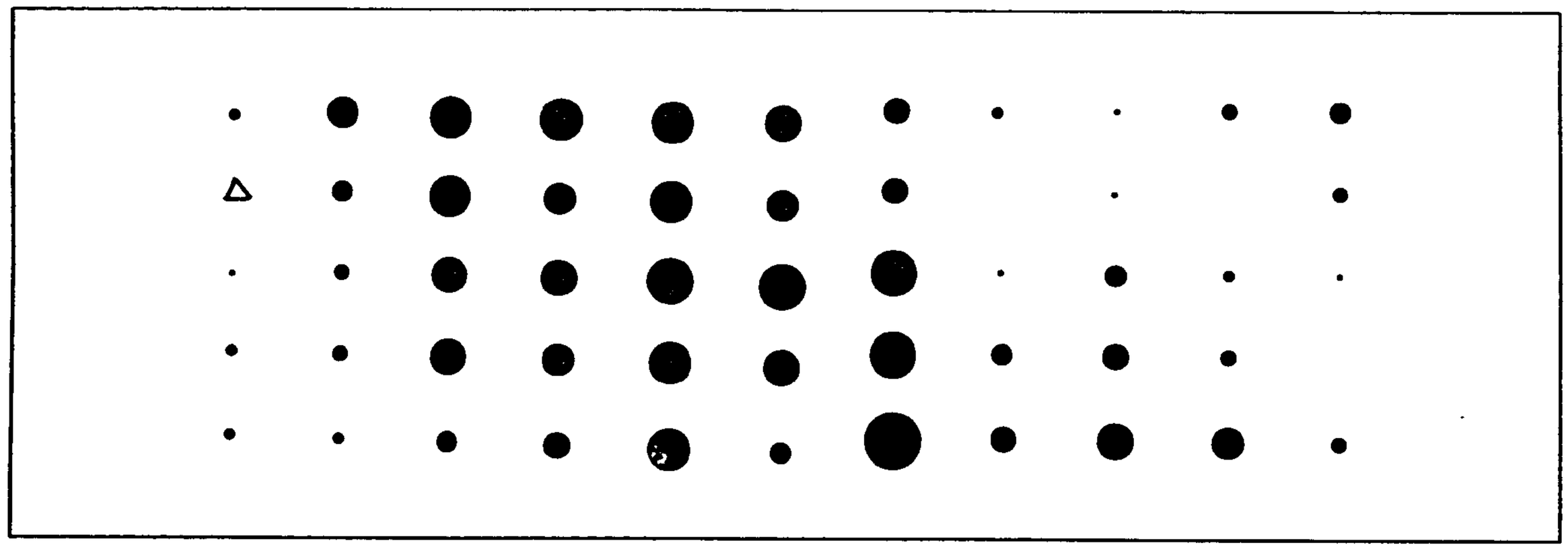

XY Vector Scale: 1cm=3.5cm Height Bubble Scale: 1cm radius=14cm

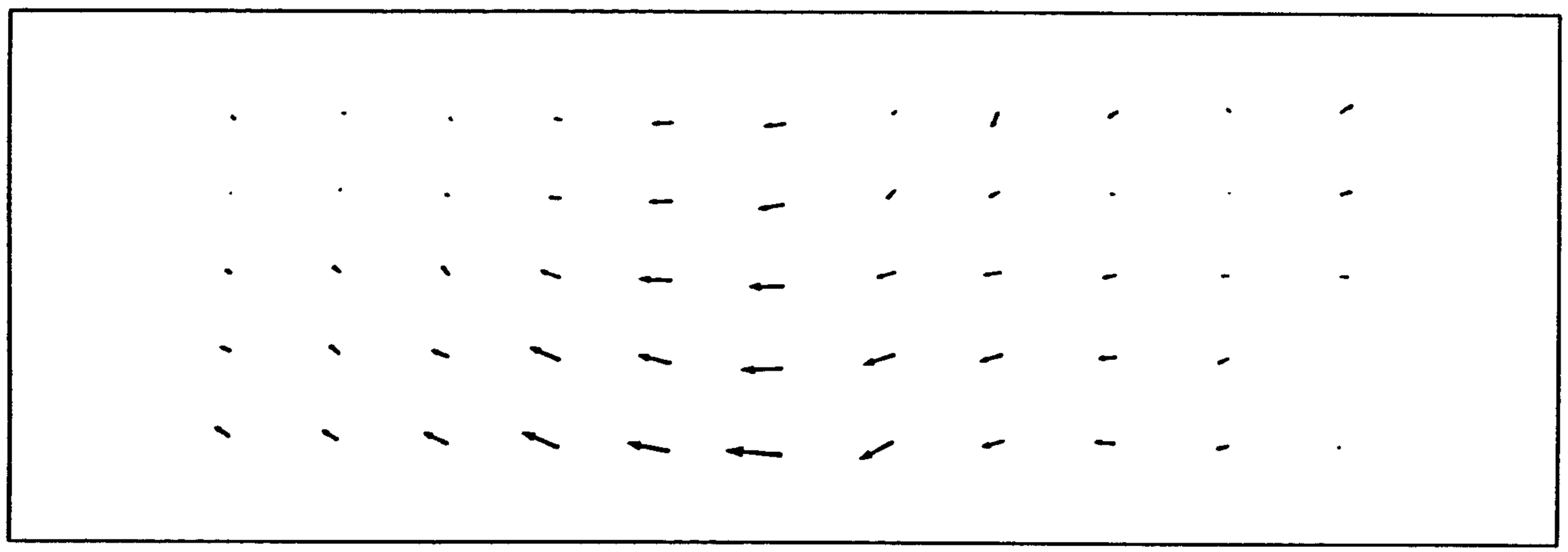

Figure C.14.2 - XY Vector Residual Plot and Height Bubble Residual Plot
(Centre Strip, With GPS, Two 3-D Control Point At Points 4 And 52)